The role of FOX Genes on Chromosome 6 on Breast Cancer

by

Fahed Elian

A thesis submitted in partial fulfillment of the requirements for the degree of

Doctor of Philosophy

Medical Sciences – Medical Genetics

University of Alberta

Abstract

The transcription factors *FOXC1, FOXQ1, and FOXF2* (FOX cluster on chromosome 6) are members of the forkhead family that play a role in a plethora of biological processes during development and tumorigenesis. Emerging studies in the last decade have suggested a role of the FOX cluster in breast cancer (BC). The majority of the research however has focused on one subtype of BC known as basal/triple negative breast cancer. Very limited studies have investigated the role of the FOX cluster in other BC subtypes such as luminal and HER2 subtypes. Thus, studies that examine the role of the FOX cluster in other subtypes of BC are needed.

In this thesis, I examined the expression, copy numbers, and mutations of the FOX cluster genes across BC subtypes in BC patient samples and cell lines. I revealed for the first time that *FOXQ1* expression varied across breast cancer subtypes and most importantly that low expression of *FOXQ1* is associated with poor prognosis in BC patients. Moreover, I showed that *FOXC1* expression also varied across BC subtypes and that the protein of *FOXC1* is more stable in basal/TNBC cell lines. I also showed that the FOX cluster genes had copy number variation in BC subtypes, however I showed that their mRNA expression is independent from copy number variations. Finally, I found three novel mutations of *FOXC1* in 3 different BC patients that were predicted to be likely-pathogenic, and that *FOXC1* expression is significantly positively correlated with *FOXF2* expression in BC patients.

My findings suggest dual roles of the FOX cluster in BC in different BC subtypes. Based upon my research I suggest that the FOX cluster acts more like “onco-genes” in basal BC, but a “tumor-suppressor genes” in HER2 and luminal BC subtype.

Preface

Parts of Chapter 1 of this thesis has been published as Elian, F.A.; Yan, E.; Walter, M.A. *FOXC1, the new player in the cancer sandbox*. *Oncotarget* **2018**, *9*, 8165–8178. I wrote the review and designed all the figures. E. Yan provided help with drafting role of FOXC1 in HCC, HL, and NHL. M.A. Walter was the supervisory author and was involved in manuscript composition.

Chapter 2 of this thesis is submitted to *Breast Cancer: Targets and Therapy Journal* and currently under review as Elian, F.A; Are, U; Ghosh, S; Nuin, P; Footz, T; McMullen, TPW, Brindley, D.N; and Walter, M.A "*FOXQ1 is differentially expressed across breast cancer subtypes with low expression associated with poor overall survival*". I conceived and planned the experiments. I conducted the qPCR and RT-qPCR experiments, overall survival analysis, statistical analysis, interpreted and analyzed the K-means clustering. I took the lead on writing the manuscript and made all the tables and figures. U.A, helped with conducting some of the qPCR experiments. S.G carried out Cox regression analysis using the SPSS program and helped with interpreting the data of univariate and multivariate analysis. P.N carried out the K-means clustering. T.F designed the PCR primers, helped with interpreting the qPCR data, and reviewed the manuscript. T.P.W.M provided the breast patient and normal breast tissues. D.N.B provided the cDNA and DNA from these tissues and also helped with interpreting the data and reviewing the manuscript. M.A.W helped with interpreting the data and reviewed the manuscript. M.A W was the supervisory author and was involved with the concept formation and manuscript composition.

All other work in this thesis are my original work.

To my mother, whose unconditional love and support sustains my life.

To my father, who never fails to be there for me.

To Mike, whose wisdom enlightened my life.

To my nieces, Leanne and Maria, I love you both.

Acknowledgements

This section of my thesis is the hardest to write. Words cannot describe my gratitude to all those who have supported me these last few years and have helped me to complete my PhD's thesis.

Mike, my mentor, my supervisor, and my friend; thank you for trusting me from the first day we worked together. You saw in me and nurtured abilities and skills that I could not have recognized without your support. You took me under your wing and provided me a space in your lab where I felt comfortable to dream, imagine, grow, believe, learn, and act. Your wisdom is limitless and has impacted and enriched my life beyond my PhD studies. You value my opinions and ensure I am always heard and have space to get involved. I have, and continue to learn a lot from you, and I know that everything I have gained under your guidance will positively impact my career and my life. What separates you from many supervisors in academia is your emotional intelligence that I have experienced firsthand and learned from. You supported me in every academic or non-academic aspect of my life during my PhD studies. The lab did not feel the same after you left on sabbatical, and, at times, I felt that motivation was low on my end to maintain that drive and push harder each day, but you always went out of your way to maintain communication and to support me in any possible way. Thanks, Mike, for being the family I never had in Canada.

To my committee members, Dave and Ing Swie, thank you for your guidance, contributions and suggestions throughout my PhD studies. Dave, thank you for always being there for me when I needed your support, providing me with reference letters, and going above and beyond to make my research progress. Ing Swie, thank you for challenging my research ideas and hypotheses to make me a better critical thinker and a better scientist. You thought of me highly and expected the best from me, which always motivated me during my studies. As well, I would also like to give thanks to my external examiners Dr. Brian Brooks and Dr. Daniel Graf for agreeing to be on my PhD defense examining committee and for sharing their time. I also want to thank Daniel for sharing his time as an examiner on my candidacy committee. I will miss the fun times, beers, and great conversations we always used to have at TGIFs. In addition, I am thankful to our former and current graduate coordinators, Dr. Sarah Hughes and Dr. Rachel Wevrick, for their wise advice regarding my scientific career. Also, special thanks to our department staff Heather and Shari who helped immensely with my scholarship applications, logistical support, and with planning the MGSA research day and many other social events in our department.

The experiments in this thesis could not be done without the help of our lab technician, Tim Footz. Tim, you are professional, hardworking, organized, smart, and are uniquely gifted at making experiments work! But, above all of that; you are a welcoming and helpful colleague. I'm thankful that I got to know you and learn how to do lab experiments from you. I will miss our walks to McDonalds and it'Dog! Also, I cannot forget to thank Paulo, whose help in bioinformatics was critical for some of the chapters in this thesis.

I have many friends to thank. Wael, I have known you for more than 20 years and yet you still impress me with your kindness, energy, and support. I know I would not be where I am at right now without your help, brother. André, Edmonton is really a cold city, I mean, it's literally cold, but somehow you made it feel like home. I did not know that when we met during our executive terms, and we both made the "Mr. Macky" reference, that it was going to be a friendship that I will cherish a lot. Thank you for proofreading my manuscripts. Also, thank you for all the road trips and fun adventures we shared together over the past years. To Oday, my undergrad and travel buddy, aka Rafeeq, whose passion for science is contagious. Thank you for all the years of support and for all the great times we always had in every place we traveled to. Vanessa, thank you for being there for me through all the ups and downs, on campus and off campus, and for encouraging me to finish my PhD thesis. Thank you Marwan and Kinda, Toronto always felt like home because of both of you, thanks for hosting me every time I visited the 6IX. Joel, Ping and Maryam, thank you for organizing many ski trips and camping trips, they were great ways for me to unwind and disconnect from my PhD. Finally, thanks to my summer students, Elizabeth and Ubah, who made me develop a greater understanding and appreciation for learning and sharpen my leadership and communication skills. I feel privileged to have had the opportunity to mentor both of you and proud to call you my friends.

To my GSA family—Chantal, Dylan, Marc, Mo, Sasha, Beth, Masoud, Zhihong, Courtney, Julie, Lisa, Mahsa, & Laura—thank you so much for making the last two years of my graduate school very memorable. Working alongside you was a pleasure and am so proud of the work we did together over the past couple years.

I would also like to express my sincere thanks and appreciation to the members of the GSA office support team, GSA board members, GSA Council members, and all members of University administration—in particular the former university President Dr. David Turpin, for the collaborative work we have done over the past year. The relationships we built together have truly made my presidency a pleasure. I commend members of University administration for the incredible and supportive leadership they have shown in this challenging climate. I would also like to give thanks to all of the members of the Faculty of Graduate Studies and Research leadership team—in particular the Dean and Vice-Provost Dr. Brooke Milne—for their contributions to the thoughtful discussions and collegial working relationships we have developed over the past year. It has been a great pleasure to serve alongside all of you.

For Francesca, I simply cannot thank you enough for all what you have done to support me these past few months. Writing a thesis during a pandemic is not fun, but you made it doable with all your unconditional support and care. Thank you for making me believe that eventually everything will work out.

Finally, this work would not have been done without my family's support, both emotionally and financially. To my mother, my role model, your love and support are exemplary. I rarely share with anyone how much you have positively impacted and enriched my life. But I hope you know

how lucky I feel every day that I have you in my life. Your actions taught me what life should mean to us and how we should live it. Learning from you while I was growing up; you being a professional dentist, raising me and my siblings, and making time for your hobbies and loved ones showed me that nothing in this life is impossible. I owe you everything. To my father, who led by example. Your story inspires me every day; a refugee child who had to flee his home country to then later become a successful medical doctor and the most caring father I could ever ask for. Thanks for all the insightful conversations and lessons you share with me, and thank you for all the love and care you show to me. They have shaped the man who I am today. I learned from you that respect and trust are earned, and that hard work and dedication always pay off. To my siblings, Shadi, Shaden, and Farah. I can't imagine a world without you. Every time I doubted myself, I found at least one if not all of you there to support me and keep my wheels in motion. I am lucky to have friends in my life that I can trust unconditionally, and that I can lean on, anytime. I love you.

Table of Contents

ABSTRACT ..... **II**

PREFACE ..... **III**

ACKNOWLEDGEMENTS ..... **V**

TABLE OF CONTENTS ..... **VIII**

LIST OF TABLES ..... **X**

LIST OF FIGURES ..... **XI**

LIST OF ABBREVIATIONS ..... **XIII**

CHAPTER 1 ..... **1**

INTRODUCTION **1**

1.1 Breast cancer 2

1.1.1 Intrinsic BC subtypes *4*

1.2 The FOX family 6

1.2.1 FOXC1: background *7*

1.2.2 FOXQ1: background *13*

1.2.3 FOXF2: background *14*

1.3 The FOX family and cancer 14

1.3.1 FOXC1 and breast cancer *15*

1.3.2 FOXQ1 and breast cancer *19*

1.3.3 FOXF2 and breast cancer *22*

1.4 Hypothesis and Aims 24

CHAPTER 2 ..... **25**

2.1 Chapter Abstract 27

2.2 Introduction 28

2.3 Materials and Methods 30

2.3.1 Tissue samples 30

2.3.2 Overall survival analysis 30

2.3.3 RT-qPCR 32

2.3.4 Copy number variation 33

2.3.5 K-means Clustering 34

2.4 Results 35

2.4.1 FOXQ1 mRNA expression varies between BC patient subtypes *35*

2.4.2 Low expression of FOXQ1 is associated with poorer overall survival in breast cancer patients *36*

2.4.3 Relation of FOXQ1 copy numbers in BC subtypes to mRNA levels *37*

2.4.4 FOXQ1 expression is an independent predictor of overall survival in BC patients when adjusted to FOXF2 and FOXM1 expressions *39*

2.5 Discussion 39

2.6 Tables and Figures 46

CHAPTER 3 ..... **59**

3.1 Chapter Abstract 61
3.2 Introduction 63
3.3 Materials and Methods 65
3.3.1 Tissue samples *65*
3.3.2 Cell lines and cell culture *66*
3.3.3 RT-qPCR *66*
3.3.4 FOXC1 copy number variation *67*
3.3.5 Immunoblot analysis *68*
3.3.6 Protein stability *69*
3.3.7 FOXC1 sequence analysis *70*
3.3.8 K-Means clustering *71*
3.4 Results 72
3.4.1 FOXC1 expression in BC subtypes *72*
3.4.2 The impact of DNA mutation and amplification on FOXC1 expression in TNBC *74*
3.4.3 The effects of activated epidermal growth factor receptor (EGFR) on FOXC1 levels in TNBC *75*
3.4.4 FOXC1 is more stable in TNBC cell lines *76*
3.5 Discussion 77
3.5.1 FOXC1 expression in BC *78*
3.5.2 Investigation of FOXC1 over-expression mechanisms in TNBC *82*
3.6 Tables and Figures 85

CHAPTER 4 ..... **101**

4.1 Chapter Abstract 103
4.2 Introduction 105
4.3. Materials and Methods 107
4.3.1. FOXC1, FOXF2, and FOXQ1 expression, copy numbers, and sequence analyses *107*
4.3.2 Copy number variation (CNV) and mRNA correlation studies *108*
4.3.3 Co-expression analysis of FOXC1, FOXF2, and FOXQ1 ..... *109*
4.4 Results 109
4.4.1. FOXC1, FOXF2, and FOXQ1 genetic alterations in basal BC and other BC subtypes *109*
4.4.2. Relation of FOX cluster copy numbers in BC patients to mRNA expression levels *111*
4.4.3. FOXC1 mutations in the TCGA-BRCA patients *112*
4.5. Discussion 113
4.6 Figures 119

CHAPTER 5 ..... **130**

5.1 Significance 131
5.2 General discussion and Future Directions 132

REFERENCES **140**

APPENDIX **162**

List of Tables

Chapter 2: *FOXQ1 is differentially expressed across breast cancer subtypes and is associated with poor overall survival*

Table 2. 1: BC patient demographic 47

Table 2. 2: Hazard ratios from the univariate Cox's regression analysis for the TCGA-BRCA database..... 48

Table 2. 3: Cox's regression analysis for *FOXQ1* expression based on the median cut-off stratified by BC subtypes and adjusted for BC subtypes the TCGA-BRCA database 49

Table 2. 4: Cox's regression analysis for *FOXQ1, FOXF2, and FOXM1* expression based on the median cut-off..... 50

Table 2. 5: BC cell line names and types that were used for standard K-means clustering. 51

Chapter 3: *FOXC1 is Over-expressed and is More Stable in Basal/Triple Negative Breast Cancer*

Table 3. 1: Patient demographic 86

Table 3. 2: BC cell line names and types that were used for unsupervised K-means clustering.. 87

List of Figures

Chapter 1: *Introduction*

Figure 1. 1: *FOXC1* schematic structure and *FOXC1* missense mutations. 10

Figure 1. 2: FOXC1 function and activity in human diseases. 12

Figure 1. 3: FOXC1-Signaling Pathways in BLBC. 18

Chapter 2: *FOXQ1 is differentially expressed across breast cancer subtypes and is associated with poor overall survival*

Figure 2.1: *FOXQ1* is under-expressed in luminal and HER2 breast cancer patient samples..... 52

Figure 2. 2: Low *FOXQ1* expression predicts poor overall survival in BC patient..... 53

Figure 2. 3: Low *FOXQ1* expression predicts poor overall survival in BC patient subtypes..... 54

Figure 2. 4: *FOXQ1* has more copies in TNBC compared to control samples. 55

Figure 2. 5: *FOXQ1* expression is independent of its CNV in BC cell lines..... 57

Chapter 3: *FOXC1 is Over-expressed and is More Stable in Basal/Triple Negative Breast Cancer*

Figure 3. 1: *FOXC1* is over-expressed in TNBC compared to luminal patient samples and is under-expressed in luminal compared to normal breast tissue..... 88

Figure 3. 2: *FOXC1* expression varies among BC cell lines and is highly expressed in basal (TNBC) cell lines. 90

Figure 3. 3: *FOXC1* sequence analysis on TNBC cell line showed no pathogenic mutations. 91

Figure 3. 4: The TNBC cell lines HS-587T and BT-549 have extra copies of *FOXC1*. 93

Figure 3. 5: *FOXC1* expression varies among BC cell lines and is independent of its CNV. 94

Figure 3. 6: FOXC1 levels in TNBC cell line HS-578T cells are independent of short-term EGF stimulation..... 95

Figure 3. 7: FOXC1 levels in TNBC cell line BT-549 cells are independent of short-term EGF stimulation..... 96

Figure 3. 8: FOXC1 levels in TNBC cell line MDA-MB-231 cells are independent of short-term EGF stimulation. 97

Figure 3. 9: FOXC1 levels are upregulated in TNBC cell line BT-549 but not HS578T after a time-course of EGF stimulation. 98

Figure 3. 10: FOXC1 protein half-life is longer in TNBC cell lines (HS-578T and BT-549). .. 100

Chapter 4: *in silico analysis of FOX gene cluster—FOXC1, FOXF2, and FOXQ1—in Breast Cancer patients*

Figure 4. 1: *in silico* analysis of *FOXC1, FOXF2, and FOXQ1* (FOX cluster) genetic alterations in the TCGA-BRCA dataset. 121

Figure 4. 2: Graphical summary of the FOX cluster genes' alterations found in the TCGA-BRCA patient samples. 123

Figure 4. 3: Weak correlation between *FOXC1* mRNA levels and CNV in the TCGA-BRCA patients. 124

Figure 4. 4: *FOXF2* mRNA and FOXQ1 mRNA levels are not correlated with CNV in the TCGA-BRCA patients. 126

Figure 4. 5: The FOX cluster genes' co-expression and correlation analysis in the TCGA-BRCA patients. 128

Figure 4. 6: FOXC1 mutations in the TCGA-BRCA patient samples. 129

List of Abbreviations

BC	breast cancer
HER2	human epidermal growth factor 2
TNBC	triple negative breast cancer
IHC	immunohistochemistry
ER	estrogen receptor
PR	progesterone receptor
PAM50	the prediction analysis of microarray 50
EGFR	epidermal growth factor receptor
FHD	forkhead domain
TF	transcription factor
ARS	Axenfeld Rieger syndrome
AD	activation domain
NLS	nuclear localization sequence
ID	inhibitory domain
FOXC1	forkhead box C1
FOXQ1	forkhead box Q1
HOXA-1	homebox A1
SMO	Smoothened
Hh	Hedgehog
MAPK	mitogen activated protein kinase
PI3K	phosphatidylinositol-4,5-bisphosphate 3-kinase
Patched 1	patched 1
GLI2	Glioma-Associated Oncogene Family Zinc Finger 2 (
EpRas	mouse mammary epithelial
CDH1	E-cadherin
HMLE	human mammary epithelial cells
CSC	cancer stem cell
FOXF2	forkhead box F2
GI	gastrointestinal
CNV	copy number variation
DBD	DNA binding domain
GEPIA	Gene Expression Profiling Interactive Analysis
TCGA	Cancer Genome Atlas
BRCA	invasive breast carcinoma project
KM	Kaplan-Meier
TPM	Transcript per million
CCLE	Cancer Cell Line Encyclopedia
HR	Hazard ratio
CI	Confidence intervals
Hepatocellular carcinoma	HCC
HL	Hodgkin's lymphoma
NHL	non-Hodgkin's lymphoma
HTRTOA3	FOXC1 stably-transfected non-BC HeLa cells

DMEM	Dulbecco's modified Eagle's medium
EGF	epidermal growth factor
SF	serum free
Akt	protein kinase B
ERK	extracellular signal-regulated kinase
BRCA1	breast cancer type 1
IEG	immediate early gene
WT	wild type
SIFT	sorting intolerant from tolerant
PolyPhen-2	polymorphism

Chapter 1

Introduction

The first medical description of cancer was found in an Egyptian text originally written in 2500 BC: "a bulging tumor in the breast….like touching a ball of wrappings." Discussing treatment, the ancient scribe noted: "There is none."

—The Emperor of All Maladies

1.1 Breast cancer

Breast cancer (BC) is one of the most common life threatening malignancies in women [1]. Epidemiologically, it was estimated that 2.1 million women worldwide will be diagnosed with BC in 2018; and approximately 600,000 women with BC died [2]. BC incidence, however, varies worldwide with estimated 92/100,000 BC incidence in North America compared to 27/100,000 in eastern Asia and Africa [3,4]. Moreover, women who develop BC in North America and western countries are usually between the age of 40 and 50, while women who develop BC in Asian countries are typically between the age of 60 and 70 [5–8].

BC is a heterogeneous disease, and this term encompasses a variety of entities with distinct morphological features and clinical behaviors [9]. In the clinic, BC is further subdivided into luminal BC, human epidermal growth factor receptor-2 (HER2 or ERBB2) BC, triple negative breast cancer (TNBC) [10]. These subtypes are mainly decided based on the levels of immunohistochemistry (IHC) markers, such as estrogen receptor (ER), progesterone receptor (PR), and HER2.

Luminal BC is known as the most heterogenous BC in many features such as copy number changes, patient outcomes, and mutations [11]. Luminal BC is suggested to originate from either luminal precursors cells or luminal progenitor cells that grow uncontrollably[12]. Luminal tumors are suggested to have high levels of the hormonal receptors ER and PR; and count up to 60-70% of total BC cases [13]. There are two isoforms of ER; ERα and ERβ both of which are nuclear receptors and transcription factors that are encoded by *ESR1* and *ESR2* genes respectively [14]. The mechanisms that lead for ER aberrant expression in BC are complex including alternative splicing of ERα and Erβ, epigenetics and post-translational regulation [15,16].

Both ERα and ERβ are activated by binding to estrogen family members (steroidal hormones) such as estrone, estradiol, and estriol [15,16]. Once activated by its ligand, ER translocates to the nucleus and binds to DNA at estrogen response elements in promoters of genes that are regulated by ER[17]. ERβ is usually lost in BC where its expression is associated with better BC prognosis [18]. On the other hand, the ERα isoform is present at high levels in luminal BC and its levels are measured in the clinic to diagnose BC. ERα was suggested to activate genes that play critical role in BC cell's proliferation and survival [19,20]. ER positive BC, such as luminal BC, benefits from therapy that target ER (endocrine therapy) such as aromatase inhibitors and tamoxifen [21,22]. PR also has two major isoforms PR A and PR B encoded by *PGR* gene, and similar to ER, it is a transcription factor that has been suggested to play a role in breast tumorigenesis [23].

HER2 BC is proliferative and aggressive form of BC. HER2 BC accounts for about 15-25% of all BC cases. The *HER2* (*ERBB2/Neu*) gene—a member of the ERBB receptor family—is located on chromosome 17 and encodes a HER2 protein with molecular weight of 185 kD [24]. HER2 is structurally different from the rest of the ERBB receptor family members because it lacks a known ligand-binding domain [25,26]. The absence of the ligand-binding activity in HER2 receptor makes it one of the preferential receptors for homo/hetero-dimerization within the ERBB family receptors [27]. HER2 plays a critical role in BC invasion, proliferation, survival, differentiation, and angiogenesis [28–30]. Therapies that target and block HER2 signaling such as humanized antibodies and small molecule tyrosine kinase inhibitors are shown efficacy in the clinic [24,31].

TNBC accounts for about 10-15% of all BC cases and its main characteristics are that TNBC is more frequent in younger patients (<50 years), more prevalent in African-American women, and often present as interval cancers [32]—cancers are detected after a normal

mammogram screening but before the next scheduled mammogram screening which usually occur every 2 years [33]. TNBC is considered the most aggressive form of all BC subtypes and has the worst prognosis. TNBC lacks effective targeted therapies, this is in part due to the lack of biomarkers such as ER, PR, and HER2 expressions, but also the high level of heterogeneity observed even within TNBC [34].

The BC classification into different subtypes using clinical factors—histological grade, lymph node metastasis, tumor size, and age—benefits clinicians, pathologists, and researchers through the provision of precise BC prognosis, diagnosis, and treatment. As a result targeted therapies have been developed for BC subtypes based on this classification and have proved effective [35–37]. Although pathological/clinical classification is critical for BC diagnosis, prognosis, and treatment, it was suggested that this traditional classification could also miss other molecular intrinsic BC subtypes and limit our understanding of BC progression and metastasis. Also, it is widely accepted that BC patients within the same pathological and clinical subtype of BC can experience different outcomes, treatment response rate, overall survival rate, and relapses [38,39]. As a result, in the last two decades, efforts have been focused on further stratifying the pathological and clinical BC subtypes—to what known now as intrinsic molecular subtypes and/or surrogate BC subtypes.

1.1.1 Intrinsic BC subtypes

Almost 20 years ago, based on multigene expression profiling and hierarchical clustering, the first proposals of existing molecular intrinsic subtypes within the pathological BC subtypes were suggested [40,41]. The Prediction Analysis of Microarray 50 (PAM50) predictor, initially was introduced in 2000, is a multigene signature that further stratified traditional

pathological classification of BC (TNBC, luminal, HER2) into intrinsic molecular subtypes based on multigene differential expression [40]. Further studies were conducted using the PAM50 predictor to stratify BC and suggested four main intrinsic molecular BC subtypes; luminal A, luminal B, HER2 enriched, and basal-like (basal) BC [11,40,42–44 45–47].

The cell of origin of BC is not well studied and is as yet not fully understood. Tumor heterogeneity, tumor microenvironment, genetic and epigenetics are factors that contribute to BC development and complexity. The normal breast mammary epithelium is made of bilayers of epithelial cells, the luminal layer and the myoepithelium layer [48,49]. It was suggested that the luminal layer is composed of cells expressing estrogen and/or progesterone and/or keratins such as keratin 18 and 19. On the other hand, the myoepithelial layer (basal layer) is composed of cells that express p63 and/or keratins 5 and 14 [50,51]. It was suggested that different cells of origin contribute to different BC subtype development [42,52]. For example, the basal-like BC cell gene signature is closest to those of the luminal progenitor cells in the breast mammary gland [42,52]. In addition, ER negative luminal progenitor cells were also suggested as the origin of basal-like BC [53]. On the other hand, the cell of origin that may give rise to luminal and HER2 BC is debatable and remain elusive [54].

Luminal B was suggested to have higher levels of proliferation and cell cycle markers genes such as *MKI67,* but lower luminal markers such as *PGR* compared to luminal A. Furthermore, luminal B BC cells have higher *TP53* but lower *PIK3CA* mutations frequency compared to luminal A [55–57]. In addition, luminal A has a good prognosis compared to luminal B, where the latter has higher recurrence rate, lower overall survival rate, more invasive and proliferative [58,59].

HER2 BC cells were suggested to harbor the highest frequency of mutations across all BC subtypes—approximately 30% and 70% of *PIK3CA* and *TP53* mutations respectively were detected in HER2 BC cells [60,61]—*MKI67* encodes a protein that plays a critical role in cell proliferation [62], *TP53* encodes a protein that plays a vital role in DNA damage repair [63], apoptosis and cell cycle, and *PIK3CA* gene encodes p110α proteins, one of the catalytic subunit of the PI3K pathway (frequently activated in BC and plays a role in proliferation [64].

Basal BC was suggested to have high levels of additional immunohistochemistry markers such as basal cytokeratins CK5/6, CK14, CK17, and epidermal growth factor receptor (EGFR) and lack the overexpression of ER, PR, and HER2 thus referred to as TNBC [65]. Basal BC is an intrinsic subtype of TNBC, where 80% of TNBC are of the basal BC [66]. Very similar to TNBC, basal BC usually presents with high stage—the cancer spread to other parts of the body—aggressive clinical features, poor prognosis, and a propensity to metastasize to the brain and lung.

Emerging data suggested that the forkhead genes; *FOXC1, FOXQ1, and FOXF2* play a role in TNBC, in particular in basal BC, and that *FOXF2* and *FOXC1* expression can be used as prognostic markers for basal/TNBC [67,68]. However, their expressions and roles in basal/TNBC are controversial and not well studied. Moreover, very limited studies have investigated their expressions and roles in other BC subtypes such as luminal and HER2. Thus the emerging roles of three FOX genes on chromosome 6 in oncogenesis warranted a deeper examination at a molecular level in BC.

1.2 The FOX family

The FOX protein family, otherwise known as the Forkhead box protein family, is a group of highly evolutionarily conserved proteins [69] with a common DNA-binding domain of 110 amino acids known as the forkhead box or "winged helix" domain (FHD) [70,71]. The general structure of the FHD consists of three α-helices, three β-sheets, and two "wing" regions situated on either side of a third β-sheet – this produces the "butterfly-like" characteristic that inspired the moniker of the "winged helix domain" [69].

The orthologue of this functionally diverse family was found nearly three decades ago in *Drosphila melanogaster*, in which a mutation in the homeotic gene *forkhead* (*fkh*) was found to inhibit gene expression and manifest aberrant head structures [72]. Since then, more than fifty different forkhead proteins have been discovered in humans, classified in subgroups ranging from FOXA to FOXS based on similarity within the forkhead box and outside the forkhead box [69,71,73].

The FOX family members are highly conserved transcription factors (TFs) that have a major role in a plethora of biological functions such as embryonic and adult development i.e. heart, stomach, limbs, and eyes development, and are connected to chromatin remodeling as well as nuclear localization[71,73,74]. Moreover, FOX proteins play a significant role in immune response; they can activate genes that play a major role in the differentiation of specific immune leukocyte population and therefore optimizing immune responses and sustaining immune homeostasis [75–81].

1.2.1 *FOXC1*: background

FOXC1, which is also known as Mf1, Fkh-1[71] or FREAC3 [82], is a single exon gene located at 6p25.3 encoding a 533 aa protein that localizes to the nucleus, where it can bind to the DNA

and regulate gene expression [83]. *FOXC1* is an essential component of mesodermal [84], neural crest [85] and ocular development [86–88] and is often studied and discussed in relation to Axenfeld Rieger syndrome (ARS). ARS can be caused by *FOXC1* mutations [71,89] and involves the abnormal development of the anterior segment of the eye. Importantly, 50% of ARS patients go on to develop high ocular pressure [90]. *FOXC1* is also associated with Dandy-Walker malformation, which is a condition in which patients suffer from an underdeveloped cerebellum and enlarged posterior fossa [89,91]. While this gene is undoubtedly an integral developmental transcription factor – the deletion of both *FOXC1* alleles in mice leads to not only issues in ocular development, but it also gives rise to hydrocephalic, cardiac, organogenesis, and skeletal anomalies, and neonatal mortality [83,84,92].

Like others of the FOX family, the phosphoprotein FOXC1 [90] possesses the "winged-helix" structure in its DNA binding domain (DBD) (Figure 1.1). The third α-helix of the "winged helix" crosses perpendicularly to the DNA helical axis, creating a sequence-specific contact with the major groove in the core base sequence GTAAATAAA-3' [93–95] to which FOXC1 has a strong affinity, as determined through *in vitro* experiments [82]. There are additional protein-DNA contacts possible in the second wing region [95]. *FOXC1* regulates transcription through its N- and C- terminal activation domains as well as a phosphorylated transcription inhibitory domain [83].

FOXC1 point mutations have been reported and studied [96–103]. These mutations have been shown to reduce FOXC1 protein level, FOXC1 transactivation, and/or FOXC1's DNA binding ability [99,100,104]. To date, 31 missense variants in ARS patients have been identified in *FOXC1*, 29 of which occur within the forkhead domain (Figure 1.1).

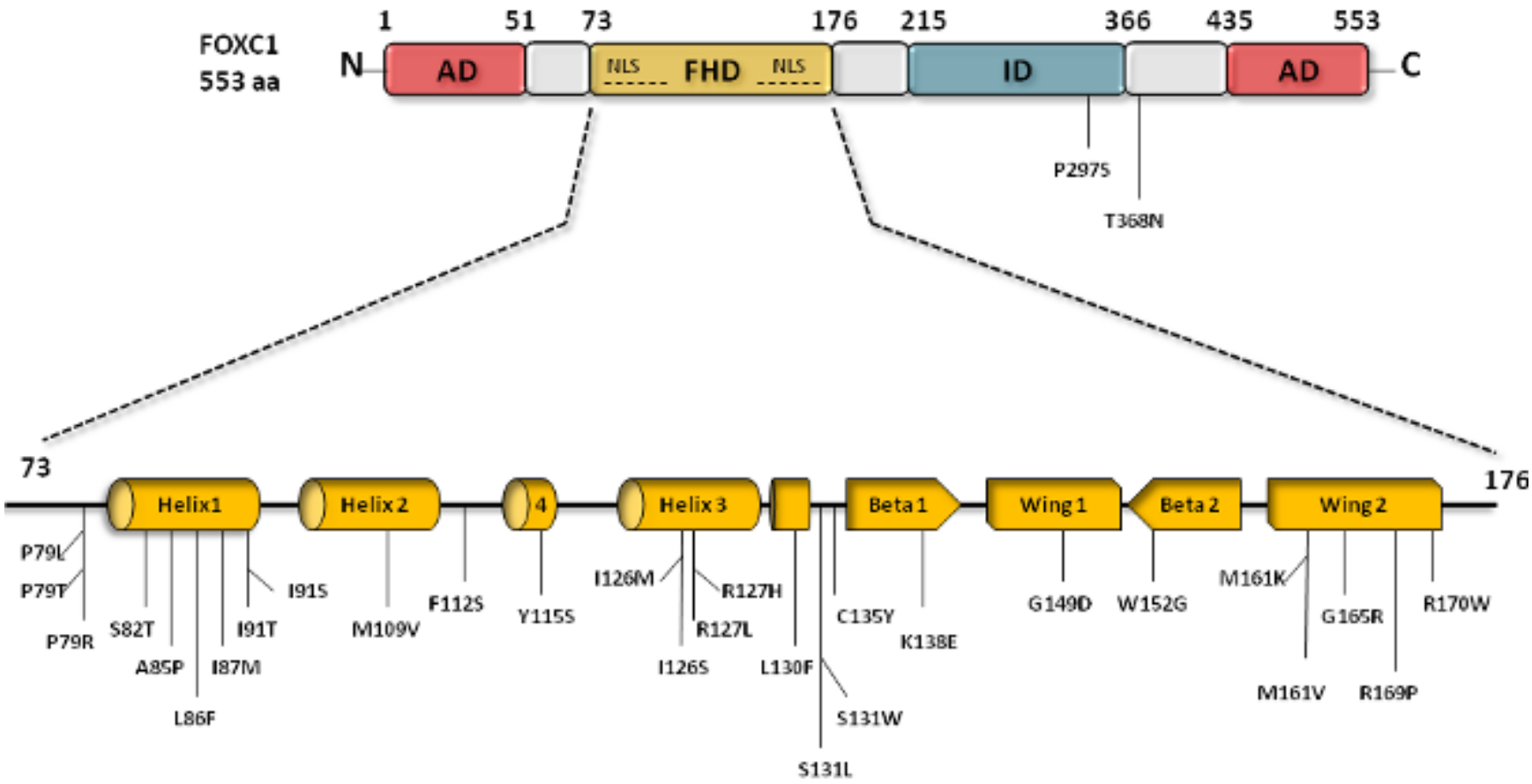
FOXC1
553 aa
1
51
73
176
215
366
435
553
N
AD
NLS
FHD
NLS
ID
AD
C
P297S
T368N
73
176
Helix1
Helix 2
4
Helix 3
Beta 1
Wing 1
Beta 2
Wing 2
P79L
P79T
P79R
S82T
A85P
I87M
L86F
I91T
I91S
M109V
F112S
Y115S
I126M
I126S
R127H
R127L
L130F
S131L
S131W
C135Y
K138E
G149D
W152G
M161K
M161V
G165R
R169P
R170W

Figure 1. 1: *FOXC1* schematic structure and *FOXC1* missense mutations.

FOXC1 protein contains two activation domains (AD) that are located at the N-terminus 1-51 aa, and the C-terminus 435-553 aa, both of which play a main role in FOXC1 activation [83,105]. Engineered FOXC1 proteins that lack either the N- or/and C- terminus have reduce activity and improper functions. FOXC1 protein localizes to the cell nucleus via two nuclear localization sequences (NLS), and binds to DNA via the forkhead domain (FHD) 73-176 aa. To date 28 point mutations have been identified in the FHD of FOXC1, most of which are linked to ocular defects and malformations. Deletion of the inhibitory domain (ID) 435-533 aa. significantly increases FOXC1 activity. In contrast to the two ADs that activate FOXC1, specific residues in the ID experience post-translational phosphorylation and as a result inhibit FOXC1function.

Elian, Yan, and Walter. FOXC1, the New Player in the Cancer Sandbox. Oncotarget. Impact Journals; 2018; 9: 8165–78.

Normally, FOXC1 is localized to the nucleus where it binds to DNA to activate or inactivate other genes. Missense and nonsense mutations within the *FOXC1* forkhead domain that alter FOXC1 translocation to the nucleus reduce its function. For example, Saleem and colleagues functionally characterized various mutations throughout the forkhead domain of FOXC1 (Figure 1.1). They found that FOXC1 with either the S82T, L86F, F112S, or I126M mutation displayed 80-100% nuclear localization compared to wild-type FOXC1, 61-80% for either P79L, P79T, or S131L, 41-60% for I91T, and 0-20% for either I91S or R127H [100,104,105]. These mutations had been shown to reduce FOXC1 activity due to impaired FOXC1 translocation to the nucleus. Aside from nuclear translocation, mutations within the FHD of FOXC1 can impair binding activity of FOXC1 to its target genes. Specifically, the R127H and S131L mutations in α-helix3 reduced FOXC1 binding to DNA by 90 % compared to wild-type FOXC1 binding efficiency [100,105,106]. Moreover, some mutations in the FHD were reported to cause other molecular defects to FOXC1. In particular, the I87M, R127H, and H128R mutations reduce protein stability, alter binding specificity, and extend protein half-life, respectively [100,105,106].

Missense mutations that alter FOXC1 translocation to the nucleus, binding to DNA, and protein stability consequently reduce FOXC1 function. In addition, recently, gain of function mutations have also been found to be rare causes of dominant glaucoma [103]. Together these mutations consequences are likely to be responsible for the developmental anomalies in ARS (Figure 1.2) and lymphedema-distichiasis patients.

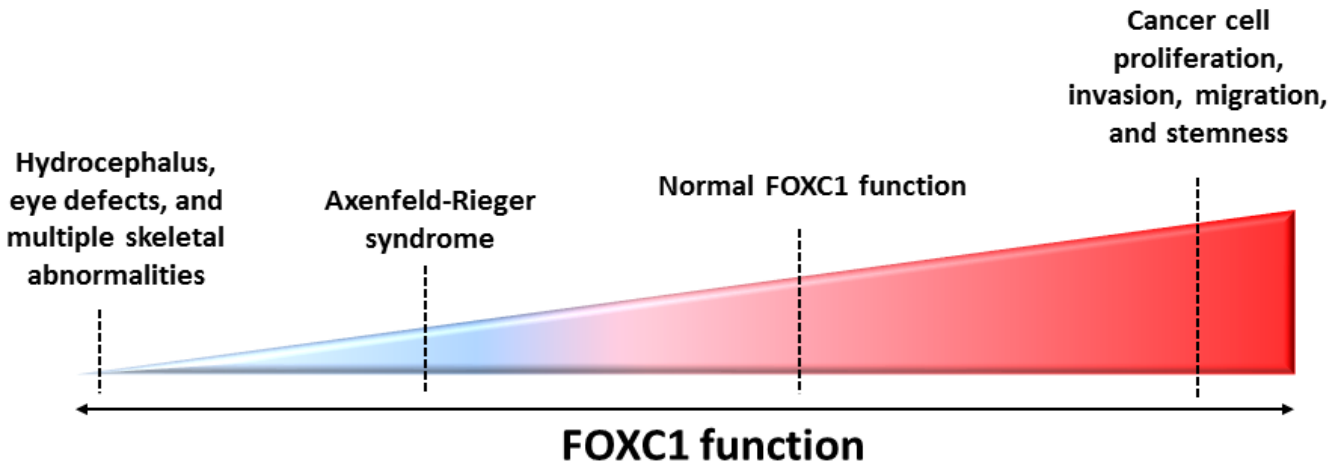

Figure 1. 2: FOXC1 function and activity in human diseases.

FOXC1 has been shown to play an integral role in development and adulthood, with both increased and decreased FOXC1 function linked to abnormal disease phenotypes. For example, due to profound defects in ocular development, hydrocephaly, cardiac organogenesis and skeletal anomalies, homozygous null *Foxc1* mice do not survive past birth [84]. Mutations in *FOXC1* are shown to hinder FOXC1-DNA binding activity, FOXC1 protein level and stability, as well as FOXC1 translocation to the nucleus – all of these defects resulting in Axenfeld-Rieger Syndrome (ARS). More recently, FOXC1 has been demonstrated to have a key role in cancer progression. Contrary to the reduced *FOXC1* function observed in ARS, recent studies are linking high *FOXC1* protein levels to the development of more aggressive phenotypes in cancers such as breast cancer, hepatocellular carcinoma, and endometrial cancer.

Elian, Yan, and Walter. FOXC1, the New Player in the Cancer Sandbox. Oncotarget. Impact Journals; 2018; 9: 8165–78.

1.2.2 *FOXQ1*: background

The Forkhead box Q1 (*FOXQ1*) gene, initially named "HFH-1", is another member that belongs to the FOX family of transcription factors, mainly known to play regulatory roles in embryonic development and cellular processes such as the cell cycle, differentiation, and proliferation [107,108]. Like other members of the family, the *FOXQ1* gene harbours an evolutionary conserved fork head or winged helix domain.

FOXQ1 is a single exon gene located in chromosome 6p25.3 and produces a 403-aa protein that contains a fork head motif (also known as DBD) and putative activation domains [108]. In 2001, the human *FOXQ1* gene was first isolated and characterized by Bieller et al [108]. By comparing nucleotides sequences, they found human *FOXQ1* gene to share 82% homology with the coding region of murine *FOXQ1* gene known as *Hfh-1L* [108].

In human tissues, *FOXQ1* is highly expressed in the stomach, trachea, bladder, and salivary gland [108]. The deletion of both *FOXQ1* alleles in mice produces variable phenotypes, however 50% of mice that lack both alleles of *FOXQ1* die before birth [109,110]. A DNA-binding core sequence 5'-TGTTT-3' was suggested for FOXQ1 [111], however another study suggested that 5'-GTTT-3' is the core binding sequence of FOXQ1 [112]. FOXQ1 was suggested to play a role in development, aging, cell cycle regulation and cancer [113 114,115 116117].

As a transcription factor, FOXQ1 protein functions to regulate smooth muscle and epithelial differentiation [114,115] and hair development/differentiation [118,119] and glucose metabolism [120]. Moreover, A study done by Martinez-Ceballos et al. identified *FOXQ1* as a

Homeobox A1 (*Hoxa-1*) target gene in embryonic stem cells [121]. *Hoxa-1* is a transcription factor known to regulate embryonic stem cell differentiation [122].

1.2.3 *FOXF2*: background

The forkhead box F2 (*FOXF2*) otherwise formally known as FREAC2 or FKHL6 is another member of the FOX transcription factor family that was suggested to play a critical role in embryonic development [123,124]. Similar to *FOXC1* and *FOXQ1*, *FOXF2* is also located at 6p25.3 and has DBD and transcriptional activation domains [123]. *FOXF2* gene has two exons that encodes a 444-aa protein that is important in regulating embryogenesis, extra cellular matrix (ECM) synthesis, and tissue homeostasis[125,126]. Recently, a role for FOXF2 in cochlear development in human and mice was also suggested [127]. *FOXF2* is specifically expressed in the mesenchyme of the respiratory, gastrointestinal (GI), and urinary tracts, and is known to act as a mesenchymal regulator [125,128]. Moreover, mice that lack both alleles of *FOXF2* die shortly after birth in which they showed abnormal tongue development and also developed cleft palate suggesting a role of *FOXF2* in palatogenesis [129]—the process where primary and secondary palatal shelves initiate, grow and fuse during embryogenesis [130].

1.3 The FOX family and cancer

In recent years, a number of FOX family members have been linked to tumorigenesis, carcinogenesis, and the survival of malignant cell growth [131]. Members of the FOXA, FOXC, FOXM, FOXO, and FOXP subclasses of FOX proteins, in particular, were found to have direct effects on the initiation, maintenance, progression, and drug resistance of cancers [131,132]. For example, the removal of *FOXM1*, which is known to play an integral role in G1-S and G2-M cell cycle progression and mitotic spindle integrity [70], results in the inability to commence mitosis in

mice [133]. Furthermore, the overexpression of *FOXM1* accelerates the proliferation and progression of prostate cancers in mouse models [134]. The widely studied FOXO proteins are key negative regulators of tumor suppression, as the simultaneous deletion of *FOXO1*, *FOXO3*, and *FOXO4* alleles in somatic cells invokes thymic lymphomas and systemic haemangiomas in mouse models [135]. As such, many FOX family members are desirable new avenues for further research as possible therapeutic targets in cancer treatment.

1.3.1 *FOXC1* and breast cancer

Currently, out of all the associations *FOXC1* has with different forms of cancer such as hepatocellular carcinomas, endometrial cancer, and lymphoma [136–143], *FOXC1's* relationship with BC, specifically basal, is the most elucidated. Recently, a central role in basal BC for FOXC1 has been clearly established [144–151]. As indicated in (Figure 1.3), FOXC1 is associated with basal through critical signaling pathways [144,149,150] and is directly linked to tumor metastasis and invasion [144,147,149,150].

As a transcription factor of the functionally versatile FOX family, FOXC1 has a role in many gene regulatory pathways [91,145,149,150,152,153]. Of these pathways, the most intriguing from the perspective of cancer biology are those involved in cell growth, proliferation, differentiation, invasion, and cancer stem cell growth (Figure 1.3).

FOXC1 was suggested to be exclusively over-expressed in basal BC when compared to other BC molecular subtypes in multiple, independent, gene expression microarray datasets [147]. Ray and his colleagues determined a significant positive correlation between high FOXC1 activity and *FOXC1* mRNA expression and basal BC [147]. Further expansion on these

relationships yielded that brain metastasis-free survival was significantly tied to high *FOXC1* mRNA levels. Moreover, the ectopic overexpression of *FOXC1* invoked more aggressive BC phenotypes, including epithelial-mesenchymal transition, increased cell proliferation, increased migration, and increased invasion [147]. This association of increased *FOXC1* levels with basal and poor prognosis appears to be the result of the aggressive cell phenotypes that result from over-expression of *FOXC1* [144,147,150]. Knockdown of *FOXC1* expression by siRNA in basal cell lines significantly decreased cell proliferation, migration, and invasion [147,149]. Furthermore, several studies have reported on the interaction between *FOXC1* and signaling pathways. For example, FOXC1 can regulate the basal BC cells by activating the Nf- kB signaling pathway (Figure 1.3) [144]. FOXC1 also mediates the function of EGFR [149], which has previously been suggested as a surrogate biomarker in basal BC [151]. While the activation of EGFR leads to the upregulation of FOXC1 expression through ERK- and Akt, FOXC1 is a necessary component in EGF-invoked cell proliferation, migration, and invasion (Figure 1.3) [149].

More recently, Han et al., 2015 found that FOXC1 interacts with Gli2 in different basal BC cell lines through direct binding, and that FOXC1 mediates the non-canonical Smoothened (SMO)-Independent Hedgehog (Hh) signaling that establishes the basal stem-like phenotype and anti-Hh sensitivity (Figure 1.3) [150]. These findings clearly suggest that FOXC1 is a specific biomarker for basal BC. However, the role of FOXC1 and its expression in other BC subtypes such as HER2 and luminal is still not fully studied. Moreover, there are no studies that have examined the copy number variation and mutation status of *FOXC1* in BC. For a better understating of FOXC1's role in BC, studies that examine its expression, copy number, and mutation status across BC subtypes are needed.

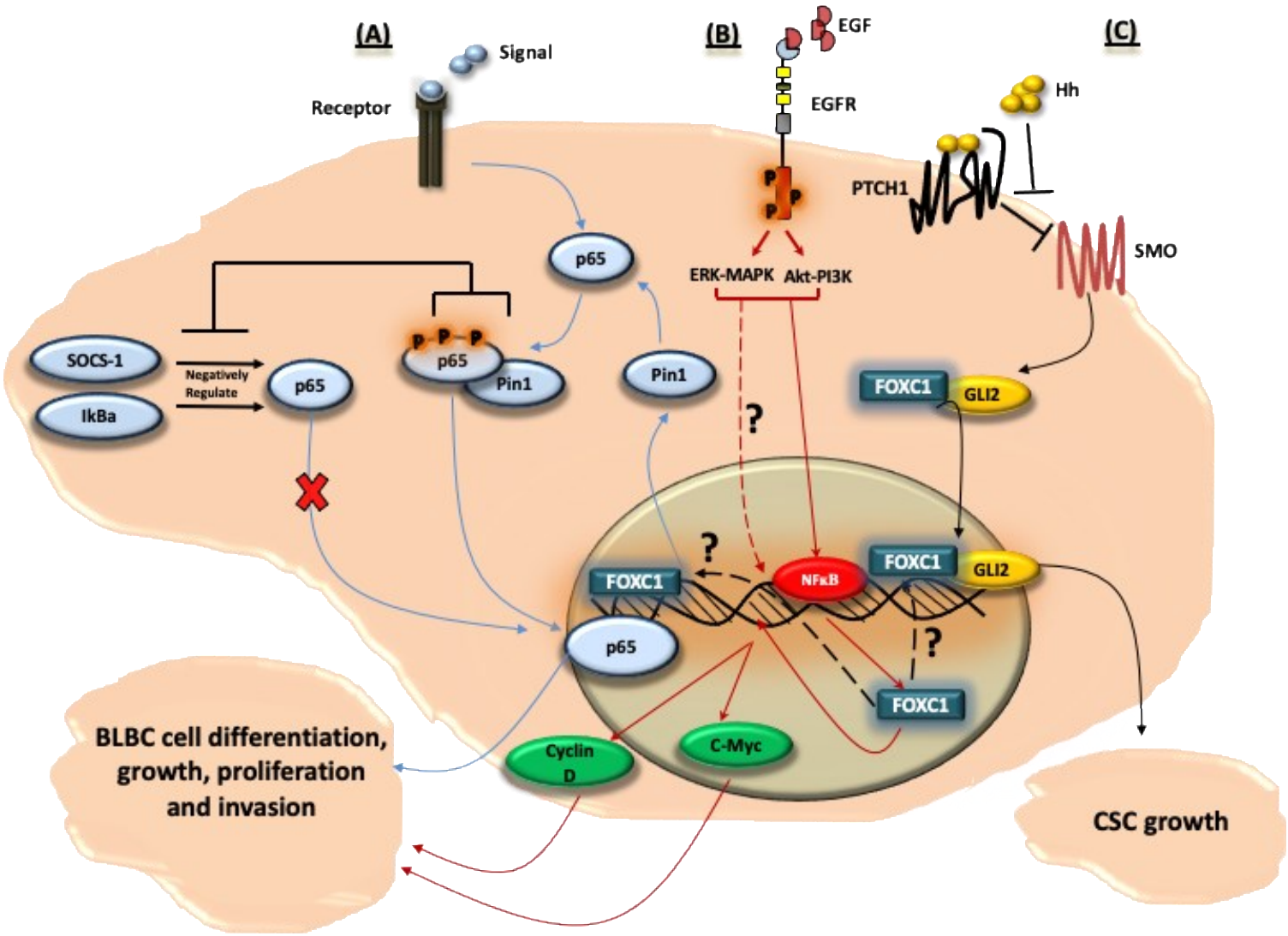
(A)
Signal
Receptor
(B)
EGF
EGFR
(C)
Hh
PTCH1
SMO
p65
ERK-MAPK
Akt-PI3K
SOCS-1
IkBa
Negatively Regulate
p65
p65
Pin1
Pin1
?
FOXC1
GLI2
?
FOXC1
NFκB
FOXC1
GLI2
p65
?
FOXC1
Cyclin D
C-Myc
BLBC cell differentiation, growth, proliferation and invasion
CSC growth

Figure 1. 3: FOXC1-Signaling Pathways in BLBC (basal BC).

(A) FOXC1 regulates the function of the NF- κB pathway in BLBC cell; NF- κB pathway can be activated as a cellular response to stimuli (i.e. TNFα, Interleukin 1) that plays a vital role in adaptive immune function and mediating inflammatory response. Once activated, the NF- κB subunit p65 get phosphorylated and translocated to the nucleus where it binds to DNA. The p65 activity is negatively regulated by the ubiquitin ligase cytokine signal inhibitor SOCS-1 [154] that sends p65 to the proteasome for degradation, and by IκBα that plays a role in the steady-state cytoplasmic localization of p65 dimers, thus preventing p65 nuclear localization and DNA binding [155]. The NF- κB pathway activity has been linked to tumorigenesis. In BLBC cell, FOXC1 regulates the expression of Pin1, a peptidyl-prolyl isomerase, that regulates the activity of p65 [154] and has been linked to tumor development [156]. Pin1 physically binds to p65 in the cytoplasm. This physical binding thus blocks p65 association with SOCS-1 and IκBα, as a result inhibits the p65 degradation. This then leads to p65 phosphorylation and p65 translocation to the nucleus. p65 binds to DNA and activates genes that enhances BLBC cell growth and proliferation. (B) EGFR, via MAPK-ERK and PI3K-Akt pathways, upregulates FOXC1 in BLBC; upon activation of EGFR by the ligand EGF, two of the classical pathways Mitogen-Activated Protein Kinase (MAPK) and Phosphatidylinositol-4,5-bisphosphate 3-kinase (PI3K) can be activated. The PI3K and MAPK pathways thus upregulate FOXC1 protein and mRNA expression through the ERK and Akt proteins. It has been shown that Akt and ERK phosphorylate and activate NF- κB that leads to its translocation to the nucleus [157]. NF- κB then would bind to FOXC1 promoter region and increases FOXC1 transcription activity. FOXC1 then would enhance the expression of the transcription factor c-Myc and Cyclin D, in which both play a key role in BLBC cell growth, proliferation, and invasion. (C) FOXC1 activates Smoothened-independent Hedgehog Signaling; the ligand Hh binds to the receptor Patched 1 (PTCH1) which allow SMO to activate the transcription factor Glioma-Associated Oncogene Family Zinc Finger 2 (GLI2). FOXC1 can activate GLI2 independently from SMO, where the FOXC1 N-terminal domain (aa 1-68) binds directly to a certain internal region of GLI2 (aa 898-1168), increasing GLI2-DNA transcription activity. FOXC1 activation of the non-canonical Hh signaling can result in cancer stem cell growth and expansion, consequently produces the BLBC stem-like phenotype.

Elian, Yan, and Walter. FOXC1, the New Player in the Cancer Sandbox. Oncotarget. Impact Journals; 2018; 9: 8165–78.

1.3.2 *FOXQ1* and breast cancer

Over the years, a growing body of studies have established *FOXQ1*'s functional role in BC development and progression. *FOXQ1* has been identified to act as an important driver of BC metastasis and invasion [68,158–161]. For example, Zhang et al. have shown that the ectopic expression of *FOXQ1* in both human and mouse mammary epithelial cells leads to cell migration and invasion *in vitro* [158]. When the metastatic abilities of overexpressing *FOXQ1* mouse mammary epithelial (EpRas) cells were investigated *in vivo*, in comparison to the control, more long-distance metastases were observed in the lung sections of mice injected with overexpressing *FOXQ1* EpRas cells [158]. Meaning that high expression of *FOXQ1* is associated with cancer metastasis. As well, the overexpression of *FOXQ1* has been previously demonstrated to increase the invasive and metastatic abilities of BC cell lines. [68,161].

According to Han et al.'s study, *FOXQ1* is a direct target of tumor-suppressive microRNA in breast cancer [159]. Specifically, microRNA miRNA-937 directly binds to *FOXQ1* gene and downregulates its expression to inhibit BC progression [159]. This was elucidated from *in-vitro* functional assays, to which the silencing of *FOXQ1* and ectopic expression of miRNA-937 both similarly supressed the proliferation, migration, and invasiveness of BC cell lines (MDA-MB-231 and MCF-7) [159] Notably, the overexpression of miRNA-937 was correlated with the under expression of *FOXQ1* in BC cell lines. When a bioinformatics analysis was performed, the putative binding site of miR-937 was located in the 3' untranslated region of *FOXQ1* gene, providing evidence for *FOXQ1* expression being regulated by tumor-suppressive microRNA in breast cancer [159].

Moreover, it has recently emerged that *FOXQ1* contributes to the metastasis-promoting function of RNA-binding protein HuR (also known as *ELAVL1*) in BC [162]. HuR is an abundantly expressed post-transcriptional regulator reported to regulate the stability and expression of mRNAs of genes involved in cell proliferation, cell survival, local angiogenesis, the evasion of cancer cells from immune recognition, and cancer cell invasion and metastasis [163]. *FOXQ1* was suggested as a direct target of HuR. Subsequently, the targeting of *FOXQ1* by HuR was correlated with BC metastasis when the loss of cell invasion from HuR CRISPR knock out MDA-MB-231 cells were partially restored from the overexpression of FOXQ1 [162]. Interestingly, *FOXQ1* expression has also been suggested to have an inverse association with the expression of CDH1 (E-cadherin), an epithelial marker whose downregulation is a critical feature of epithelial-to-mesenchymal transition (EMT) [162]. Loss/downregulation of E-cadherin expression is a critical EMT stage for tumor progression as it increases the invasion and metastatic abilities of tumor cells to spread from the primary tumor site to distant tissues and organs [164].

A number of studies have revealed *FOXQ1*'s function in promoting EMT [68,158,160]. This was marked by significant cell morphological changes of overexpressing *FOXQ1* human mammary epithelial cells (HMLE) cells from an epithelial to mesenchymal phenotype, paired with the downregulation of epithelial cell markers E-cadherin, β-catenin, and γ-catenin, and the upregulation of mesenchymal markers fibronectin, vimentin, and N-cadherin. Moreover, it has been suggested that FOXQ1 induces EMT by directly binding to 3 E-boxes in E-cadherin's promoter region and repressing E-cadherin expression.

Another mechanism for EMT-induction proposed is FOXQ1's involvement with TGF-β signaling, a growth factor known to exhibit both tumor suppressor and tumor promoter functions [158]. In the advanced stages of tumorigenesis, TGF- β signaling is known to act as a tumor

promoter, and functions to stimulate EMT and tumor proliferation and migration [165]. TGF- β has been found to regulate *FOXQ1* expression, as the level of *FOXQ1* mRNA expression increased in mouse mammary epithelial (EpRas) cells treated with TGF- β for 5 days [158].

FOXQ1 has been also linked to the induction and maintenance of cancer stem cell (CSC)-like properties. Overexpressing *FOXQ1* in BC cell lines and subsequent analyses of these cells through flow cytometry showed significant prevalence of cell populations with the $CD44^{high}/CD24^{low}$ configuration [166]. Moreover, silencing *FOXQ1* with siRNA significantly supressed the induction of the $CD44^{high}/CD24^{low}$ CSC population and reduced the levels of mRNA expressions of mesenchymal markers laminin V and fibronectin [167]. Moreover, *FOXQ1* overexpression altered the expression level of genes associated with CSC maintenance, such as *DACH1*, *ZEB1*, and *TWIST2* [168].

Emerging evidence shows that *FOXQ1* is overexpressed in TNBC and that *FOXQ1* overexpression contributes to the development of aggressive BC phenotypes [68,107,158,168]. Evaluating the gene expression profiles of all 49 members of the FOX family, the authors discovered that the expression of *FOXQ1* is higher in the highly invasive and mesenchymal-like BC MDA-MB-231 cells, compared to non-invasive epithelial BC MCF7 cells. Additionally, *FOXQ1* knockdown caused the TNBC BC cells to display more apical-basal polarity and structural organization, in which are opposite to the phenotypes (epithelial structure disorganization and loss of basal polarity) necessary for cancer development and progression.

Very recently, a reciprocal regulation between *FOXQ1* and *FOXF2* was proposed [161]. Through loss- and gain-of function experiments, the authors found that the deregulation of the negative feedback loop between *FOXQ1* and *FOXF2* enhanced the migration and invasion

abilities of basal BC cells, as well as the induction of EMT and acquisition of multidrug resistance Wnt/β-catenin-signaling pathway has been suggested to mediate this negative feedback loop, as *FOXQ1* and *FOXF2* have been previously linked to the activity of this pathway in other cancers [169,170].

Although, *FOXQ1* role and expression are studied in basal/TNBC subtypes, there are no reports that have investigated its role in other subtypes of BC. Moreover, the prognostic value in BC of *FOXQ1* expression is not fully studied and needs further investigations. Similar to *FOXC1*, there are no studies that have investigated *FOXQ1* copy numbers and their impact on *FOXQ1* expression in BC.

1.3.3 *FOXF2* and breast cancer

Like other members of the FOX family such as *FOXC1* and *FOXQ1, FOXF2* has been associated with numerous types of cancers including breast, colon, esophageal, lung, liver, and prostate cancers [171]. However, various studies have especially linked the dysregulation of *FOXF2* to BC progression and metastasis [17217367174175]. *FOXF2* has been reported to be overexpressed specifically in basal/TNBC breast cancer compared to the other BC subtypes [173].

Moreover, the deregulation of *FOXF2* has been attributed to facilitating invasion and metastasis of BC cells by possibly playing a role in EMT [172173]. In this complex process, epithelial cells dedifferentiate into migratory mesenchymal cells through a series of changes that include reorganization of the cytoskeleton, loss of apico-basal polarization of the cell, and a loss of cellular adhesions. These are the changes important in promoting tumorigenic progression; cancer cells acquire increased invasiveness and metastatic potential through EMT, and spread from the primary tumor site to distant tissues and organs [176,177].

Recent studies have revealed that FOXF2 play an important role in basal/TNBC development and progression through EMT [172173174]. However, the question of whether FOXF2 promotes or inhibits EMT in basal/TNBC is controversial and has been disputed, due to inconsistent findings between studies [178]. Wang et al. study found that the deficiency of FOXF2 activates EMT of basal/TNBC cells [172]. Their study revealed that knocking down *FOXF2* caused basal/TNBC cells to change from an epithelial to a mesenchymal morphology, which is typically observed in EMT. Additionally, they observed increased mRNA expression of mesenchymal markers in *FOXF2*-knockdown basal/TNBC cell lines. Their study also showed that the knockdown of *FOXF2* increased the metastatic ability of basal/TNBC cells *in vitro* and *in vivo.* Their findings concluded that FOXF2 functions as a suppressor of EMT in basal/TNBC [172]. In contrast, Lo et al. study found that knocking down *FOXF2* down-regulated the expression of EMT-programming genes (VIM, ZEB1, FOXC2) and significantly inhibited cell migration, and invasion [173]. Additionally, their microarray based gene expression analyses have revealed significant *FOXF2* co-expression with EMT related genes (NAI2/Slug, VIM, CDH11) and the metastasis-promoting gene GLI2. Overall, Lo et al. findings support that FOXF2 functions to act as a promoter of EMT and metastatic progression in basal/TNBC breast cancer [173].

It appears that studies that investigated *FOXF2* expression and role in basal/TNBC are conflicted and consistent. Moreover, the role and expression of *FOXF2* other BC subtypes are not well studied. While the correlation of *FOXF2* and *FOXQ1* expressions with each other has been investigated before [161], there are no reports that have examined the correlation of *FOXF2* and *FOXC1* expressions with each other in BC, or between *FOXC1* and *FOXQ1* with each other in BC. Due to their suggested roles in BC, and since they are within 300 kilobase from each other

on chromosome 6p25, studies that investigate *FOXC1, FOXQ1, and FOXF2* in BC simultaneously are needed.

1.4 Hypothesis and Aims

A role for each of the members of *FOXC1, FOXQ1, and FOXF2* (FOX) cluster has been reported or basal/TNBC. It appears that these three FOX genes each has a role in basal/TNBC cells invasion and metastasis through the activation of EMT and BC cell stemness. However, why these genes are overexpressed in basal/TNBC is not known—*FOXC1* is not necessary for mouse mammary ductal morphogenesis [179], while *FOXF2* and *FOXQ1* roles in mammary ductal morphogenesis are unknown. Moreover, the expression of these genes in other BC subtypes such as luminal and HER2 are not fully studied. Finally, conflicted data has been reported regarding the expression of the FOX cluster genes in basal/TNBC.

I hypothesized that similar to basal/TNBC subtypes, the FOX cluster has a role in other BC subtypes and that their expression is also altered. I also hypothesized that since the FOX cluster genes are located within 300 kilobase from each other, their copy number alterations are correlated among the 3 genes and that their expression is also correlated with each other in BC.

Therefore, in this thesis, the expression of *FOXQ1*, copy numbers, and prognostic values were investigated across BC subtypes in BC patient samples and cell lines (Chapter 2). I also investigated the expression of *FOXC1* across BC subtypes in BC patient samples and cell lines. Furthermore, the copy numbers of *FOXC1* and protein stability were also investigated (Chapter 3). Finally, I investigated the expression and copy numbers of the FOX cluster in expanded panel of BC patients' online dataset-TCGA-BRCA (Chapter 4).

Chapter 2

FOXQ1 is differentially expressed across breast cancer subtypes with low expression associated with poor overall survival

It is the molecule that has the glamour, not the scientists.

—Francis Crick

This chapter is submitted to *Breast Cancer: Targets and Therapy Journal* and currently under review as Elian, F.A; Are, U; Ghosh, S; Nuin, P; Footz, T; McMullen, TPW, Brindley, D.N; and Walter, M.A "*FOXQ1 is differentially expressed across breast cancer subtypes with low expression associated with poor overall survival*".

Note: I conceived and planned the experiments. I conducted the qPCR and RT-qPCR experiments, overall survival analysis, and statistical analysis, interpreted and analyzed the K-means clustering. I took the lead on writing the manuscript and made all the tables and figures. U.A, helped with running some of the qPCR experiments. S.G carried out Cox regression analysis using the SPSS program and helped with interpreting the data of univariate and multivariate analysis. P.N carried out the K-means clustering. T.F designed the PCR primers and helped with interpreting the qPCR data. T.P.W.M provided the breast patient and normal breast tissues. D.N.B provided the cDNA and DNA from these tissues and also helped with interpreting the data and reviewing the manuscript. M.A.W helped with interpreting the data and reviewed the manuscript. M.A W was the supervisory author and was involved with concept formation and manuscript composition.

2.1 Chapter Abstract

Forkhead box Q1 (*FOXQ1*) has been shown to contribute to the development and progression of cancers, including ovarian and breast cancer (BC). However, research exploring *FOXQ1* expression, copy number variation (CNV) and prognostic value across different BC subtypes is limited. Our purpose was to evaluate *FOXQ1* mRNA expression, CNV, and prognostic value across BC subtypes.

We determined *FOXQ1* expression and CNV in BC patient tumors using RT-qPCR and qPCR respectively. We also analyzed *FOXQ1* expression and CNV in BC cell lines in the CCLE database using K-means clustering. The prognostic value of *FOXQ1* expression in the TCGA-BRCA database was assessed using univariate and multivariate Cox's regression analysis as well as using the online tools OncoLnc, GEPIA, and UALCAN.

Our analyses reveal that *FOXQ1* mRNA is differentially expressed between different subtypes of BC and is significantly decreased in luminal BC and HER2 patients when compared to normal breast tissue samples. Furthermore, analysis of BC cell lines showed that *FOXQ1* mRNA expression was independent of CNV. Moreover, patients with low *FOXQ1* mRNA expression had significantly poorer overall survival compared to those with high *FOXQ1* mRNA expression. Finally, low *FOXQ1* expression had a critical impact on the prognostic values of BC patients and was an independent predictor of overall survival when it was adjusted for BC subtypes and to two other FOX genes, *FOXF2* and *FOXM1*.

Our study reveals for the first time that *FOXQ1* is differentially expressed across BC subtypes and that low expression of *FOXQ1* is indicative of poor prognosis in patients with BC.

2.2 Introduction

Breast cancer (BC) is well known as a highly heterogeneous disease comprised of distinct molecular subtypes [9,34]. Each BC subgroup differs from each other in terms of biological characteristics, risk factors, treatment responses, and patient survival outcomes [9,34]. This variability in BC behaviours and characteristics presents major clinical challenges and implications with regard to prognosis and BC management [180,181]. Therefore, much effort has been made to stratify heterogeneous BC subtypes, in order to increase our knowledge of the pathobiology of BC as well as to discover new treatments [182–185]. Typically, BC tumors have been divided into subtypes according to immunohistochemical (IHC) markers of estrogen receptor (ER), progesterone receptor (PR), and human epidermal growth factor receptor 2 (HER2), with the combination of differential gene expression [186]. Hence, there are three major subtypes of BC, and these subtypes are luminal (ER positive), triple negative breast cancer (TNBC), and HER2 BC [186]. Through the use of well-defined standard IHC markers to identify BC tumor subtype, clinicians can determine what therapeutic options are most effective. However, clinicians are now increasingly shifting towards looking at genetic differences to develop more personalized medicine approaches [187]. With this move to precision medicine for cancer treatment, there has been an increasing need for the identification of new potential biomarkers across the different subtypes of BC.

Forkhead box (FOX) family members are highly conserved transcription factors that have a major role in a plethora of biological functions. These family members have a common DNA-binding domain (DBD) composed of 100 monomeric amino acids that is known as the forkhead box or “winged helix” domain [69]. Many FOX transcription factors have been linked to tumorigenesis, carcinogenesis, and the survival of malignant cell growth [73,131]. Members of the

FOXA, FOXC, FOXM, FOXO, and FOXP subclasses of FOX proteins are found to have direct effects on the initiation, maintenance, progression, and drug resistance of cancers [73]. *FOXQ1* is another member of the FOX protein superfamily of transcription factors that regulate the expression of genes necessary for embryonic development, cell proliferation, differentiation, and apoptosis [107]. This single-exon gene is located on chromosomal region 6p25.3 and its encoded protein is characterized by a distinctive evolutionarily conserved DBD [188]. Functionally, *FOXQ1* plays a role in a diverse range of important biological processes such as angiogenesis, epithelial differentiation, smooth muscle differentiation, mucin secretion, and natural killer cell effector function activation [69,107,114,189]. Moreover, FOXQ1 has been associated with the aggressive phenotype of cancers such as breast, colorectal, ovarian, and pancreatic cancers, since altered *FOXQ1* expression has been previously detected in human tumor specimens [112,158,168,190–192].

Increasing numbers of studies have examined the role of *FOXQ1* in tumor progression and it has been suggested that supressing *FOXQ1* expression may decrease invasion, and migration in two TNBC cell lines [159,162]. *FOXQ1* has also been suggested as potentially being a driving force in the heterogeneity of BC [183]. Thus, additional knowledge of the role of *FOXQ1* in BC could have the potential to improve the diagnosis and treatment of BC tumors. In particular, the role and expression of *FOXQ1* in luminal and HER2 BC needs to be determined.

In this study, we investigated *FOXQ1* mRNA expression and copy number variation (CNV) across BC patient subtypes and cell lines. Furthermore, we assessed the prognostic significance of *FOXQ1* for BC patients. Our results revealed for the first time that *FOXQ1* mRNA is differentially expressed in TNBC, luminal, and HER2 BC patients and cell lines. We found that *FOXQ1* expression is significantly lower in luminal and HER2 positive tumors and that low expression of *FOXQ1* predicts poor overall survival in BC patients. We also found that *FOXQ1* has more copies

in tumors from TNBC patients compared to normal breast tissue samples. Interestingly, *FOXQ1* mRNA expression is independent of its CNV in BC cell lines. Our findings highlight that low expression of *FOXQ1* mRNA is associated with significantly poorer survival for different classes of BC.

2.3 Materials and Methods

2.3.1 Tissue samples

BC patients' samples were obtained with approval of the University of Alberta Health Research Ethics Board (Pro00018758) with written informed consent. The tumor samples from BC patients were collected at surgery and frozen in liquid nitrogen within 20 min of devitalization for further experiments. Normal human breast tissue was obtained from breast reduction surgery. BC subtypes have been defined using immunohistochemistry (IHC) markers; ER, Estrogen receptor; PR, Progesterone; and HER2, Human Epidermal Receptor (Table 2.1).

2.3.2 Overall survival analysis

Kaplan-Meier curves were generated using the online analysis tools OncoLnc (http://www.oncolnc.org) [193] and Gene Expression Profiling Interactive Analysis (GEPIA, http://gepia.cancer-pku.cn/) [194]. OncoLnc and GEPIA use patient survival data and level 3 RNA sequencing expression data of BC tumor samples from the Cancer Genome Atlas (TCGA) invasive breast carcinoma project (BRCA) database (https://portal.gdc.cancer.gov/projects/TCGA-BRCA). Patient samples (n=1006) and (n=1055) from TCGA-BRCA were used to generate the Kaplan-Meier (KM) curves in OncoLnc and GEPIA online tools respectively. Patient samples in OncoLnc and GEPIA were divided into high and low groups based on the median and the quartile of *FOXQ1* expression in BRCA database.

The median cut-off divided patients into two groups, high *FOXQ1* expression group are above the 50th percentile, and low *FOXQ1* expression group are below the 50th percentile. For the quartile cut-off analysis, patients were categorized into two groups, high *FOXQ1* expression group are above the third quartile (higher than 75th percentile), and low *FOXQ1* expression group are below the first quartile (lower than 25th percentile). More details on the mRNA expression data and their normalization can be found in (http://www.oncolnc.org) [193]. The log-rank test was used for the hypothesis evaluation. In regard to the censorship method, we used right censoring method in which the patients who did not experience the event (death) during the study duration and had no available further follow up data were censored. The mean age at diagnosis of the BC patients in TCGA-BRCA database is 58.4± 13.2 years and the median follow up time is 27.7 months where the median follow-up time for the overall survival time to event is 41.8 months and the median follow-up time for the overall survival time to censor is 25.0 months [195].

Kaplan-Meier survival curves were generated of *FOXQ1* expression in BC subtypes using UALCAN online tool (http://ualcan.path.uab.edu/index.html) [196]. TCGA-BRCA patient samples were divided into two groups, high and low *FOXQ1* expression groups. Patients with *FOXQ1* transcript per million (TPM) above the third quartile (higher than 75th percentile) were categorized as high *FOXQ1* expression group, while patients with *FOXQ1* TPM below the third quartile (lower than 75th percentile) were categorized as low/medium *FOXQ1* expression group. Subsequently, patients within each group were further stratified into TNBC, luminal, and HER2 BC subtypes. Log-rank test was used to generate the *p* value to test statistical significance of survival correlation between BC subtypes and *FOXQ*1 expression.

SPSS version 25 (IBM Corp. Released 2017. IBM SPSS Statistics for Windows, Version 25.0. Armonk, NY: IBM Corp.) was used to run the Cox's regression hazard model. p-value <0.05 was used for statistical significance. We used the TCGA-BRCA data (https://portal.gdc.cancer.gov/projects/TCGA-BRCA) to conduct the univariate overall survival of Cox's regression analysis for *FOXQ1* expression. 1006 TCGA-BRCA patients data with high and low *FOXQ1* expression with respect to the median and quartile cut-off were downloaded from OncoLnc (http://www.oncolnc.org) [193]. OncoLnc includes only patients who have all the necessary clinical data for each cancer such as age, sex, and grade as well as gene expression. More details on TCGA_BRCA patient data used for *FOXQ1* Cox regression analysis can be found in (Supplementary Table 2.1; Appendix). Uunadjusted and adjusted Cox's regression hazard model was used to determine the association of *FOXQ1*, *FOXF2*, and *FOXM1* with overall survival, more details can be found in (Supplementary table 2.2; Appendix).

Finally, we also used TCGA-BRCA data (https://portal.gdc.cancer.gov/projects/TCGA-BRCA) to conduct Cox's regression analysis of *FOXQ1* expression adjusted to BC subtypes. 1006 BC patient data with high and low FOXQ1 expression with respect to the median were downloaded. Then, we identified each BC patient subtype as TNBC, luminal, and HER2 as previously described in [197]. More details on the latter analysis can be found in (Supplementary table 2.3; Appendix).

2.3.3 RT-qPCR

RT-qPCR was conducted according to the detailed protocol as previously described [198]. Total RNA was extracted from BC patients' tumor samples and human breast normal tissue using the RNAqueous kit (Ambion, Streetsville, ON, Canada) according the manufacturer's

instruction. cDNA was synthesised from 1 µg RNA using Superscript II reverse transcriptase [199]. RT-qPCR assays were performed with a QuantiTect SYBR Green PCR kit (Applied Biosystems Foster City, CA, United States) and analyzed on a LightCycler 96 Real-Time PCR System (Roche Life Science, Penzberg, Germany), at least three times with each reaction in triplicate. mRNA levels were normalized to *TFRC* through the ΔΔCt method and changes in mRNA levels were described in fold change compared to the control samples. Primers for *FOXQ1 and TFRC* were designed using the Primer3 software (http://primer3.ut.ee/); *FOXQ1:* F: 5′-CGGAGATCAACGAGTACCTCA-3′, R: 5′-CAGTCGTTGAGCGAAAGGTT-3′; *TFRC* F: 5′-AACAACAGATTTCGGGAATGC-3′, R: 5′-CGTAGGGAGAGAGGAAGTGATA-3′. For statistical analyses, we first compared *FOXQ1* expression in all four groups; normal breast tissue, TNBC, luminal, and HER2, using one-way ANOVA. Then, one-tailed unpaired Student's t-tests and Bonferroni correction were used for multiple comparisons to assess statistical differences.

2.3.4 Copy number variation

FOXQ1 gene copy number in BC patients was quantified through Real-time qPCR, as previously described [200] to determine if the altered dosage of *FOXQ1* gene affected expression levels in BC tumors. Genomic DNA was extracted from human breast normal tissue and from TNBC, luminal, and HER2 BC patient tumor samples using the EZ-10 Spin Column Genomic DNA Minipreps Kit (Bio Basic Inc., Markham, ON, Canada) according to the manufacturer's instructions. Real-time qPCR was then conducted on the genomic DNA of all samples to measure *FOXQ1* dosage. PCR reactions for normal breast tissue, TNBC, luminal, and HER2 BC patient tumor samples (Table 1) were analyzed in triplicate. Normal breast tissue samples were used as a control to normalize *FOXQ1* dosage. We used the ΔΔCT method as our quantification

strategy, with *GJA5* selected as an internal control gene. Average CT values of triplicates were calculated for each sample. ΔCT for each sample was then calculated by subtracting the average CT number of *FOXQ1* from that of *GJA5. FOXQ1:* F: 5′-CGGAGATCAACGAGTACCTCA-3′, R: 5′-CAGTCGTTGAGCGAAAGGTT-3′; *GJA5* F: 5′-AGTTCCCAGCCAATAGACAGC-3′, R: 5′-AAGGCTGAGTAGAGGGAGGAG-3′. We used a two-tailed unpaired Student's t-tests for comparisons of each BC subtype with normal breast tissues to assess statistical differences.

2.3.5 K-means Clustering

K means clustering analysis was performed to investigate and compare *FOXQ1* CNV and its mRNA expression. In order to conduct K-means clustering, we first identified the ideal number of clusters. Our initial approach was to compare the biological ideal number of clusters, which is 3 clusters, based on cell line annotation and classification; TNBC, luminal, and HER2(supervised K-means clustering). For the unsupervised ideal number of clusters, we used the elbow method [201] to determine the ideal statistical number of clusters for K-means with the scikit-learn's method of the MinMaxScaler module used with a sum of squares distance and fit between 1 and 15 possible clusters [201]. We then devised Python scripts to identify the cluster sets by applying standard supervised K-means clustering using both number of clusters (supervised and unsupervised) and *FOXQ1* mRNA expression and copy number variation (CNV) as seeds as described [202]. The mRNA and CNV data of *FOXQ1* were obtained from Cancer Cell Line Encyclopedia online (CCLE) database [203]. K-means clustering performed 1000 iterations using the Euclidean distance and using seeds between 1 and 3 clusters and 1 and 4 clusters**.** Thirty-six BC cell lines were used for the analysis and the cell lines' names and types are listed in (Table 2). Cell lines were grouped as TNBC, luminal, and HER2 BC cell lines as described [204,205]. CCLE CNV data of BC cell lines were obtained using genome-wide human Affymetrix SNP

Array 6.0 [203]. The mRNA data on the CCLE website were produced by Affymetrix Human Genome U133 Plus 2.0 Array followed by Robust Multiarray Averaging (RMA) method of microarray normalization and were uploaded as log(2) gene expression signal [203]. The log(2) *FOXQ1* expression data in each for each of the 36 BC cell lines from CCLE were obtained and then scaled to values between 0 and 1 using the equation;

$$zi = \frac{\{xi - \min(x)\}}{\{\max(x) - \min(x)\}}$$

where $x = (x_1, \ldots\ldots, x_n)$ producing z_i as the scaled value for *FOXQ1* mRNA expression in each of the 36 BC cell lines. CNV raw data created by Affymetrix (CEL file) were normalized to copy number estimates using a GenePattern pipeline [203]. The median of the scaled *FOXQ1* expression values was used as a cut-off, where cell lines with values above the median were considered as relative high expression of *FOXQ1* cell lines, while cell lines with *FOXQ1* expression below the median were considered as relative low expression of *FOXQ1* cell lines.

2.4 Results

2.4.1 *FOXQ1* mRNA expression varies between BC patient subtypes

To evaluate *FOXQ1* expression across the different subtypes of BC, RT-qPCR assays were conducted on TNBC, luminal, and HER2 BC patient samples and on normal breast tissue samples (Table 2.1). One-way ANOVA analysis showed that *FOXQ1* mRNA expression varied between BC patients' subtypes, $F(30,52) = 3.8$, $p=0.026$. Furthermore, we found that *FOXQ1* expression was significantly lower in luminal BC when it was compared to normal breast tissue (Figure 2.1). The mRNA level of *FOXQ1* was lower in HER2 BC compared to normal breast tissue ($p=0.02$) (Figure 2.1). Interestingly, *FOXQ1* mRNA levels were lower in luminal and HER2 BC compared to TNBC ($p=0.017$ and $p=0.029$, respectively) (Figure 2.1). These results

indicate that *FOXQ1* mRNA levels were differentially expressed among BC patients and that *FOXQ1* could potentially have different roles based on the BC subtype.

2.4.2 Low expression of *FOXQ1* is associated with poorer overall survival in breast cancer patients

Kaplan-Meier curves were performed on the TCGA-BRCA dataset using the OncoLnc [193], GEPIA [194], and UALCAN [196] online tools to investigate whether *FOXQ1* mRNA expression is prognostic for life expectancy. BC patients were divided into two risk groups with high and low *FOXQ1* expression levels with respect to the quartile and the median used as the cut off value. BC patients with low *FOXQ1* mRNA expression had significantly shorter overall survival time compared to those with high *FOXQ1* mRNA expression (Figure 2.2, p=0.00473 and p=0.0479) and (Supplementary Figure 2.1, p=0.0087 and p=0.042).

In addition, a univariate Cox's regression analysis was conducted for overall survival on the TCGA-BRCA patient data with respect to the expression of *FOXQ1.* The results of the univariate Cox's regression analysis in Table 2.2 indicate that BC patients who have high *FOXQ1* expression (>= 50th percentile) were significantly associated with 29% lower risk of death as compared to BC patients who have low *FOXQ1* expression (p=0.048). Further analysis was conducted, comparing the highest quartile and the lowest quartile of *FOXQ1* expression. The results indicate that *FOXQ1* high expression (>= 75th percentile) were significantly associated with about 51% lower risk of BC patient's death as compared to the low *FOXQ1* expression (below 25th percentile) with a p-value of 0.006 (Table 2.2).

Furthermore, using UALCAN online tool, we examined the correlation of *FOXQ1* expression and BC subtypes by dividing patients into two groups; high and low/medium *FOXQ1*

expression cohorts (Figure 2.3). Kaplan-Meier curves indicate that patients with low/medium *FOXQ1*expression had significantly shorter overall survival time than those with high expression of *FOXQ1* (Figure 2.3, p=0.011). Subsequently, using the TCGA_BRCA data, we conducted Cox's regression analysis for *FOXQ1* expression stratified by BC subtype as well as *FOXQ1* expression adjusted for BC subtype (Table 2.3). For HER2 subtype, high *FOXQ1* expression was significantly associated with about 73% lower risk of death as compared to low *FOXQ1* expression (Table 2.3, p=0.024). The same trend was observed for luminal and TNBC subtypes indicating that high *FOXQ1* expression showed a reduced risk of death by 19% and 32% respectively. However, these associations were not statistically significant (Table 2.3).

When adjusting for BC subtype, high *FOXQ1* expression showed a 32% lower risk of death (Table 2.3, p=0.036). The unadjusted analysis from Table 2.2 and adjusted analysis from Table 2.3 indicate that *FOXQ1* is an independent predictor of overall survival in BC patients. Together, these results demonstrate that low expression of *FOXQ1* predicts poor overall survival in patients with BC.

2.4.3 Relation of *FOXQ1* copy numbers in BC subtypes to mRNA levels

It has recently been suggested that CNV correlates with gene expression in BC cell lines and patient tissue [206]. To determine *FOXQ1* CNV in the subtypes of BC patients, qPCR assays were conducted on TNBC, luminal, and HER2 BC patient DNA samples (Table 2.1) and on normal breast tissue DNA samples. The copies of *FOXQ1* were significantly higher in TNBC patients compared to normal breast tissue p=0.03 (Figure 2.4). Although *FOXQ1* appeared to have a trend for more copies in HER2 BC patients, this did not reach statistical significance (Figure 2.4, p=0.08).

Unsupervised and supervised K-means clustering analyses (Table 2.4 and Figure 2.5), were performed to identify clusters of BC cell lines as well as to investigate any associations between *FOXQ1* mRNA expression and copy number. Unsupervised K-means clustering identified 4 clusters among BC cell lines for *FOXQ1* mRNA compared to their copy number (Table 2.4 and Figure 2.5A).

We found some cell lines clusters that have similar copy number (orange cluster vs red cluster, Figure 2.5A) but different mRNA expression (Figure 2.5A). We also found similar results after we conducted supervised K-means clustering, where some cell line clusters had high and/or low *FOXQ1* mRNA expression but similar ranges of variation in relative copy number (Figure 2.5B). For the supervised K-means clustering, we choose 3 as the number of clusters to correspond to the 3 different subtypes of BC; TNBC, luminal, and HER2 (see K-means clustering in method's section). Interestingly, unsupervised and supervised K-means clustering analyses suggests that the steady state level of *FOXQ1* mRNA expression appears to be independent of gene copy number in BC cell lines. Thus, *FOXQ1* mRNA expression levels are not correlated with *FOXQ1* CNV in BC subtypes. However, consistent with our results where *FOXQ1* expression was lower in luminal and HER2 BC patient tumors (Figure 2.1), we found that *FOXQ1* expression was low in all luminal and HER2 cell lines (Figure 2.5 A and B). Similar to our observation of increased expression of *FOXQ1* in TNBC patient tumors compared to luminal and HER2 (Figure 2.1), we found that *FOXQ1* has elevated expression in some TNBC cell lines as compared to luminal and HER2 BC cell lines (Figure 2.5 A and B). Interestingly we found numerous TNBC cell lines to cluster with other luminal and/or HER2 cell lines and have low *FOXQ1* expression. This difference of *FOXQ1* mRNA expression within the TNBC

classification might be attributed to the distinct subgroups (basal A and basal B) that exists within TNBC cell lines [205].

2.4.4 *FOXQ1* expression is an independent predictor of overall survival in BC patients when adjusted to *FOXF2* and *FOXM1* expressions

We also investigated the overall survival of *FOXQ1* adjusted for *FOXF2* and *FOXM1* expressions. We evaluated *FOXF2 and FOXM1* genes due to their critical role in BC initiation, proliferation, migration, and invasion [172,207,208].

TCGA-BRCA patient were divided into low and high expressing *FOXF2, FOXM1,* and *FOXQ1* groups using the medians as cut-off values, followed by a univariate and multivariate Cox's regression overall survival analysis. *FOXM1* high expression was associated with 1.5 times higher risk of BC patient death as compared to *FOXM1* low expression values (p=0.013; Table 2.5). Adjusted Cox's regression model with *FOXQ1*, *FOXM1* and *FOXF2* expressions indicated that *FOXQ1* and *FOXM1* were significantly associated with overall survival (Table 2.5; p=0.05 and p=0.011 respectively). The results indicate that *FOXQ1* and *FOXM1* were independent predictors of overall survival in BC patients. Having high expression of *FOXQ1* was associated with 32% lower risk for overall survival when adjusted for *FOXF2* and *FOXM1* (p=0.050; Table 2.5). Higher expression of *FOXM1* was associated with 1.6 times higher risk of death when adjusted for *FOXQ1* and *FOXF2* expressions, this association was statistically significant (p=0.011; Table 2.5). Our results show that *FOXQ1* expression correlates inversely with overall survival in BC patients, and that *FOXQ1* expression is an independent predictor of BC overall survival when adjusted to the expression of *FOXF2* and *FOXM1* in BC patients.

2.5 Discussion

FOXQ1 plays an important role in BC tumor re-initiation [209], stemness and chemoresistance [160], epithelial-mesenchymal transition (EMT), invasion, and metastasis [158]. Increasing evidence supports the hypothesis that *FOXQ1* can be used as a biomarker for cancer prognosis and diagnosis. Indeed, high levels of *FOXQ1* expression can predict poor overall survival in hepatocellular carcinoma, gastric, colorectal, pancreatic, and non-small cell lung cancers [191,210–212]. However, the prognostic value of *FOXQ1* in BC is not well known. In particular, the expression of *FOXQ1* in other subtypes of BC, specifically luminal and HER2 BC, is not well studied. Thus, a molecular understanding of the mechanism of altered expression of *FOXQ1* warrants further investigation. In this study, we report for the first time that *FOXQ1* mRNA is differentially expressed across different types of BC patients and cell lines. In contrast to the earlier studies of a limited number of BC cell lines [68,158,159,168], our studies of an expanded panel of thirty-six BC cell lines show that *FOXQ1* has low expression in many TNBC cell lines and in all luminal, HER2 BC patients and cell lines. We also show that this low expression of *FOXQ1* is associated with poor prognosis in BC subtypes and that *FOXQ1* expression is an independent predictor of overall survival in BC patients.

In order to understand *FOXQ1* expression across BC subtypes, we investigated *FOXQ1* expression in BC tumor tissues (Table 2.1). *FOXQ1* expression across BC subtypes was analyzed in TNBC, luminal, and HER2 tumor tissues (Figure 2.1). Two previous papers [168,183] studied *FOXQ1* expression data of BC tumors from the TCGA-BRCA database and found an overexpression of *FOXQ1* in TNBC compared with luminal BC [168] and with HER2 BC [183]. Similarly, it was suggested that *FOXQ1* is overexpressed in BC tumor tissue compared with normal adjacent tissue [159], however it was not clear what BC subtypes were used for this analysis. Consistent with these studies, we found that *FOXQ1* is overexpressed in TNBC tumor

tissues when compared with luminal BC tumors tissues (p=0.017) (Figure 2.1). As well, *FOXQ1* mRNA levels are higher TNBC compared with HER2 BC (p=0.029) (Figure 2.1). Importantly, we reveal for the first time that *FOXQ1* is expressed at lower levels in luminal BC (p=0.008) and in HER2 BC (p=0.029) when each subtype was compared with unmatched normal breast tissue (Figure 2.1). Together these results reveal that significant differences of *FOXQ1* expression occurs in BC subtypes, with *FOXQ1* high expression in TNBC and *FOXQ1* low expression in luminal and HER2.

We further investigated the impact of *FOXQ1* expression on BC patients' overall survival. Using the OncoLnc [193], and GEPIA [194] online tools, overall survival curves identified two risk groups with high and low *FOXQ1* mRNA expression levels (Figure 2.2 and Supplementary Figure 2.1). We found that BC patients with low *FOXQ1* expression had significantly shorter overall survival than BC patients with high *FOXQ1* expression (Figure 2.2, and Supplementary Figure 2.1). Univariate Cox regression analysis for *FOXQ1* expression, where BC patients who have high *FOXQ1* expression were significantly associated with lower risk of death as compared to BC patients who have low *FOXQ1* expression (Table 2.2). Kaplan-Meier curves also showed that TNBC, luminal, and HER2 BC patients with low *FOXQ1* expression have significantly poor overall survival compared to TNBC, luminal, and HER2 BC patients with high *FOXQ1* expression (Figure 2.3). When adjusting for BC subtype, high *FOXQ1* expression showed significantly lower risk of death (Table 2.3) indicating that *FOXQ1* is an independent predictor of overall survival in BC patients. This suggests that low expression of *FOXQ1* in BC patients is significantly correlated with poor prognosis.

Importantly, we found *FOXQ1* has lower expression in HER2 BC patient tissues (Figure 2.1) and that HER2 BC patients with low *FOXQ1* expression had significantly shorter overall

survival compared to HER2 BC patients with high *FOXQ1* expression (Table 2.3, Figure 2.3). This is an interesting result giving that HER2 BC, in comparison to other BC subtypes, is normally known to respond well to numerous targeted therapies that favourably impact patients overall survival [213]. On other hand, TNBC lacks targeted therapy and is considered to have a clinically aggressive phenotype compared to other BC subtypes [214]. Although TNBC patient tissue had higher *FOXQ1* mRNA expression compared to luminal and HER2 (Figure 2.1), those TNBC patients with low expression of *FOXQ1* appeared to have poorer overall survival compared to those with high *FOXQ1* expression (Table 2.3 and Figure 2.3). This suggests that, clinically and case-by-case, BC patients in the TNBC cohort who have low *FOXQ1* expression could have poorer clinical outcomes. Further studies that focus on stratifying the TNBC subtype further using gene signatures and cancer stages could reveal better understating of *FOXQ1* expression in TNBC.

Intriguingly, while it has been reported that high *FOXQ1* expression predicts poor overall survival in hepatocellular carcinoma, gastric, colorectal, pancreatic, and non-small cell lung cancers [191,210–212], we found that high expression of *FOXQ1* favourably impacts overall survival in BC (Table 2.2 and 2.3), suggesting a dual role of FOXQ1 across human cancers. Dual role of other FOX genes in cancers has been reported before. High expression of FOXF2 enhanced EMT, migration and invasion of lung cancer cells [215] in contrast to in BC [172] where low expression of FOXF2 induced EMT and was associated with poor overall survival. In addition, high expression of FOXA1 was associated with poor overall survival in prostate cancer [216], while high expression of FOXA1 favourably impacted BC prognosis [217,218]. Our data also contrasts the findings of Qiao *et al.* who suggested that overall survival was significantly poorer in BC patients with high *FOXQ1* expression [68]. Qiao Y *et al* [68] used the van de Vijver cohort to

generate Kaplan-Meier plots of their overall survival analysis but the number of patients within that cohort who had high and low levels of *FOXQ1* were not indicated [68]. Moreover, Van de Vijver *et al.* [47] included microarray data of 295 BC tumors, some of which were lymph-node/ER-positive and some of which were lymph-node/ER-negative. OncoLnc [193], GEPIA [194], and UALCAN [196], on the other hand, use up-to-date RNA sequencing data of the TCGA-BRCA database. In our study, we applied OncoLnc and GEPIA (respectively) to obtain Kaplan-Meier curves on BC tumors (n=1006 and n=1055), with high (n=503 and n=524), and low (n=503 and n=531) levels of *FOXQ1* expression (Figure 2.2 and Supplementary Figure 2.1). The TCGA-BRCA data was also used to perform the adjusted and unadjusted Cox regression (see methods and Supplementary tables 2.1, 2.2, and 2.3). The differences in numbers of BC tumor tissue samples, BC subtypes, and assays used could explain why we obtained different clinical outcomes of *FOXQ1* expression compared to Qiao *et al.* [68].

We also measured *FOXQ1* CNV in BC samples (Table 2.1) to determine if altered copy number could underlie the differences in mRNA expression levels in TNBC, luminal, and HER2 tumors (Figure 2.4). Although there are numerous studies that have identified an association between copy number alteration and altered gene expression, how CNVs alter gene expression in BC is not well understood [206,219,220]. We found that *FOXQ1* copy number is significantly amplified in TNBC compared with normal breast tissue (Figure 2.4). In contrast, no significant changes in *FOXQ1* copy number were found in luminal and HER2 BC compared to control samples (Figure 2.4). To explore the possible ramifications of these findings further, we performed K-means clustering to investigate and compare *FOXQ1* CNV and its mRNA expression. Our K-means clustering analyses took two approaches; unsupervised (Figure 2.5A) and supervised (Figure 2.5B). For the supervised K-means clustering we determined the

biological ideal number of clusters based on BC cell lines classification, TNBC, luminal, and HER2. For the unsupervised K-means we used the elbow method [201] to identify the ideal statistical number of clusters. For both methods, the numbers of clusters and the *FOXQ1* expression and CNV were used as seeds. We found that some clusters have high copy number with low mRNA expression, while other clusters have high mRNA expression with no CNV (Figure 2.5 A and B). Intriguingly, this suggests that *FOXQ1* expression is independent from *FOXQ1* copy number in BC cell lines.

Several interesting patterns, however, emerge from our K-means clustering analysis. Our supervised analysis investigated if *FOXQ1* expression and CNV correlate within a specific BC subtype more than others. Intriguingly, while it was expected that TNBC cell lines would cluster together based on *FOXQ1* expression and CNV (Figure 2.5B), we found some TNBC cell lines also cluster with HER2 and with HER2 and luminal BC cell lines (red and black clusters, Figure 2.5B). Furthermore, our unsupervised analysis identified 4 clusters (Table 2.4 and Figure 2.5A), an extra cluster compared to the supervised method (Table 2.4 and Figure 2.5B). This suggests that *FOXQ1* expression and CNV could potentially identify a sub-population of BC within TNBC, HER2, and luminal BC cell lines. This supports the findings of Yang *et al*., that suggest that *FOXQ1* expression could drive the heterogeneity of BC subtypes [183]. Consistent with our findings of low levels of *FOXQ1* expression in luminal and HER2 BC patient tumors (Figure 2.1), we found *FOXQ1* mRNA to be low in all luminal and HER2 BC cell lines (Figure 2.5 A and B). Interestingly, while other studies reported *FOXQ1* overexpression in TNBC cell lines [158,159], our results show that *FOXQ1* has low expression in many TNBC cell lines (Figure 2.5 A and B), but *FOXQ1* is overexpressed in some TNBC cell lines (Figure 2.5 A and B). The difference in *FOXQ1* overexpression across TNBC cell lines is striking. It has been previously

suggested that, on the basis of molecular features and morphology and invasion potential, TNBC might be further subdivided into basal A and basal B types [205]. Basal A has a less differentiated and more epithelial like morphology, whereas basal B has a more mesenchymal-like morphology which is more invasive [205]. Basal B has additionally been characterized as exhibiting more stem-cell like characteristics ('stemness'), as cells of this subgroup have been found to possess the $CD44^{+}/CD24^{-/low}$ phenotype [205] normally associated with mammary cancer stem cells (CSCs) [221,222]. Moreover, a role of *FOXQ1* in stemness [160,167], and EMT [158] has been reported. This could provide an explanation of why *FOXQ1* is overexpressed in certain TNBC cell lines rather than other *FOXQ1* TNBC cell lines (Figure 2.5 A and B). Further classification of TNBC cell lines into basal A and B could provide a clearer picture of the difference consequences of *FOXQ1* expression between these two TNBC subtypes.

The underlying mechanisms altering *FOXQ1* expression in BC subtypes, therefore, remain elusive. This is not surprising given the lack of knowledge on the regulatory machinery controlling the expression of transcription factors such as *FOXQ1* in either development or in cancer. While it has been suggested that FOXQ1 regulates more than 30 genes that play roles in BC stemness and EMT [158,160,167], there is no specific transcriptional signature that has been proposed for FOXQ1 in development or cancer. The actual number of genes regulated by FOXQ1 is unknown, but this could number in the thousands based upon similar analyses of the direct targets of the related FOXC1 transcription factor [147,223]. Thus while a "transcriptional addiction in cancer" has been proposed [224], it remains a challenge to precisely identify in cancer how and when transcription factors are themselves regulated and activated, and then to understand the target genes regulated by the activity of these transcription factors in normal and disease states [225]. Epigenetics, gene function redundancy, tissue specificity, predicting enhancer-

promoter regions, and the role of coactivators are a few among many other challenges to studying transcription factors in cancer [225]. Future studies that reveal the regulation of FOXQ1 expression, together with the identification of transcriptional targets of FOXQ1, might reveal how FOXQ1 expression is controlled and the consequences of its dysregulation of this regulation in BC.

Our research, and that from other groups [68,191,210–212], clearly demonstrate that *FOXQ1* is another member of the FOX class of transcription factors with a key emerging role in cancer [73,131]. Previous studies have investigated the role of *FOXQ1* expression, regulation, and function in relation to the expression of *FOXF2* and *FOXM1* genes, function and roles in BC and other diseases. Our findings that *FOXQ1* is an independent predictor of overall survival in BC when adjusted to *FOXM1* and *FOXF2* expressions highlights the prognostic significance of *FOXQ1* expression in BC patients (Table 2.5). *FOXQ1* and *FOXM1* expressions levels have previously been shown to have prognostic value in colorectal cancer patients [211]. Moreover, a recent study suggested that *FOXQ1* expression is negatively regulated by FOXF2 in BC cells [161]. *FOXQ1*, *FOXF2*, and *FOXC1* are all located within a 300 kb region of chromosome 6, physically linking in close proximity three FOX transcription factors with substantial roles in BC [67,131,147,172], development [69,88,114,126,127,189], and in several diseases [86,226–231]. Our results suggest that *FOXQ1* expression in BC patients could have significant prognostic value for survival from BC.

2.6 Tables and Figures

Table 2.1: BC patient demographic

Patient	Age	ER_IHC	PR_IHC	HER2_IHC	Tumor Size(cm)
TNBC					
MT2673	43	Neg	Neg	Neg	2.1
MT2112	67	Neg	Neg	Neg	3.5
MT3624	57	Neg	Neg	Neg	1.1
MT3473	52	Neg	Neg	Neg	1.1
MT3800	60	Neg	Neg	Neg	4.1
MT2881	47	Neg	Neg	Neg	7
Luminal BC					
MT3504	55	Pos	Neg	Neg	2.3
MT3874	56	Pos	Neg	Neg	3.5
MT2348	65	Pos	Neg	Neg	1.9
MT3387	51	Pos	Neg	Neg	1.9
MT3193	53	Pos	Neg	Neg	3.2
MT3756	31	Pos	Neg	Neg	1.8
HER2 BC					
MT3866	59	Neg	Neg	Pos	1.4
MT2151	53	Neg	Neg	Pos	0.8
MT2160	59	Neg	Neg	Pos	0.9
GT363	80	Neg	Neg	Pos	5
MT2520	50	Neg	Neg	Pos	NULL
MT2730	74	Neg	Neg	Pos	1.5

ER, Estrogen receptor; PR, Progesterone; HER2, Human Epidermal Receptor 2; TNBC, Triple Negative Breast Cancer; IHC Immunohistochemistry; Neg, negative; Pos, positive; cm, Centimeters; Null, size of the tissue samples is small (1-3 mm^3).

Table 2.2: Hazard ratios from the univariate Cox's regression analysis for the TCGA-BRCA database

	Median cut-off				Quartile cut-off			
Variable	**β estimate**	**HR**	**95% CI**	***p*-value**	**β estimate**	**HR**	**95% CI**	***P*-value**
FOXQ1 expression	-0.344	0.709	(0.504-0.999)	**0.049**	-0.712	0.49	(0.296-0.812)	**0.006**

HR, hazard ratio; CI, confidence intervals

Table 2.3: Cox's regression analysis for *FOXQ1* expression based on the median cut-off stratified by BC subtypes and adjusted for BC subtypes the TCGA-BRCA database

Variables	β estimate	HR	95% CI	*P*-value
HER2 subtype (n=77)				
FOXQ1 (Low Expression)				
High Expression	-1.31	0.27	(0.09-0.84)	**0.024**
Luminal Subtype (n=707)				
FOXQ1 (Low Expression)				
High Expression	-0.21	0.81	(0.53-1.25)	0.341
TNBC Subtype (n=175)				
FOXQ1 (Low Expression)				
High Expression	-0.39	0.68	(0.28-1.62)	0.383
Adjusted for BC subtypes				
FOXQ1 (Low Expression)				
High Expression	-0.39	0.68	(0.47-0.98)	**0.036**

HR, hazard ratio; CI, confidence intervals
The reference category is presented in the parentheses

Table 2.4: Cox's regression analysis for *FOXQ1, FOXF2, and FOXM1* expression based on the median cut-off

		Univariate			Multivariate			
Variables	**β estimate**	**HR**	**95% CI**	***P*-value**	**Coefficient**	**HR**	**95% CI**	***P*-value**
***FOXQ1* expression**	-0.344	0.709	(0.504-0.999)	**0.049**	-0.389	0.678	(0.459-1.001)	**0.05**
***FOXF2* expression**	-0.221	0.802	(0.570-1.127)	0.204	0.062	1.064	(0.716-1.583)	0.758
***FOXM1* expression**	0.437	1.548	(1.096-2.188)	**0.013**	0.465	1.591	(1.112-2.278)	**0.011**

HR, hazard ratio; CI, confidence intervals

Table 2.5: BC cell line names and types that were used for standard K-means clustering.

Cell line types were sorted as described in [204,205]. The mRNA expression and CNV of *FOXQ1* in 36 BC cell lines were obtained from CCLE online database [203]. Cell lines with no defined subtypes were not considered for consistency. Four clusters were used for unsupervised K-means clustering, while 3 clusters were used for supervised clustering. For supervised and unsupervised clustering, cell lines within each column that have the same color are grouped together. These clusters and data are plotted in Figure 2.4.

BC cell line subtype	*FOXQ1* Relative Expression	*FOXQ1* Relative CNV	Unsupervised K-Means clusters	Supervised K-Means clusters
TNBC				
CAL-148	0.046847	-0.1		
DU4475	0.071856	-0.1		
CAL-51	0.047552	0		
HCC1395	0.093519	0.41		
BT-549	0.036633	0.04		
HCC1806	1	0.49		
MDA-MB-231	0.71962	0.41		
CAL-120	0.550194	0.29		
CAL-851	0.63156	0.28		
HDQ-P1	0.797992	0.20		
HCC38	0.344311	0.51		
Hs 578T	0.373547	0.24		
HCC1187	0.327932	0.3		
HCC1143	0.686685	-0.15		
HCC70	0.713632	-0.09		
HCC1937	0.775097	-0.48		
MDA-MB-436	0.551427	-0.33		
MDA-MB-157	0.037161	0.02		
HCC2157	0.058471	-0.82		
BT-20	0.057591	-0.67		
Luminal				
CAMA-1	0.031349	0.08		
MDA-MB-415	0.070447	-0.16		
EFM-192A	0.034519	0.18		
BT-483	0.068158	-0.05		
KPL-1	0.095104	-0.15		
MCF-7	0.024833	0		
MDA-MB-175	0.435717	-0.24		
MDA-MB-134	0	-0.01		
HCC1428	0.054773	-0.48		
HER2				
MDA-MB-453	0.023248	-0.07		
HCC1569	0.016555	-0.08		
HCC2218	0.027474	-0.03		
HCC202	0.012328	0.14		
HCC1954	0.441881	0.09		
JIMT-1	0.447693	-0.22		
AU565	0.054773	-0.54		

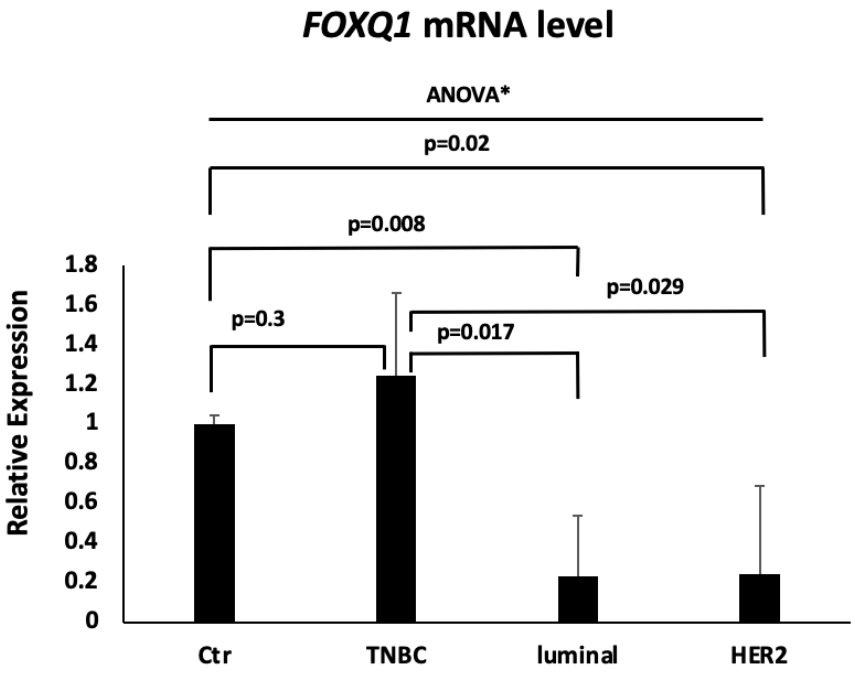

Figure 2.1: *FOXQ1* is under-expressed in luminal and HER2 breast cancer patient samples.

one-way ANOVA analysis was used to asses statistical difference in all groups *F(30,52) = 3.8, p=0.026 followed by unpaired t-tests and Bonferroni corrections were used for multiple comparisons. α= 0.05, adjusted α= 0.0125. qPCR experiments were conducted to measure *FOXQ1* mRNA levels in normal breast tissue (Ctr, n=6) acquired from reduction mammoplasties, TNBC (n=6), luminal (n=6), and HER2 (n=6) BC patient samples. The ΔΔCT method was used for analysis and *TFRC* was used as a reference gene. Error bars represent standard error of the mean (SEM).

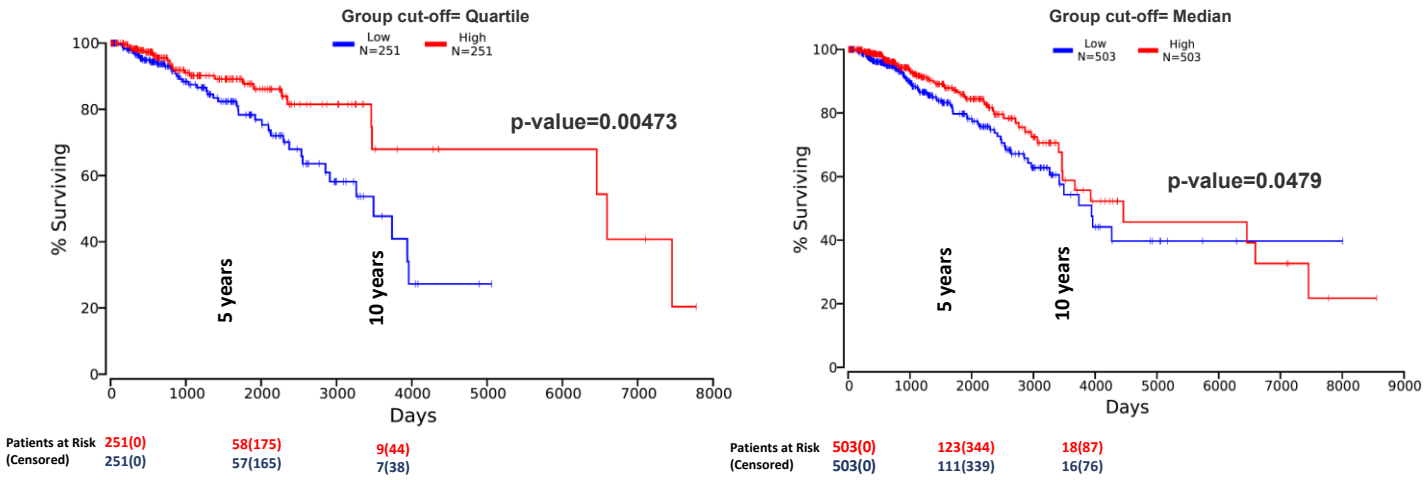

Figure 2.2: Low *FOXQ1* expression predicts poor overall survival in BC patient.

Kaplan-Meier (KM) analysis identified low and high-risk BC patient groups based upon significant differences of *FOXQ1* mRNA in BRCA-TCGA database. BC patients were divided with high and low *FOXQ1* expression levels with respect to the quartile and the median used as the cut off value. This graph was generated using the bioinformatics online tool OncoLnc (http://www.oncolnc.org) [193] and then modified to include the number of patients at risk at 0, 5 and 10 years.

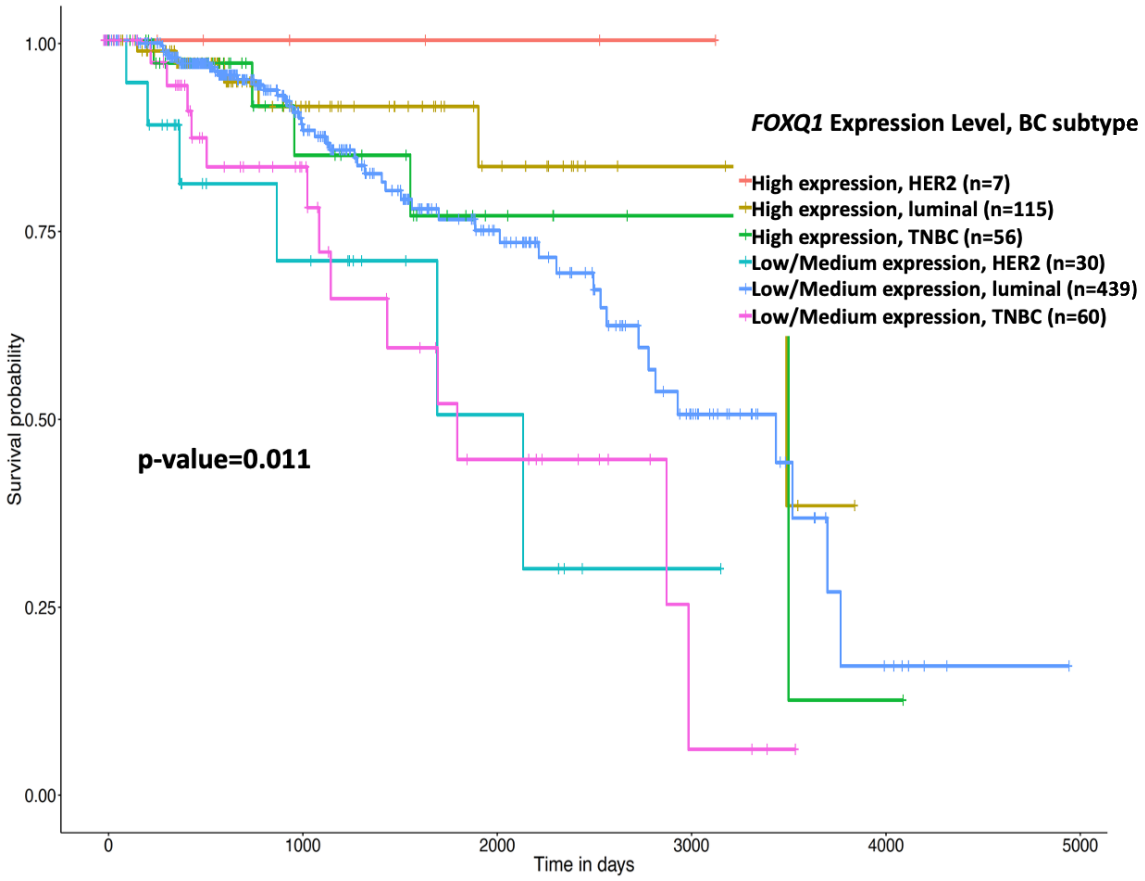

Figure 2.3: Low *FOXQ1* expression predicts poor overall survival in BC patient subtypes.

Kaplan-Meier (KM) analysis of the effect of high and low/medium *FOXQ1*expression on overall survival of HER2, luminal, and TNBC patients shows a cumulative significance of p=0.011. This graph was generated and modified using the bioinformatics online tool UALCAN online tool (http://ualcan.path.uab.edu/index.html) [196].

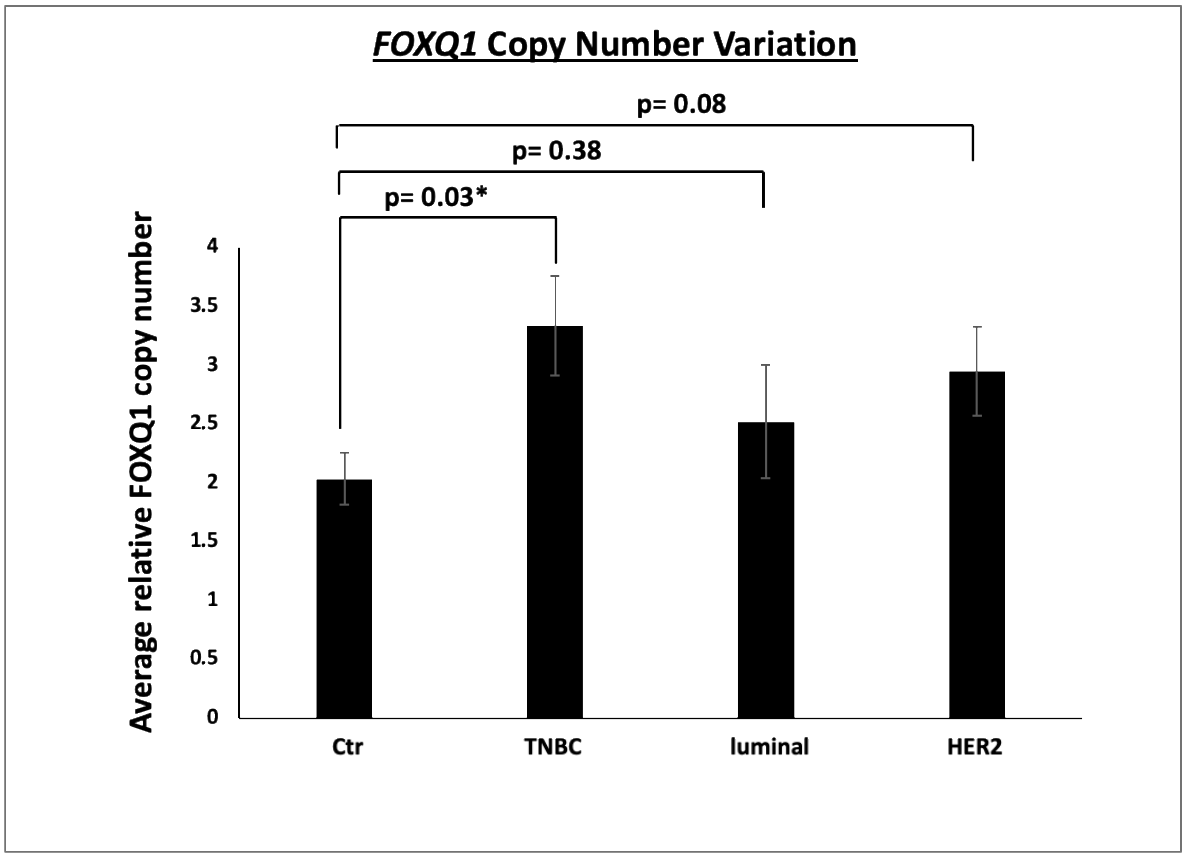

Figure 2.4: *FOXQ1* has more copies in TNBC compared to control samples.

qPCR experiments were conducted on genomic DNA to measure *FOXQ1* dosage in TNBC, luminal, and HER2 BC patient tumor tissues. The ΔCT method was used for analysis and *GJA5* was used as a reference gene. *FOXQ1* dosage was calculated using $2^{[\Delta CT\ sample - \Delta CT\ control]}$. Control (Ctr) samples are normal breast tissue samples acquired from reduction mammoplasties. Ctr (n=6), TNBC (n=6), luminal (n=6), and HER2 (n=6). Two-tailed unpaired Student's t-tests were used for comparisons of each BC subtype with normal breast tissue to assess statistical differences. Error bars represent standard error of the mean (SEM). * < 0.05.

A

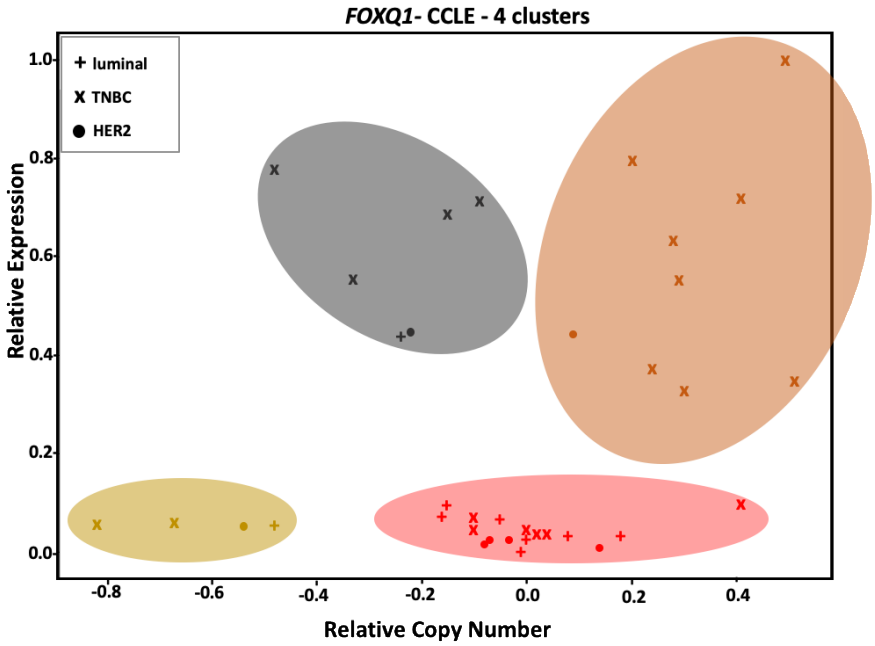
FOXQ1- CCLE - 4 clusters
luminal
TNBC
HER2
Relative Expression
Relative Copy Number
1.0
0.8
0.6
0.4
0.2
0.0
-0.8
-0.6
-0.4
-0.2
0.0
0.2
0.4

B

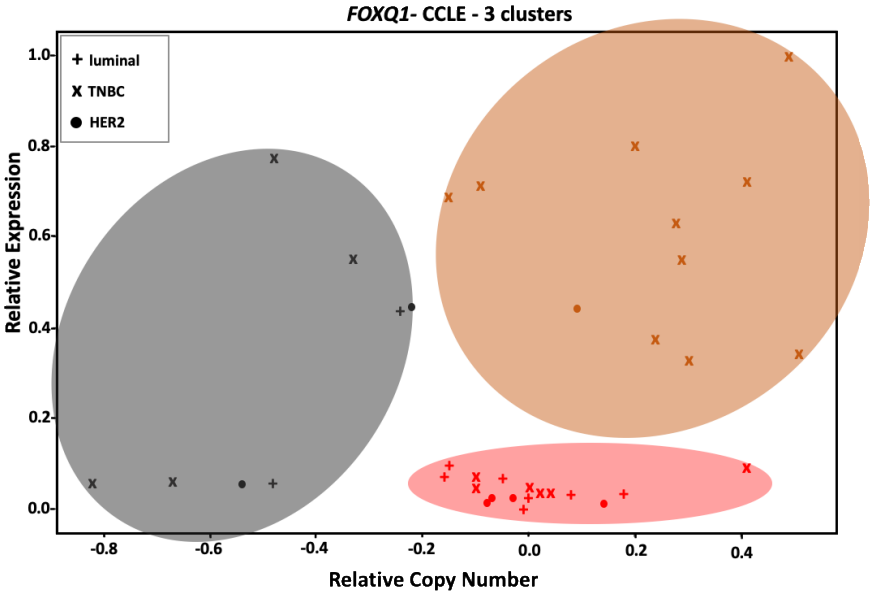
FOXQ1- CCLE - 3 clusters
luminal
TNBC
HER2
Relative Expression
Relative Copy Number
1.0
0.8
0.6
0.4
0.2
0.0
-0.8
-0.6
-0.4
-0.2
0.0
0.2
0.4

Figure 2.5: *FOXQ1* expression is independent of its CNV in BC cell lines

(A) unsupervised and **(B)** supervised K-means clustering analyses show different clusters of BC cell lines that have similar ranges of CNV but different FOXQ1 expression (the orange cluster vs the red cluster). Unsupervised clustering identified an extra cluster in BC cell lines compared to supervised clustering (the olive cluster, lower left).

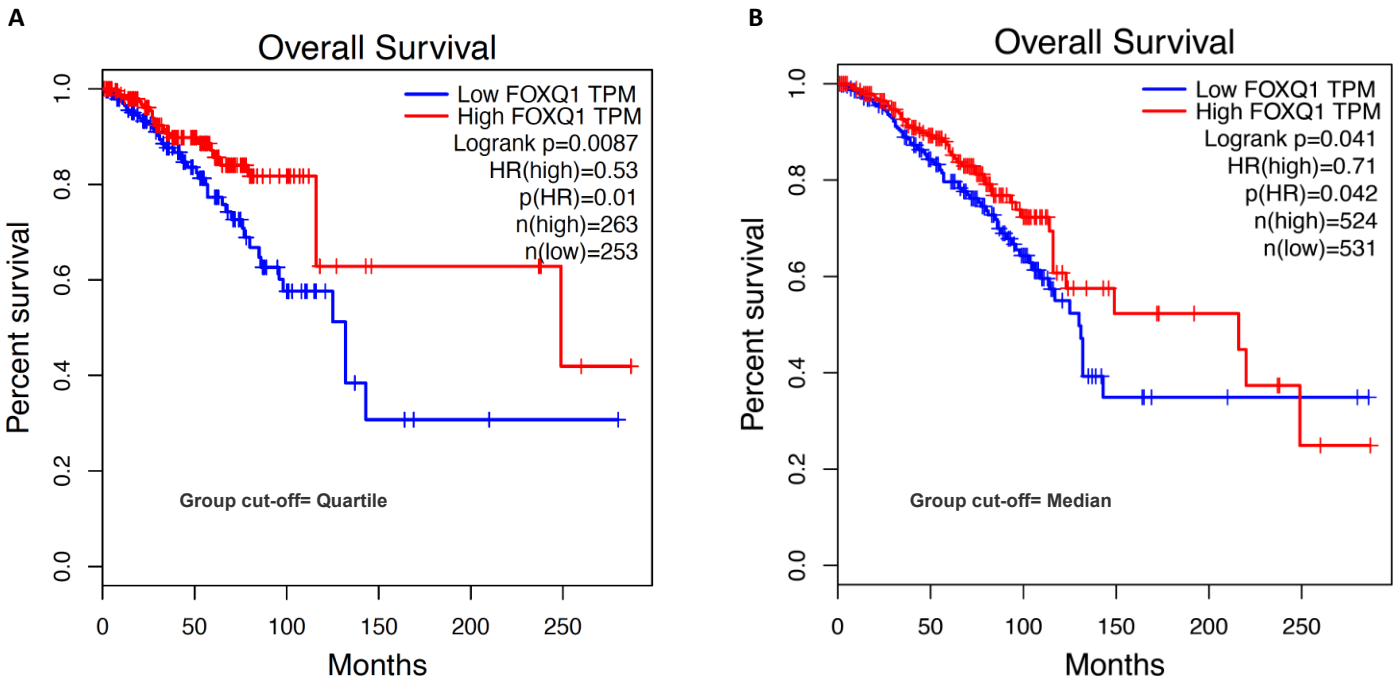

Supplementary Figure 2.1: Overall survival curve identified low and high-risk groups based upon significant differences of *FOXQ1* mRNA in BRCA-TCGA database.

(A) The quartile and (B) the median were used for group cut-off. The hazard ratio (HR) was calculated based on Cox PH Model. TPM, transcript per million. This graph was generated using the bioinformatics online tool GEPIA, (http://gepia.cancer-pku.cn/) [194]. Patients with higher *FOXQ1* are highlighted in red, whereas patients with lower *FOXQ1* expression are highlighted in blue.

Chapter 3

FOXC1 is Over-expressed and is More Stable in Basal/Triple Negative Breast Cancer

A little doubt is better than total credulity.

—Al-Ma'arri (973 - 1057)

Note: Dr. Paulo Nuin conducted the K-means clustering. Tim Footz generated the FOXC-HeLa stable cell line.

All other experiments were carried out by Fahed Elian.

3.1 Chapter Abstract

Rapidly accumulating evidence implicates forkhead box C1 (*FOXC1*) in basal/Triple Negative Breast Cancer (TNBC). Recently additional studies have demonstrated that *FOXC1* is also a major player in hepatocellular carcinoma (HCC), endometrial cancer, Hodgkin's lymphoma (HL), non-Hodgkin's lymphoma (NHL), and others.

The *FOXC1* gene encodes a transcription factor that is crucial to mesodermal, neural crest, and ocular development. Loss of function mutations in *FOXC1* have been shown to cause autosomal dominantly inherited Axenfeld-Rieger's Syndrome (ARS), a developmental disorder associated in eye anomalies and glaucoma. Interestingly, while *FOXC1* missense mutations that cause ARS reduce FOXC1 activity, increased FOXC1 function now appears to be often linked to more aggressive cancer phenotypes in TNBC, HCC, HL, and NHL.

I have investigated the mechanism(s) by which FOXC1 activity is increased in BC. Samples were obtained from TNBC tumors, luminal BC tumors or from breast tissue from normal patients. Using quantitative PCR, I found that *FOXC1* was significantly over-expressed in TNBC patients as compared to luminal. In contrast, *FOXC1* mRNA was significantly less abundant in luminal samples as compared to either control or TNBC samples. My studies of *FOXC1* copy-number variation (CNV) in TNBC cell lines reveals that cell lines that have higher levels of FOXC1 protein (HS-578T, BT-549) have extra copies of *FOXC1*. This contrasts with a cell line with lower expression of FOXC1 protein, MDA-MB-231, which has a deletion of *FOXC1* in this TNBC cell line. However, in a larger panel of 42 BC cell lines, K-means clustering analysis of available online data of *FOXC1* mRNA and CNV revealed that *FOXC1* expression is independent of CNV.

Sequence-analysis of *FOXC1* in TNBC cell lines did not detected pathogenic mutations in any cell line. A silent-mutation (C18T; pR6R) was however found in the cell line HS-578T. I also found that, acting indirectly, the epidermal growth factor receptor (EGFR) significantly upregulated FOXC1 protein levels under EGF time-course stimulation. My findings suggest that increased FOXC1 function in TNBC results from over-expression of *FOXC1* in tumors of TNBC patients that appears to be the result of changes to FOXC1 stability and EGFR signaling pathways. Interestingly, FOXC1 protein half-life was significantly longer in the TNBC cell lines (HS-578T and BT-549) compared to FOXC1 protein's half-life in HeLa cells that stably express FOXC1.

3.2 Introduction

In recent years, it has become apparent that this diversity is the result of distinct genetic, epigenetic, and transcriptomic alterations [232]. Advances in genetics have resulted in the identification of genes mutated in some BC patients, and have allowed improvements in diagnostics, family counseling, and treatments [233]. BC is classified into three molecular subtypes, luminal BC (70 % of all cases), human epidermal growth factor receptor (HER2)- positive BC (20 % of all cases), and triple negative-breast cancer (10 % of all cases) based on the levels of estrogen receptor (ER), progesterone receptor (PR), and HER2 [234]. Clinically, triple negative breast cancer (TNBC), is considered one of the most aggressive forms of BC subtypes that is highly metastatic with a poor prognosis, short overall survival time, and high relapse incidences [61]. Pathologically, TNBC, lacks a known biomarker/s, is a heterogenous disease, and has intrinsic subtypes in which all of that makes its treatment a medical challenge [235,236]. For these reasons, BC researchers and clinicians have tirelessly dedicated their effort to stratify TNBC in order to have a better understating of its pathology hence improving treatment options. As a result, several studies have identified an intrinsic subtypes within TNBC based on differential gene/s expression such as basal/TNBC intrinsic subtype (approximately more than 80% of TNBC are of the basal-like BC) [65,182]. Furthermore, basal/TNBC BC cell lines can be further subdivided into basal A and B based on differences in molecular features (basal markers such as cytokeratins 5/6/14, P-cadherin), morphology and invasion potential [205,237].

Emerging data suggest that forkhead box FOXC1 is a sensitive biomarker for TNBC [131,147,148]. FOXC1 is a member of the forkhead box gene family, a group of highly evolutionarily conserved genes with critical roles in embryonic and adult development. FOXC1 is transcriptional factor that binds to DNA and directly regulates the expression of other genes.

FOXC1 is an essential component of proper mesodermal [86], neural crest [85] and ocular development [86–88]. In recent years, a number of FOX family members have been linked to tumorigenesis, carcinogenesis, and the survival of malignant cell growth[73,238].

FOXC1 is critically involved in basal/TNBC and is associated with TNBC's aggressive, invasive tumor phenotype through FOXC1's regulation of key cancer signaling pathways [131,146] and these pathways' contributions to tumor metastasis and invasion. FOXC1 is suggested as consistently and exclusively over-expressed in basal/TNBC when compared to other BC molecular subtypes in multiple independent gene expression microarray datasets [147]. Further expansion on these relationships yielded that brain metastasis-free survival was significantly tied to high FOXC1 mRNA levels. Moreover, the ectopic overexpression of FOXC1 invoked more aggressive BC phenotypes, including epithelial-mesenchymal transition, increased cell proliferation, increased migration, and increased invasion [147]. This association of increased FOXC1 levels with basal/TNBC and poor prognosis appears to be the result of the aggressive cell phenotypes that result from over-expression of FOXC1. More recently, FOXC1 has been shown to mediate non-canonical Smoothened (SMO)-Independent Hedgehog (Hh) signaling [150]. FOXC1 activation of non-canonical Hh signaling can result in cancer stem cell growth and expansion, consequently producing the basal/TNBC stem-like phenotype and anti-Hh sensitivity [150]. These findings suggest that FOXC1 appears to be specific biomarker for basal/TNBC that contributes to the aggressive phenotype of basal/TNBC. However, the expression of *FOXC1* among other BC subtypes and how and why FOXC1 is overexpressed in basal/TNBC are not well studied. In addition, *FOXC1* DNA mutation status, protein stability, and copy-number variation (CNV) in TNBC are also unknown.

In this chapter, I show that *FOXC1* was significantly over-expressed in TNBC patients as compared to luminal BC. In contrast, *FOXC1* mRNA was significantly less expressed in luminal samples as compared to either control or TNBC samples, indicating that FOXC1 expression varies between BC subtypes. *FOXC1* expression was not correlated with its mutation/s and/or CNV. FOXC1 levels were regulated by the epidermal growth factor receptor (EGFR) in a ligand dependent fashion. I reveal for the first time that FOXC1 protein half-life was significantly longer in the basal/TNBC cell lines (HS-578T and BT-549) compared to FOXC1 protein's half-life in HeLa cells. My results suggest that increased FOXC1 function in TNBC results from over-expression of FOXC1 in tumors of TNBC patients that appears to be the result of changes to FOXC1 stability and levels. While further understanding of the mechanism(s) underlying FOXC1's activation and stability in cancer is needed, this knowledge could explain why FOXC1 levels are abundant in TNBC hence contributing to the aggressive phenotype of TNBC cells.

3.3 Materials and Methods

3.3.1 Tissue samples

BC patients' samples were obtained with approval of the University of Alberta Health Research Ethics Board (Pro00018758) with written informed consent. The tumor samples from BC patients were collected at surgery and frozen in liquid nitrogen within 20 min of devitalization for further experiments. Normal human breast tissue was obtained from breast reduction surgery. BC subtypes have been defined using immunohistochemistry (IHC) markers; ER, Estrogen receptor; PR, Progesterone; and HER2, Human Epidermal Receptor (Table 3.1).

3.3.2 Cell lines and cell culture

The following TNBC cell lines were used in this thesis chapter: HS-578T (human breast cancer cells, ATCC HTB-1126); MDA-MB-231 (human breast cancer cells, ATCC HTB-26); BT-549 (human breast cancer cells, ATCC HTB-122); and FOXC1 stably-transfected non-BC HeLa cells (HTRTOA3) that was generated with the T-REx™ system (Invitrogen, Carlsbad, CA) to create Tetracycline-inducible Xpress-FOXC1 protein expression according to the manufacturer's instructions.

All cells were grown at 37°C in Dulbecco's modified Eagle's medium (DMEM) containing 10% FBS, penicillin, and streptomycin (100 μg/ml), and were maintained in a 5% CO_2 atmosphere. For the HTRTOA3 cells, antibiotics blasticidine (Cedarlame, Burlington, ON) and zeocin (Life Technologies Inc.) of final concentrations of (2 μg/ml) and (40 μg/ml) respectively were added to the medium to select cells that express FOXC1 as well as Tetracycline (Invitrogen, Carlsbad, CA) of final concentration of (1 μg/ml) was used in the medium to activate FOXC1 expression as required.

3.3.3 RT-qPCR

RT-qPCR was conducted according to the detailed protocol as previously described [198]. Total RNA was extracted from BC patients' tumor samples (Table 3.1) and human breast normal tissue using the RNAqueous kit (Ambion, Streetsville, ON, Canada) according the manufacturer's instruction. cDNA was synthesised from 1 μg RNA using Superscript II reverse transcriptase [199]. qPCR assays were performed with a QuantiTect SYBR Green PCR kit (Applied Biosystems Foster City, CA) and analyzed on a LightCycler 96 Real-Time PCR System (Roche Life Science, Penzberg, Germany), at least three times with each reaction in triplicate. mRNA

levels were normalized to *HPRT1* (reference gene) through the ΔΔCt method and changes in mRNA levels were described in fold change compared to the control samples. Primers for *FOXC1 and HPRT1* were designed using the Primer3 software (http://primer3.ut.ee/); *FOXC1:* F: 5′-TAGCTGTCAAATGGCCTTCCC-3′, R: 5′-CTTTTCCTGCTTTGGGGTTCG-3′; *HPRT1* F: 5′-GCCAGACTTTGTTGGATTTGA-3′, R: 5′-GGCTTTGTATTTTGCTTTTCCAG-3′. For statistical analyses, we first compared *FOXC1* expression in all three groups; normal breast tissue, TNBC, and luminal, using one-way ANOVA. Then, one-tailed unpaired Student's t-tests and Bonferroni correction were used for multiple comparisons to assess statistical differences.

3.3.4 *FOXC1* copy number variation

FOXC1 gene copy number in BC cell lines was quantified through Real-time qPCR, as previously described [200]. Briefly, genomic DNA was extracted from human BC lines; BT-549, HS-578T, and MDA-MB-231 using the EZ-10 Spin Column Genomic DNA Minipreps Kit (Bio Basic Inc., Markham, ON, Canada) according to the manufacturer's instructions. Real-time qPCR was then conducted on the genomic DNA of all samples to measure *FOXC1* dosage. PCR reactions were analyzed in triplicate. DNA from patient samples with a known WT copies of *FOXC1* [86,227,229,239] were used to normalize *FOXC1* dosage. DNA from patient samples with a known *FOXC1* duplication were used as a control [226]. The ΔΔCT method was used as quantification strategy, with *GJA5* selected as an internal control gene. Average CT values of triplicates were calculated for each sample. ΔCT for each sample was then calculated by subtracting the average CT number of *FOXC1* from that of *GJA5. FOXC1* dosage was calculated using $2^{-[\Delta CT\ BC\ sample - \Delta CT\ WT\ sample]}$. *FOXC1:* F: 5′-TAGCTGTCAAATGGCCTTCCC-3′, R: 5′-

CTTTTCCTGCTTTGGGGTTCG-3′; *GJA5* F: 5′-AGTTCCCAGCCAATAGACAGC-3′, R: 5′-AAGGCTGAGTAGAGGGAGGAG-3′.

3.3.5 Immunoblot analysis

BT-549, HS-578T, and MBA-MB-231 BC cell lines were serum starved for 16 hours before they were treated with epidermal growth factor (EGF). For EGF dose-response experiment, cells were treated with EGF (10 ng/mL or 50 ng/mL or 100 ng/mL) for 15 minutes or serum free medium with PBS+1%BSA (vehicle) as negative control. For time-response experiment, cells were treated with EGF (50 ng/mL) for 0, 15, 45, 90, 120 and 180 minutes. The same experiment was conducted on the same cell lines but using PBS+1%BSA (vehicle) as a control instead of EGF.

To obtain total lysates from BT-549, HS-578T, and MBA-MB-231 BC cell lines, cells were lysed in ice-cold Mammalian Protein Extraction Reagent (IGEPAL ® CA-680, 0.05 M Tris pH 8.0, 0.15 MNaCl, 1 mM PMSF, 0.05% Protease Inhibitor Cocktail). The lysates were then centrifuged at 4°C for 15 min at 21,000 x *g*. The supernatant was collected, and protein was quantified using the Bradford protein dye assay. Absorbance at λ=595 nm was measured by a Beckman DU 640 spectrophotometer (Beckman Instrument, Fullerton, CA). Bovine Serum Albumin (BSA) was used as a standard. Following protein quantification, protein samples were boiled in SDS-loading buffer for 5 min and stored at -80°C for SDS-polyacrylamide gel electrophoresis (SDS-PAGE) applications. For the staining of total cell lysates, aliquots containing 20 µg of protein from each cell lysate were used. Protein samples were separated by electrophoresis through 8.5-10% SDS-polyacrylamide gels at 180 volts for 48 minutes. Pre-stained protein markers (Sigma) were used for molecular weight standards.

Following SDS-PAGE, Proteins were electrophoretically transferred onto Trans-blot nitrocellulose membranes (BioRad, Hercules, CA). Blots were blocked with 3-5% skim milk in 0.05% Triton X -TBS (blocking buffer) for 25 min to reduce the background. Membranes were then probed with the respective primary antibody in blocking buffer at 4°C overnight after washed twice with 0.05% Triton X –TBS for 10 min, membranes were then incubated with HRP-conjugated IgG secondary antibody for 1 hour at room temperature, washed with TBS buffer for 10 min. Secondary antibodies were detected by enhanced chemiluminescence (SuperSignal® West Femto Maximum Sensitivity Substrate, Thermo Scientific, Rockford, IL) and light detection with Image Station 4000MM. Band intensities were detected using ImageJ software. For statical analysis, two-tailed unpaired Student's t-tests was used for to assess statistical differences. P value <0.05 was considered significant.

The following antibodies were used from Cell Signaling ™ (Danvers, MA) : pEGFR (1173) (1:1000), FOXC1 (1:1000), pERK Thr 202/Tyr204 (1:1000), pAkt Ser 473 (1:1000), Tubulin (1:5000), HRP-conjugated anti-Mouse (1:1500), and HRP-conjugated anti-Rabbit (1:2000).

3.3.6 Protein stability

Protein stability assay was conducted as previously described [90,200]. BT-549 and HS-578T BC cell lines and HTRTOA3 cell line were treated with cycloheximide (50 μg/ml) for 0–4 h. To activate the expression of FOXC1 in HTRTOA3 cell line, cells were treated Tetracycline (Invitrogen, Carlsbad, CA) of final concentration of (1 μg/ml) 24 hours before cycloheximide treatment. For immunoblotting experiments, the cells were first rinsed 2 times with 5 ml of PBS. Cells then were gently scraped and harvested at different time points in 50 μl of lysis buffer

(IGEPAL® CA-630, 0.05 M Tris pH 8.0, 0.15 M NaCl, 1 mM PMSF, 0.05% protease inhibitor cocktail) and then incubated on ice for 15 min. Next, cells were centrifuged at 14,000*g* for 5 min at 4°C. The supernatants were transferred to a new tube, quantified, denatured at 95°C for 5 min and size-separated on an 8% SDS-PAGE gel. Samples were subjected to FOXC1 antibody (1:1000) Cell Signaling ™ (Danvers, MA), anti-α-tubulin (Santa Cruz Biotechnology) 1:2000 and anti-Xpress (1:5000). The band intensities were quantified with ImageJ software. α-Tubulin was used as a loading control. Band intensities were normalized to that of α-Tubulin, then scaled to 0 time point of cycloheximide exposure. Error bars represent standard deviation for the slopes. The decay of FOXC1 followed first order kinetics. The slope of the decay line was calculated by standard linear regression, and the protein half-life was determined accordingly. A two-tailed Student's *t*-test was applied to determine statistical significance using slopes over the time of cycloheximide treatment. Three independent experiments were carried out to determine the rates of decay of FOXC1proteins. A p value < 0.05 was considered significant.

3.3.7 *FOXC1* sequence analysis

Genomic DNA was isolated from BT-549, HS-578T, and MBA-MB-231 BC cell lines using the EZ-10 Spin Column Genomic DNA Minipreps Kit (Bio Basic Inc., Markham, ON). FOXC1 genes were PCR amplified using the following primers *FOXC1a:* 45-F: 5′-GTTTGCGCCTGGAAGCTG-3′, 45-R: 5′-CTGCTGTCGGGGCTCTCG-3′; *FOXC1b:* 42-F: 5′-ATCAAGACCGAGAACGGTACG-3′, 43-R: 5′- GGGGTTCGATTTAGTTCGGCT-3′; using the following conditions: denaturation at 95.0˚C for 3:00 followed by 5 cycles of 95.0˚C (0.30 min), 64.0-56.0˚C for 0:30 (2˚C decrease per cycle touchdown), 72.0˚C for 0:30 and then 30 cycles of 95.0˚C (0.30 min), 54.0˚C (0.30 min) and 0:30 min final extension at 72.0˚C. FailSafe buffer J (Epicentre Biotechnologies, Madison, WI) was used in conjunction with Taq polymerase

(New England Biolabs, Whitby, ON). PCR products were purified on separation columns (Qiagen Inc. Toronto, ON), and sequenced on a 3130XL Genetic Analyzer at The Applied Genomics Core of the University of Alberta. For sequencing reads, the following primers were used *FOXC1* 44-R: 5′-GCGGCACCTTGACGAAGC-3′, *FOXC1* 41-F: 5′-CCCAAGGACATGGTGAAGC-3′; *FOXC1* 42-F: 5′-ATCAAGACCGAGAACGGTACG-3′; *FOXC1* 43-F 5′-ACAGAGGATCGGCTTGAACA-3′.

3.3.8 K-Means clustering

Unsupervised K means clustering analysis was performed to investigate and compare *FOXC1* CNV and its mRNA expression. We used the elbow method [201] to determine the ideal statistical number of clusters for K-means with the scikit-learn's method of the MinMaxScaler module used with a sum of squares distance and fit between 1 and 15 possible clusters [201]. We then devised Python scripts to identify the cluster sets by applying standard supervised K-means clustering using number of clusters and *FOXC1* mRNA expression and copy number variation (CNV) as seeds as described in [202]. The mRNA and CNV data of *FOXC1* were obtained from Cancer Cell Line Encyclopedia online (CCLE) database [203,240]. K-means clustering performed 1000 iterations using the Euclidean distance and using seeds between 1 and 12 clusters**.** 42 BC cell lines were used for the analysis and cell lines were grouped as luminal A, luminal B, HER2, Basal A and Basal B as described [204,205,237]. CCLE CNV data of BC cell lines were obtained using genome-wide human Affymetrix SNP Array 6.0 [203]. The mRNA data on the CCLE website were produced by Affymetrix Human Genome U133 Plus 2.0 Array followed by Robust Multiarray Averaging (RMA) method of microarray normalization and were uploaded as log(2) gene expression signal [203]. The log(2) *FOXC1* expression data in each of the 42 BC cell lines from CCLE were obtained and then scaled to values between 0 and 1 using the equation;

$zi = \frac{\{xi - \min(x)\}}{\{\max(x) - \min(x)\}}$ where $x = (x_1, \ldots\ldots, x_n)$ producing z_i as the scaled value for *FOXC1* mRNA expression in each of the 42 BC cell lines. CNV raw data created by Affymetrix (CEL file) were normalized to copy number estimates using a GenePattern pipeline [203]. The median of the scaled *FOXC1* expression values was used as a cut-off, where cell lines with values above the median were considered as relative high expression of *FOXC1* cell lines, while cell lines with *FOXC1* expression below the median were considered as relative low expression of *FOXC1* cell lines.

3.4 Results

3.4.1 FOXC1 expression in BC subtypes

To study the expression of *FOXC1* in BC subtypes, I conducted RT-qPCR assays on TNBC and luminal BC patient samples and on normal breast tissue samples (Table 3.1). One-way ANOVA analysis showed that *FOXC1* mRNA expression varied between BC patients' subtypes and normal breast tissue, $F(2,17) = 10.8$, p=0.0009. I conducted unpaired t-tests for multiple comparison between luminal, TNBC, and normal breast tissue (Figure 3.1). I found that *FOXC1* expression was significantly higher in TNBC when it was compared to luminal BC (p=0.0002, Figure 3.1). Although *FOXC1* showed a trend of higher expression in TNBC when it was compared to normal breast tissues, it did not reach the statistical significance (p=0.07, Figure 3.1). Interestingly, *FOXC1* mRNA levels were significantly lower in luminal compared to TNBC and normal breast tissue (Figure 3.1), which suggest that *FOXC1* is differentially expressed in BC subtypes and could potentially have different roles in TNBC and luminal subtypes.

I next further examined *FOXC1* expression in a larger panel of 42 BC cell lines (Figure 3.2). *FOXC1* mRNA data in 42 BC cell lines were obtained from the CCLE website [203,240]. BC cell lines were grouped into luminal, A and B; TNBC, basal A and B, as shown in (Figure 3.2) to resemble the intrinsic heterogeneity and subtypes of BC as described in [204,205,237]. I was not able to obtain HER2 BC patient samples when the RT-qPCR was preformed (Figure 3.1), hence *FOXC1* expression was not investigated in that subtype patient samples. For that reason, I included HER2 BC cell lines in my analysis of *FOXC1* expression in the larger panel of BC cell lines (Figure 3.2). Consistent with my findings of low levels of *FOXC1* expression in luminal BC patient tumors (Figure 3.1), I found *FOXC1* mRNA to be low in all luminal A and B cell lines except for one luminal A cell line, MDA-MB-175-VII, that had *FOXC1* expression value above the median cut-off (Figure 3.2). I also found high *FOXC1* expression in most of the TNBC, Basal A and B cell lines, which consistent with my findings of high expression of *FOXC1* in TNBC patient samples (Figure 3.2 and 3.1 respectively).

Although it was previously suggested that *FOXC1* is consistently and exclusively over-expressed in basal/TNBC cell lines [147], I found HER2 cell lines (HCC1569, JIMT-1, and HCC1954) also had high expression of *FOXC1* (Figure 3.2). Moreover, I found *FOXC1* expression varied in basal/TNBC cell lines, where some basal cell lines such as HCC1187, HCC1806, CAL-51, HS-578T, and HCC38 had high expression of *FOXC1* but DU4475, MDA-MB-436, HCC1937, and CAL-148 had low expression of *FOXC1* (Figure 3.2). Together, these results show that *FOXC1* levels are elevated in basal/TNBC and under-expressed in luminal BC, however, the underlying mechanisms of the over expression and/or under-expression of *FOXC1* are not fully known in BC.

3.4.2 The impact of DNA mutation and amplification on *FOXC1* expression in TNBC

I examined whether *FOXC1* DNA mutations and/or gene amplification impact the high expression of *FOXC1* in TNBC cell lines. I first conducted a qPCR to sequence *FOXC1* in TNBC cell lines, HS-578T, BT-549, and MDA-MB-231. I used these cell lines since they have different mRNA levels of *FOXC1* (Figure 3.2), to investigate if *FOXC1* mutation and/or CNV are the driver of the variable mRNA levels in these cell lines. The sequence-analysis of *FOXC1* showed no pathogenic mutations in any cell line (Figure 3.3.). A silent-mutation (C18T; pR6R) was however found in the cell line HS-578T (Figure 3.3). I next examined *FOXC1* CNV. A qPCR was conducted to measure *FOXC1* DNA dosage in TNBC cell lines. I also used DNA samples from patients with known WT [86,227,229,239] and duplicated copies [226] of *FOXC1* respectively as my controls. I found that cell lines with high *FOXC1* expression (HS-578T, BT-549) had extra copies of *FOXC1* (Figure 3.4). This contrasts with the lower expression of *FOXC1* cell line, MDA-MB-231, that had a deleted copy of *FOXC1* (Figure 3.4).

To further investigate whether *FOXC1* CNV is associated with its expression, K-means clustering was conducted on *FOXC1* mRNA and CNV values in 42 BC cell lines downloaded from the CCLE website [203,240] (Table 3.2). Unsupervised K-means clustering identified 12 clusters among BC cell lines for *FOXC1* mRNA compared to their copy number (Table 3.2 and Figure 3.5). I found some cell lines clusters that have similar copy number of *FOXC1* (C11 vs C10, C1 vs C10, C3 vs C2) but different mRNA expression (Table 3.2 and Figure 3.5). I also found some cell line clusters had similar *FOXC1* mRNA expression but different variation in relative copy number (C4 vs C5, C4 vs C7, C6 vs C9, C1 vs C8, Figure 3.5). Although I found high expression and more copies of *FOXC1* in HS-578T and BT-549 (Figure 3.2 and 3.4) and low expression and a deleted copy of *FOXC1* in MDA-MB-231 (Figure 3.2 and 3.4), K-means

analysis suggests that the steady state level of *FOXC1* mRNA expression appears to be independent of gene copy number in 42 BC cell lines. Thus, *FOXC1* mRNA expression levels are not correlated with *FOXC1* CNV in BC subtypes.

Furthermore, K-means clustering based on *FOXC*1 expression and CNV revealed that while some clusters had cell lines of the same BC subtype (C0, C4, and C5, Table 3.2) other clusters had cell lines of different BC subtypes clustered together (C10, C1, C3, and C11, Table 3.2) suggesting that *FOXC1* expression and CNV are not exclusive markers for a specific subtype of BC cell lines.

3.4.3 The effects of activated epidermal growth factor receptor (EGFR) on FOXC1 levels in TNBC

I examined whether EGFR activation, via its ligand epidermal growth factor (EGF), impacts the levels of FOXC1 in TNBC cell lines. It was suggested that EGFR, a membrane receptor protein, could serve as surrogate biomarker in TNBC [219,241]. TNBC cell lines, HS-578T, BT549, and MDA-MB-231 were treated with 10ng/ml, 50ng/ml, and 100ng/ml of EGF for 15 minutes then followed by immunoblotting analysis. Cells were serum free (SF) for 16 hours prior EGF treatment. Vehicle was used as a negative control.

Consistent with my findings of high mRNA expression of *FOXC1* in HS-578T and BT-549 (Figure 3.2), and low mRNA expression of *FOXC1* in MDA-MB-231 (Figure 3.2), I found high and detectable levels of FOXC1 protein in HS-578T (Figure 3.6) and BT-549 (Figure 3.7), and low levels of FOXC1 protein in MDA-MB-231 (Figure 3.8). EGF treatment stimulated the activation of EGFR as EGFR phosphorylation (activated form of EGFR) was significantly more after 15 minutes (short-term) of 10 ng/ml, 50 ng/ml, and 100 ng/ml treatment in HS-578T

(Figure 3.6) and BT-549 (Figure 3.7), and after 50 ng/ml and 100 ng/ml in MDA-MB-231 (Figure 3.8) when it was compared to serum-free samples.

I then examined the activation of the EGFR downstream singling pathways such as phosphatidyl-inositol 3-kinase (PI3K) and mitogen-activated protein kinases (MAPK), both of which are important for TNBC cell proliferation and metastasis [242]. Therefore, I examined the activation of the protein kinase B (Akt) and the extracellular signal-regulated kinase (ERK) that are downstream proteins of PI3K and MAPK pathways respectively. ERK and Akt are known to be activated by EGFR and play a role in TNBC proliferation and survival [243,244]. Both ERK and Akt phosphorylation (active forms) levels were significantly more after EGF stimulation in HS-578T (Figure 3.6), BT-549 (Figure 3.7), and in MDA-MB-231 (Figure 3.8) compared to serum-free samples. However, I found no significant changes in FOXC1 levels in any of the cell lines after short-term of EGF treatment (Figure 3.6, 3.7, and 3.8). This directly contrasts the findings of longer-term (3 hours) of EGF treatment, where increased levels of FOXC1 in BT-549 cells were detected (Figure 3.9). Notably, no significant changes in FOXC1 levels were seen in HS-578T under the same treatment, suggesting that may be there unknown signaling pathway regulate FOXC1 levels in HS-578T cells that is independent of EGFR signaling pathway. Nevertheless, my findings in BT-549 suggests that FOXC1 levels are impacted by EGFR activation and EGFR's activated downstream pathways in an indirect fashion after long-term treatment with EGF.

3.4.4 FOXC1 is more stable in TNBC cell lines

Finally, I investigated whether FOXC1 protein is more stable in TNBC cell lines (HS-578T, BT-549). HeLa FOXC1 sable cell line (HTRTOA3) that has a tetracycline-inducible

Xpress-FOXC1 protein expression was used as a control. To measure FOXC1 half-life in HS-578T, BT-549, and HTRTOA3, *de novo* protein synthesis was blocked using cycloheximide as our lab previously described in [90,200]. To induce FOXC1 protein expression in the HTRTOA3 cell line, cells were treated with tetracycline for 24 hours prior cycloheximide treatment. Then, the 3 cell lines were treated with cycloheximide for 4 hours, and the amount of FOXC1 protein in HS-578T, BT-549, and HTRTOA3 was analyzed by immunoblotting as shown in (Figure 3.10). Interestingly, I found that the half-life of FOXC1 was significantly longer in TNBC cell lines BT-549 and HS-578T compared to the half-life of FOXC1 in HTRTOA3 cell line (Figure 3.10). FOXC1 half-life was approximately three times and two times longer in BT-549 and HS-578T respectively compared to half-life of FOXC1 in HTRTOA3, suggesting that FOXC1 protein is more stable in TNBC cell lines.

3.5 Discussion

In the last decade, a role for FOXC1 in TNBC has been reported [131,144–147,149,151,245]. FOXC1 was also suggested as exclusively overexpressed in basal/TNBC and to be directly linked to TNBC metastasis and invasion [144,147]. FOXC1 is associated with TNBC through critical signaling pathways [144,145,149,150]. However, gaps in the literature regarding *FOXC1* expression and role in BC exist. First, the how and why of *FOXC1* being exclusively overexpressed in basal/TNBC rather than other BC subtypes has yet to be answered. Second, the mechanisms underlying FOXC1's altered expression, including the status of *FOXC1* mutation, CNV, and protein stability in basal/TNBC have yet to be investigated. Finally, very limited reports have explored *FOXC1* expression across the BC subtypes. In this chapter, I showed that *FOXC1* expression varies among BC subtypes in BC patients and cell lines, where *FOXC1* is highly expressed in TNBC and under-expressed in luminal and HER2. I also found that TNBC (also

known as basal BC where more than 80% of TNBC are known as basal BC) cell lines HS-578T and BT-549 (both cell lines have high levels of FOXC1 mRNA and protein) had more copies of *FOXC1* and MDA-MB-231 (with low levels of FOXC1 mRNA and protein) had a deleted copy of *FOXC1*. However, my studies of an expanded panel of 42 BC cell lines showed that *FOXC1* mRNA expression is independent of its CNV. Furthermore, *FOXC1* sequence analysis showed no pathogenic mutations of *FOXC1* in TNBC cell lines. Instead, my studies suggest that FOXC1 overexpression in TNBC appears to be the result of increased protein levels by EGFR and/or FOXC1 stability. Protein studies showed that FOXC1 levels were regulated by EGFR, and protein-stability studies revealed that FOXC1 had longer half-life in TNBC cell lines compared to FOXC1 half-life in stably expressing FOXC1 HeLa cells.

3.5.1 FOXC1 expression in BC

The expression of *FOXC1* across BC subtypes is very limited, controversial, and not well studied. For that reason, I investigated *FOXC1* expression across BC subtypes in BC patient tissues, normal breast tissue as well as in BC cell lines. BC is a heterogenous disease that encompasses several diseases making its treatment a clinical challenge. Traditionally, BC subtypes are classified as TNBC, HER2 and luminal BC based on the levels of the immunohistochemistry (IHC) markers ER, PR, and HER2 [61]. However, almost a decade ago, a surrogate BC subtypes based on different protein levels were suggested and was adapted for the clinic. These surrogate subtypes are TNBC, HER2 enriched, luminal A and luminal B BC [246]. Where IHC-TNBC (ER/PR/HER2 negative) and IHC-HER2 (ER and PR negative/HER2 positive). luminal A and B are classified based on a combination of the traditional pathological markers (ER, PR, and HER2) and Ki67—a nuclear marker of cell proliferation that is highly expressed in BC cells and associated with poor prognosis [247,248]—that is encoded by the gene

MKI67. As a result, luminal BC can be further grouped as IHC-luminal A (ER and PR positive/HER2 negative/Ki67<14%), IHC-luminal B/HER2 negative (ER and PR positive/HER2 negative/Ki67>14%), and IHC-luminal B/HER2 positive (ER and PR positive/HER2 positive/Ki67>14%) [249]. Moreover, the luminal BC surrogate classification was further modified to include what is known as luminal A-like (high ER/PR, low Ki67 and histologic grade 1) and luminal B-like (low ER/PR, high Ki67, histologic grade 3) in order to improve BC prognosis, diagnosis and treatment [250,251].

In this chapter, I used BC patient samples and normal breast tissue (Table 3.1) that were provided by Dr. Todd McMullen (Department of Surgery, University of Alberta). Dr. McMullen's lab used ER, PR, and HER2 markers to identify the BC subtypes of those patients (Table 3.1). However, the cut-off values of ER and PR levels as well as Ki67 in those patient tissues were not provided. Hence, I used the traditional BC subtyping method to group patient tissues, where tissues that had negative or positive expressions of (ER, PR, and HER2) were categorized as TNBC and luminal respectively (Table 3.1) and then were subjected to RT-qPCR analysis (Figure 3.1). I found *FOXCI* was significantly overexpressed in TNBC patients when compared to luminal and was significantly under-expressed in luminal compared to normal breast tissue (Figure 3.1). My findings of high expression of *FOXC1* in TNBC and low expression of *FOXC1* in luminal were in line with those of others who had also investigated *FOXC1* expression in BC patients [147,252,253]. *FOXC1* expression was higher in TNBC compared to non-TNBC BC [147,253], and *FOXC1* expression was low in luminal subtype [252]. However, multiple comparisons and statistical analyses of *FOXC1* expression between luminal and TNBC, or between luminal or TNBC and normal breast tissue were not reported [252,253]. Taken together, my findings and those of others show that *FOXC1* is differentially expressed across BC patient

subtypes suggesting that *FOXC1* expression varies among BC subtypes and thus could have different roles based on BC subtypes.

In order to further investigate *FOXC1* expression across BC subtypes, I examined *FOXC1* mRNA levels in an expanded panel of 42 BC cell lines (Figure 3.2). BC cell lines were grouped as luminal A, luminal B, basal, and HER2 as described by Neve *et al.,* [205] and Liu *et al*., [237]. Basal BC cell lines can be further subdivided into basal A and B based on differences in molecular features, morphology and invasion potential [205,237] (Figure 3.2). Of note, basal BC cell lines are ER/PR/HER2 negative, resembling TNBC in that regard, and are known to have high expression of cytokeratin 5/6 and/or EGFR [11,40,42–44,254]. For the rest of this discussion section, I will be using "basal" to refer to the results analyses that were conducted in TNBC cell lines that were obtained from CCLE, while "TNBC" for the wet-lab results and experiments that were conducted in TNBC cell lines (this is mainly because the basal markers levels were not measured in the TNBC cell lines I used for the wet lab experiments).

Consistent with my findings of low levels of *FOXC1* expression in luminal BC patient tumors (Figure 3.1), I found *FOXC1* mRNA to be low in all luminal A and B cell lines except for one luminal A cell line, MDA-MB-175-VII, that had *FOXC1* expression value above the median cut-off (Figure 3.2). I also found high *FOXC1* expression in most of the basal (TNBC) compared to luminal BC cell lines, which is consistent with my findings of high expression of *FOXC1* in TNBC patient samples compared to luminal patient samples (Figure 3.2 and 3.1 respectively).

Intriguingly, other studies of limited number of luminal, HER2, and basal BC cell lines suggested that *FOXC1* is high in all of the basal cell lines, and low in all luminal and HER2 cell lines [253,255,256]. However, my studies of expanded panel of 42 cell lines showed that *FOXC1*

expression varied in basal (TNBC) cell lines. I found most of the basal cell lines had high expression of *FOXC1* (Figure 3.2) which is consistent with other studies [253,255,256], but I also found some basal cell lines had low expression of *FOXC1,* in particular the basal A cell lines (DU4475, MDA-MB-436, HCC1937, and CAL-148) (Figure 3.2). Moreover, I found HER2 cell lines (HCC1569, JIMT-1, and HCC1954) had high expression of *FOXC1* (Figure 3.2) in contrast to other studies that suggested that *FOXC1* is exclusively high in basal cell lines (n=7) compared to luminal (n=3) and HER2 (n=2) cell lines [256]. It is worth mentioning that conflicting results regarding *FOXC1* expression in identically-named BC cell lines have been reported previously [147,255–257].

My findings of low expression of *FOXC1* in some of the basal BC cell lines are striking (DU4475, MDA-MB-436, HCC1937, and CAL-148, Figure 3.2). A few possibilities, however, behind the low expression of *FOXC1* in these cell lines, can be considered. Pathogenic mutations in the breast cancer type 1 (*BRCA1*) gene—encodes a tumor suppressor protein that plays a critical role in cell cycle control, DNA damage repair, and transcriptional regulation— are associated with higher risk of developing BC [258,259]. It has shown that basal BC and tumors arising from *BRCA1* mutation carriers share remarkable histological and morphological similarities [260–262] and that BRCA1 regulates genes associated with basal BC [263]. Interestingly, it was suggested that BRCA1 suppressed the transcription of *FOXC1* in basal BC and that high expression of *FOXC1* in basal BC subtype was a result of impaired BRCA1 function [256]. Moreover, *FOXC1* DNA methylation—epigenetic mechanism that supresses DNA transcription [264]—has been suggested to regulate *FOXC1* expression in BC [265–268]. *FOXC1* methylation was significantly lower in BC patients harboring mutations in *TP53* gene (tumor suppressor gene[269]) compared to patients who had wild-type *TP53* [267]. In addition, it was shown that *FOXC1*

methylation is significantly less in BC patients who received chemotherapy [265,266], and in invasive ductal BC patients compared to those of ductal BC *in situ* patients (pre-invasive BC) [267,268]. Therefore, to understand the mechanisms behind *FOXC1* low expression in some of the basal A BC cell lines, future studies that investigate mutation status of *BRCA1* and *TP53* as well as the epigenetic regulation of *FOXC1* expression are warranted.

I also found *FOXC1* expression is under-expressed in luminal BC patient samples and cell lines (Figure 3.2). Very recently, a study has suggested subtype-specific negative regulation of *FOXC1* expression in luminal BC and that low expression of *FOXC1* is critical for luminal BC metastasis [252]. High expression of *FOXC1* in luminal BC patients was associated with significant better overall survival outcomes compared to those who had low expression of *FOXC1* [252]. This directly contrasts other studies that suggested high expression of *FOXC1* is associated with poor prognosis in TNBC patients [147,253]. Moreover, *FOXC1* methylation was found to be higher in luminal BC compared to TNBC [267], suggesting again the importance of epigenetic regulation of *FOXC1* in different BC subtypes. Together, these studies may explain my findings of low expression of *FOXC1* in luminal BC (Figure 3.1 and 3.2).

My studies and those from others showed that the expression of *FOXC1* varies in BC subtypes, where *FOXC1* is over-expressed in TNBC and under-expressed in luminal and HER2. Moreover, I highlight the importance of studying *FOXC1* expression in expanded number of cell lines in order to have a fulsome picture on *FOXC1* expression in BC-subtypes cell lines.

3.5.2 Investigation of *FOXC1* over-expression mechanisms in TNBC

FOXC1 levels are elevated in TNBC compared to other BC subtypes (Figure 3.1 and 3.2), however, the underlying mechanisms of this over expression of *FOXC1* are not fully

known. *FOXC1* point mutations have been reported and studied in other diseases. These mutations have been shown to alter FOXC1 protein level, FOXC1 transactivation, and/or FOXC1's DNA binding ability [86,99,100,104,226,227,229,239]. There have been no reports on the impact of *FOXC1* DNA mutation/s and/or CNV on the expression of *FOXC1* in TNBC. Therefore, I investigated the copy number and sequence of *FOXC1* in TNBC cell lines, HS-578T, BT-549, and MDA-MB-231.

My results showed no pathogenic mutations of *FOXC1* in any cell line (Figure 3.3). However, I found that cell lines with high *FOXC1* expression (HS-578T, BT-549) had extra copies of *FOXC1* (Figure 3.4). This contrasts with the lower expression of *FOXC1* cell line, MDA-MB-231, that had a deleted copy of *FOXC1* (Figure 3.4). Although I found *FOXC1* CNV in these TNBC cell lines, unsupervised K-means analysis suggested that the steady level of *FOXC1* mRNA expression appeared independent of gene copy number in 42 BC cell lines (Table 3.2 and Figure 3.5). Therefore, *FOXC1* expression is not correlated with *FOXC1* CNV in BC cell lines. Moreover, while I expected that BC cell lines of the same subtype to cluster together, I found some clusters had cell lines from different BC subtypes clustered together (C10, C1, C3, and C11, Table 3.2 and Figure 3.5). Although, other groups [147,253] suggested the exclusivity of *FOXC1* expression in BC cell lines based on their subtypes, my K-means findings suggested that *FOXC1* expression and CNV are not exclusive markers for a specific subtype of BC cell lines. This perhaps may be attributed to *FOXC1* CNV in BC cell lines, which were not investigated in other studies [147,253]. Nevertheless, my findings suggest that there were no pathogenic mutations of *FOXC1* found in TNBC cell lines (n=3) and that *FOXC1* expression is independent of its CNV in basal BC cell lines.

FOXC1 protein levels were also reported to be overexpressed in basal BC cell lines and that FOXC1's role in basal BC is mediated via signaling pathways [144,145,149,150]. EGFR signaling pathway/s play a critical role in cell proliferation and survival and EGFR has previously been suggested as a surrogate biomarker in TNBC [219,241]. I investigated the impact of EGFR signaling on FOXC1 protein levels in TNBC cell lines. Post-transitional modification of EGFR such as phosphorylation of its tyrosine residue/s is critical for EGFR activation, signaling, and degradation. To activate EGFR, TNBC cell lines were treated with EGF (EGFR ligand) and EGFR phosphorylation and its downstream signaling proteins such as ERK and Akt were detected using western-blotting. ERK and Akt are known to be activated by EGFR thus play a role in TNBC proliferation and survival [243,244]. Although EGF short-term treatment in TNBC cell lines activated EGFR and its downstream signaling proteins ERK and Akt, no significant changes in FOXC1 levels in any of the cell lines were detected (Figure 3.6, 3.7, and 3.8). This suggests that FOXC1 is not an immediate early gene (IEG) induced by EGFR, where IEGs response was suggested between 0-20 minutes after EGF treatment [270,271]. However, FOXC1 levels were increased after 1.5-3 hours of EGF treatment in BT-549, suggesting that FOXC1 is indirectly regulated by EGFR and FOXC1 is thus a delayed early (primary) gene [270,271]. My results are consistent with other group that showed FOXC1 levels are increased but after 24 hours of EGF stimulation [149]. FOXC1 fits in the criteria of IEGs based on other studies of genes response to growth factor stimulation. It was suggested that transcription factors and cell cycle regulators are examples of IEG in response to growth factors [270,271]. Moreover, IEGs are shorter and contain fewer exons compared to delayed early (primary) gene [270,271] and *FOXC1* is a single exon gene. For future studies, investigating FOXC1 mRNA levels after EGF time-course may provide more in depth understating for the role of EGFR regulation of FOXC1 mRNA and

protein expression. Nevertheless, my findings and those of others showed that EGFR indirectly regulates the levels of FOXC1 in TNBC cell lines.

Finally, the stability of FOXC1 protein in TNBC cell lines were investigated. FOXC1 is shown to have a short half-life of ~60-80 minutes [90,200]. Thus, I investigated if increased amounts of FOXC1 in TNBC might be the result of FOXC1 protein being more stable in TNBC cells. Interestingly, the half-life of FOXC1 was 2 times and 3 times longer in HS-578T and BT-549 respectively, as compared to HeLa cells that stably express FOXC1 protein (Figure 3.10). The mechanism/s behind the increased stability of FOXC1 in TNBC remain elusive. Taken together, my studies of FOXC1 protein showed that FOXC1 is also highly expressed in HS-578T and BT-549 cells, consistent with FOXC1 mRNA expression in both cell lines. I also showed that FOXC1 levels are regulated indirectly by EGFR and that FOXC1 is a delayed primary response gene under EGF stimulation. Finally, I showed that FOXC1 protein is more stable in TNBC cell lines and this increased stability may explain its overexpression in TNBC. Together, my findings suggest that FOXC1 protein levels are indirectly regulated by EGFR and FOXC1 protein is more stable in TNBC. Further research on mechanisms that regulate FOXC1 proteins and mRNA stability are needed and could be fruitful.

3.6 Tables and Figures

Table 3.1: Patient demographic

Patient	Age at diagnosis	ER_IHC	PR_IHC	HER2_IHC	Tumor Size (cm)
TNBC					
MT3795	57	Neg	Neg	Neg	2.1
MT3061	36	Neg	Neg	Neg	3.2
MT3626	22	Neg	Neg	Neg	1.2
MT1995	41	Neg	Neg	Neg	5.6
MT3800	60	Neg	Neg	Neg	4.1
MT3473	52	Neg	Neg	Neg	1.1
MT3663	48	Neg	Neg	Neg	5.5
MT2881	47	Neg	Neg	Neg	7
MT3436	57	Neg	Neg	Neg	1.5
MT3332	53	Neg	Neg	Neg	3
CT141	58	Neg	Neg	Neg	1.2
Luminal					
MT3559	57	Pos	Pos	Pos	4.8
CT149	53	Pos	Pos	Pos	3.1
MT2519	47	Pos	Pos	Pos	2.2
MT3219	43	Pos	Pos	Pos	2.4
MT1109	51	Pos	Pos	Pos	2.3
GT1116	31	Pos	Pos	Pos	7

ER, Estrogen receptor; PR, Progesterone; HER2, Human Epidermal Receptor 2; TNBC, Triple Negative Breast Cancer; IHC Immunohistochemistry; Neg, negative; Pos, positive; cm, Centimeters; Null, size of the tissue samples is small (1-3 mm^3).

Table 3.2: BC cell line names and types that were used for unsupervised K-means clustering. Cell line types were sorted as described in [204,205,237]. The mRNA expression and CNV of *FOXC1* in 42 BC cell lines were obtained from CCLE online database [203,240]. Clusters and data are plotted in Figure 3.5.

BC Cell line	Relative *FOXC1* Expression	Relative *FOXC1* CNV	BC Subtype	Unsupervised K-means clusters
HCC1187	1	0.3	Basal A	C0
HCC1806	0.843807	0.49	Basal A	
HCC38	0.751667	0.51	Basal B	
MDA-MB-468	0.696302	0.4	Basal A	
HDQ-P1	0.606991	0.2	Basal B	C7
Hs 578T	0.790665	0.24	Basal B	
HCC1569	0.733482	0.22	HER2	
CAL-120	0.721358	0.29	Basal B	
CAL-85-1	0.715902	0.28	Basal B	
CAL-51	0.804607	0	Basal B	C2
BT-549	0.684381	0.04	Basal B	
HCC1954	0.604769	0.09	HER2	
MDA-MB-157	0.594261	0.02	Basal B	
MCF7	0.50536	0	Basal B	
HCC70	0.718327	-0.09	Basal A	C10
HCC1143	0.675288	-0.15	Basal A	
JIMT-1	0.665589	-0.22	HER2	
MDA-MB-175-VII	0.596282	-0.24	Luminal A	
HCC2157	0.7157	-0.82	Basal A	C4
BT-20	0.521115	-0.67	Basal A	
HCC1395	0.576278	0.41	Basal B	C5
MDA-MB-231	0.516468	0.41	Basal B	
DU4475	0.409578	-0.1	Basal A	C1
MDA-MB-436	0.380683	-0.33	Basal A	
MDA-MB-361	0.331178	-0.25	Luminal B	
KPL-1	0.314811	-0.15	Luminal A	
EFM-192A	0.406547	0.18	Luminal B	C8
EFM-19	0.311578	0.03	Luminal A	
HCC1937	0.315821	-0.48	Basal A	C6
HCC1428	0.095575	-0.48	Luminal A	
HCC2218	0.1667	-0.03	HER2	C3
HCC1419	0.163063	0.02	Luminal B	
MDA-MB-134-VI	0.117397	-0.01	Luminal A	
MDA-MB-453	0.106082	-0.07	HER2	
HCC202	0.088705	0.14	HER2	
BT-474	0.083451	0.01	Luminal B	
BT-483	0.073146	-0.05	Luminal A	
CAMA-1	0.061022	0.08	Luminal A	
AU565	0.121035	0.34	HER2	C9
MDA-MB-415	0.109921	-0.16	Luminal A	C11
CAL-148	0.01273	-0.1	Basal A	
HCC1500	0	-0.2	Luminal A	

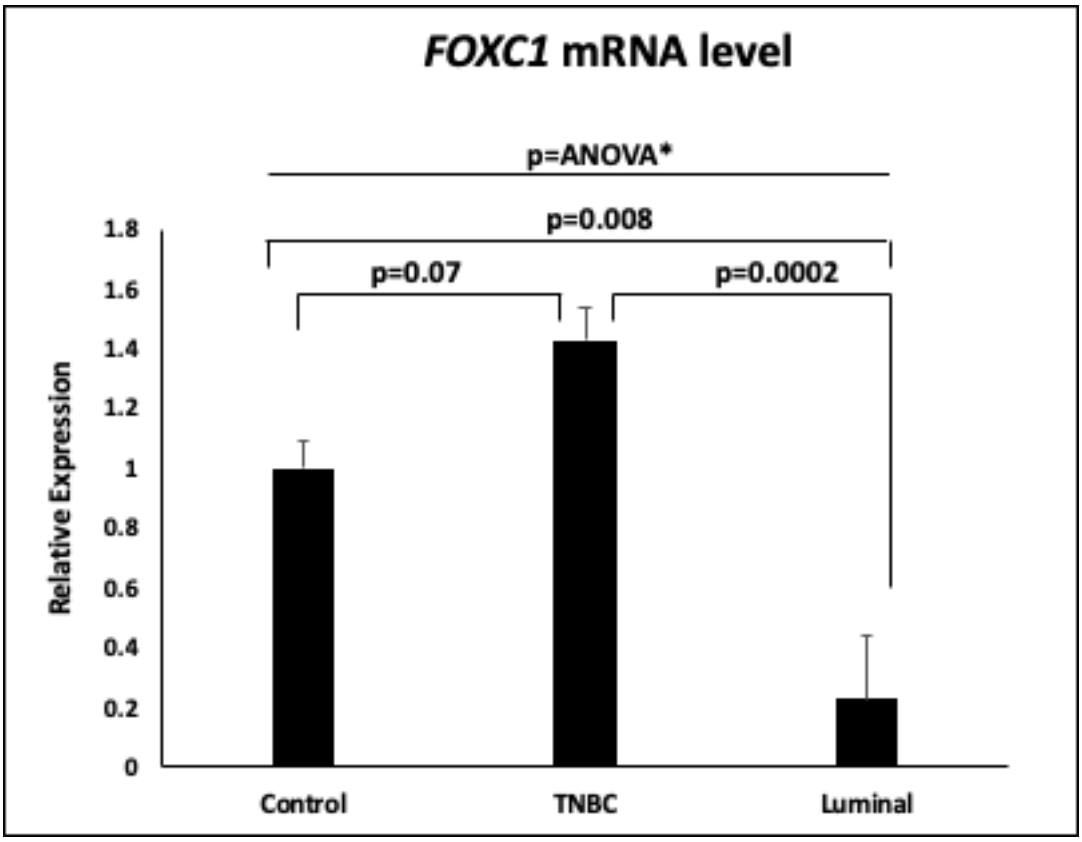

Figure 3.1: *FOXC1* is over-expressed in TNBC compared to luminal patient samples and is under-expressed in luminal compared to normal breast tissue.

one-way ANOVA analysis was used to asses statistical difference in all groups *$F(2,17) = 10.8$, $p = 0.0009$ followed by unpaired t-tests and Bonferroni corrections were used for multiple comparisons. $\alpha = 0.05$, adjusted $\alpha = 0.0166$; *$p < 0.0166$. qPCR experiments were conducted to measure *FOXC1* mRNA levels in normal breast tissue (Control, n=3) acquired from reduction mammoplasties, TNBC (n=11), and luminal (n=6) patient samples. mRNA levels were normalized to *HPRT1* (reference gene) through the $\Delta\Delta$Ct method and changes in mRNA levels were described in fold change compared to the control samples. Error bars represent standard error of the mean (SEM).

Cancer Cell Line Encyclopedia (CCLE)

↓

***FOXC1* mRNA values in 42 BC cell lines**

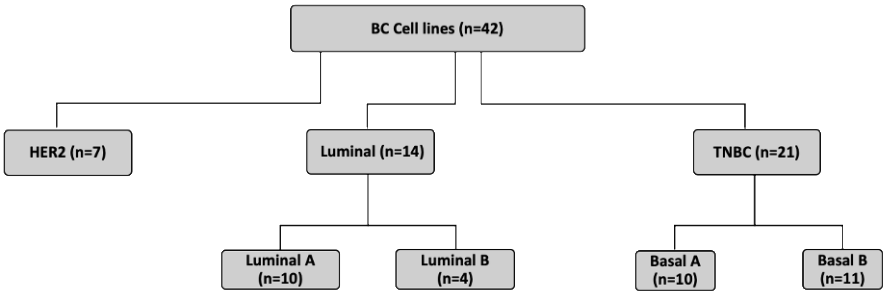

↓

BC Cell line	BC Subtype	Relative *FOXC1* Expression
HCC1187	**Basal A**	**1**
HCC1806	**Basal A**	**0.8438**
CAL-51	**Basal B**	**0.8046**
Hs 578T	**Basal B**	**0.7907**
HCC38	**Basal B**	**0.7517**
HCC1569	HER2	0.7335
CAL-120	**Basal B**	**0.7214**
HCC70	**Basal A**	**0.7183**
CAL-85-1	**Basal B**	**0.7159**
HCC2157	**Basal A**	**0.7157**
MDA-MB-468	**Basal A**	**0.6963**
BT-549	**Basal B**	**0.6844**
HCC1143	**Basal A**	**0.6753**
JIMT-1	HER2	0.6656
HDQ-P1	**Basal B**	**0.607**
HCC1954	HER2	0.6048
MDA-MB-175-VII	Luminal A	0.5963
MDA-MB-157	**Basal B**	**0.5943**
HCC1395	**Basal B**	**0.5763**
BT-20	**Basal A**	**0.5211**
MDA-MB-231	**Basal B**	**0.5165**
MCF7	**Luminal A**	**0.50536**
DU4475	Basal A	0.4096
EFM-192A	**Luminal B**	**0.4065**
MDA-MB-436	Basal A	0.3807
MDA-MB-361	**Luminal B**	**0.3312**
HCC1937	Basal A	0.3158
KPL-1	**Luminal A**	**0.3148**
EFM-19	**Luminal A**	**0.3116**
HCC2218	HER2	0.1667
HCC1419	**Luminal B**	**0.1631**
AU565	HER2	0.121
MDA-MB-134-VI	**Luminal A**	**0.1174**
MDA-MB-415	**Luminal A**	**0.1099**
MDA-MB-453	HER2	0.1061
HCC1428	**Luminal A**	**0.0956**
HCC202	HER2	0.0887
BT-474	**Luminal B**	**0.0835**
BT-483	**Luminal A**	**0.0731**
CAMA-1	**Luminal A**	**0.061**
CAL-148	Basal A	0.0127
HCC1500	**Luminal A**	**0**

Cell lines with relative high expression of *FOXC1*

Median cut-off

Cell lines with relative low expression of *FOXC1*

Figure 3.2: ***FOXC1* expression varies among BC cell lines and is highly expressed in basal (TNBC) cell lines.**

relative *FOXC1* expression is high in most basal (TNBC) cell lines, and in particular, in basal B cell lines. While relative *FOXC1* expression is low in all luminal cell lines except of the luminal A BC cell line MDA-MB-175-VII. *FOXC1* mRNA data in 42 BC cell lines were obtained from Cancer Cell Line Encyclopedia online (CCLE) database [203,240]. BC cell lines were further grouped as luminal A and luminal B—luminal— , HER2, and Basal A and Basal B—TNBC—as described in [204,205,237]. The mRNA data on the CCLE website were produced by Affymetrix Human Genome U133 Plus 2.0 Array followed by Robust Multiarray Averaging (RMA) method of microarray normalization and were presented as log2 gene expression signal. The log2 *FOXC1* expression data in 42 BC cell lines from CCLE were obtained and then were scaled between 0 and 1 as presented in this figure. The median of the scaled *FOXC1* expression values was used as a cut-off, where cell lines with values above the median were considered as relative high expression of *FOXC1* cell lines, while cell lines with *FOXC1* expression below the median were considered as relative low expression of *FOXC1* cell lines.

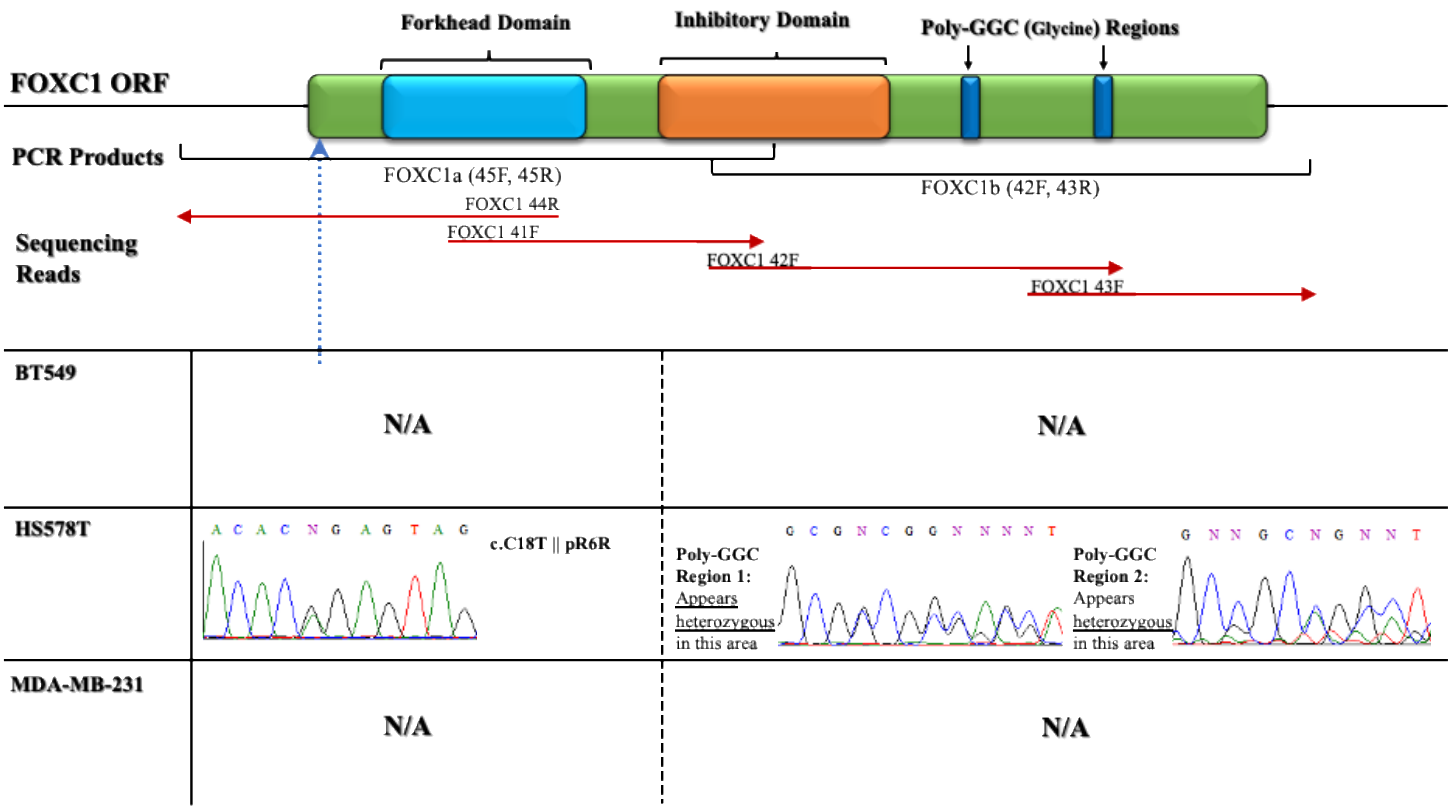

Figure 3.3: *FOXC1* sequence analysis on TNBC cell line showed no pathogenic mutations.

DNA sequencing completed in cell lines BT-549, HS-578T, and MDA-MB-231, including PCR and sequencing primers used as shown in the figure. Silent mutation in HS-578T cell line in the open reading frame (ORF) at position 18 from the open reading frame [C18T], with changes in the protein at amino acid 6 [pR6R].

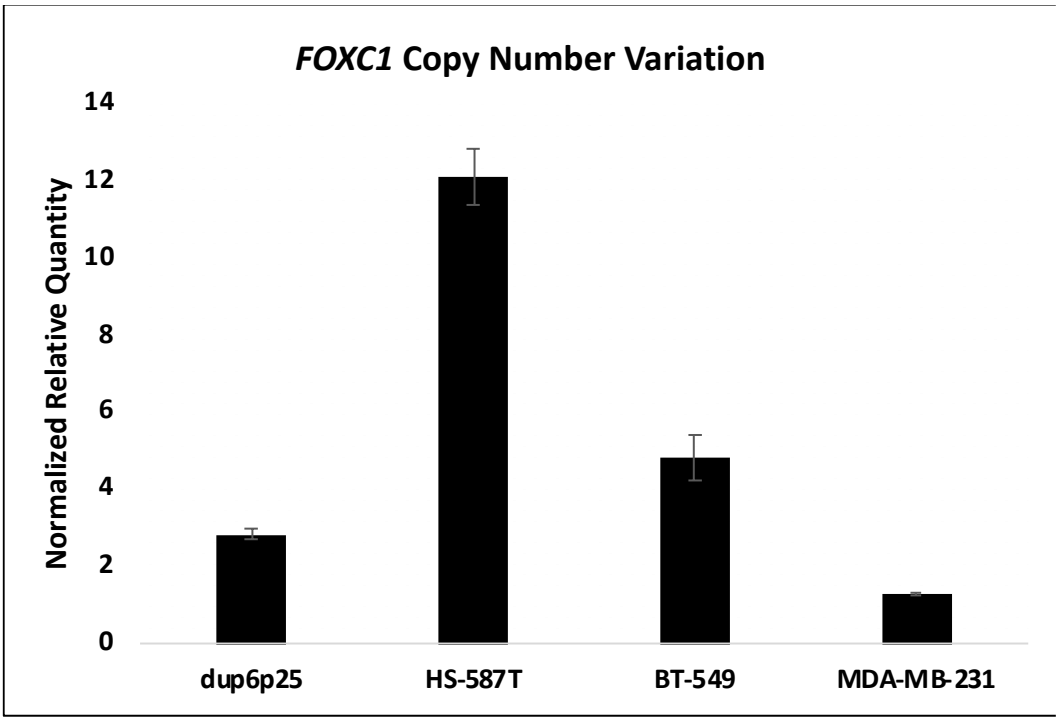

Human cells	*FOXC1* Copy Number	Interpretation
WT	2	Normal *FOXC1*
FOXC1 Duplication (dup6p25)	2.5 +/- 0.05	Duplicated *FOXC1*

TNBC cells	*FOXC1* Copy Number	Interpretation
Hs 578T	12 +/- 2	Extra *FOXC1* copies
BT-549	5 +/- 1	Extra *FOXC1* copies
MDA MB-231	1+/- 0.5	Deleted *FOXC1*

Figure 3.4: The TNBC cell lines HS-587T and BT-549 have extra copies of *FOXC1*.

qPCR experiments were conducted on genomic DNA to measure *FOXC1* dosage in TNBC cell lines. The ΔΔCT method was used as quantification strategy, with *GJA5* selected as an internal control gene. Average CT values of triplicates were calculated for each sample. ΔCT for each sample was then calculated by subtracting the average CT number of *FOXC1* from that of *GJA5*. *FOXC1* dosage was calculated using $2^{[\Delta CT\ BC\ sample - \Delta CT\ WT\ sample]}$. *FOXC1* dosage was normalized to DNA from patient samples (n=4) with a known wild-type (WT) copies of *FOXC1* [86,227,229,239]. DNA from patient samples (n=3) with a known *FOXC1* duplication (dup6p25) were used as a control [226]. Error bars represent standard error of the mean (SEM).

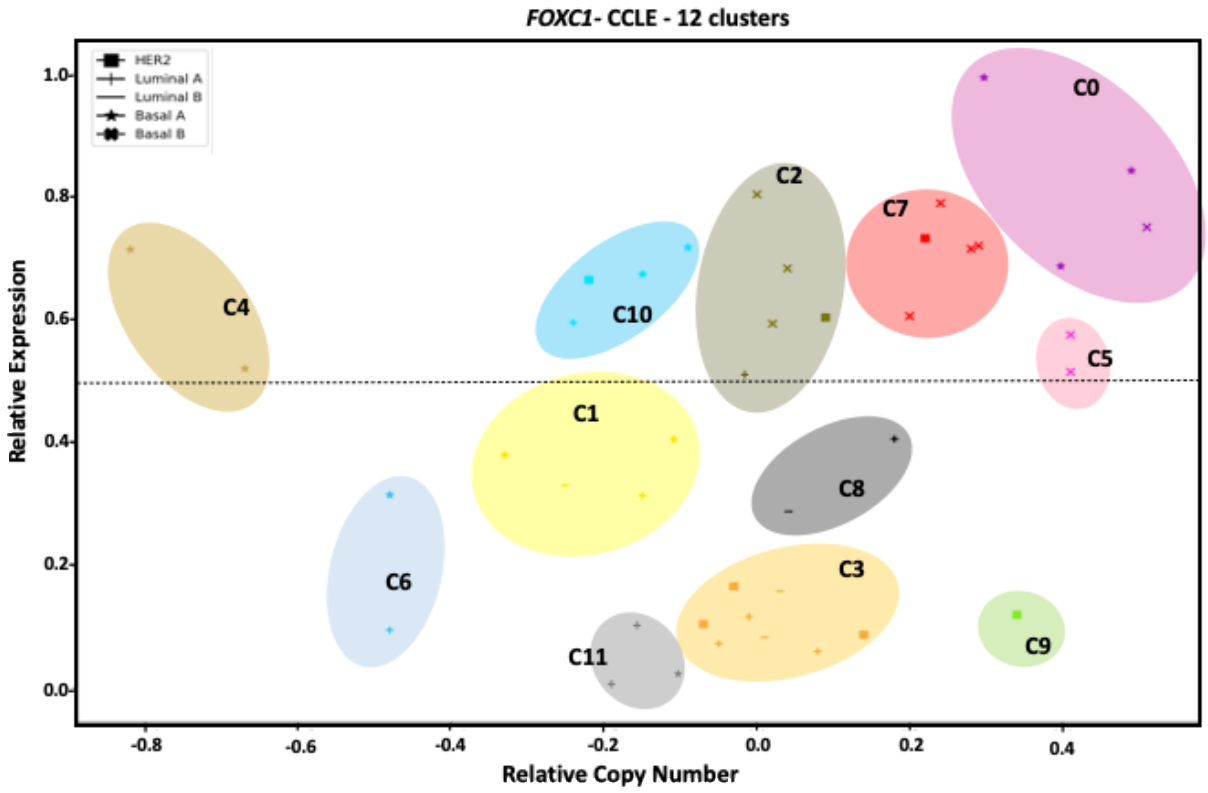

Figure 3.5: *FOXC1* expression varies among BC cell lines and is independent of its CNV.

FOXC1 mRNA and CNV data in 42 BC cell lines were obtained from Cancer Cell Line Encyclopedia online (CCLE) database [203,240]. (See methods section for more details). BC cell lines were further grouped as luminal A and luminal B—luminal— , HER2, and Basal A and Basal B—TNBC—as described in [204,205]. Unsupervised K-means clustering analysis shows different clusters of BC cell lines that have similar ranges of CNV but different *FOXC1* expression (i.e., the orange cluster vs the olive cluster, the yellow cluster vs the blue cluster, and the green cluster vs the purple cluster), indicating that *FOXC1* expression is independent of its CNV. The median of *FOXC1* expression values was used as a cut-off, where cell lines with values above the median were considered as high expression of *FOXC1* cell lines, while cell lines with *FOXC1*expression below the median were considered low expression of *FOXC1* cell lines.

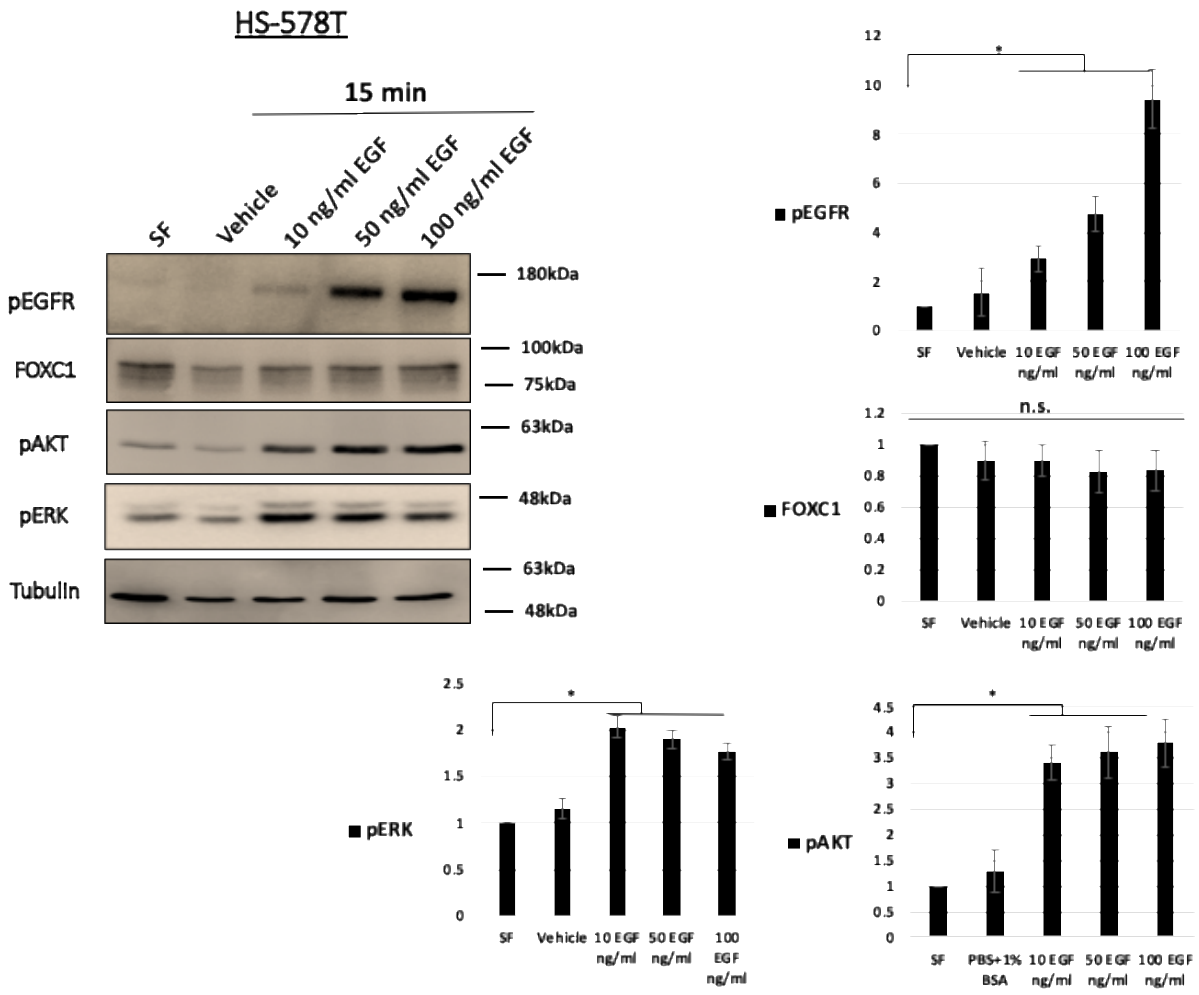

Figure 3.6: FOXC1 levels in TNBC cell line HS-578T cells are independent of short-term EGF stimulation.

A dose-course of EGF stimulation was applied to in HS-578T cells. Immunoblotting experiments were performed HS-578T after a dose course treatment as indicated. Antibodies that detect the phosphorylated tyrosine residue of EGFR (1173), the endogenous level of FOXC1, the phosphorylated Erk 1/2 (Thr 202, Tyr 204), and the phosphorylated Akt (Ser 473) were used. Samples were 16 hr serum starved. SF= culture media with serum Free. Vehicle = PBS+1%BSA. Tubulin was used as a loading control. Band intensities were normalized to that of Tubulin, then scaled to the SF control. Three independent experiments were used. Paired Student's t-test was applied for statistical analysis. Error bars represent standard error of the mean (SEM). *P < 0.05

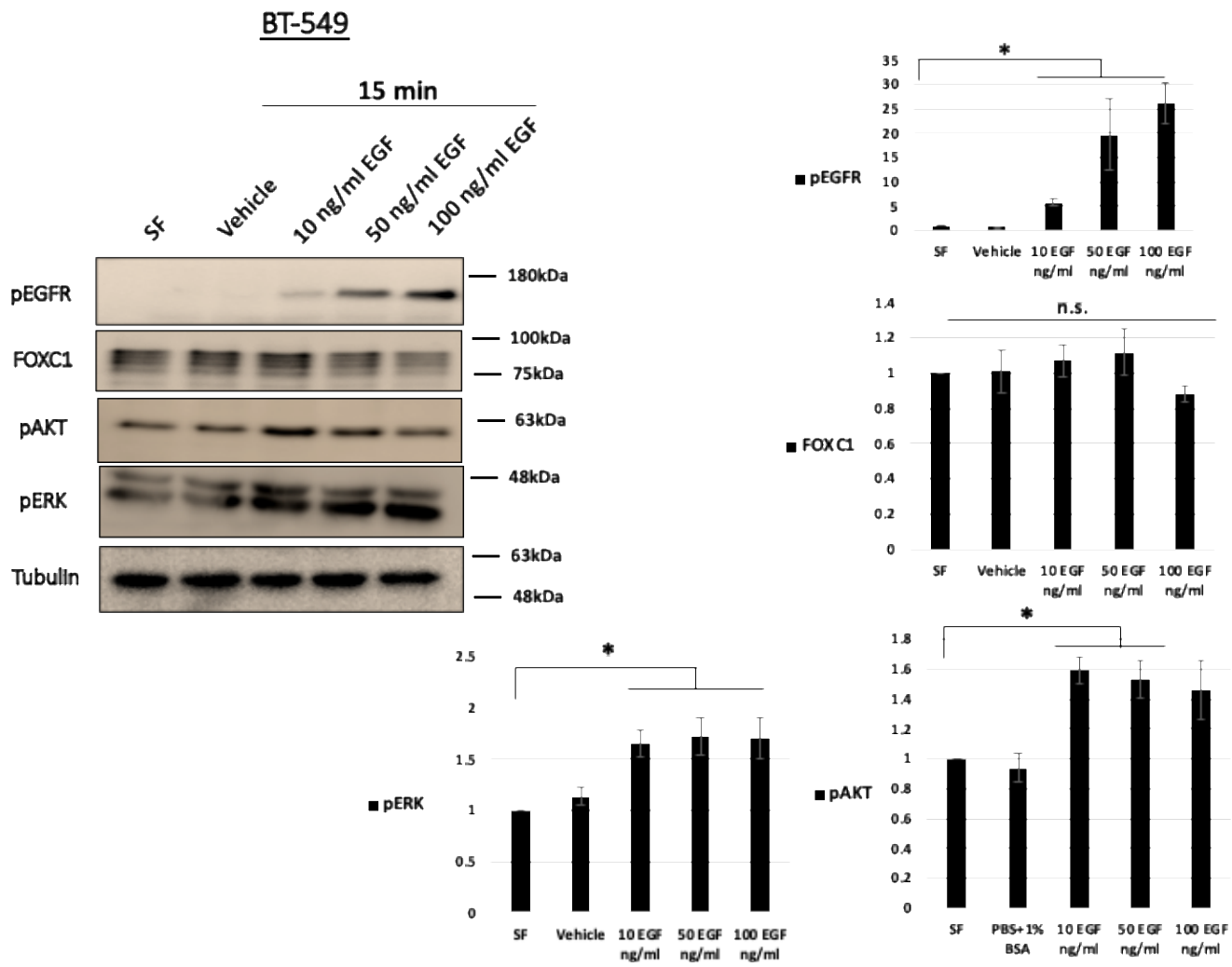

Figure 3.7: FOXC1 levels in TNBC cell line BT-549 cells are independent of short-term EGF stimulation.

A dose-course of EGF stimulation was applied to in BT-549 cells. Immunoblotting experiments were performed BT-549 after a dose course treatment as indicated. Antibodies that detect the phosphorylated tyrosine residue of EGFR (1173), the endogenous level of FOXC1, the phosphorylated Erk 1/2 (Thr 202, Tyr 204), and the phosphorylated Akt (Ser 473) were used. Samples were 16 hr serum starved. SF= culture media with serum Free. Vehicle = PBS+1%BSA. Tubulin was used as a loading control. Band intensities were normalized to that of Tubulin, then scaled to the SF control. Three independent experiments were used. Paired Student's t-test was applied for statistical analysis. Error bars represent standard error of the mean (SEM). *P < 0.05

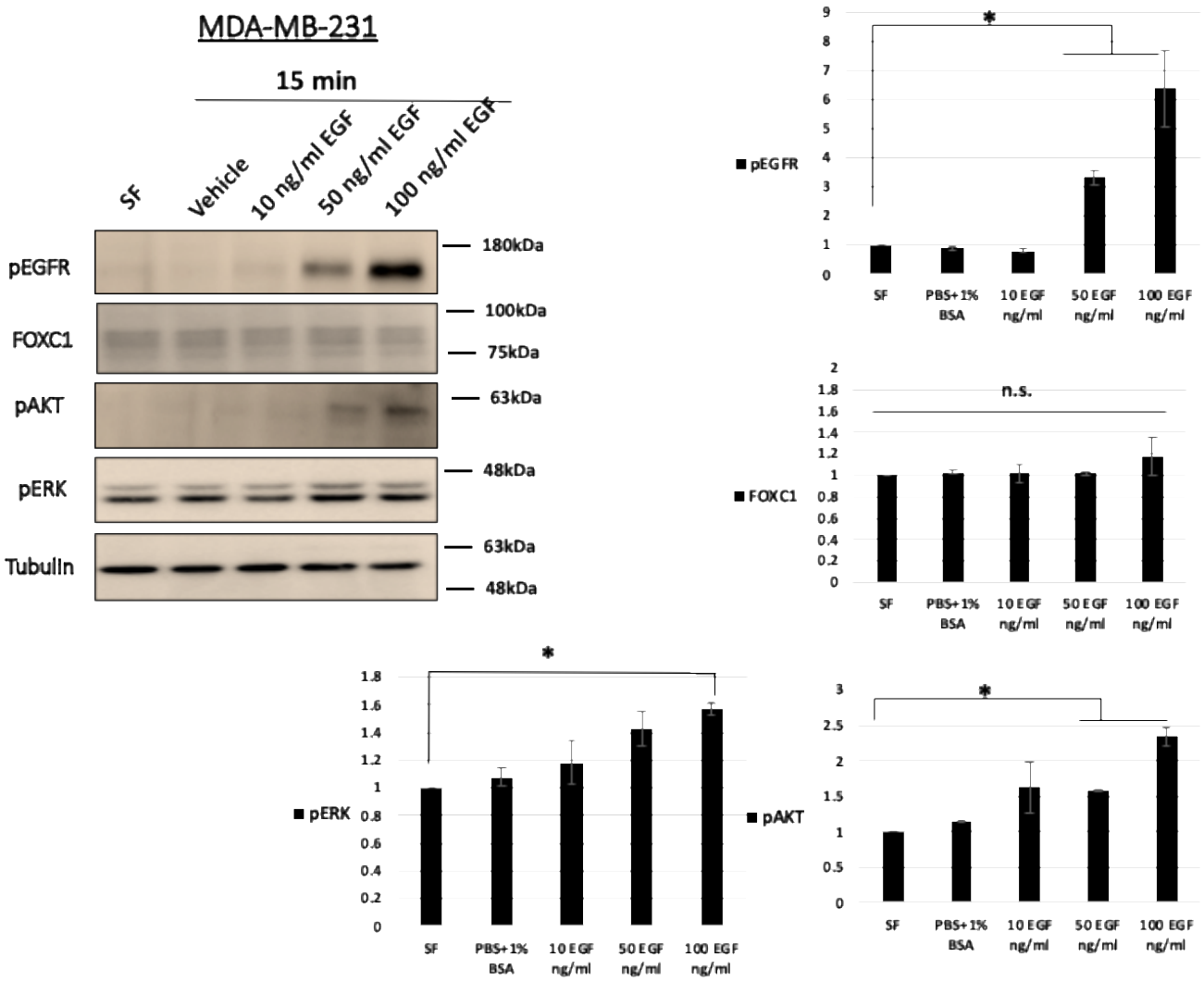

Figure 3.8: FOXC1 levels in TNBC cell line MDA-MB-231 cells are independent of short-term EGF stimulation.

A dose-course of EGF stimulation was applied to in MDA-MB-231 cells. Immunoblotting experiments were performed MDA-MB-231 after a dose course treatment as indicated. Antibodies that detect the phosphorylated tyrosine residue of EGFR (1173), the endogenous level of FOXC1, the phosphorylated Erk 1/2 (Thr 202, Tyr 204), and the phosphorylated Akt (Ser 473) were used. Samples were 16 hr serum starved. SF= culture media with serum Free. Vehicle = PBS+1%BSA. Tubulin was used as a loading control. Band intensities were normalized to that of Tubulin, then scaled to the SF control. Three independent experiments were used. Paired Student's t-test was applied for statistical analysis. Error bars represent standard error of the mean (SEM). *P < 0.05. n.s. not significant.

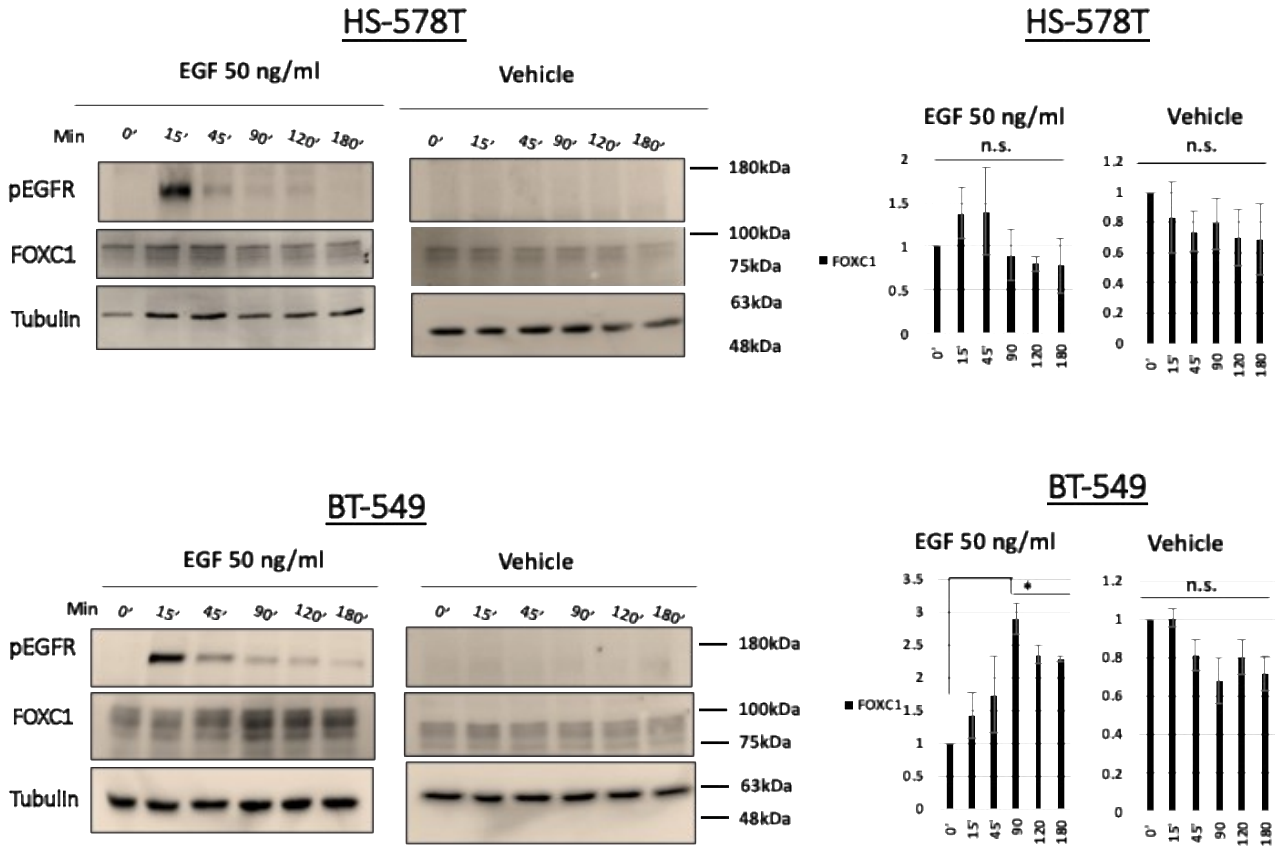

Figure 3.9: FOXC1 levels are upregulated in TNBC cell line BT-549 but not HS578T after a time-course of EGF stimulation.

A time-course of EGF (50 ng/ml) stimulation was applied to in HS-578T and BT-549 cells and an immunoblotting experiment were performed. Antibodies that detect the phosphorylated tyrosine residue of EGFR (1173) and the endogenous level of FOXC1 were used. Samples were 16 hr serum starved prior EGF stimulation. Vehicle = PBS+1%BSA. Tubulin was used as a loading control. Band intensities were normalized to that of Tubulin. Two independent experiments were used for HS-578T and three independent experiments were used for BT549). Paired Student's t-test was applied for statistical analysis. Error bars represent standard error of the mean (SEM). *P < 0.05. n.s. not significant.

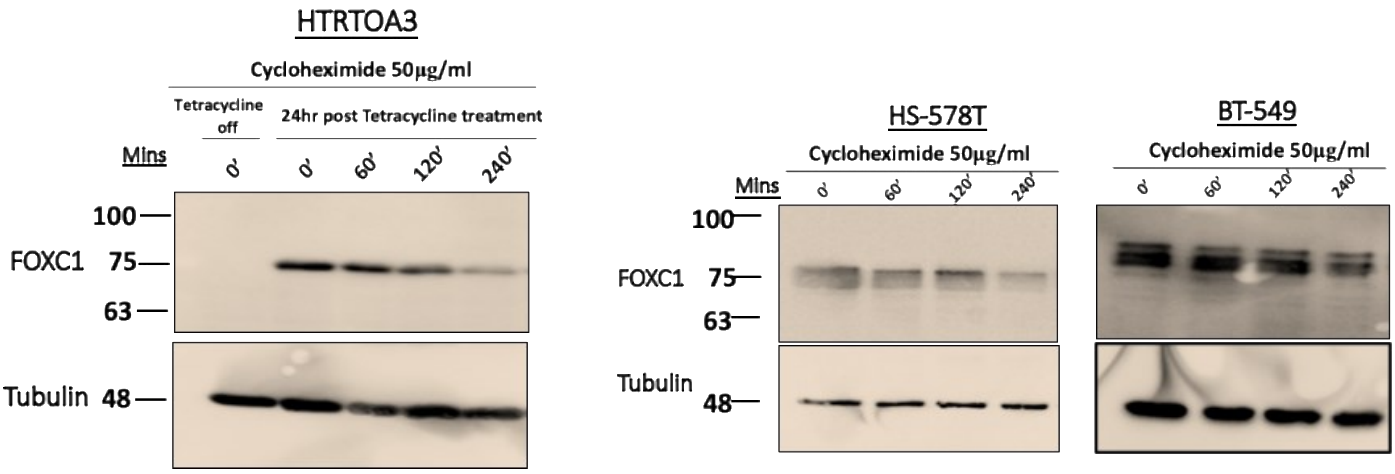
HTRTOA3
Cycloheximide 50µg/ml
Tetracycline off
24hr post Tetracycline treatment
Mins
0'
0'
60'
120'
240'
100
FOXC1
75
63
Tubulin
48
HS-578T
Cycloheximide 50µg/ml
Mins
0'
60'
120'
240'
100
FOXC1
75
63
Tubulin
48
BT-549
Cycloheximide 50µg/ml
0'
60'
120'
240'

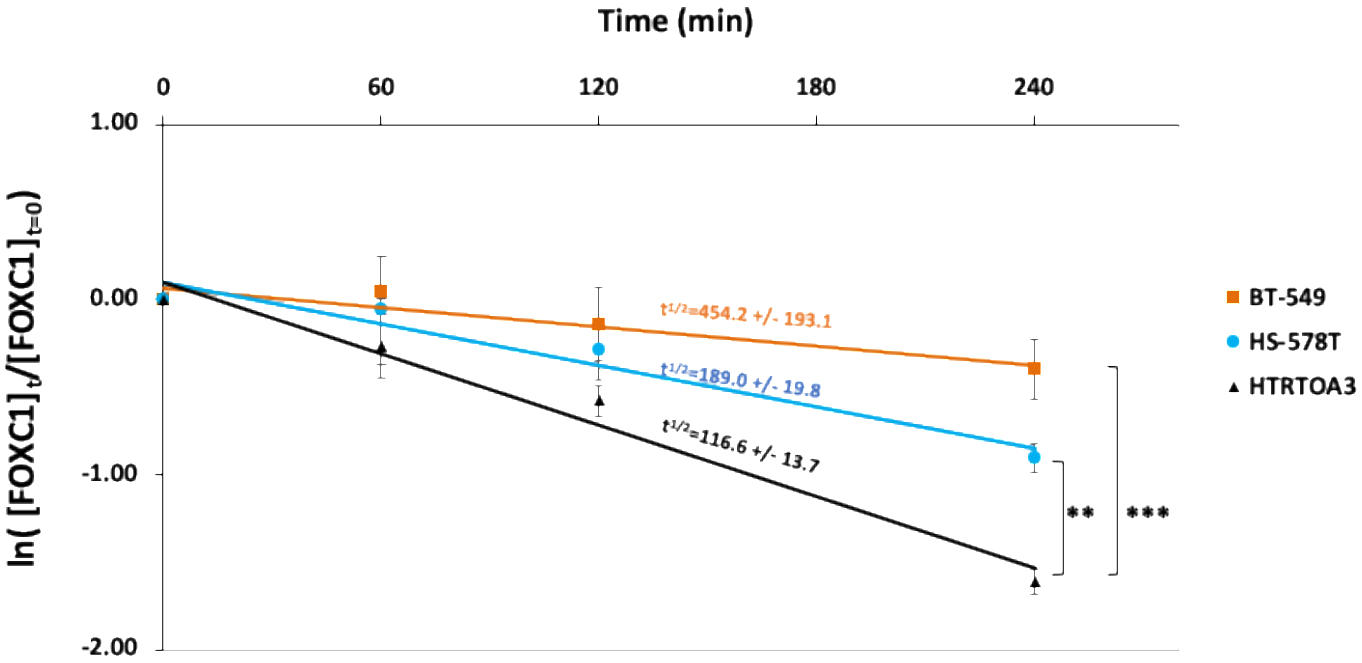
Time (min)
0
60
120
180
240
1.00
0.00
-1.00
-2.00
ln([FOXC1]t/[FOXC1]t=0)
t1/2=454.2 +/- 193.1
t1/2=189.0 +/- 19.8
t1/2=116.6 +/- 13.7
**
***
BT-549
HS-578T
HTRTOA3

Figure 3.10: FOXC1 protein half-life is longer in TNBC cell lines (HS-578T and BT-549).

A FOXC1 stable cell line (HTRTOA3) was generated with the T-REx(TM) system (Invitrogen) to create Tetracycline-inducible Xpress-FOXC1 protein expression. HTRTOA3 cells were treated with tetracycline 24 hr before cycloheximide treatment. Immunoblotting experiments were performed to measure FOXC1 levels after cycloheximide (50 μg/ml) treatment for the indicated time points. Band intensities were normalized to α-Tubulin, then scaled to 0' cycloheximide time point. The decay of FOXC1 followed first order kinetics. The slope of the decay line was calculated by standard linear regression, and the protein half-life was determined accordingly. Error bars represent standard deviation of the average of $\log_e x$ (x=time point) of 3 independent replicates. FOXC1 $t^{1/2}$= 116.6 +/- 13.7 mins, 189.0 +/- 19.8 mins, and 454.2+/- 193.1 mins in HTRTOA3, HS-578T, and BT-549 respectively. Paired t-test was conducted on the slopes of 3 independent experiments. **P < 0.01, ***P < 0.001.

Chapter 4

in silico analysis of FOX gene cluster—*FOXC1*, *FOXF2*, and *FOXQ1*— in Breast Cancer patients

If two oncogenes were insufficient to create cancers, then how many activated proto-oncogene and inactivated tumor suppressors were required?

—Siddhartha Mukherjee

Note: all experiments were carried out by Fahed Elian.

4.1 Chapter Abstract

Located within a 300 kilobase region of chromosome 6, FOXC1, FOXF2, and FOXQ1 (FOX cluster) are members of the forkhead box (FOX) transcription factor gene family that play critical roles in embryonic and adult development. In the last decade, several studies have proposed novel roles of the FOX cluster in breast cancer (BC) such as facilitating BC cells' invasion, metastasis, proliferation, chemoresistance, and stemness. However, the relationship of their copy number, mutations profile, and gene expression is yet to be investigated.

In this chapter, I examined the expression and copy number variations of the FOX gene cluster (*FOXC1, FOXF2,* and *FOXQ1*) on chromosome 6 in BC patients. Using the TCGA-BRCA database, I confirmed that mRNA expression for these three genes varied across BC subtypes. The FOX cluster high gene expression appears to overlap in basal BC, while FOX cluster low expression appears to overlap in HER2 and luminal BC. While some BC patients had amplification or deletion of the FOX cluster genes, I found that their mRNA expressions are independent of CNV. Moreover, *FOXF2* and *FOXQ1* expressions were moderately and positively correlated with each other in BC patients. As well, novel, *in silico*-predicted pathogenic mutations in *FOXC1* forkhead and activation domains were detected in several BC patients and in different BC subtypes.

My findings thus identified subpopulations within the BC patient cohort and across BC subtypes based on the FOX genes' mRNA expression. These subpopulations had high frequency of alteration of the FOX genes' expression, where 26.8% of BC patients had high expression of the FOX genes and 24.4% of BC patients had low expression of the FOX genes. These findings also highlight the complexity of the FOX cluster roles in BC subtypes where their expression

alteration varies across BC subtypes, and in some cases within the same BC subtypes, suggesting different roles of these transcription factors based on each BC subtype. Together, my findings suggest that the FOX cluster acts more like “onco-genes” in basal BC, but a “tumor-suppressor genes” in HER2 and luminal BC subtype.

4.2 Introduction

Triple negative breast cancers (TNBC) are defined as tumors that lack the overexpression of estrogen receptor (ER), progesterone receptor (PR), and human epidermal growth factor receptor 2 (HER2)[9]. Unlike most other BC subtypes, targeted agents specifically aimed at TNBC are not available since the molecular targets such as ER or HER2 that confirm responsiveness to the targeted therapies for HER2 and luminal BC are not expressed [34,182,272]. This lack of targeted therapies combined with the high morbidity associated with TNBC indicates that a better understanding of the molecular mechanisms of TNBC and the development of effective targeted therapy are urgently needed.

In the last two-decades, several studies have investigated TNBC heterogeneity based on gene expression profiling in order to improving its prognosis, diagnosis, and treatment [11,65,66,182,235,236,273,274]. Consequently, basal BC was suggested as an intrinsic subtype of TNBC. All basal BC are considered TNBC and approximately more than 80% of TNBC are of the basal BC subtype [182]. Basal BC is known to be phenotypically aggressive, highly metastatic, and histologically of high grade [275]. As a result, to improve basal BC prognosis in BC patients, screening of an additional immunohistochemistry markers such as basal cytokeratins (CK) CK5/6, CK14, CK17, and epidermal growth receptor (EGFR) to increase accuracy have been recommended [262,276,277]. However, there is no internationally accepted definition for basal BC, and there is no genetic test available in clinical practice to identify these tumors. In the last decade, growing evidence suggested a role for FOXC1, FOXQ1, and FOXF2 in BC, in particular, in basal BC [131,146–148,27867,178,279,280158,161,167,168,183,209,281].

The three related forkhead box transcription factor genes, FOXC1, FOXF2, and FOXQ1 (FOX cluster) are located within a 300 kilobase region of chromosome 6 with critical roles in embryonic and adult development. FOXC1 is directly linked to tumor metastasis and invasion through critical signaling pathways [144,145,147,149,150]. FOXC1 was suggested to be exclusively over-expressed in basal BC when compared to other BC molecular subtypes in multiple independent gene expression microarray datasets [147]. Dysregulation of FOXF2 has also been associated with BC and metastasis [67,172]. FOXF2 is specifically overexpressed in basal BC [173,174,279,280]. Moreover, FOXF2 levels were suggested to predict the prognosis, high risk of early-onset relapse and metastasis in BC patients [67]. Recent studies have revealed that FOXF2 plays an important role in basal BC development and progression through epithelial-to-mesenchymal transition (EMT), a biological process important in embryonic tissue development, wound healing, and tumorigenesis [177]. However, the question of whether FOXF2 promotes or inhibits EMT in basal BC is controversial and has been disputed, due to inconsistent findings among studies[178]. Lastly, FOXQ1 also has been associated with basal BC (chapter 2) [209,282]. Several studies have found that FOXQ1 plays an important role in BC stemness and chemoresistance [160], EMT transition, invasion, and metastasis [158].

There are no reports, however, that investigated the frequencies of FOX cluster genetic alterations such as mRNA level alterations, gene amplification, deletion, and mutations across basal BC patients or any other BC subtype patients simultaneously. Moreover, the impact of CNVs that involve the entire chromosome 6p25 FOX gene cluster on their mRNA levels across BC patient subtypes are not fully studied. Finally, the co-expression of these genes in basal BC and other BC subtypes and their mutation profiles are yet to be determined. In this chapter, I showed that the FOX cluster expression varies across BC subtypes. I also showed that high

mRNA levels are the predominant alterations of the FOX cluster in basal BC subtype in contrasts to luminal and HER2 subtypes where low expression of the FOX cluster overlapped with each other in BC patients. Although, CNV studies revealed DNA amplification and deletion of the entire FOX cluster in basal, HER2, and luminal BC patients, correlation studies showed that the FOX cluster genes' expressions were independent of their CNV. Moreover, FOXC*1* mRNA levels had a weak correlation with either *FOXF2* or *FOXQ1*. On the other hand, *FOXF2* and *FOXQ1* mRNA levels were moderately and positively correlated in BC patients. Thus, I hypothesized that investigating he high or low expressions of the FOX cluster genes simultaneously could reveal distinct BC patients' groups within BC subtypes that may therefore have more aggressive BC phenotype.

4.3. Materials and Methods

4.3.1. *FOXC1, FOXF2, and FOXQ1* expression, copy numbers, and sequence analyses

The PanCanAtlas 2018 of the TCGA-BRCA https://gdc.cancer.gov/about-data/publications/pancanatlas [283] were used in this Chapter and it was obtained from cBioPortal website https://www.cbioportal.org/ [284,285]. RNAseq mRNA data were used for expression analysis of *FOXC1, FOXF2, and FOXQ1* in the TCGA-BRCA BC patients. The mRNA z-scores represent the relative expression of each gene in a tumor sample to each gene's expression distribution in all tumor samples. Therefore, z-score represents the standard deviations away from the mean of each gene expression in all samples. DNA sequence analysis for mutations in the TCGA-BRCA data was preformed using the TCGA-BRCA whole-exome DNA sequence data. TCGA-BRCA Copy number data were generated by the GISTIC2 from "masked copy number segment" files, and numeric copy number variation values followed a "noise" cut-off

values as numbers smaller than -0.3 =”loss“ (-1) numbers more than 0.3=”gain” (+1) and numbers between -0.3 and 0.3 are “neutral”. cBioPortal apply +/- 2 which exceed the high-level thresholds, where copy numbers variation larger than 2 is considered “amplified” or smaller than -2 is “deep deletion” (probably homozygous deletion). I used Oncoprint tool on cBioPortal to detect *FOXC1, FOXF2, and FOXQ1* genes amplification and deep deletions in (Figure 4.1). cBioPortal automatically generated the threshold cut-off values for these genes copy numbers in each of 1084 TCG-BRCA BC. Therefore, this method would not detect copy number gain or hemizygous deletion for *FOXC1, FOXF2, and FOXQ1* genes across all BC patients and would only detect “amplification” or “deep deletions” based on the cut off value automatically used by cBioPortal. The TCGA-BRCA copy number data that were generated using GISTIC are available at https://docs.gdc.cancer.gov/Data/Bioinformatics_Pipelines/CNV_Pipeline/.

mRNA z-scores, gene expression heat map, copy number, and sequence data analysis were generated using the Oncoprint tool the online database website cBioPortal for cancer genomics [284,285]. cBioPortal used data of tumor samples (n=1084) of the the PanCanAtlas 2018 of the TCGA-BRCA https://gdc.cancer.gov/about-data/publications/pancanatlas [283]. More details on cBioPortal’s datasets and tools can be found in https://www.cbioportal.org/ [284,285].

4.3.2 Copy number variation (CNV) and mRNA correlation studies

TCGA-BRCA mRNA z-scores (RNAseq V2 RSEM) of *FOXC*1, *FOXF2, and FOXQ1* in each sample relative to diploid samples across the 1068 patient samples were used for this analysis. Log2 copy number values for *FOXC*1, *FOXF2, and FOXQ1* were generated using Affymetrix SNP6. Genes’ mRNA z-scores and Log2 copy number values were obtained from the

PanCanAtlas 2018 of the TCGA-BRCA https://gdc.cancer.gov/about-data/publications/pancanatlas [283] using the cBioPortal https://www.cbioportal.org/ [284,285].

4.3.3 Co-expression analysis of *FOXC1, FOXF2,* and *FOXQ1*

FOXC1, FOXF2, and *FOXQ1* mRNA expression correlation was analyzed in the TCGA-BRCA database using the co-expression analysis tool on cBioPortal. Spearman and Pearson were used for correlation analysis. *FOXC1, FOXF2,* and *FOXQ1* log2 mRNA values of normalized RSEM RNAseq V2 [286] in 1082 patient and normal samples were obtained from the from The PanCanAtlas 2018 of the TCGA-BRCA https://gdc.cancer.gov/about-data/publications/pancanatlas [283].

4.4 Results

4.4.1. *FOXC1, FOXF2, and FOXQ1* genetic alterations in basal BC and other BC subtypes

In order to study *FOXC1, FOXF2, and FOXQ1* (FOX cluster) genetic alterations across BC subtypes, I investigated simultaneously for all three genes, the features of mutations, amplification, deletion, and expression in 1084 BC patient samples and normal breast tissues that were obtained from TCGA-BRCA database [283]. (Figure 4.1). The BC intrinsic subtypes in these samples are basal, 171 samples (15.8%); luminal A, 499 samples (46.0%); luminal B, 197 samples (18.2%); HER2, 78 samples (2%) and normal (normal-like BC), 36 samples (3.3%); and 103 (9.5%) samples that did not match any of the BC subtype criteria.

I found high levels of *FOXC1* and *FOXQ1* expressions in basal BC compared to other BC subtypes (Figure 4.1). *FOXC1* and *FOXQ1* were highly expressed in 87% and 41% of basal BC patient samples respectively (Figure 4.1). This is consistent with my RT-qPCR findings where

FOXC1 and *FOXQ1* expressions in basal (TNBC) BC patient samples and cell lines were higher compared to other BC subtypes (chapter 3 and 2 respectively). Moreover, consistent with my findings of low expressions of *FOXC1* in luminal patient samples and cell lines (Chapter 3), *FOXC1* expression appeared at low levels in 9.5% and 32% in luminal A and B BC patient samples respectively (Figure 4.1). Similarly, *FOXQ1* appeared at low levels in 14.5% and 31.5% in luminal A and B BC subtypes respectively (Figure 4.1), which is also consistent with my findings of low levels of *FOXQ1* in luminal BC patient samples compared to normal breast tissue as well as to other BC subtypes (chapter 2). I also found that *FOXF2* expression appeared at high levels in 22% in basal BC but also at low levels in 19% of the same BC subtype cohort (Figure 4.1). Moreover, *FOXF2* mRNA expressions also varied within the luminal A BC patient samples, where high or low levels of *FOXF2* were detected in 11% and 10% of the luminal A BC group respectively (Figure 4.1). Taken together, my findings of the FOX cluster expression in the TCGA-BRCA patient samples are in line with my findings presented in Chapters 2 and 3. Moreover, my findings in (Figure 4.1) highlight the complexity of the FOX cluster roles in BC subtypes where their expression alteration varies across BC subtypes, and in some cases within the same BC subtypes, suggesting different roles of these transcription factors across BC subtypes.

In order to understand the genetic alterations of the FOX cluster, such as their frequencies and type of genetic alterations across BC patients, a summary of my findings of the FOX cluster genes' alterations in Figure 4.1 is presented in Figure 4.2. The combined frequencies of FOX cluster alterations, including gene expression alterations (high and low), gene amplification, gene deletion, and mutations were detected in 54% of 1084 patient cases. Notably, the frequencies of FOX cluster altered expression levels were the highest compared to copy number variation and mutation frequencies across BC patients, where high levels and low levels of the FOX cluster

mRNA were found in 27% and 24% of all patient samples respectively (Figure 4.2). On the other hand, low frequencies of FOX cluster CNV such as amplification and deletion were found in 0.7% and 0.8% of BC patient samples, and multiple alterations such as high/low mRNA levels and CNV were detected in only 1.75% of total BC patients (Figure 4.2). The latter suggests that the altered mRNA expressions of FOX cluster in BC patients may not be the result of FOX cluster CNV. At each gene level, *FOXC1*, *FOXF2*, and *FOXQ1* gene alterations' frequencies were 30%, 28%, and 30% of 1084 patient samples (Figure 4.1 and Figure 4.2). In these patients, the highest alteration frequencies were of *FOXC1* mRNA high expression (16% of all cases) and low levels of mRNA expression of *FOXF2* (14% of all cases) and *FOXQ1* (17% of all cases) (Figure 4.2).

4.4.2. Relation of FOX cluster copy numbers in BC patients to mRNA expression levels

I examined whether FOX cluster expressions are correlated with their CNV in BC patients. Therefore, Spearman and Pearson analysis were conducted to examine the correlation of copy numbers and mRNA levels in 1084 BC and normal tissues. I first investigated the copy numbers of *FOXC1* and their impact on *FOXC1* mRNA levels. Spearman and Pearson analyses showed a weak correlation between *FOXC1* CNV and mRNA expression levels (Figure 4.3; Spearman $r=0.15$, $n=1068$, $p<0.0001$; Pearson $r=0.26$, $n=1068$, $p<0.0001$; note: cBioPortal website generated the p values). This is in line with my K-means findings in chapter 3 where multiple clusters of BC cell lines with variable *FOXC1* mRNA levels but similar CNV (Chapter 3).

I then examined *FOXF2* and *FOXQ1* CNV's impact on their expression. I found that there was no correlation between *FOXF2* CNV and mRNA levels in BC patient and normal samples (Figure 4.4 A; Spearman $r=-0.04$, $n=1068$, $p=0.198$; Pearson $r=-0.04$, $n=1068$, $p=0.181$). Similarly, *FOXQ1* CNV had no impact on *FOXQ1* mRNA levels in BC subtype and normal samples (Figure

4.4 B; Spearman r=0.01, n=1068, p=0.742; Pearson r=0.05, n=1068, p=0.119). The latter is consistent with my findings in chapter 2 where I showed that *FOXQ1* mRNA levels are not impacted by *FOXQ1* CNV in BC cell lines. Taken together, FOX cluster expression is not correlated with their CNV in BC patients.

Finally, I examined whether FOX cluster genes are co-expressed in BC patients. Overlap of FOX cluster expression was found in BC patients as shown in Figure 4.1. Therefore, the co-expression of *FOXC1* and *FOXF2,* or *FOXC1* and *FOXQ1,* or *FOXF2 and FOXQ1* mRNA were examined in 1082 BC patient and normal samples using Spearman and Pearson correlation analyses (Figure 4.5). I found a weak correlation between *FOXC1*and *FOXF2* mRNA levels (Figure 4.5; Spearman r=0.31, n=1082, p<0.0001; Pearson r=0.18, n=1082, p<0.0001), and between *FOXC1* and *FOXQ1* (Figure 4.5; Spearman r=0.34, n=1082, p<0.0001; Pearson r=0.34, n=1082, p<0.0001). However, a moderate correlation between FOXF2 and FOXQ1 mRNA levels was found in BC patient and normal samples (Figure 4.5; Spearman r=0.58, n=1082, p<0.0001; Pearson r=0.54, n=1082, p<0.0001).

Taken together, my findings showed that the FOX cluster mRNA levels were not impacted by CNV and a weak to a moderate correlation between *FOXC1, FOXF2 and FOXQ1* mRNA levels in BC patients.

4.4.3. FOXC1 mutations in the TCGA-BRCA patients

I next examined whether the TCGA-BRAC patients harbor DNA mutations of the FOX cluster genes. I found no mutations of *FOXF2* or *FOXQ1* in BC patients. I showed in Chapter 3 that DNA sequencing studies of *FOXC*1 in basal (TNBC) BC cell lines showed no pathogenic mutations. Interestingly, however, I found 3 mutations in the *FOXC1* gene in three BC tumor

samples with unknown significance that were not previously reported. These mutations are 2 missense mutations c.373A>G (p.S125G) and c.1628C>T (p.S543F), and c.258delinsTAA (p.I87Kfs*16) truncating mutation (Figure 4.6). The 2 mutations p.S125G and p.I87Kfs*16 are in the forkhead domain of FOXC1, a domain known to be critical for FOXC1 ability to binding to DNA and activate or inactivate genes. The p.S543F mutation is located in the activation domain at the C-terminal of FOXC1 protein. I further examined these mutations in *in silico* bioinformatics programs such as sorting intolerant from tolerant (SIFT) and polymorphism (PolyPhen-2) that predict DNA mutation pathogenicity [287]. SIFT predicted deleterious impact and PolyPhen-2 predicted a probably damaging impact for all tested mutations, p.S125G, p.S543F, and p.I87Kfs*16.

4.5. Discussion

Roles for each of the genes, within the *FOXC1*, *FOXF2*, and *FOXQ1* (FOX) gene cluster in BC have been previously suggested [67,131,146–148,158,161,167,168,178,183,209,278–281]. In particular, different studies have indicated several roles of these genes in basal BC cells' stemness, invasion, metastasis, prognosis, and treatment [144,145,147,149,150,158,160,173,174,177,209,279,280,282]. However, the combined expression and CNV of these three genes in basal BC or other subtypes have not been investigated before. Therefore, in this chapter, I examined the FOX cluster's genetic alterations such as their mRNA level alterations, gene amplification/deletion, and DNA mutations in the TCGA-BRCA database.

In order to have a fulsome picture of the FOX cluster genetic alterations in BC subtypes, combined data on mRNA expression levels, gene amplification and deletion of the FOX cluster genes were investigated in 1084 BC patients from the TCGA-BRCA dataset [283]. In this thesis,

separately, *FOXC1* and *FOXQ1* genetic alterations (mRNA levels and CNV) in BC subtypes were investigated in Chapter 3 and Chapter 2 respectively, where I found *FOXC1* and *FOXQ1* mRNA levels were higher in basal BC compared to other subtypes. I confirmed these findings in expanded panel of BC patients (1084 patient samples) in which high levels of *FOXC1* and *FOXQ1* expressions in basal BC compared to other BC subtypes were found (Figure 4.1). Moreover, I also found low expressions of *FOXC1* and *FOXQ1* in luminal and HER2 BC subtypes (Figure 4.1), which also confirms my findings of low expressions of *FOXC1* and *FOXQ1* in luminal and HER2 BC subtypes (Chapter 3 and 2).

Although, *FOXF2* mRNA levels and CNV were not investigated in Chapters 2 or 3, their mRNA levels and CNV in BC patients were investigated in this chapter. The investigation of *FOXF2* mRNA levels and CNV were included for the following reasons: (1) an established role of *FOXF2* in BC has been previously proposed by other groups [67,172–174,279,280] (2) a selective maintaining for more than 500 million years of the FOX cluster genes—*FOXC1*, *FOXF*2, and *FOXQ1*—have been previously suggested, and that their sequential expression pattern is critical for vertebrate development [69,74,288,289] and (3) limited and conflicted studies have investigated the mRNA expression levels, gene amplification/deletion, and mutations of *FOXF2* across all BC subtypes [171]. Therefore, investigation of *FOXF2* genetic alterations in BC subtypes and in relation to *FOXC1* and *FOXQ1* are warranted.

Interestingly, I found that *FOXF2* expression appeared at high levels in some of basal BC patient samples but also at low levels in other patient samples within the same BC subtype cohort (Figure 4.1). Moreover, *FOXF2* mRNA levels also varied within the luminal A BC cohort (high 11% vs low 10%; Figure 4.1). However, *FOXF2* expression appeared to be mostly at low levels in HER2 and luminal B patient samples (low 9/78 vs high 4/78 and low 45/197 vs high 9/197

respectively; Figure 4.1). My findings regarding *FOXF2* mRNA levels in BC subtypes are in concordance with other literature data [67,173,279,280,290]. Although, both high and low levels of *FOXF2* mRNA were reported in basal BC, more studies support that *FOXF2* mRNA levels are low [67,279,280,290] than high [173] in basal BC. Moreover, my findings of low expression of *FOXF2* in luminal and HER2 were in line with those of others who had also investigated *FOXF2* expression in BC cell lines [173]. However, in the discrepant study [173], the authors did not investigate variation of *FOXF2* mRNA expression across luminal subtypes A and B (Figure 4.1). Their results differ from mine, where in luminal BC I found low and high mRNA levels of *FOXF2* and they found only low mRNA levels of *FOXF2*, could perhaps result different experimental designs. I used, RNAseq data of 1084 (Luminal A=499, Luminal B= 197 samples) BC patients for *FOXF2* mRNA analysis, where the authors of [173] used a limited number of luminal cell lines (n=7) to analyze *FOXF2* expression, without further subtyping of the luminal cell lines into luminal A and B. Thus, the limited number of luminal cell lines used in [173] and the lack of further grouping of luminal cell lines into luminal A and B might undermined the variation of *FOXF2* expression in luminal BC. It was also suggested that low expression of *FOXF2* in BC is due to epigenetic regulation of *FOXF2,* such as DNA methylation, that supresses its transcription, and consequently its expression [290] [173]. Hence, epigenetic regulation appears to be one of the most thoroughly investigated mechanism that suppress the FOX cluster expressions in BC [265–268].

Another notable finding in (Figure 4.1) that some patients showed an overlap of mRNA expressions of the three genes of the FOX cluster in all BC subtypes. The majority of the patients that had an overlap of high expressions of *FOXC1, FOXF2, and FOXQ1* were of the basal BC subtypes, indicating that high expressions of these genes simultaneously maybe be critical for

these BC subtypes. On the other hand, overlap of low expressions of the three genes were found in luminal A and B patients, suggesting that the FOX cluster is more likely to act as a tumor suppressor in luminal BC. The latter could be supported by the findings that low expression of each of the FOX cluster genes is associated with poor prognostic outcomes. Which was suggested before for low expression of *FOXC1* in luminal [252], low expression of *FOXF2* in luminal and HER2 [67,173,280] and low expression of *FOXQ1* (Chapter 2). For future research, investigating the mechanisms that drive high (in basal) or low (in luminal and HER2) or variable expression (variable expressions were found for *FOXF2* or for *FOXQ1* within the same BC subtype in figure 4.1) of the FOX cluster—by focusing on stratifying the BC subtype cancer stages and treatment history—could reveal better understanding of the variation of the FOX cluster expression in BC subtypes and across BC patients.

CNV (amplification and deletion) of the FOX cluster were detected in BC subtypes (Figure 4.1). Moreover, these CNV overlapped for the three genes in most of the patient where they were detected (Figure 4.1). However, I found that CNV of the FOX cluster incidence frequencies were low (0.7% and 0.8% amplification and deletion across BC patients respectively, Figure 4.2) and that alterations of the mRNA levels of the FOX cluster are the most common genetic alterations in BC patients compared to CNV and gene mutations (Figure 4.2)—of note, the CNV data of the FOX cluster were obtained from the TCGA-BRCA 2018 study [283] and via cBioPortal. CNV were generated using GISTIC algorithm (see method section). The cBioPortal uses specific thresholds for the GISTIC data to detect gene amplification (high level of amplification) and gene deep deletion (probably homozygous deletion). Therefore, gene copy number gain or hemizygous deletion were not reported in Figure 4.1.

Furthermore, my studies of CNV and mRNA expression showed that the FOX cluster mRNA expressions is not correlated with its CNV in BC subtypes (Figure 4.3 and 4.4). This is consistent with my previous results where I found no correlations between *FOXQ1* mRNA expression and its CNV and between *FOXC1* expression and its CNV in BC cell lines (Chapter 2 and 3 respectively).

There are no studies in the literature that have investigated the intra-gene relationship of the mRNA expressions between the FOX cluster genes in BC. In order to understand the relationship between the genes of the FOX cluster, I conducted correlations studies of their co-expressions in BC patients. As shown in Figure 4.5, the expression of *FOXC1* mRNA had a weak but significant correlation with either the expression of *FOXF2* or *FOXQ1* mRNA in BC patients. However, the expressions of *FOXF2* and *FOXQ1* had a moderate but significant correlation where their mRNA levels were positively correlated across BC patients (Figure 4.5). This directly contrasts the findings that *FOXF2* negatively regulates the expression of *FOXQ1* in basal BC cell lines, where exogenous overexpression of *FOXF2* in basal BC cell lines reduced the mRNA levels of *FOXQ1* [161]. However, the same group also reported that they did not find a negative correlation between *FOXF2* and *FOXQ1* mRNA expressions when it was investigated in basal BC patients—the negative correlation was only and exclusively observed in basal cell lines (n=2) after exogenously overexpressing or downregulating the expression of *FOXF2* [161]. The latter research group suggested sequential expression and chromatin modifications such as DNA methylation and acetylation (epigenetic regulations that are critical for transcription machinery deactivation and activation) to support the findings of no negative correlation between *FOXF2* and *FOXQ1* in basal BC patients. Nevertheless, this once again highlights the

importance of using an expanded panels of BC patient samples and cell lines in order to have a better understating of the complex role that transcription factors play in BC.

The final notable findings in this chapter were the mutations in the *FOXC1* DNA forkhead and activation domains (Figure 4.6). As shown in Chapter 3, DNA sequence analysis of *FOXC1* in basal (TNBC) cell lines (n=3) showed no pathogenic mutations in any of the cell lines. However, I found 2 missense mutations c.373A>G (p.S125G) and c.1628C>T (p.S543F), and 1 truncating mutation c.258delinsTAA (p.I87Kfs*16) in 3 different patient samples in the TCGA-BRCA patient dataset (Figure 4.6). The p.I87Kfs*16 and p.S125G mutations were in the forkhead domain of *FOXC1*, a DNA-binding domain of 110 amino acids that is critical for FOXC1 function [131]. The p.S543F mutation was found in FOXC1 activation domain at the C-terminal—a domain that is critical for the transactivation of FOXC1 [83,131]. Although *in silico* analysis using SIFT and PolyPhen-2 predicted that these three mutations are pathogenic, to validate the impact of these mutations on FOXC1 function, wet-lab experiments are needed. However, a previous study from our lab showed that using SIFT and PolyPhen-2 predictions for *FOXC1* mutations are very likely to be specific and sensitive [287]. Moreover, previous studies from our laboratory showed that missense and nonsense mutations within the *FOXC1* forkhead domain can alter FOXC1 translocation to the nucleus, ability to bind to DNA, activate transcription, and bind to other proteins, all of which were shown to reduce FOXC1 function [99,100,104,131]. Therefore, further analysis of these p.I87Kfs*16, p.S125G, p.S543F mutations could reveal novel mechanism/s of FOXC1's role in BC.

In conclusion, I showed in this chapter that the FOX cluster mRNA levels are altered in BC patients and that their mRNA alteration in BC is subtype dependent. FOX cluster high and low levels of mRNA were detected in 26.8% and in 24.4% of BC patients respectively. Most

importantly, FOX cluster mRNA expression was high in basal BC but low in luminal and HER2 BC suggesting a harmonized dual role of the FOX cluster in different BC subtypes. Since several studies have suggested independent roles for each of *FOXC1, FOXF2, and FOXQ1* in chemoresistance [68,256,265,280], my findings shed the light on the importance of investigating these genes simultaneously in BC; patients who have altered expression of *FOXF2, FOXC1,* and *FOXQ1* may have higher resistance to BC therapeutics compared to patients who do not have an altered expression of the FOX cluster. Further investigation of the latter could be fruitful.

4.6 Figures

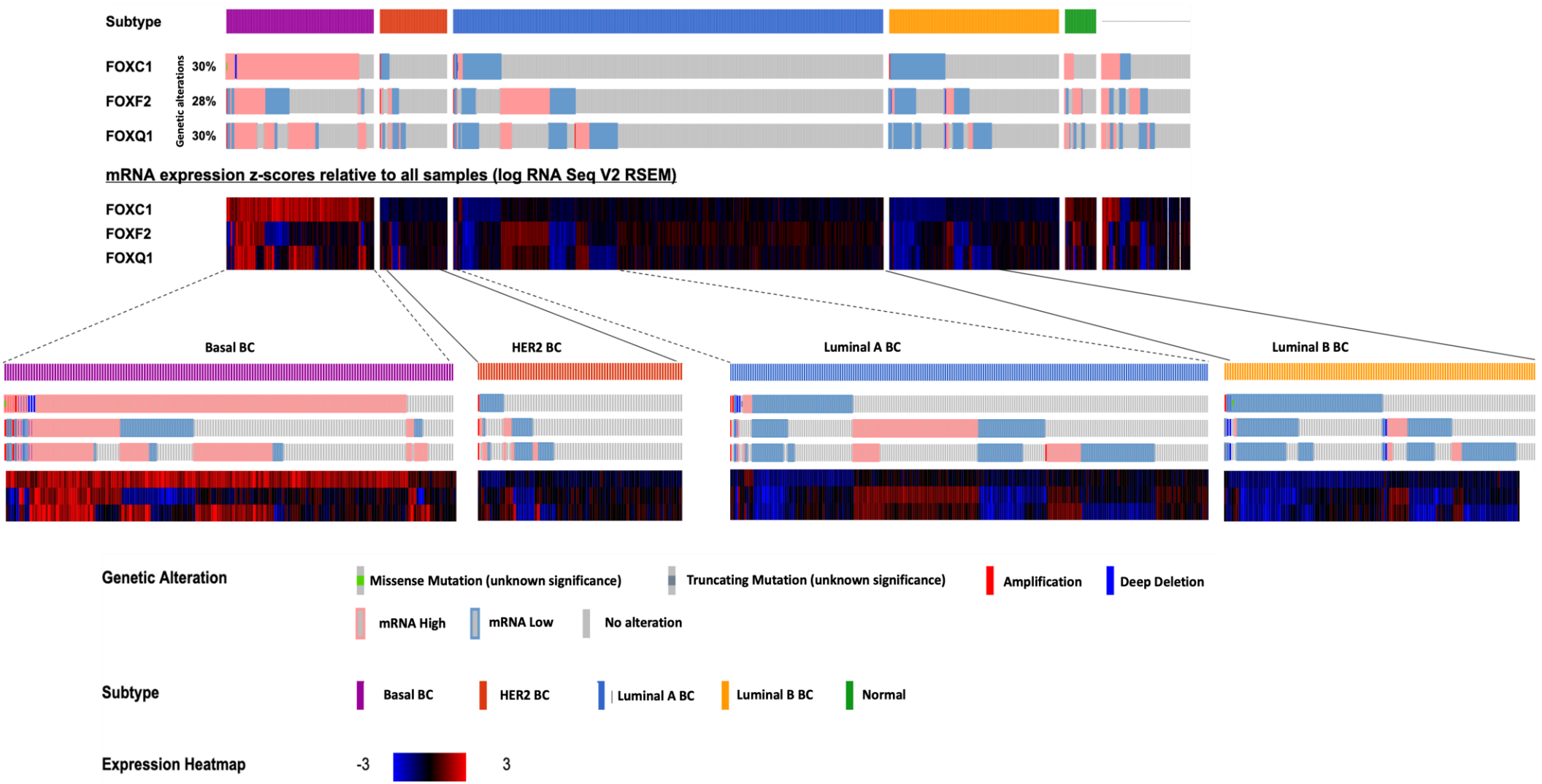
Subtype
FOXC1
FOXF2
FOXQ1
Genetic alterations
30%
28%
30%
mRNA expression z-scores relative to all samples (log RNA Seq V2 RSEM)
FOXC1
FOXF2
FOXQ1
Basal BC
HER2 BC
Luminal A BC
Luminal B BC
Genetic Alteration
Missense Mutation (unknown significance)
Truncating Mutation (unknown significance)
Amplification
Deep Deletion
mRNA High
mRNA Low
No alteration
Subtype
Basal BC
HER2 BC
Luminal A BC
Luminal B BC
Normal
Expression Heatmap
-3
3

Figure 4.1: *in silico* analysis of *FOXC1, FOXF2, and FOXQ1* (FOX cluster) genetic alterations in the TCGA-BRCA dataset.

FOX cluster's genetic alterations (high and low levels of mRNA, gene amplification, deletion, missense and truncating mutations) were detected in 54% of all BC patient samples (580/1084), where each *FOXC1*, *FOXF2*, and *FOXQ1* is altered in 30%, 28%, and 30% in all BC patients respectively. FOX cluster genes are highly expressed in basal BC patient samples, in particular, *FOXC1* is highly expressed in a majority of basal BC patients compared to other BC subtypes. On the other hand, low expression of the FOX cluster is detected in many of the luminal and HER2 BC patients. Low or high expressions of *FOXF2,* and low or high expression of *FOXQ1* were detected in different patients for the same BC subtype, highlighting the complexity of these transcription factors' roles in BC subtypes. Two DNA missense and one truncating mutations were found in *FOXC1* in 3 different BC patients. RNAseq and whole-genome sequencing data of 1084 BC patients samples from the the PanCanAtlas 2018 of the TCGA-BRCA https://gdc.cancer.gov/about-data/publications/pancanatlas [283] were used in this analysis. 1084 samples BC subtypes are luminal A, n=499; luminal B, n=197; basal, n=171; HER2, n=78; normal, n=36, not applicable; n=103. Colours presentation of genetic alterations: light red, mRNA high; light blue, mRNA low; dark red, amplification (more copies, indicates high-level of amplification); dark blue, deep deletion (possibly a homozygous deletion), middle green square, missense mutation; middle grey square, truncating mutation; grey, no alterations. Colors for subtypes: purple, basal BC; red, HER2 BC; blue, luminal A; yellow, luminal B; green, normal samples (although cBioPortal indicate that they do not store any adjacent normal data in their data base, however when I applied the PAM50 subtype filter, results gave back normal as one of the subtypes. I think the normal samples here are referring to Normal-like BC). *FOXC1*, *FOXF2*, and *FOXQ1* mRNA expression z-scores relative to all samples (log RNA Seq V2 RSEM) were used to generate the gene expressions' heatmap. This figure was generated and modified using Oncoprint tool, cBioPortal for cancer genomics [284,285].

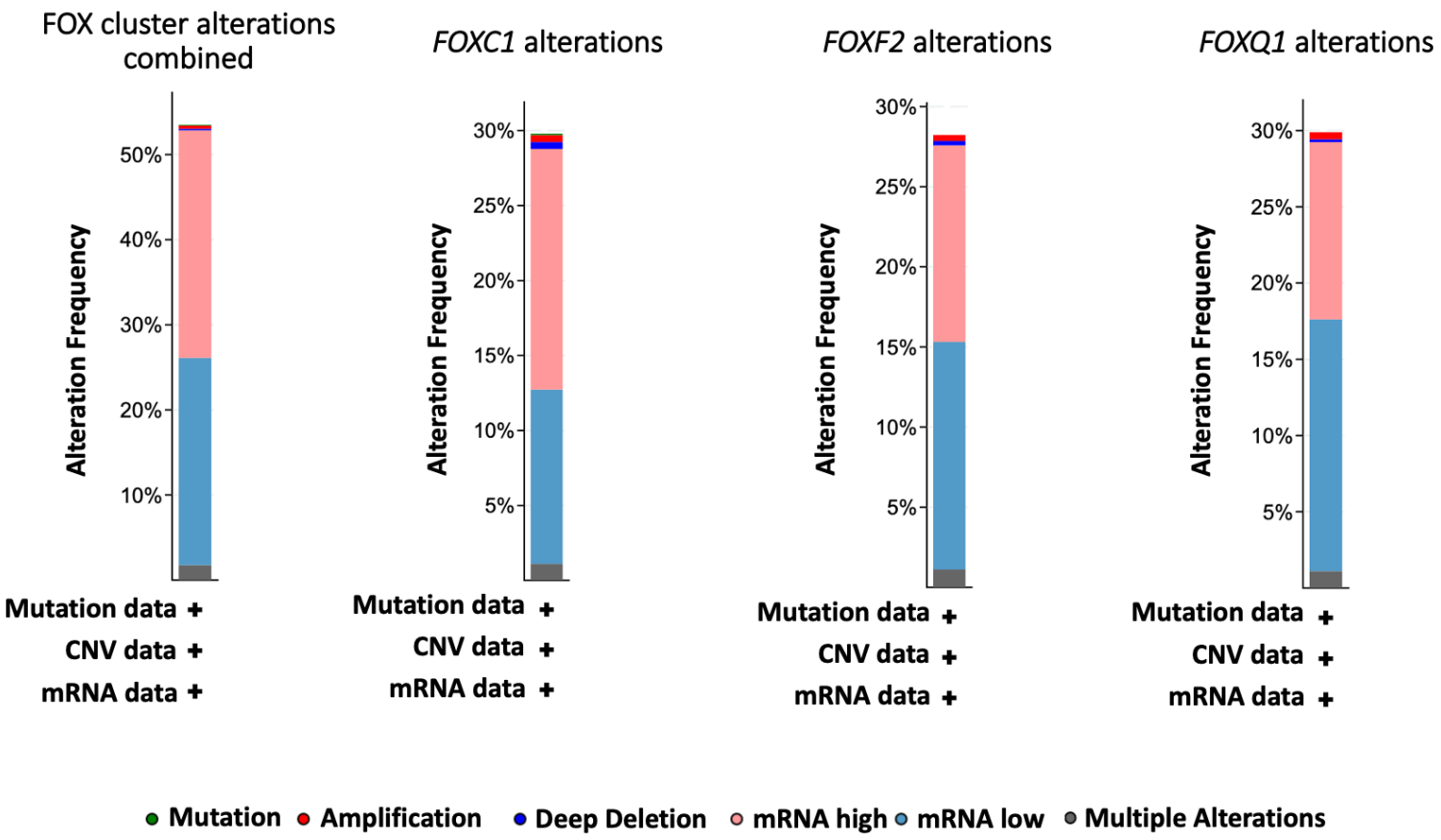
FOX cluster alterations combined
FOXC1 alterations
FOXF2 alterations
FOXQ1 alterations
Alteration Frequency
50%
40%
30%
20%
10%
30%
25%
20%
15%
10%
5%
Mutation data +
CNV data +
mRNA data +
Mutation
Amplification
Deep Deletion
mRNA high
mRNA low
Multiple Alterations

Figure 4.2: Graphical summary of the FOX cluster genes' alterations found in the TCGA-BRCA patient samples.

The frequency of the FOX cluster genes' alterations combined counted for 53.5% of 1084 patient samples, where mRNA high alterations cases are detected in 290 cases (26.8%), low mRNA expression are detected in 264 cases (24.4%), and amplification and deletions in 8 cases (0.73%) and 9 cases (0.84%) respectively. Detected multiple alterations (mRNA levels and CNV) of *FOXC1*, and *FOXQ1*, and *FOXQ1* were in 19 cases (1.8%) of all alterations in patients' cases. *FOXC1* mRNA alterations were of high mRNA expression in 174 cases (16.1%) and of low expression in 126 cases (11.6%). *FOXC1* amplifications and deep deletions were detected in 9 cases (0.83%) and in 12 cases (1.1%) respectively. Missense mutations and truncating mutation were only detected in *FOXC1*. *FOXF2* mRNA alterations were of high mRNA expression in 133 cases (12.3%) and of low expression in 154 cases (14.2%). *FOXF2* amplification and deep deletion were detected in 8 cases (0.73%) and in 9 cases (0.83%) respectively. *FOXQ1* mRNA alterations were of high mRNA expression in 126 cases (11.6%) and of low expression in 179 cases (16.5%). *FOXQ1* amplification and deep deletion were detected in 6 cases (0.55%) and in 10 cases (0.92%) respectively. Colours presentation of genetic alterations in the figure: light red, mRNA high; light blue, mRNA low; dark red, amplification (more copies, indicates high-level of amplification); dark blue, deep deletion (possibly a homozygous deletion), green, mutations; grey, multiple alterations. This figure was generated and modified from cBioPortal [284,285].

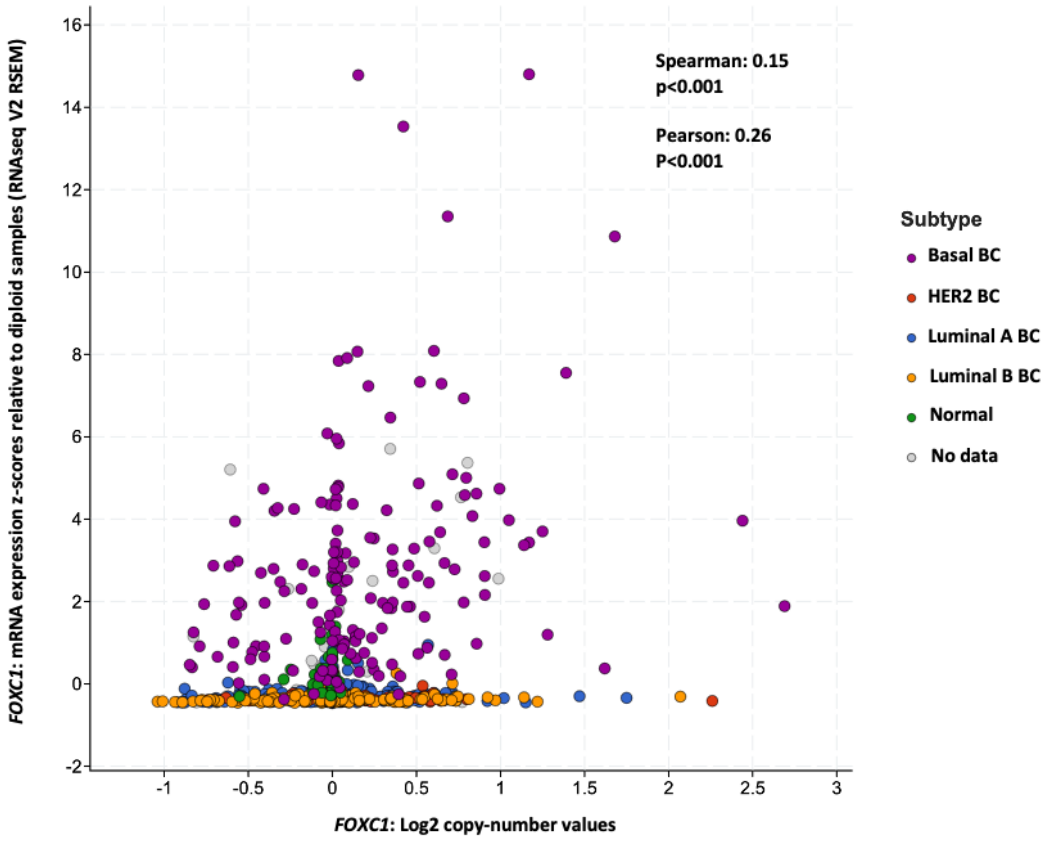

Figure 4.3: Weak correlation between *FOXC1* mRNA levels and CNV in the TCGA-BRCA patients.

Correlation between *FOXC1* mRNA levels and CNV was investigated in 1068 BC patient and normal samples. mRNA expression levels are plotted as mRNA z-scores (RNAseq V2 RSEM) of *FOXC*1 in each sample relative to diploid samples of *FOXC1* across the 1068 patient samples. Log2 copy number values for *FOXC1* gene were generated using Affymetrix SNP6. Both *FOXC1* mRNA z-scores and Log2 copy number values were obtained from the the PanCanAtlas 2018 of the TCGA-BRCA https://gdc.cancer.gov/about-data/publications/pancanatlas [283] Spearman and Pearson analyses were used to determine correlation between gene mRNA levels and CNV. Colors for subtypes: purple, basal BC; red, HER2 BC; blue, luminal A; yellow, luminal B; green, normal samples (although cBioPortal indicate that they do not store any adjacent normal data in their data base, however when I applied the PAM50 subtype filter, results gave back normal as one of the subtypes. I think the normal samples here are referring to Normal-like BC). $p<0.05$ is considered significant. This figure was generated and modified using Oncoprint tool, cBioPortal for cancer genomics [284,285].

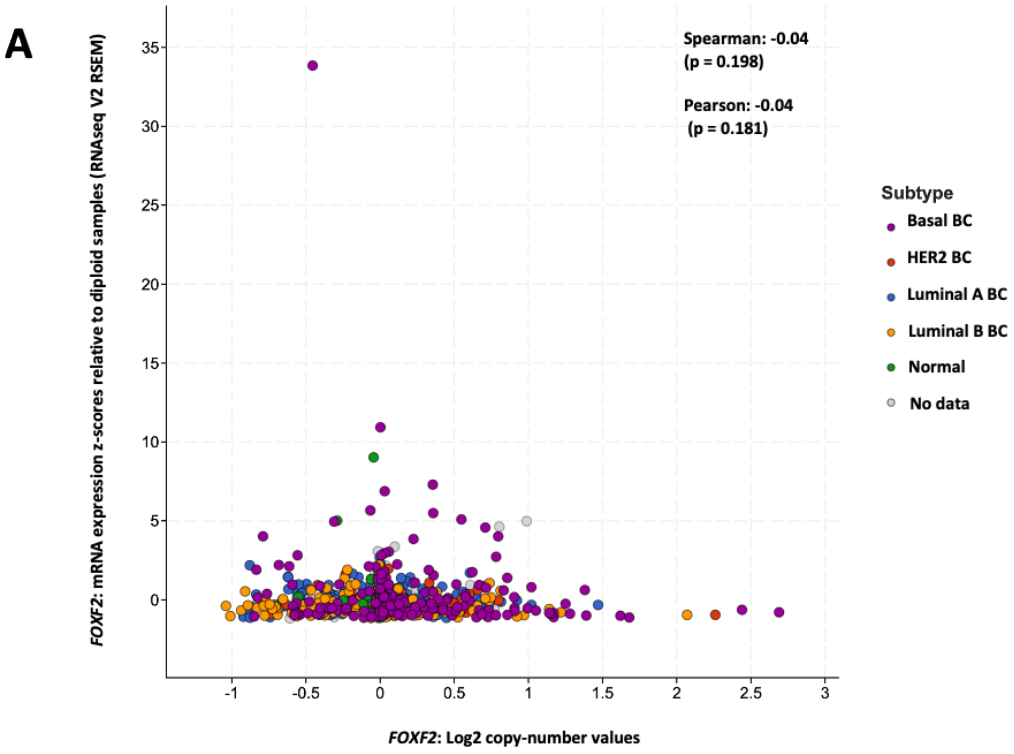
A
Spearman: -0.04
(p = 0.198)
Pearson: -0.04
(p = 0.181)
Subtype
Basal BC
HER2 BC
Luminal A BC
Luminal B BC
Normal
No data
FOXF2: mRNA expression z-scores relative to diploid samples (RNAseq V2 RSEM)
FOXF2: Log2 copy-number values

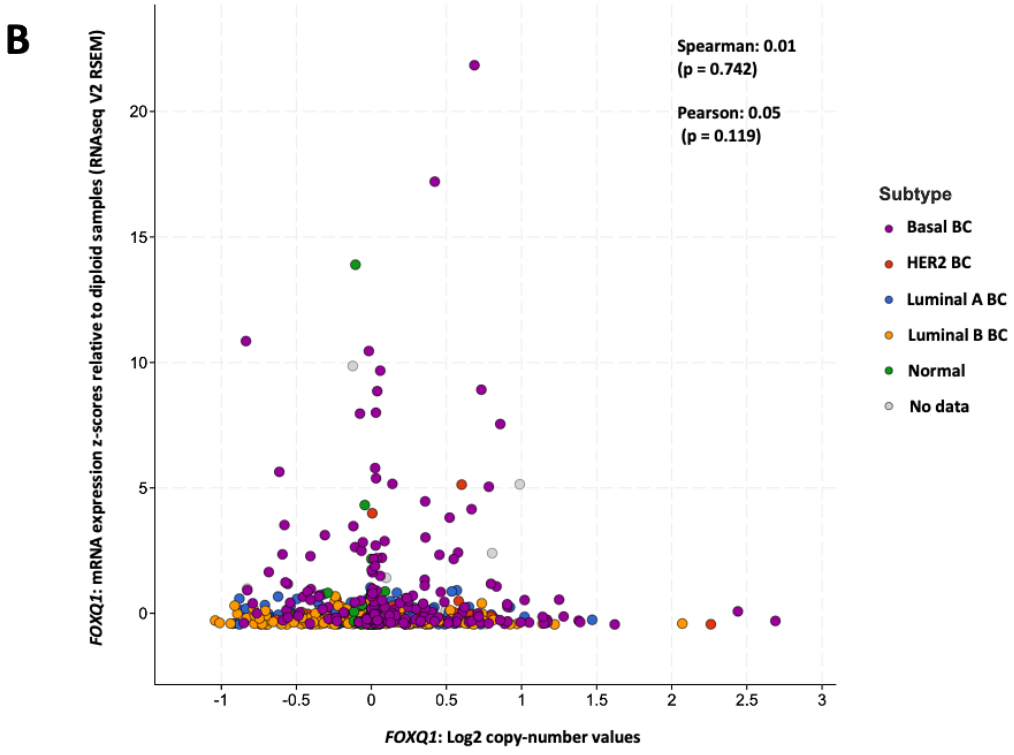
B
Spearman: 0.01
(p = 0.742)
Pearson: 0.05
(p = 0.119)
Subtype
Basal BC
HER2 BC
Luminal A BC
Luminal B BC
Normal
No data
FOXQ1: mRNA expression z-scores relative to diploid samples (RNAseq V2 RSEM)
FOXQ1: Log2 copy-number values

Figure 4.4: *FOXF2* mRNA and FOXQ1 mRNA levels are not correlated with CNV in the TCGA-BRCA patients.

Correlation between (A) *FOXF2* mRNA levels and CNV and between (B) *FOXQ1* mRNA levels and CNV were investigated in 1068 BC patient and normal samples. mRNA expression levels are plotted as mRNA z-scores (RNAseq V2 RSEM) in each sample relative to diploid samples across the 1068 patient samples. Log2 copy number values for *FOXF2 and FOXQ1* genes were generated using Affymetrix SNP6. Both mRNA z-scores and Log2 copy number values were obtained from the PanCanAtlas 2018 of the TCGA-BRCA https://gdc.cancer.gov/about-data/publications/pancanatlas [283]. Spearman and Pearson analyses were used to determine correlation between gene mRNA levels and CNV. Colors for subtypes: purple, basal BC; red, HER2 BC; blue, luminal A; yellow, luminal B; green, normal samples (although cBioPortal indicates that they do not store any adjacent normal data in their data base, however when I applied the PAM50 subtype filter, results gave back normal as one of the subtypes. I think the normal samples here are referring to Normal-like BC). $p<0.05$ is considered significant. This figure was generated and modified using Oncoprint tool, cBioPortal for cancer genomics [284,285].

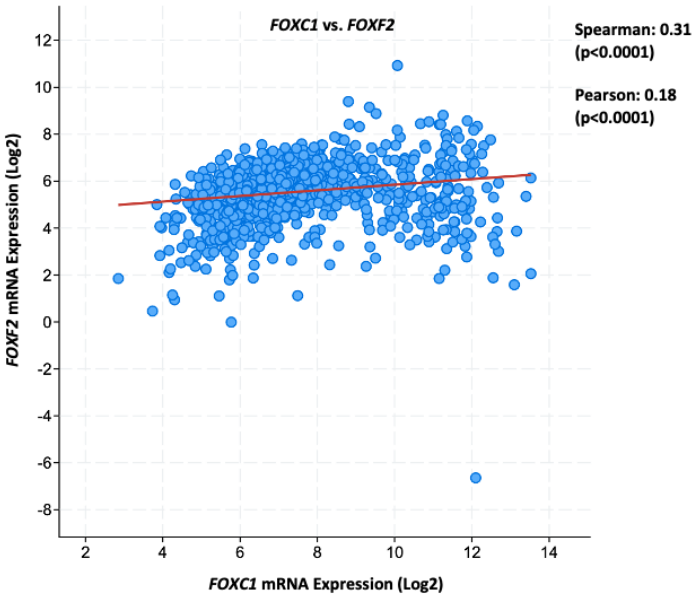
FOXC1 vs. FOXF2
Spearman: 0.31
(p<0.0001)
Pearson: 0.18
(p<0.0001)
FOXF2 mRNA Expression (Log2)
FOXC1 mRNA Expression (Log2)

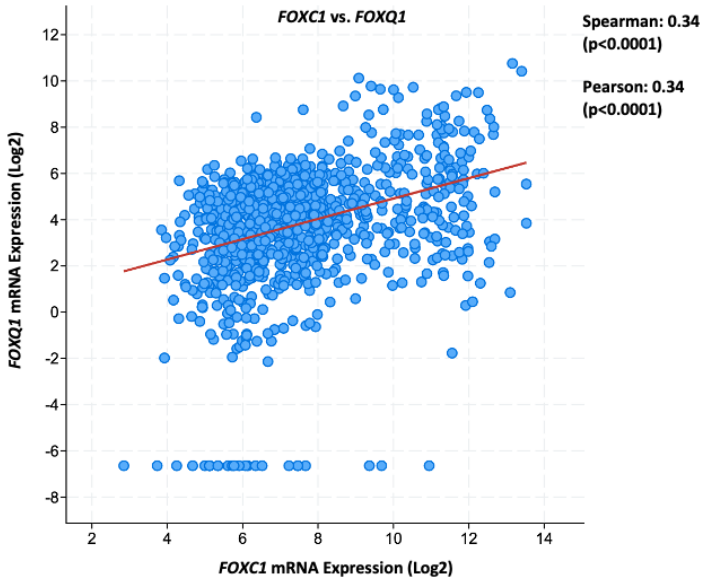
FOXC1 vs. FOXQ1
Spearman: 0.34
(p<0.0001)
Pearson: 0.34
(p<0.0001)
FOXQ1 mRNA Expression (Log2)
FOXC1 mRNA Expression (Log2)

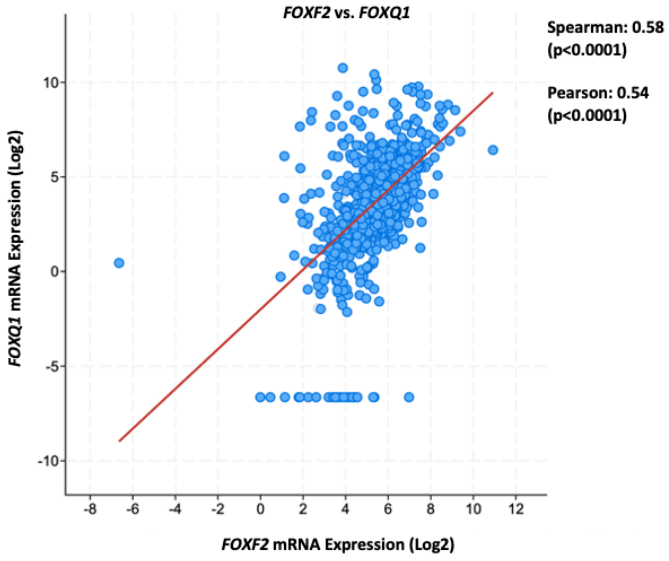
FOXF2 vs. FOXQ1
Spearman: 0.58
(p<0.0001)
Pearson: 0.54
(p<0.0001)
FOXQ1 mRNA Expression (Log2)
FOXF2 mRNA Expression (Log2)

Figure 4.5: The FOX cluster genes' co-expression and correlation analysis in the TCGA-BRCA patients.

FOXC1 mRNA levels have a weak correlation with either *FOXF2* or *FOXQ1*. *FOXF2* and *FOXQ1* mRNA levels have a moderate correlation. *FOXC1, FOXF2,* and *FOXQ1* log2 mRNA values of normalized RSEM RNAseq V2 [286] in 1082 patient were obtained the PanCanAtlas 2018 of the TCGA-BRCA https://gdc.cancer.gov/about-data/publications/pancanatlas[283]. Spearman and Pearson analyses were used to determine correlation coefficients. $p<0.05$ is considered significant. This figure was generated and modified using Oncoprint tool, cBioPortal for cancer genomics [284,285].

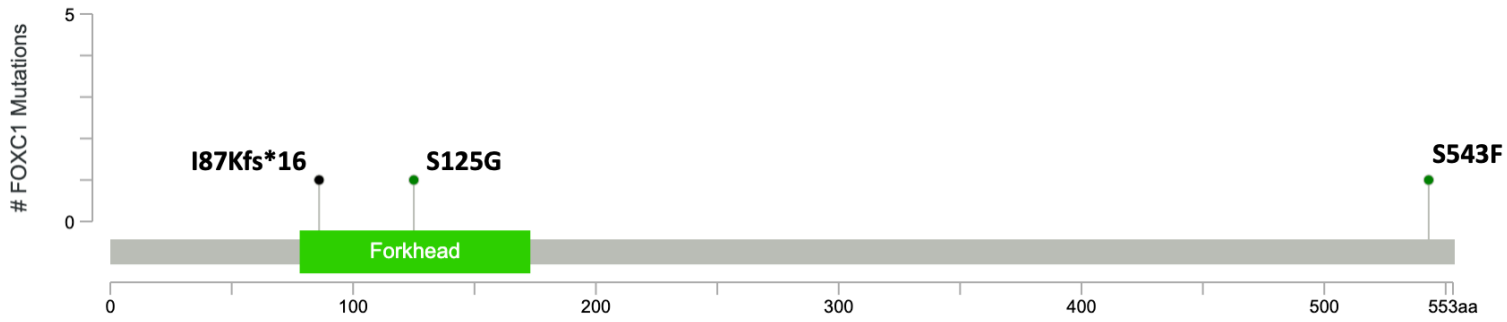

Figure 4.6: FOXC1 mutations in the TCGA-BRCA patient samples.

The missense mutations c.373A>G (p.S125G) and c.1628C>T (p.S543F), and c.258delinsTAA (p.I87Kfs*16) truncating mutation were detected in 3 different BC patients. As shown, 2 mutations are in the forkhead domain of FOXC1 and 1 mutation is in the activation domain of FOXC1 at the c-terminal. Allele frequencies of p.S125G, p.S543F, p.I87Kfs*16 are 0.41, 0.05, and 0.25 respectively. cBioPortal website was used for DNA sequence analysis. cBioPortal uses whole exome sequence data of the the PanCanAtlas 2018 of the TCGA-BRCA https://gdc.cancer.gov/about-data/publications/pancanatlas [283]. This figure was generated and modified using Oncoprint tool, cBioPortal for cancer genomics [284,285].

Chapter 5

Overall Discussion and Future Directions

Science would be ruined if—like sports—it were to put competition above everything else.

—Benoit Mandelbrot

5.1 Significance

Clinically, the transcription factors (TF) *FOXC1, FOXF2, and FOXQ1 (FOX)* have been proposed as an emerging prognostic "biomarker" for breast cancer (BC). Particularly, several roles of each of the FOX genes have been suggested in basal/TNBC. However, a significant gap in the literature regarding the FOX genes role in other BC subtypes is discernible. This is mainly due to the very limited studies that investigated the FOX genes mRNA expressions, copy number variation, prognostic value, and mutations across BC subtypes in BC patients and cell lines. In particular, the expression of the FOX genes in other subtypes of BC, specifically luminal and HER2, is not well studied. Therefore, a molecular understanding of FOX genes expression across BC subtypes warrants further investigation. In this thesis I mainly focused on investigating the mRNA expression, the copy number variation (CNV), and the mutations of the FOX genes across BC subtypes in BC patients and cell lines.

First, the mRNA expression, the CNV, the relationship between CNV and mRNA expression, and the prognostic value of *FOXQ1* across BC subtypes were investigated (Chapter 2). Second, the mRNA expression, the CNV, and the relationship between CNV and mRNA expression of *FOXC1* across BC subtypes, as well as the mutations and the protein stability of FOXC1 in TNBC cell lines were investigated (Chapter 3). Finally, the FOX cluster (*FOXC1, FOXF2, and FOXQ1*) genes' expressions, CNV, and mutations in an expanded panel of BC patients were also investigated simultaneously (Chapter 4). Consequently, my findings: (1) highlighted for the first time that *FOXQ1* mRNA was differentially expressed across BC patients and cell lines where FOXQ1 was significantly lower in luminal and HER2. This low expression of *FOXQ1* mRNA was associated with significantly poorer overall survival for different classes of BC, therefore suggesting a potential prognostic value of *FOXQ1* in BC (2) revealed that

altered expression of *FOXC1* in BC patient tissues compared to normal breast tissue. My studies highlighted the importance of using an extended panel of BC cell lines (n=42) in order to have a better understating of *FOXC1* expression across BC subtypes. I also demonstrated that FOXC1 protein levels are indirectly regulated by EGFR signaling pathway and that FOXC1 protein is more stable in TNBC cell lines, suggesting altered protein stability as a potential mechanism behind the overexpression of FOXC1 in these cell lines and (3) that simultaneous high or low expressions of the FOX genes in BC is subtype specific; and novel mutations of *FOXC1* were detected in BC patients.

Taken together, my studies suggested a prognostic value of *FOXQ1* in BC patients, and advanced our knowledge in order to address some of the discrepancies regarding FOX cluster genes' expression across BC subtypes. The variation of FOX genes' expression across BC patients is striking and suggests different roles of these genes in different BC subtypes. Previous studies have suggested a role of each of the FOX genes in chemoresistance and cancer cell stemness in BC. Thus determining the mechanisms by which FOX genes' levels are significantly elevated or under expressed—while also taking into consideration the treatment history, subtype of BC, stage, age, histological grade—in some of BC patients are urgently needed and consequently could underlie the poor prognoses for these patients.

5.2 General Discussion and Future Directions

The FOX genes expression results in BC cell lines previously reported in the literature, in particular for *FOXC1* [147,255–257] are conflicting and inconsistent. BC cell lines have been widely used in the past to study the biological mechanisms that drive cancer cell's metastasis, survival, proliferation, and drug resistance. They do not require intensive effort to maintain, they are

readily genetically engineered, and they are costly efficient all of which made them a prefect tool for many research studies. However, several reports in the last decade have suggested striking findings regarding BC cell lines. Indeed, the fact that many drugs fail in clinical trials suggested the reconsideration of using cancer cell lines as tumor models [291]. Moreover, remarkable differences were found between cell lines and tumor biology such as in signaling pathways and drug responsiveness [292,293]. Furthermore, several studies that have investigated to which extent cell lines accurately represent tumors' genomics profile—gene mutation, copy number variation and transcriptome [237,294–296]— showed significant differences between tumor tissues and cell lines. Regarding BC, Neve and colleagues were the first group to report significant differences within the 52 commercially available BC cell lines [205]. Their study has introduced the commonly used subtyping of BC cell lines; luminal A, luminal B, basal, and HER2. Basal cell lines were suggested as TNBC cell lines and based on differences in molecular features and biological characteristics such as morphology and invasion potential, basal cell lines are further subdivided into basal A and basal B. Basal A has been discovered to appear less differentiated and more epithelial like, whereas basal B has shown a more mesenchymal-like morphology and is more highly invasive. Moreover, basal B has also been characterized as exhibiting more cancer "stemness". It has been suggested that basal A cell lines resemble the basal tumors we have in the clinic more than the basal B cell lines [204,205,297]. Together, this might explain why several studies have reported inconsistent expressions of *FOXC1* in identically-named cell lines, or in different cell lines but of the basal subtypes and luminal subtypes [147,255–257]. For these reasons, I have investigated the FOX genes' expression in BC patient tissue samples and normal breast tissue using RT-qPCR (chapter 2, n=24; chapter 3, n=20), and in an expanded number of BC cell lines. I then confirmed my findings in expanded panel of BC patients in the TCGA-BRCA

database (chapter 4, n=1086). In the latter, the mRNA levels of FOX genes were measured using RNAseq [283]. Moreover, I applied the intrinsic BC subtypes as described in [204,205,237] for BC cell lines such as basal A and B, and luminal A and B to study *FOXC1* expression. Where some basal A and B cell lines had high levels of *FOXC1* mRNA, other basal A cell lines showed low levels of FOXC1 (chapter 3), suggesting variation of *FOXC1* expression in basal cell lines. These differences in BC cell lines of the same subtypes could in part explain the previous conflicting results of *FOXC1* [147,255–257].

Interestingly, MDA-MB-231 (basal B), one of the most widely used BC cell lines in metastasis—40% of total citations on PubMed Lie *et al* 2019—did not recapitulate the genomic profile (CNV and mutations), and had low similarities with the metastatic basal BC samples of the MET500 dataset [237]. The MET500 is a dataset of 500 metastatic BC patients' transcriptome and whole-exome sequencing data [298]. Several studies have investigated the FOX genes' expression, regulation, and role using MDA-MB-231 cell line as one of their studied models [147,161,208]. Where often the term "metastasis basal BC" was linked with the MDA-MB-231 results. This might explain why the authors in one study found that *FOXF2* negatively regulated *FOXQ1* in MDA-MB-231, however, no negative correlation between the two genes was found in basal patients' database—in this study an exclusive negative mechanism of *FOXQ1* regulation (through physical binding to FOXF2 promoter with other corepressors) was proposed in "basal" BC based on findings in MDA-MB-231 and not MCF7 (suggested as luminal BC cell line). Thus, in this thesis I used MDA-MB-231 and expanded BC cell lines to examine *FOXQ1* and *FOXC1* expressions and CNVs. This resulted in a better understating of the FOX genes' expression in basal BC cell lines, where my findings showed variation of FOX genes expression in both basal BC cell lines and patients and across BC subtypes (chapter 2 and 3). These

differences could be missed if only a limited number of basal BC cell lines were used. Therefore, for future studies of FOX genes' expression in basal BC and across other BC subtypes, it will be possible to better understand the variability of FOX genes expression if (1) expanded panel of cell lines are used (2) BC patients tumor tissues or BC patient publicly available data are used or both (3) further grouping of basal and luminal cell lines and if when available conducting RT-qPCR using known basal markers such as CD44, CK5/4/17, or luminal markers such as ER to validate the BC cell lines (4) and when applicable considering 3D tissue culturing techniques [299,300].

Notable findings in this thesis were the low expression of FOX genes in luminal and HER2. More importantly, my findings that *FOXQ1* low expression is significantly associated with poor overall survival in BC are intriguing. Moreover, simultaneous low expression of the FOX cluster genes was detected in approximately 12% of the luminal B patient samples. As discussed in chapter 3 and 4, DNA methylation (epigenetic mechanism that regulates transcription) has been suggested to regulate *FOXC1* transcription hence reduce its expression in BC [265–268]. It was also suggested that low expression of *FOXF2* in BC was due to epigenetic DNA methylation [290] [173]. Therefore, DNA methylation may be a mechanism to supress *FOXQ1* expression in luminal and HER2 BC as it was shown to supress its neighbour genes, *FOXC1 and FOXF2*. Moreover, very recently, two groups have suggested a negative regulation of FOXC1 expression by EZH2—a methyltransferase enzyme that plays a role in transcriptional suppression by adding methyl groups to histone H3 at lysine 27 (H3K27me3) [253252]. Of note, one of these studies has suggested this negative regulation of *FOXC1* as a subtype-specific in luminal—where they did not find this negative regulation of *FOXC1* in basal/TNBC cell lines—which directly contrasts the other group who suggested EZH2 negative regulation of *FOXC1* in

basal/TNBC. Nevertheless, EZH2 may possibly plays a part in *FOXQ1* and *FOXF2* downregulation in luminal and HER2.

Interestingly, I found that FOXC1 protein half-life was significantly longer in basal/TNBC cell lines compared to HeLa cell lines that stably express FOXC1 (HS-578T and BT-549, chapter 3). Previous study from our labratory has shown that the phosphorylation of FOXC1 through the activation of the ERK1/2 mitogen-activated protein kinase (MAPK) pathway is critical in stabilizing FOXC1 in HeLa cells [90]. ERK1/2 was suggested to phosphorylate the Ser-272 residue of the inhibitory domain of FOXC1 residue thus increase its stability and prevent proteasomal degradation. My findings and those of others [149] have shown that EGFR signaling activation as well as ERK1/2 activation via its ligand EGF increased the levels of FOXC1 protein (in this thesis it was after 1-3 hours of EGF stimulation). Therefore, EGFR activation may conceivably play a role in FOXC1 stability in BC via ERK1/2 post-translational modification of FOXC1 protein. Future studies that investigate FOXC1 stability with or without EGF stimulation and in the presence or absence of ERK1/2 inhibitor could reveal a novel mechanism of FOXC1 regulation in BC. Furthermore, signaling pathways that activate *FOXC1* or are activated by *FOXC1* in basal/TNBC have been proposed, however, the crosstalk between these pathways and the underlining mechanisms for their compensation still needs to be elucidated [301]. Although the EGFR signaling pathway was suggested to upregulates the expression, activity, and protein levels of *FOXC1*, the how and why of *FOXC1* being exclusively expressed in basal/TNBC rather than in other BC molecular subtypes has yet to be answered. Recently, Chung and colleagues [157] have shown that NF-κB binds to the promoter region of FOXC1 once EGFR is activated by EGF. NF-κB—activates a pathway that has been linked to tumorigenesis—binding to FOXC1 can increase FOXC1 transcription activity (Fig 3). It would

be interesting to know if FOXC2 [302] is also involved in this cancer circuit. The factors that bind to and regulate FOXC1, for example in response to EGFR pathway activation, are still being discovered.

The copy numbers of the FOX genes were also investigated in this thesis. Although, my results showed that FOX genes have more copies in BC, in particular in basal/TNBC, K-means analysis suggested that the expression of FOX genes is independent of CNV. Similar findings were reported regarding the correlation between EGFR CNV and EGFR expression in TNBC [303,304]. Copy number changes could be due to aberrations of chromosome number or gene number [219], chromosomal duplication/deletion, or inversion/translocation [305]. However, the most prevalent modes for CNVs for the chromosomal region 6p21-25 where the FOX cluster is localized are isochromosome formation, unbalanced chromosome translocation, and focal amplification [306]. The determination of the types of chromosomal aberrations is complex, making it difficult to elucidate a specific mechanism responsible for the formation of more copies of the FOX genes in BC. However, there are no reports that have investigated the prognostic impact of FOX genes CNV in BC. Previous study that investigated EGFR CNV and mRNA found that there was no correlation between CNV and EGFR mRNA expression, however further analysis of the EGFR CNV showed that CNV had significant prognostic value in TNBC patients compared to those who did not have EGFR CNV [219] , suggesting that, beyond any role in mRNA expression, CNVs have functional consequences. Future studies that examine FOX genes CNVs and their impact on BC prognosis could be fruitful.

Variation in FOX genes' expression across BC subtypes and within the same BC subtypes were reported in this thesis. My results are consistent with other studies and suggest complex roles of FOX genes in BC. Indeed, it was suggested that the ectopic expression of

FOXQ1 promotes tumor growth in colorectal cancer by inhabiting apoptosis [191]. At the same time, *FOXQ1* over-expression did not impact BC proliferation in 4T1 highly metastatic mouse cell line and induced cell death in BC cells lines MCF7 and BT-20 [158] suggesting a tumor suppressive role of *FOXQ1*. High expression of FOXF2 enhanced EMT, migration and invasion of lung cancer cells [215] and in TNBC [173] in which directly contrasts other group's findings where low expression of FOXF2 induced EMT and was associated with poor overall survival in BC [172]. Moreover, dual functionality of other FOX genes in cancers have also been reported before. For example, high expression of FOXA1 was associated with poor overall survival in prostate cancer [216], while high expression of the same protein favourably impacted BC prognosis [217,218]. In addition, FOXA1 activated luminal genes and repressed basal genes in ER positive and ER negative BC cells respectively [307], indicating different roles of FOXA1 in different BC subtypes. Therefore, future studies that focus on stratifying the BC subtypes further using basal and luminal markers, gene signatures, and cancer stages could reveal better understating of the FOX cluster genes' expression in BC. Moreover, further analysis for long-term and short-term overall survival of BC using patients' FOX expression, age, grade, tumor size, and lymph-node status could provide more details on FOX cluster on overall survival of BC patients [308,309].

In summary, "I start with the premise that all human disease is genetic," said Paul Berg—a biochemist and Nobel laureate in chemistry. Indeed, breast tumorigenesis is undoubtedly dictated by genes, and breast tumors are known to arise as a result of multiple accumulated genetic insults—genes' expression alteration, mutations, copy number variation, and post-transcriptional and translational modifications. In addition, breast tumors are challengingly heterogenous—including molecular and pathological differences between breast tumors across breast cancer patients or within the tumor cells of a single tumor. Moreover, breast tumor's

microenvironment, is very complex, and contains a variety of cells such as immune cells and cancer stem cell (CSC) which makes treatments for BC challenging[310–312].

While it is widely accepted that breast tumors are not caused by a single altered gene and phenotype, investigating multiple genes at once was almost impossible 20 years ago. Fortunately, the completion of the revolutionary "Human Genome Project" and advances in sequencing such as whole exome sequencing and RNA sequencing have all together resulted with a reservoir of genetic data that are readily available for further analyses and examination. Moreover, scientific collaborative efforts between basic science researchers, clinical researchers, oncologists, pathologists, bioinformaticians, and industry have strengthened our fight against breast cancer and resulted with valuable public database such as Cancer Genome Atlas and Cancer Cell Line Encyclopedia. The availability of these data that are rich with genetic information such as gene expression, mutation, copy number alteration associated with clinical data of each patient have certainly advanced research towards better understating of the breast tumorigeneses. Indeed, all of this has facilitated my studies to answer some of remaining questions regarding the FOX genes on chromosome 6 and their genetic alterations across breast cancer subtypes. The mRNA expression. copy number variation, and mutation analyses of these genes were feasible thanks to advanced technologies and available public database. Clinical data regards breast cancer patients were also critical in analyzing the prognostic value of the FOX genes in breast cancer patients. To better enhance our understating for cancer progression, now than ever—because the global COVID-19 pandemic our planet is facing and with all physical distancing measures are in place—the need of available online genetic database as well as the expanding of national and international collaborative research efforts are crucial. Inevitably, all of this will lead for better diagnosis, prognosis, and treatment of breast cancer.

References

1. Edwards, B. K. *et al.* Annual report to the nation on the status of cancer, 1975-2002, featuring population-based trends in cancer treatment. *Journal of the National Cancer Institute* **97**, 1407–1427 (2005).

2. Bray, F. *et al.* Global cancer statistics 2018: GLOBOCAN estimates of incidence and mortality worldwide for 36 cancers in 185 countries. *CA. Cancer J. Clin.* **68**, 394–424 (2018).

3. Torre, L. A., Siegel, R. L., Ward, E. M. & Jemal, A. Global cancer incidence and mortality rates and trends - An update. *Cancer Epidemiology Biomarkers and Prevention* **25**, 16–27 (2016).

4. Ginsburg, O. *et al.* The global burden of women's cancers: a grand challenge in global health. *The Lancet* **389**, 847–860 (2017).

5. Leong, S. P. L. *et al.* Is Breast cancer the same disease in Asian and Western countries? *World J. Surg.* **34**, 2308–2324 (2010).

6. Bhoo Pathy, N. *et al.* Breast cancer in a multi-ethnic Asian setting: Results from the Singapore-Malaysia hospital-based breast cancer registry. *Breast* **20**, S75–S80 (2011).

7. Raina, V. *et al.* Clinical features and prognostic factors of early breast cancer at a major cancer center in North India. *Indian J. Cancer* **42**, 36–41 (2005).

8. Agarwal, G., Pradeep, P. V., Aggarwal, V., Yip, C. H. & Cheung, P. S. Y. Spectrum of breast cancer in Asian women. *World J. Surg.* **31**, 1031–1040 (2007).

9. Badve, S. *et al.* Basal-like and triple-negative breast cancers : a critical review with an emphasis on the implications for pathologists and oncologists. *Nat. Rev.* 157–167 (2011). doi:10.1038/modpathol.2010.200

10. Wolff, A. C. *et al.* American Society of Clinical Oncology/College of American Pathologists guideline recommendations for human epidermal growth factor receptor 2 testing in breast cancer. *J. Clin. Oncol.* **25**, 118–45 (2007).

11. Koboldt, D. C. *et al.* Comprehensive molecular portraits of human breast tumours. *Nature* **490**, 61–70 (2012).

12. Skibinski, A. & Kuperwasser, C. The origin of breast tumor heterogeneity. *Oncogene* **34**, 5309–5316 (2015).

13. Deroo, B. J. & Korach, K. S. Estrogen receptors and human disease. *Journal of Clinical Investigation* **116**, 561–570 (2006).

14. Herynk, M. H. & Fuqua, S. A. W. Estrogen receptor mutations in human disease. *Endocrine Reviews* **25**, 869–898 (2004).

15. Hua, H., Zhang, H., Kong, Q. & Jiang, Y. Mechanisms for estrogen receptor expression in

human cancer 11 Medical and Health Sciences 1112 Oncology and Carcinogenesis 06 Biological Sciences 0604 Genetics. *Experimental Hematology and Oncology* **7**, 24 (2018).

16. Hamilton, K. J., Hewitt, S. C., Arao, Y. & Korach, K. S. Estrogen Hormone Biology. in *Current Topics in Developmental Biology* **125**, 109–146 (Academic Press Inc., 2017).

17. Whitesell, L. *et al.* HSP90 empowers evolution of resistance to hormonal therapy in human breast cancer models. *Proc. Natl. Acad. Sci. U. S. A.* **111**, 18297–18302 (2014).

18. Sugiura, H. *et al.* Expression of estrogen receptor β wild-type and its variant ER βcx/β2 is correlated with better prognosis in breast cancer. *Jpn. J. Clin. Oncol.* **37**, 820–828 (2007).

19. Chang, E. C., Frasor, J., Komm, B. & Katzenellenbogen, B. S. Impact of estrogen receptor β on gene networks regulated by estrogen receptor α in breast cancer cells. *Endocrinology* **147**, 4831–4842 (2006).

20. Grober, O. M. V. *et al.* Global analysis of estrogen receptor beta binding to breast cancer cell genome reveals an extensive interplay with estrogen receptor alpha for target gene regulation. *BMC Genomics* **12**, (2011).

21. Abe, O. *et al.* Effects of chemotherapy and hormonal therapy for early breast cancer on recurrence and 15-year survival: An overview of the randomised trials. *Lancet* **365**, 1687–1717 (2005).

22. Abe, O. *et al.* Relevance of breast cancer hormone receptors and other factors to the efficacy of adjuvant tamoxifen: Patient-level meta-analysis of randomised trials. *Lancet* **378**, 771–784 (2011).

23. Graham, J. D. *et al.* Progesterone receptor A and B protein expression in human breast cancer. in *Journal of Steroid Biochemistry and Molecular Biology* **56**, 93–98 (Elsevier Ltd, 1996).

24. Roskoski, R. The ErbB/HER family of protein-tyrosine kinases and cancer. *Pharmacol. Res.* 1–41 (2013). doi:10.1016/j.phrs.2013.11.002

25. Wilson, K. J., Gilmore, J. L., Foley, J., Lemmon, M. a & Riese, D. J. Functional selectivity of EGF family peptide growth factors: implications for cancer. *Pharmacol. Ther.* **122**, 1–8 (2009).

26. Maruyama, I. N. Mechanisms of activation of receptor tyrosine kinases: monomers or dimers. *Cells* **3**, 304–30 (2014).

27. Karunagaran, D. *et al.* ErbB-2 is a common auxiliary subunit of NDF and EGF receptors : implications for breast cancer. *EMBO Rep.* **15**, 254–264 (1996).

28. Wolff, A. C. *et al.* Human epidermal growth factor receptor 2 testing in breast cancer: American Society of Clinical Oncology/College of American Pathologists Clinical Practice Guideline Focused Update. *Archives of Pathology and Laboratory Medicine* **142**, 1364–1382 (2018).

29. Barnes, C. J. & Kumar, R. Biology of the epidermal growth factor receptor family. *Cancer treatment and research* **119**, 1–13 (2004).

30. Bazley, L. A. & Gullick, W. J. The epidermal growth factor receptor family. in *Endocrine-Related Cancer* **12**, (Endocr Relat Cancer, 2005).

31. Schroeder, R. L., Stevens, C. L. & Sridhar, J. Small molecule tyrosine kinase inhibitors of ErbB2/HER2/Neu in the treatment of aggressive breast cancer. *Molecules* **19**, 15196–15212 (2014).

32. Tischkowitz, M. *et al.* negative breast cancer. *BMC Cancer* **11**, 1–11 (2007).

33. Van Bommel, R. M. G. *et al.* Interval breast cancer characteristics before, during and after the transition from screen-film to full-field digital screening mammography. *BMC Cancer* **17**, (2017).

34. Feng, Y. *et al.* Breast cancer development and progression: Risk factors, cancer stem cells, signaling pathways, genomics, and molecular pathogenesis. *Genes Dis.* **5**, 77–106 (2018).

35. Nahta, R. & Esteva, F. J. Trastuzumab: triumphs and tribulations. *Oncogene* **26**, 3637–43 (2007).

36. Kawajiri, H. *et al.* Pertuzumab in combination with trastuzumab and docetaxel for HER2-positive metastatic breast cancer. *Expert Rev. Anticancer Ther.* **15**, 17–26 (2015).

37. Du, F. Le *et al.* Is the future of personalized therapy in triple-negative breast cancer based on molecular subtype? *Oncotarget* **6**, 12890–12908 (2015).

38. Eroles, P., Bosch, A., Alejandro Pérez-Fidalgo, J. & Lluch, A. Molecular biology in breast cancer: Intrinsic subtypes and signaling pathways. *Cancer Treatment Reviews* **38**, 698–707 (2012).

39. Rakha, E. A. & Ellis, I. O. Modern classification of breast cancer: Should we stick with morphology or convert to molecular profile characteristics. *Advances in Anatomic Pathology* **18**, 255–267 (2011).

40. Perou, C. M. *et al.* Molecular portraits of human breast tumours. *Nature* **406**, 747–752 (2000).

41. Sørlie, T. *et al.* Gene expression patterns of breast carcinomas distinguish tumor subclasses with clinical implications. *Proc. Natl. Acad. Sci. U. S. A.* **98**, 10869–10874 (2001).

42. Prat, A. *et al.* Phenotypic and molecular characterization of the claudin-low intrinsic subtype of breast cancer. *Breast Cancer Res.* **12**, (2010).

43. Prat, A. & Perou, C. M. Deconstructing the molecular portraits of breast cancer. *Molecular Oncology* **5**, 5–23 (2011).

44. Prat, A., Parker, J. S., Fan, C. & Perou, C. M. PAM50 assay and the three-gene model for identifying the major and clinically relevant molecular subtypes of breast cancer. *Breast Cancer Res. Treat.* **135**, 301–306 (2012).

45. Paik, S. *et al.* A Multigene Assay to Predict Recurrence of Tamoxifen-Treated, Node-Negative Breast Cancer. *N. Engl. J. Med.* **351**, 2817–2826 (2004).

46. Bernard, P. S. *et al.* Supervised risk predictor of breast cancer based on intrinsic subtypes. *J. Clin. Oncol.* **27**, 1160–1167 (2009).

47. van de Vijver, M. J. *et al.* A Gene-Expression Signature as a Predictor of Survival in Breast Cancer. *N. Engl. J. Med.* **347**, 1999–2009 (2002).

48. Santagata, S. *et al.* Taxonomy of breast cancer based on normal cell phenotype predicts outcome. *J. Clin. Invest.* **124**, 859–870 (2014).

49. Visvader, J. E. & Stingl, J. Mammary stem cells and the differentiation hierarchy: Current status and perspectives. *Genes and Development* **28**, 1143–1158 (2014).

50. Hennighausen, L. & Robinson, G. W. Signaling Pathways in Mammary Gland Development. *Developmental Cell* **1**, 467–475 (2001).

51. Bissell, M. J., Rizki, A. & Mian, I. S. Tissue architecture: The ultimate regulator of breast epithelial function. *Current Opinion in Cell Biology* **15**, 753–762 (2003).

52. Lim, E. *et al.* Aberrant luminal progenitors as the candidate target population for basal tumor development in BRCA1 mutation carriers. *Nat. Med.* **15**, 907–913 (2009).

53. Shehata, M. *et al.* Phenotypic and functional characterisation of the luminal cell hierarchy of the mammary gland. *Breast Cancer Res.* **14**, (2012).

54. Visvader, J. E. & Stingl, J. Mammary stem cells and the differentiation hierarchy: Current status and perspectives. *Genes and Development* **28**, 1143–1158 (2014).

55. Martín, M. *et al.* Abstract P6-08-10: Prospective study of the impact of the Prosigna^{TM} assay on adjuvant clinical decision-making in women with estrogen receptor-positive, HER2-negative, node-negative breast cancer: A GEICAM study. in *Cancer Research* **75**, P6-08-10-P6-08–10 (American Association for Cancer Research (AACR), 2015).

56. Prat, A. *et al.* Prognostic significance of progesterone receptor-positive tumor cells within immunohistochemically defined luminal a breast cancer. *J. Clin. Oncol.* **31**, 203–209 (2013).

57. Chia, S. K. *et al.* A 50-gene intrinsic subtype classifier for prognosis and prediction of benefit from adjuvant tamoxifen. *Clin. Cancer Res.* **18**, 4465–4472 (2012).

58. Creighton, C. J. The molecular profile of luminal B breast cancer. *Biologics: Targets and Therapy* **6**, 289–297 (2012).

59. Ellis, M. J. *et al.* Outcome prediction for estrogen receptor-positive breast cancer based on postneoadjuvant endocrine therapy tumor characteristics. *J. Natl. Cancer Inst.* **100**, 1380–1388 (2008).

60. Roberts, S. A. *et al.* An APOBEC cytidine deaminase mutagenesis pattern is widespread in human cancers. *Nat. Genet.* **45**, 970–976 (2013).

61. Prat, A. *et al.* Clinical implications of the intrinsic molecular subtypes of breast cancer. *Breast* **24**, S26–S35 (2015).

62. Sobecki, M. *et al.* The cell proliferation antigen Ki-67 organises heterochromatin. *Elife* **5**, (2016).

63. Hafner, A., Bulyk, M. L., Jambhekar, A. & Lahav, G. The multiple mechanisms that regulate p53 activity and cell fate. *Nature Reviews Molecular Cell Biology* **20**, 199–210 (2019).

64. Fruman, D. A. *et al.* The PI3K Pathway in Human Disease. *Cell* **170**, 605–635 (2017).

65. Bastien, R. R. *et al.* PAM50 breast cancer subtyping by RT-qPCR and concordance with standard clinical molecular markers. *BMC Med. Genomics* **5**, (2012).

66. Lehmann, B. D. & Pietenpol, J. A. Identification and use of biomarkers in treatment strategies for triple-negative breast cancer subtypes. *Journal of Pathology* **232**, 142–150 (2014).

67. Kong, P.-Z., Yang, F., Li, L., Li, X.-Q. & Feng, Y.-M. Decreased FOXF2 mRNA Expression Indicates Early-Onset Metastasis and Poor Prognosis for Breast Cancer Patients with Histological Grade II Tumor. *PLoS One* **8**, e61591 (2013).

68. Qiao, Y. *et al.* FOXQ1 regulates epithelial-mesenchymal transition in human cancers. *Cancer Res.* **71**, 3076–3086 (2011).

69. Hannenhalli, S. & Kaestner, K. H. The evolution of Fox genes and their role in development and disease. *Nat. Rev.* **10**, 233–240 (2009).

70. Myatt, S. S. & Lam, E. W.-F. The emerging roles of forkhead box (Fox) proteins in cancer. *Nat. Rev. Cancer* **7**, 847–859 (2007).

71. Zhu, H. Forkhead box transcription factors in embryonic heart development and congenital heart disease. *Life Sci.* **144**, 194–201 (2016).

72. Weigel, D., Jürgens, G., Küttner, F., Seifert, E. & Jäckle, H. The homeotic gene fork head encodes a nuclear protein and is expressed in the terminal regions of the Drosophila embryo. *Cell* **57**, 645–658 (1989).

73. Lam, E. W., Brosens, J. J., Gomes, A. R. & Koo, C. Y. Forkhead box proteins: tuning forks for transcriptional harmony. *Nat. Rev. Cancer* **13**, 482–495 (2013).

74. Carlsson, P. & Mahlapuu, M. Forkhead transcription factors: Key players in development and metabolism. *Developmental Biology* **250**, 1–23 (2002).

75. Zaiss, D. M. W. & Coffer, P. J. Forkhead box transcription factors as context-dependent regulators of lymphocyte homeostasis. *Nat. Rev. Immunol.* 1 (2018). doi:10.1038/s41577-018-0048-9

76. Hori, S., Nomura, T. & Sakaguchi, S. Control of Regulatory T Cell Development by the Transcription Factor Foxp3. *Science (80-.).* **299**, 1057–1061 (2003).

77. Liu, Y. *et al.* FoxA1 directs the lineage and immunosuppressive properties of a novel regulatory T cell population in EAE and MS. *Nat. Med.* **20**, (2014).

78. Ouyang, W., Beckett, O., Flavell, R. A. & Li, M. O. An Essential Role of the Forkhead-Box Transcription Factor Foxo1 in Control of T Cell Homeostasis and Tolerance. *Immunity* **30**, 358–371 (2009).

79. Kerdiles, Y. M. *et al.* Foxo1 links homing and survival of naive T cells by regulating L-selectin, CCR7 and interleukin 7 receptor. *Nat. Immunol.* **10**, 176–84 (2009).

80. Kerdiles, Y. M. *et al.* Foxo Transcription Factors Control Regulatory T Cell Development and Function. *Immunity* **33**, 890–904 (2010).

81. Harada, Y. *et al.* Transcription factors Foxo3a and Foxo1 couple the E3 ligase Cbl-b to the induction of Foxp3 expression in induced regulatory T cells. *J. Exp. Med.* **207**, 1381–91 (2010).

82. Pierrou, S., Enerback, S. & Carlsson, P. Selection of High-Affinity Binding Sites for Sequence-Specific, DNA Binding Proteins from Random Sequences of Oligonucleotides. 99–105 (1995).

83. Berry, F. B., Saleem, R. A. & Walter, M. A. FOXC1 transcriptional regulation is mediated by N- and C-terminal activation domains and contains a phosphorylated transcriptional inhibitory domain. *J. Biol. Chem.* **277**, 10292–7 (2002).

84. Kume, T. *et al.* The Forkhead/Winged Helix Gene Mf1 Is Disrupted in the Pleiotropic Mouse Mutation congenital hydrocephalus. *Cell* **93**, 985–996 (1998).

85. Hong, H. K., Lass, J. H. & Chakravarti, A. Pleiotropic skeletal and ocular phenotypes of the mouse mutation congenital hydrocephalus (ch/Mf1) arise from a winged helix/forkhead transcriptionfactor gene. *Hum Mol Genet* **8**, 625–637 (1999).

86. Mears, A. J. *et al.* Mutations of the Forkhead/Winged-Helix Gene, FKHL7, in Patients with Axenfeld-Rieger Anomaly. *Am. J. Hum. Genet.* **63**, 1316–1328 (1998).

87. Nishimura, D. Y. *et al.* A Spectrum of FOXC1 Mutations Suggests Gene Dosage as a Mechanism for Developmental Defects of the Anterior Chamber of the Eye. *Am. J. Hum. Genet.* **68**, 364–372 (2001).

88. Doucette, L. P., Rasnitsyn, A., Seifi, M. & Walter, M. A. The interactions of genes, age, and environment in glaucoma pathogenesis. *Surv. Ophthalmol.* **60**, 310–326 (2015).

89. Mortemousque, B. *et al.* Axenfeld-Rieger anomaly: a novel mutation in the forkhead box C1 (FOXC1) gene in a 4-generation family. *Arch. Ophthalmol. (Chicago, Ill. 1960)* **122**, 1527–33 (2004).

90. Berry, F. B., Mirzayans, F. & Walter, M. A. Regulation of FOXC1 Stability and Transcriptional Activity by an Epidermal Growth Factor-activated Mitogen-activated Protein Kinase Signaling Cascade. *J. Biol. Chem.* **281**, 10098–10104 (2006).

91. Somerville, T. D. D. & Somervaille, T. C. P. Tissue-inappropriate derepression of *FOXC1* is frequent and functional in human acute myeloid leukemia. *Mol. Cell. Oncol.* **3**, e1131355 (2016).

92. Kume, T., Deng, K. & Hogan, B. L. Murine forkhead/winged helix genes Foxc1 (Mf1) and Foxc2 (Mfh1) are required for the early organogenesis of the kidney and urinary tract. *Development* **127**, 1387–1395 (2000).

93. Pierrou, S., Hellqvist, M., Samuelsson, L., Enerbäck, S. & Carlsson, P. Cloning and characterization of seven human forkhead proteins: binding site specificity and DNA bending. *EMBO J.* **13**, 5002–12 (1994).

94. Clark, K. L., Halay, E. D., Lai, E. & Burley, S. K. Co-crystal structure of the HNF-3/fork head DNA-recognition motif resembles histone H5. *Nature* **364**, 412–20 (1993).

95. Lines, M. A., Kozlowski, K. & Walter, M. A. Molecular genetics of Axenfeld – Rieger malformations. *Hum Mol Genet* **11**, 25–28 (2002).

96. Furukawa-Hibi, Y., Kobayashi, Y., Chen, C. & Motoyama, N. FOXO Transcription Factors in Cell-Cycle Regulation and the Response to Oxidative Stress. *Antioxid. Redox Signal.* **7**, 752–760 (2005).

97. Ito, Y. A. *et al.* Analyses of a Novel L130F Missense Mutation in FOXC1. *Arch. Ophthalmol.* **125**, 128 (2007).

98. Ito, Y. A. *et al.* Severe molecular defects of a novel FOXC1 W152G mutation result in aniridia. *Invest. Ophthalmol. Vis. Sci.* **50**, 3573–9 (2009).

99. Murphy, T. C. *et al.* The wing 2 region of the FOXC1 forkhead domain is necessary for normal DNA-binding and transactivation functions. *Investig. Ophthalmol. Vis. Sci.* **45**, 2531–2538 (2004).

100. Saleem, R. A., Banerjee-Basu, S., Berry, F. B., Baxevanis, A. D. & Walter, M. A. Analyses of the Effects That Disease-Causing Missense Mutations Have on the Structure and Function of the Winged-Helix Protein FOXC1. *Am. J. Hum. Genet.* **68**, (2001).

101. Saleem, R. A., Banerjee-Basu, S., Murphy, T. C., Baxevanis, A. & Walter, M. A. Essential structural and functional determinants within the forkhead domain of FOXC1. *Nucleic Acids Res.* **32**, 4182–93 (2004).

102. Fetterman, C. D., Mirzayans, F. & Walter, M. A. Characterization of a novel FOXC1 mutation, P297S, identified in two individuals with anterior segment dysgenesis. *Clin. Genet.* **76**, 296–9 (2009).

103. Medina-Trillo, C. *et al.* Hypo- and Hypermorphic FOXC1 Mutations in Dominant Glaucoma: Transactivation and Phenotypic Variability. *PLoS One* **10**, e0119272 (2015).

104. Saleem, R. A., Murphy, T. C., Liebmann, J. M. & Walter, M. A. Identification and Analysis of a Novel Mutation in the FOXC1 Forkhead Domain. *Investig. Opthalmology Vis. Sci.* **44**, 4608 (2003).

105. Saleem, R. A., Banerjee-Basu, S., Berry, F. B., Baxevanis, A. D. & Walter, M. A. Structural and functional analyses of disease-causing missense mutations in the forkhead domain of FOXC1. *Hum. Mol. Genet.* **12**, 2993–3005 (2003).

106. Seifi, M., Footz, T., Taylor, S. A. M. & Walter, M. A. Comparison of Bioinformatics Prediction, Molecular Modeling, and Functional Analyses of *FOXC1* Mutations in Patients with Axenfeld-Rieger Syndrome. *Hum. Mutat.* (2016). doi:10.1002/humu.23141

107. Li, Y. *et al.* Forkhead box Q1: A key player in the pathogenesis of tumors (Review). *International Journal of Oncology* **49**, 51–58 (2016).

108. Bieller, A. *et al.* Isolation and characterization of the human forkhead gene FOXQ1. *DNA Cell Biol.* **20**, 555–561 (2001).

109. Verzi, M. P., Khan, A. H., Ito, S. & Shivdasani, R. A. Transcription Factor Foxq1 Controls Mucin Gene Expression and Granule Content in Mouse Stomach Surface Mucous Cells. *Gastroenterology* **135**, 591–600 (2008).

110. Goering, W. *et al.* Impairment of gastric acid secretion and increase of embryonic lethality in Foxq1-deficient mice. *Cytogenet. Genome Res.* **121**, 88–95 (2008).

111. Overdier, D. G., Porcella, A. & Costa, R. H. The DNA-binding specificity of the hepatocyte nuclear factor 3/forkhead domain is influenced by amino-acid residues adjacent to the recognition helix. *Mol. Cell. Biol.* **14**, 2755–2766 (1994).

112. Abba, M. *et al.* Unraveling the role of FOXQ1 in colorectal cancer metastasis. *Mol. Cancer Res.* **11**, 1017–28 (2013).

113. Kaestner, K. H., Knöchel, W. & Martínez, D. E. Unified nomenclature for the winged helix/forkhead transcription factors. *Genes and Development* **14**, 142–146 (2000).

114. Hoggatt, A. M., Kriegel, A. M., Smith, A. F. & Herring, B. P. Hepatocyte nuclear factor-3 homologue 1 (HFH-1) represses transcription of smooth muscle-specific genes. *J. Biol. Chem.* **275**, 31162–31170 (2000).

115. Feuerborn, A. *et al.* The Forkhead factor FoxQ1 influences epithelial differentiation. *J. Cell. Physiol.* **226**, 710–9 (2011).

116. Wotton, K. R., Mazet, F. & Shimeld, S. M. Expression of FoxC, FoxF, FoxL1, and FoxQ1 genes in the dogfish Scyliorhinus canicula defines ancient and derived roles for fox genes in vertebrate development. *Dev. Dyn.* **237**, 1590–1603 (2008).

117. Jackson, B. C., Carpenter, C., Nebert, D. W. & Vasiliou, V. Update of human and mouse forkhead box (FOX) gene families. *Human genomics* **4**, 345–352 (2010).

118. Hong, H. K. *et al.* The winged helix/forkhead transcription factor Foxq1 regulates differentiation of hair in satin mice. *Genesis* **29**, 163–171 (2001).

119. Potter, C. S. *et al.* Evidence that the satin hair mutant gene Foxq1 is among multiple and functionally diverse regulatory targets for Hoxc13 during hair follicle differentiation. *J. Biol.*

Chem. **281**, 29245–29255 (2006).

120. Cui, Y. *et al.* The hepatic FOXQ1 transcription factor regulates glucose metabolism in mice. *Diabetologia* **59**, 2229–2239 (2016).

121. Martinez-Ceballos, E., Chambon, P. & Gudas, L. J. Differences in gene expression between wild type and Hoxa1 knockout embryonic stem cells after retinoic acid treatment or Leukemia Inhibitory Factor (LIF) removal. *J. Biol. Chem.* **280**, 16484–16498 (2005).

122. Bhatlekar, S., Fields, J. Z. & Boman, B. M. Role of HOX genes in stem cell differentiation and cancer. *Stem Cells International* **2018**, (2018).

123. Blixt, Å. *et al.* The two-exon gene of the human forkhead transcription factor FREAC-2 (FKHL6) is located at 6p25.3. *Genomics* **53**, 387–390 (1998).

124. Hellqvist, M., Mahlapuu, M., Blixt, Å., Enerbäck, S. & Carlsson, P. The human forkhead protein FREAC-2 contains two functionally redundant activation domains and interacts with TBP and TFIIB. *J. Biol. Chem.* **273**, 23335–23343 (1998).

125. Aitola, M., Carlsson, P., Mahlapuu, M., Enerb**?**ck, S. & Pelto-Huikko, M. Forkhead transcription factorFoxF2 is expressed in mesodermal tissues involved in epithelio-mesenchymal interactions. *Dev. Dyn.* **218**, 136–149 (2000).

126. Ormestad, M. *et al.* Foxf1 and Foxf2 control murine gut development by limiting mesenchymal Wnt signaling and promoting extracellular matrix production. *Development* **133**, 833–843 (2006).

127. Bademci, G. *et al.* FOXF2 is required for cochlear development in humans and mice. *Hum. Mol. Genet.* (2018). doi:10.1093/hmg/ddy431

128. Van Den Brink, G. R. & Rubin, D. C. Foxf2: A mesenchymal regulator of intestinal adenoma development. *Gastroenterology* **144**, 873–876 (2013).

129. Wang, T. *et al.* Forkhead transcription factor Foxf2 (LUN)-deficient mice exhibit abnormal development of secondary palate. *Dev. Biol.* **259**, 83–94 (2003).

130. Levi, B. *et al.* Palatogenesis: Engineering, pathways and pathologies. *Organogenesis* **7**, 242–254 (2011).

131. Elian, F. A. *et al.* FOXC1, the new player in the cancer sandbox. *Oncotarget* **9**, 8165–8178 (2018).

132. Bach, D.-H. *et al.* The Dominant Role of Forkhead Box Proteins in Cancer. *Int. J. Mol. Sci.* **19**, 3279 (2018).

133. Krupczak-Hollis, K. *et al.* The mouse Forkhead Box m1 transcription factor is essential for hepatoblast mitosis and development of intrahepatic bile ducts and vessels during liver morphogenesis. *Dev. Biol.* **276**, 74–88 (2004).

134. Kalin, T. V. *et al.* Increased levels of the FoxM1 transcription factor accelerate development and progression of prostate carcinomas in both TRAMP and LADY transgenic mice.

Cancer Res. **66**, 1712–1720 (2006).

135. Paik, J. H. *et al.* FoxOs Are Lineage-Restricted Redundant Tumor Suppressors and Regulate Endothelial Cell Homeostasis. *Cell* **128**, 309–323 (2007).

136. Nagel, S. *et al.* Oncogenic deregulation of NKL homeobox gene MSX1 in mantle cell lymphoma. *Leuk. Lymphoma* **55**, 1893–1903 (2014).

137. Nagel, S., Meyer, C., Kaufmann, M., Drexler, H. G. & MacLeod, R. A. F. Deregulated FOX Genes in Hodgkin Lymphoma. *Genes. Chromosomes Cancer* **53**, 917–933 (2014).

138. Chung, T. K. H. *et al.* Dysregulation of microRNA-204 mediates migration and invasion of endometrial cancer by regulating FOXC1. *Int. J. Cancer* **130**, 1036–1045 (2012).

139. Xu, Y. Y., Tian, J., Hao, Q. & Yin, L. R. MicroRNA-495 downregulates FOXC1 expression to suppress cell growth and migration in endometrial cancer. *Tumor Biol.* **37**, 239–251 (2016).

140. Xu, Z. Y. *et al.* FOXC1 contributes to microvascular invasion in primary hepatocellular carcinoma via regulating epithelial-mesenchymal transition. *Int. J. Biol. Sci.* **8**, 1130–1141 (2012).

141. Aravalli, R. N. & Greten, T. F. FoxC1: Novel Regulator of Inflammation-Induced Metastasis in Hepatocellular Carcinoma. *Gastroenterology* **149**, 861–863 (2015).

142. Xia, L. *et al.* Overexpression of forkhead box C1 promotes tumor metastasis and indicates poor prognosis in hepatocellular carcinoma. *Hepatology* **57**, 610–624 (2013).

143. Huang, W. *et al.* Interleukin-8 Induces Expression of FOXC1 to Promote Transactivation of CXCR1 and CCL2 in Hepatocellular Carcinoma Cell Lines and Formation of Metastases in Mice. *Gastroenterology* **149**, 1053–1067 (2015).

144. Wang, J. *et al.* FOXC1 regulates the functions of human basal-like breast cancer cells by activating NF- k B signaling. *Oncogene* **31**, 4798–4802 (2012).

145. Han, B., Qu, Y., Yu-Rice, Y., Johnson, J. & Cui, X. FOXC1-induced Gli2 activation: A non-canonical pathway contributing to stemness and anti-Hedgehog resistance in basal-like breast cancer. *Mol. Cell. Oncol.* **3**, e1131668 (2016).

146. Han, B. *et al.* FOXC1: an emerging marker and therapeutic target for cancer. *Oncogene* (2017). doi:10.1038/onc.2017.48

147. Ray, P. S. *et al.* FOXC1 Is a Potential Prognostic Biomarker with Functional Significance in Basal-like Breast Cancer. *Cancer Res.* **70**, 3870–3877 (2010).

148. Ray, P. S. *et al.* Basal-Like Breast Cancer Defined by FOXC1 Expression Offers Superior Prognostic Value: A Retrospective Immunohistochemical Study. *Ann. Surg. Oncol.* **18**, 3839–3847 (2011).

149. Jin, Y. *et al.* FOXC1 is a critical mediator of EGFR function in human basal-like breast cancer. *Ann. Surg. Oncol.* **21 Suppl 4**, 758–766 (2014).

150. Han, B. *et al.* FOXC1 Activates Smoothened-Independent Hedgehog Signaling in Basal-like Breast Cancer. *Cell Rep.* **13**, 1046–1058 (2015).

151. Jensen, T. W. *et al.* Diagnosis of Basal-Like Breast Cancer Using a FOXC1-Based Assay. *J. Natl. Cancer Inst.* **107**, 1–9 (2015).

152. Yao, T., Wang, Q., Zhang, W., Bian, A. & Zhang, J. Identification of genes associated with renal cell carcinoma using gene expression profiling analysis. *Oncol. Lett.* 73–78 (2016). doi:10.3892/ol.2016.4573

153. Wang, D. S. *et al.* miR-133 inhibits pituitary tumor cell migration and invasion via down-regulating FOXC1 expression. *Genet. Mol. Res.* **15**, 1–10 (2016).

154. Ryo, A. *et al.* Regulation of NF-kappaB signaling by Pin1-dependent prolyl isomerization and ubiquitin-mediated proteolysis of p65/RelA. *Mol. Cell* **12**, 1413–26 (2003).

155. Hayden, M. S. & Ghosh, S. NF- B, the first quarter-century: remarkable progress and outstanding questions. *Genes Dev.* **26**, 203–234 (2012).

156. Lu, K. P. Prolyl isomerase Pin1 as a molecular target for cancer diagnostics and therapeutics. *Cancer Cell* **4**, 175–80 (2003).

157. Chung, S. *et al.* Identification of EGF-NF-κB-FOXC1 signaling axis in basal-like breast cancer. *Cell Commun. Signal.* **15**, 22 (2017).

158. Zhang, H. *et al.* Forkhead Transcription Factor *Foxq1* Promotes Epithelial–Mesenchymal Transition and Breast Cancer Metastasis. *Cancer Res.* **71**, 1292–1301 (2011).

159. Han, X., Guo, X., Zhang, W. & Cong, Q. MicroRNA-937 inhibits the malignant phenotypes of breast cancer by directly targeting and downregulating forkhead box Q1. *Onco. Targets. Ther.* **12**, 4813–4824 (2019).

160. Meng, F. *et al.* PDGFR and Play Critical Roles in Mediating Foxq1-Driven Breast Cancer Stemness and Chemoresistance. *Cancer Res.* **75**, 584–593 (2015).

161. Kang, L.-J. *et al.* Reciprocal transrepression between FOXF2 and FOXQ1 controls basal-like breast cancer aggressiveness. *FASEB J.* fj.201801916R (2019). doi:10.1096/fj.201801916R

162. Wu, X. *et al.* Targeting the interaction between RNA-binding protein HuR and FOXQ1 suppresses breast cancer invasion and metastasis. *Commun. Biol.* **3**, 193 (2020).

163. Abdelmohsen, K. & Gorospe, M. Posttranscriptional regulation of cancer traits by HuR. *Wiley Interdisciplinary Reviews: RNA* **1**, 214–229 (2010).

164. Onder, T. T. *et al.* Loss of E-cadherin promotes metastasis via multiple downstream transcriptional pathways. *Cancer Res.* **68**, 3645–3654 (2008).

165. Imamura, T., Hikita, A. & Inoue, Y. The roles of TGF-β signaling in carcinogenesis and breast cancer metastasis. *Breast Cancer* **19**, 118–124 (2012).

166. Meng, F. *et al.* PDGFRα and β play critical roles in mediating Foxq1-driven breast cancer stemness and chemoresistance. *Cancer Res.* **75**, (2015).

167. Hardy, K. *et al.* Identification of chromatin accessibility domains in human breast cancer stem cells. *Nucleus* **7**, 50–67 (2016).

168. Kim, S.-H., Kaschula, C. H., Priedigkeit, N., Lee, A. V. & Singh, S. V. Forkhead Box Q1 Is a Novel Target of Breast Cancer Stem Cell Inhibition by Diallyl Trisulfide. *J. Biol. Chem.* **291**, 13495–13508 (2016).

169. Christensen, J., Bentz, S., Sengstag, T., Shastri, V. P. & Anderle, P. FOXQ1, a Novel Target of the Wnt Pathway and a New Marker for Activation of Wnt Signaling in Solid Tumors. *PLoS One* **8**, e60051 (2013).

170. Higashimori, A. *et al.* Forkhead box F2 suppresses gastric cancer through a novel FOXF2–IRF2BPL–b-Catenin signaling axis. *Cancer Res.* **78**, 1643–1656 (2018).

171. He, W. *et al.* FOXF2 acts as a crucial molecule in tumours and embryonic development. *Cell Death and Disease* **11**, (2020).

172. Wang, Q.-S., Kong, P.-Z., Li, X.-Q., Yang, F. & Feng, Y.-M. FOXF2 deficiency promotes epithelial-mesenchymal transition and metastasis of basal-like breast cancer. *Breast Cancer Res.* **17**, 30 (2015).

173. Lo, P.-K., Lee, J. S., Liang, X. & Sukumar, S. The dual role of FOXF2 in regulation of DNA replication and the epithelial-mesenchymal transition in breast cancer progression. *Cell. Signal.* **28**, 1502–1519 (2016).

174. Meyer-Schaller, N., Heck, C., Tiede, S., Yilmaz, M. & Christofori, G. Foxf2 plays a dual role during transforming growth factor beta-induced epithelial to mesenchymal transition by promoting apoptosis yet enabling cell junction dissolution and migration. *Breast Cancer Res.* **20**, 118 (2018).

175. Yu, J., Shen, W., Gao, B., Zhao, H. & Xu, J. MicroRNA-182 targets FOXF2 to promote the development of triple-negative breast cancer. *Neoplasma* **64**, 209–215 (2017).

176. Pradella, D., Naro, C., Sette, C. & Ghigna, C. EMT and stemness: flexible processes tuned by alternative splicing in development and cancer progression. *Mol. Cancer* **16**, 8 (2017).

177. Ye, X. & Weinberg, R. A. Epithelial–Mesenchymal Plasticity: A Central Regulator of Cancer Progression. *Trends Cell Biol.* **25**, 675–686 (2015).

178. Lo, P.-K. The controversial role of forkhead box F2 (FOXF2) transcription factor in breast cancer. *PRAS open* **1**, (2017).

179. Sizemore, G. M. *et al.* FOXC1 Is Enriched in the Mammary Luminal Progenitor Population, but Is Not Necessary for Mouse Mammary Ductal Morphogenesis1. *Biol. Reprod.* **89**, 10 (2013).

180. Polyak, K. Heterogeneity in breast cancer. *Journal of Clinical Investigation* **121**, 3786–

3788 (2011).

181. Blows, F. M. *et al.* Subtyping of Breast Cancer by Immunohistochemistry to Investigate a Relationship between Subtype and Short and Long Term Survival: A Collaborative Analysis of Data for 10,159 Cases from 12 Studies. *PLoS Med.* **7**, e1000279 (2010).

182. Prat, A. *et al.* Molecular characterization of basal-like and non-basal-like triple-negative breast cancer. *Oncologist* **18**, 123–33 (2013).

183. Li, Y., Tang, X.-Q., Bai, Z. & Dai, X. Exploring the intrinsic differences among breast tumor subtypes defined using immunohistochemistry markers based on the decision tree. *Sci. Rep.* **6**, 35773 (2016).

184. Buffa, F. M. *et al.* microRNA-Associated Progression Pathways and Potential Therapeutic Targets Identified by Integrated mRNA and microRNA Expression Profiling in Breast Cancer. *Cancer Res.* **71**, 5635–5645 (2011).

185. Blenkiron, C. *et al.* MicroRNA expression profiling of human breast cancer identifies new markers of tumor subtype. *Genome Biol.* **8**, R214 (2007).

186. Walker, R. A. Immunohistochemical markers as predictive tools for breast cancer. *J. Clin. Pathol.* **61**, 689–696 (2008).

187. Perez, E. A. Breast Cancer Management: Opportunities and Barriers to an Individualized Approach. *Oncologist* **16**, 20–22 (2011).

188. Katoh, M. & Katoh, M. Human FOX gene family (Review). *Int. J. Oncol.* **25**, 1495–500 (2004).

189. Jonsson, H. & Peng, S. L. Forkhead transcription factors in immunology. *Cell. Mol. Life Sci.* **62**, 397–409 (2005).

190. Gao, M., Shih, I. M. & Wang, T. L. The role of forkhead box Q1 transcription factor in ovarian epithelial carcinomas. *Int. J. Mol. Sci.* (2012). doi:10.3390/ijms131113881

191. Kaneda, H. *et al.* FOXQ1 is overexpressed in colorectal cancer and enhances tumorigenicity and tumor growth. *Cancer Res.* **70**, 2053–63 (2010).

192. Zhan, H. *et al.* FoxQ1 is a Novel Molecular Target for Pancreatic Cancer and is Associated with Poor Prognosis. *Curr. Mol. Med.* **15**, 469–477 (2015).

193. Anaya, J. OncoLnc: Linking TCGA survival data to mRNAs, miRNAs, and lncRNAs. *PeerJ Comput. Sci.* **2016**, e67 (2016).

194. Tang, Z. *et al.* GEPIA: A web server for cancer and normal gene expression profiling and interactive analyses. *Nucleic Acids Res.* (2017). doi:10.1093/nar/gkx247

195. Liu, J. *et al.* An Integrated TCGA Pan-Cancer Clinical Data Resource to Drive High-Quality Survival Outcome Analytics. *Cell* **173**, 400-416.e11 (2018).

196. Chandrashekar, D. S. *et al.* UALCAN: A Portal for Facilitating Tumor Subgroup Gene

Expression and Survival Analyses. *Neoplasia (United States)* **19**, 649–658 (2017).

197. Berger, A. C. *et al.* A Comprehensive Pan-Cancer Molecular Study of Gynecologic and Breast Cancers. *Cancer Cell* **33**, 690-705.e9 (2018).

198. Rasnitsyn, A. *et al.* FOXC1 modulates MYOC secretion through regulation of the exocytic proteins RAB3GAP1, RAB3GAP2 and SNAP25. *PLoS One* **12**, e0178518 (2017).

199. Gaetano, C. G. *et al.* Inhibition of autotaxin production or activity blocks lysophosphatidylcholine-induced migration of human breast cancer and melanoma cells. *Mol. Carcinog.* **48**, 801–809 (2009).

200. Seifi, M. *et al.* Novel PITX2 gene mutations in patients with Axenfeld-Rieger syndrome. *Acta Ophthalmol.* **94**, e571–e579 (2016).

201. Pedregosa, F. *et al.* Scikit-learn: Machine learning in Python. *J. Mach. Learn. Res.* **12**, 2825–2830 (2011).

202. Witten, D. M. & Tibshirani, R. A Framework for Feature Selection in Clustering. *J. Am. Stat. Assoc.* **105**, 713–726 (2010).

203. Barretina, J. *et al.* The Cancer Cell Line Encyclopedia enables predictive modelling of anticancer drug sensitivity. *Nature* **483**, 603–7 (2012).

204. Dai, X., Cheng, H., Bai, Z. & Li, J. Breast Cancer Cell Line Classification and Its Relevance with Breast Tumor Subtyping. *J. Cancer* **8**, 3131–3141 (2017).

205. Neve, R. M. *et al.* A collection of breast cancer cell lines for the study of functionally distinct cancer subtypes. **10**, 515–527 (2006).

206. Shao, X. *et al.* Copy number variation is highly correlated with differential gene expression: A pan-cancer study. *BMC Med. Genet.* **20**, 175 (2019).

207. Song, X., Fiati Kenston, S. S., Zhao, J., Yang, D. & Gu, Y. Roles of FoxM1 in cell regulation and breast cancer targeting therapy. *Medical Oncology* **34**, (2017).

208. S, W. *et al.* FOXF2 reprograms breast cancer cells into bone metastasis seeds. *Nat. Commun.* **10**, (2019).

209. Ross, J. B., Huh, D., Noble, L. B. & Tavazoie, S. F. Identification of molecular determinants of primary and metastatic tumour re-initiation in breast cancer. *Nat. Cell Biol.* **17**, 651–664 (2015).

210. Cui, X. *et al.* Prognostic value of FOXQ1 in patients with malignant solid tumors: A meta-analysis. *Onco. Targets. Ther.* **10**, 1777–1781 (2017).

211. Weng, W. *et al.* FOXM1 and FOXQ1 are promising prognostic biomarkers and novel targets of tumor-suppressive miR-342 in human colorectal cancer. *Clin. Cancer Res.* **22**, 4947–4957 (2016).

212. Liang, S. H. *et al.* Increased expression of FOXQ1 is a prognostic marker for patients with

gastric cancer. *Tumor Biol.* **34**, 2605–2609 (2013).

213. Mendes, D. *et al.* The benefit of HER2-targeted therapies on overall survival of patients with metastatic HER2-positive breast cancer - a systematic review. *Breast Cancer Res.* **17**, 1–14 (2015).

214. Dai, X. *et al.* Breast cancer intrinsic subtype classification, clinical use and future trends. *Am. J. Cancer Res.* **5**, (2015).

215. Kundu, S. T. *et al.* The miR-200 family and the miR-183~96~182 cluster target Foxf2 to inhibit invasion and metastasis in lung cancers. *Oncogene* **35**, 173–186 (2016).

216. Sahu, B. *et al.* Dual role of FoxA1 in androgen receptor binding to chromatin, androgen signalling and prostate cancer. *EMBO J.* **30**, 3962–3976 (2011).

217. Badve, S. *et al.* FOXA1 expression in breast cancer - Correlation with luminal subtype A and survival. *Clin. Cancer Res.* **13**, 4415–4421 (2007).

218. Albergaria, A. *et al.* Expression of FOXA1 and GATA-3 in breast cancer: The prognostic significance in hormone receptor-negative tumours. *Breast Cancer Res.* **11**, (2009).

219. Park, H. S. *et al.* High EGFR gene copy number predicts poor outcome in triple-negative breast cancer. *Mod. Pathol.* **27**, 1212–1222 (2014).

220. Hyman, E. *et al.* Impact of DNA amplification on gene expression patterns in breast cancer. *Cancer Res.* **62**, 6240–6245 (2002).

221. Al-Hajj, M., Wicha, M. S., Benito-Hernandez, A., Morrison, S. J. & Clarke, M. F. Prospective identification of tumorigenic breast cancer cells. *Proc. Natl. Acad. Sci. U. S. A.* **100**, 3983–3988 (2003).

222. Dontu, G., Al-Hajj, M., Abdallah, W. M., Clarke, M. F. & Wicha, M. S. Stem cells in normal breast development and breast cancer. *Cell Proliferation, Supplement* **36**, 59–72 (2003).

223. Berry, F. B. *et al.* FOXC1 is required for cell viability and resistance to oxidative stress in the eye through the transcriptional regulation of FOXO1A. *Hum. Mol. Genet.* **17**, 490–505 (2008).

224. Bradner, J. E., Hnisz, D. & Young, R. A. Transcriptional Addiction in Cancer. *Cell* **168**, 629–643 (2017).

225. Lambert, S. A. *et al.* The Human Transcription Factors. *Cell* **172**, 650–665 (2018).

226. Chanda, B. *et al.* A novel mechanistic spectrum underlies glaucoma-associated chromosome 6p25 copy number variation. *Hum. Mol. Genet.* **17**, 3446–3458 (2008).

227. Mirzayans, F., Mears, A. J., Guo, S. W., Pearce, W. G. & Walter, M. A. Identification of the human chromosomal region containing the iridogoniodysgenesis anomaly locus by genomic-mismatch scanning. *Am. J. Hum. Genet.* **61**, (1997).

228. Mears, A. J., Mirzayans, F., Gould, D. B., Pearce, W. G. & Walter, M. A. Autosomal

dominant iridogoniodysgenesis anomaly maps to 6p25. *Am. J. Hum. Genet.* **59**, 1321–7 (1996).

229. Walter, M. A., Mirzayans, F., Mears, A. J., Hickey, K. & Pearce, W. G. Autosomal-dominant iridogoniodysgenesis and Axenfeld-Rieger syndrome are genetically distinct. *Ophthalmology* **103**, 1907–1915 (1996).

230. Reis, L. M. *et al.* PITX2 and FOXC1 spectrum of mutations in ocular syndromes. *European Journal of Human Genetics* **20**, 1224–1233 (2012).

231. Anderlid, B. M. *et al.* Cryptic subtelomeric 6p deletion in a girl with congenital malformations and severe language impairment. *Eur. J. Hum. Genet.* **11**, 89–92 (2003).

232. Weigelt, B. & Reis-filho, J. S. Molecular profi ling currently off ers no more than tumour morphology and basic immunohistochemistry. *Breast Cancer Res.* **12**, 15–18 (2010).

233. Holbro, T. & Hynes, N. E. ErbB receptors: directing key signaling networks throughout life. *Annu. Rev. Pharmacol. Toxicol.* **44**, 195–217 (2004).

234. Braunstein, L. Z. & Taghian, A. G. Molecular phenotype, multi-gene assays, and the loco-regional management of breast Cancer. *Semin. Radiat. Oncol.* **26**, 9–16 (2015).

235. Prat, A. *et al.* Predicting response and survival in chemotherapy-treated triple-negative breast cancer. *British Journal of Cancer* **111**, 1532–1541 (2014).

236. Sikov, W. M. *et al.* Abstract S4-05: Impact of intrinsic subtype by PAM50 and other gene signatures on pathologic complete response (pCR) rates in triple-negative breast cancer (TNBC) after neoadjuvant chemotherapy (NACT) +/- carboplatin (Cb) or bevacizumab (Bev): CALGB 40603/150709 (Allianc. in *Cancer Research* **75**, S4-05-S4-05 (American Association for Cancer Research (AACR), 2015).

237. Liu, K. *et al.* Evaluating cell lines as models for metastatic breast cancer through integrative analysis of genomic data. *Nat. Commun.* **10**, 1–12 (2019).

238. Lehmann, O. J., Sowden, J. C., Carlsson, P., Jordan, T. & Bhattacharya, S. S. Fox's in development and disease. *Trends Genet.* **19**, 339–344 (2003).

239. Mears, A. J., Mirzayans, F., Gould, D. B., Pearce, W. G. & Walter, M. A. Autosomal dominant iridogoniodysgenesis anomaly maps to 6p25. *Am. J. Hum. Genet.* **59**, 1321–7 (1996).

240. Ghandi, M. *et al.* Next-generation characterization of the Cancer Cell Line Encyclopedia. *Nature* **569**, 503–508 (2019).

241. Changavi, A. A., Shashikala, A. & Ramji, A. S. Epidermal Growth Factor Receptor Expression in Triple Negative and Nontriple Negative Breast Carcinomas. *J. Lab. Physicians* **7**, 079–083 (2015).

242. Costa, R. *et al.* Targeting Epidermal Growth Factor Receptor in triple negative breast cancer: New discoveries and practical insights for drug development. *Cancer Treatment Reviews*

53, 111–119 (2017).

243. Prenzel, N., Zwick, E., Leserer, M. & Ullrich, A. Tyrosine kinase signalling in breast cancer. Epidermal growth factor receptor: Convergence point for signal integration and diversification. *Breast Cancer Research* **2**, 184–190 (2000).

244. Mirzoeva, O. K. *et al.* Basal subtype and MAPK/ERK kinase (MEK)-phosphoinositide 3-kinase feedback signaling determine susceptibility of breast cancer cells to MEK inhibition. *Cancer Res.* **69**, 565–572 (2009).

245. Yu-Rice, Y. *et al.* FOXC1 is involved in ERα silencing by counteracting GATA3 binding and is implicated in endocrine resistance. *Oncogene* 1–12 (2016). doi:10.1038/onc.2016.78

246. Gnant, M., Harbeck, N. & Thomssen, C. St. Gallen 2011: Summary of the consensus discussion. *Breast Care* **6**, 136–141 (2011).

247. Domagala, W., Markiewski, M., Harezga, B., Dukowicz, A. & Osborn, M. Prognostic significance of tumor cell proliferation rate as determined by the MIB-1 antibody in breast carcinoma: its relationship with vimentin and p53 protein. *Clin. Cancer Res.* **2**, (1996).

248. De Azambuja, E. *et al.* Ki-67 as prognostic marker in early breast cancer: A meta-analysis of published studies involving 12 155 patients. *Br. J. Cancer* **96**, 1504–1513 (2007).

249. Goldhirsch, A. *et al.* Personalizing the treatment of women with early breast cancer: Highlights of the st gallen international expert consensus on the primary therapy of early breast Cancer 2013. *Ann. Oncol.* **24**, 2206–2223 (2013).

250. Curigliano, G. *et al.* De-escalating and escalating treatments for early-stage breast cancer: The St. Gallen International Expert Consensus Conference on the Primary Therapy of Early Breast Cancer 2017. *Ann. Oncol.* **28**, 1700–1712 (2017).

251. Arnedos, M. & Gligorov, J. St Gallen International Consensus Guidelines in early breast cancer: Experts to prevent patients' overtreatment and breaking the bank? *Annals of Oncology* **30**, 1533–1535 (2019).

252. Hirukawa, A. *et al.* Targeting EZH2 reactivates a breast cancer subtype-specific anti-metastatic transcriptional program. *Nat. Commun.* **9**, 1–15 (2018).

253. Zheng, X. jin *et al.* EZH2 regulates expression of FOXC1 by mediating H3K27me3 in breast cancers. *Acta Pharmacol. Sin.* 1–9 (2020). doi:10.1038/s41401-020-00543-x

254. Cheang, M. C. U. *et al.* Basal-like breast cancer defined by five biomarkers has superior prognostic value than triple-negative phenotype. *Clin. Cancer Res.* **14**, 1368–1376 (2008).

255. Sizemore, S. T. & Keri, R. A. The forkhead box transcription factor FOXC1 promotes breast cancer invasion by inducing matrix metalloprotease 7 (MMP7) expression. *J. Biol. Chem.* **287**, 24631–24640 (2012).

256. Tkocz, D. *et al.* BRCA1 and GATA3 corepress FOXC1 to inhibit the pathogenesis of basal-like breast cancers. *Oncogene* **31**, 3667–3678 (2012).

257. Du, J. *et al.* FOXC1, a target of polycomb, inhibits metastasis of breast cancer cells. *Breast Cancer Res. Treat.* **131**, 65–73 (2012).

258. Anderson, S. F., Schlegel, B. P., Nakajima, T., Wolpin, E. S. & Parvin, J. D. BRCA1 protein is linked to the RNA polymerase II holoenzyme complex via RNA helicase A. *Nat. Genet.* **19**, 254–256 (1998).

259. Wang, Q., Zhang, H., Kajino, K. & Greene, M. I. BRCA1 binds c-Myc and inhibits its transcriptional and transforming activity in cells. *Oncogene* **17**, 1939–1948 (1998).

260. Tsuda, H., Takarabe, T., Hasegawa, T., Murata, T. & Hirohashi, S. Myoepithelial differentiation in high-grade invasive ductal carcinomas with large central acellular zones. *Hum. Pathol.* **30**, 1134–1139 (1999).

261. Fulford, L. G. *et al.* Specific morphological features predictive for the basal phenotype in grade 3 invasive ductal carcinoma of breast. *Histopathology* **49**, 22–34 (2006).

262. Livasy, C. A. *et al.* Phenotypic evaluation of the basal-like subtype of invasive breast carcinoma. *Mod. Pathol.* **19**, 264–271 (2006).

263. Gorski, J. J. *et al.* BRCA1 transcriptionally regulates genes associated with the basal-like phenotype in breast cancer. *Breast Cancer Res. Treat.* **122**, 721–731 (2010).

264. Moore, L. D., Le, T. & Fan, G. DNA methylation and its basic function. *Neuropsychopharmacology* **38**, 23–38 (2013).

265. Klajic, J. *et al.* Dnamethylation status of key cell-cycle regulators such as CDKNA2/P16 and CCNA1 correlates with treatment response to doxorubicin and 5-fluorouracil in locally advanced breast tumors. *Clin. Cancer Res.* **20**, 6357–6366 (2014).

266. Kolacinska, A. *et al.* Gene expression and pathologic response to neoadjuvant chemotherapy in breast cancer. *Mol. Biol. Rep.* **39**, 7435–7441 (2012).

267. Klajic, J. *et al.* Quantitative DNA methylation analyses reveal stage dependent DNA methylation and association to clinico-pathological factors in breast tumors. *BMC Cancer* **13**, 1–12 (2013).

268. Muggerud, A. A. *et al.* Frequent aberrant DNA methylation of ABCB1, FOXC1, PPP2R2B and PTEN in ductal carcinoma in situ and early invasive breast cancer. *Breast Cancer Res.* **12**, 1–10 (2010).

269. Olivier, M., Hollstein, M. & Hainaut, P. TP53 mutations in human cancers: origins, consequences, and clinical use. *Cold Spring Harbor perspectives in biology* **2**, (2010).

270. Avraham, R. & Yarden, Y. Feedback regulation of EGFR signalling: decision making by early and delayed loops. *Nat. Rev. Mol. Cell Biol.* **12**, 104–117 (2011).

271. Tullai, J. W. *et al.* Immediate-early and delayed primary response genes are distinct in function and genomic architecture. *J. Biol. Chem.* **282**, 23981–23995 (2007).

272. Toft, D. J. & Cryns, V. L. Minireview : Basal-Like Breast Cancer : From Molecular Profiles

to Targeted Therapies. *Mol. Endocrinol.* **25**, 199–211 (2011).

273. Schneider, B. P. *et al.* Triple-negative breast cancer: Risk factors to potential targets. *Clinical Cancer Research* **14**, 8010–8018 (2008).

274. Lehmann, B. D. *et al.* Identification of human triple-negative breast cancer subtypes and preclinical models for selection of targeted therapies. *J. Clin. Invest.* **121**, 2750–2767 (2011).

275. Smid, M. *et al.* Subtypes of breast cancer show preferential site of relapse. *Cancer Res.* **68**, 3108–14 (2008).

276. Elsheikh, S. E. *et al.* Caveolin 1 and Caveolin 2 are associated with breast cancer basal-like and triple-negative immunophenotype. *Br. J. Cancer* **99**, 327–34 (2008).

277. Nielsen, T. O. *et al.* Immunohistochemical and clinical characterization of the basal-like subtype of invasive breast carcinoma. *Clin. Cancer Res.* **10**, 5367–5374 (2004).

278. Wang, J. *et al.* FOXC1 is associated with estrogen receptor alpha and affects sensitivity of tamoxifen treatment in breast cancer. *Cancer Med.* **6**, 275–287 (2017).

279. Wang, Q.-S. *et al.* FOXF2 deficiency permits basal-like breast cancer cells to form lymphangiogenic mimicry by enhancing the response of VEGF-C/VEGFR3 signaling pathway. *Cancer Lett.* **420**, 116–126 (2018).

280. Cai, J. *et al.* FOXF2 suppresses the FOXC2-mediated epithelial–mesenchymal transition and multidrug resistance of basal-like breast cancer. *Cancer Lett.* **367**, 129–137 (2015).

281. Sehrawat, A., Kim, S.-H., Vogt, A. & Singh, S. V. Suppression of FOXQ1 in benzyl isothiocyanate-mediated inhibition of epithelial-mesenchymal transition in human breast cancer cells. *Carcinogenesis* **34**, 864–873 (2013).

282. Gambini, V. *et al.* In vitro and in vivo studies of gold(I) azolate/phosphane complexes for the treatment of basal like breast cancer. *Eur. J. Med. Chem.* **155**, 418–427 (2018).

283. Hoadley, K. A. *et al.* Cell-of-Origin Patterns Dominate the Molecular Classification of 10,000 Tumors from 33 Types of Cancer. *Cell* **173**, 291-304.e6 (2018).

284. Cerami, E. *et al.* The cBio Cancer Genomics Portal: An open platform for exploring multidimensional cancer genomics data. *Cancer Discov.* **2**, 401–404 (2012).

285. Gao, J. *et al.* Integrative analysis of complex cancer genomics and clinical profiles using the cBioPortal. *Sci. Signal.* **6**, 1–1 (2013).

286. Li, B. & Dewey, C. N. RSEM: Accurate transcript quantification from RNA-Seq data with or without a reference genome. *BMC Bioinformatics* **12**, 323 (2011).

287. Seifi, M., Footz, T., Taylor, S. A. M. & Walter, M. A. Comparison of Bioinformatics Prediction, Molecular Modeling, and Functional Analyses of FOXC1 Mutations in Patients with Axenfeld-Rieger Syndrome. *Hum. Mutat.* **38**, 169–179 (2017).

288. Mazet, F., Amemiya, C. T. & Shimeld, S. M. An ancient Fox gene cluster in bilaterian

animals. *Current Biology* **16**, R314–R316 (2006).

289. Shimeld, S. M., Boyle, M. J., Brunet, T., Luke, G. N. & Seaver, E. C. Clustered Fox genes in lophotrochozoans and the evolution of the bilaterian Fox gene cluster. *Dev. Biol.* **340**, 234–248 (2010).

290. Tian, H. P. *et al.* DNA Methylation Affects the SP1-regulated Transcription of FOXF2 in Breast Cancer Cells. *J. Biol. Chem.* **290**, 19173–19183 (2015).

291. Wilding, J. L. & Bodmer, W. F. Cancer cell lines for drug discovery and development. *Cancer Research* **74**, 2377–2384 (2014).

292. Ertel, A., Verghese, A., Byers, S. W., Ochs, M. & Tozeren, A. Pathway-specific differences between tumor cell lines and normal and tumor tissue cells. *Mol. Cancer* **5**, (2006).

293. Gillet, J. P. *et al.* Redefining the relevance of established cancer cell lines to the study of mechanisms of clinical anti-cancer drug resistance. *Proc. Natl. Acad. Sci. U. S. A.* **108**, 18708–18713 (2011).

294. Domcke, S., Sinha, R., Levine, D. A., Sander, C. & Schultz, N. Evaluating cell lines as tumour models by comparison of genomic profiles. *Nat. Commun.* **4**, (2013).

295. Chen, B., Sirota, M., Fan-Minogue, H., Hadley, D. & Butte, A. J. Relating hepatocellular carcinoma tumor samples and cell lines using gene expression data in translational research. *BMC Med. Genomics* **8**, (2015).

296. Sandberg, R. & Ernberg, I. Assessment of tumor characteristic gene expression in cell lines using a tissue similarity index (TSI). *Proc. Natl. Acad. Sci. U. S. A.* **102**, 2052–2057 (2005).

297. Dai, X., Xiang, L., Li, T. & Bai, Z. Cancer hallmarks, biomarkers and breast cancer molecular subtypes. *Journal of Cancer* **7**, 1281–1294 (2016).

298. Robinson, D. R. *et al.* Integrative clinical genomics of metastatic cancer. *Nature* **548**, 297–303 (2017).

299. Weeber, F., Ooft, S. N., Dijkstra, K. K. & Voest, E. E. Tumor Organoids as a Pre-clinical Cancer Model for Drug Discovery. *Cell Chemical Biology* **24**, 1092–1100 (2017).

300. Drost, J. & Clevers, H. Organoids in cancer research. *Nature Reviews Cancer* **18**, 407–418 (2018).

301. Elian, F. A., Yan, E. & Walter, M. A. FOXC1, the new player in the cancer sandbox. *Oncotarget* **9**, (2018).

302. Hollier, B. G. *et al.* FOXC2 expression links epithelial-mesenchymal transition and stem cell properties in breast cancer. *Cancer Res.* **73**, 1981–92 (2013).

303. Martin, V. *et al.* Molecular characterization of EGFR and EGFR-downstream pathways in triple negative breast carcinomas with basal like features. *Histol. Histopathol.* **27**, 785–792 (2012).

304. Toyama, T. *et al.* Frequently increased epidermal growth factor receptor (EGFR) copy numbers and decreased BRCA1 mRNA expression in Japanese triple-negative breast cancers. *BMC Cancer* **8**, (2008).

305. Hastings, P. J., Lupski, J. R., Rosenberg, S. M. & Ira, G. Mechanisms of change in gene copy number. *Nature Reviews Genetics* **10**, 551–564 (2009).

306. Santos, G. C., Zielenska, M., Prasad, M. & Squire, J. A. Chromosome 6p amplification and cancer progression. *Journal of Clinical Pathology* **60**, 1–7 (2007).

307. Bernardo, G. M. *et al.* FOXA1 represses the molecular phenotype of basal breast cancer cells. *Oncogene* **32**, 554–563 (2013).

308. Hallett, R. M., Dvorkin-Gheva, A., Bane, A. & Hassell, J. A. A gene signature for predicting outcome in patients with basal-like breast cancer. *Sci. Rep.* **2**, 1–8 (2012).

309. Mulligan, A. M., Pinnaduwage, D., Bull, S. B., O'Malley, F. P. & Andrulis, I. L. Prognostic effect of basal-like breast cancers is time dependent: Evidence from tissue microarray studies on a lymph node-negative cohort. *Clin. Cancer Res.* **14**, 4168–4174 (2008).

310. Hanahan, D. & Weinberg, R. a. Hallmarks of cancer: the next generation. *Cell* **144**, 646–74 (2011).

311. Place, A. E., Jin Huh, S. & Polyak, K. The microenvironment in breast cancer progression: biology and implications for treatment. *Breast Cancer Res.* **13**, 227 (2011).

312. Vitale, M., Cantoni, C., Pietra, G., Mingari, M. C. & Moretta, L. Effect of tumor cells and tumor microenvironment on NK-cell function. *Eur. J. Immunol.* **44**, 1582–1592 (2014).

Appendix

Supplementary Table 2.1: The TCGA-BRCA patient data and *FOXQ1* expression in each patient that were used Cox's regression overall survival analysis for the median cut-off and the quartile cut-off

Case Processing Summary			
Cases available in analysis	Event[a]	135	13.40%
	Censored	813	80.80%
	Total	948	94.20%
Cases dropped	Cases with missing values	0	0.00%
	Cases with negative time	0	0.00%
	Censored cases before the earliest event in a stratum	58	5.80%
	Total	58	5.80%
Total		1006	100.00%

Patient	Days	Status	FOXQ1 Expression	Group
TCGA-A1-A0SO	852	Alive	0	Low
TCGA-A2-A0EY	1925	Alive	0	Low
TCGA-A2-A0SW	1365	Dead	0	Low
TCGA-A2-A4S0	706	Alive	0	Low
TCGA-A8-A09K	912	Alive	0	Low
TCGA-AC-A5XS	588	Alive	0	Low
TCGA-AC-A7VC	1	Alive	0	Low
TCGA-AC-A8OR	40	Alive	0	Low
TCGA-B6-A0X5	2097	Dead	0	Low
TCGA-B6-A1KC	1326	Alive	0	Low
TCGA-BH-A0H0	461	Alive	0	Low
TCGA-BH-A0HW	1561	Alive	0	Low
TCGA-D8-A1X6	541	Alive	0	Low
TCGA-D8-A1XC	377	Dead	0	Low
TCGA-E2-A10C	1220	Alive	0	Low
TCGA-E2-A14U	1318	Alive	0	Low
TCGA-E2-A1LS	1604	Alive	0	Low
TCGA-E9-A3Q9	1001	Alive	0	Low
TCGA-E9-A54X	727	Alive	0	Low
TCGA-LQ-A4E4	849	Alive	0	Low
TCGA-BH-A204	2534	Dead	0.23	Low
TCGA-A8-A06Z	31	Alive	0.25	Low

TCGA-LL-A442	889	Alive	0.26	Low
TCGA-AN-A0G0	16	Alive	0.29	Low
TCGA-AC-A2FM	792	Dead	0.33	Low
TCGA-AN-A04C	54	Alive	0.35	Low
TCGA-A8-A09W	30	Alive	0.42	Low
TCGA-AO-A12B	2989	Alive	0.42	Low
TCGA-D8-A73W	385	Dead	0.42	Low
TCGA-AR-A24H	4894	Alive	0.47	Low
TCGA-C8-A1HK	366	Alive	0.5	Low
TCGA-OL-A5RZ	679	Alive	0.51	Low
TCGA-AR-A1AT	1272	Dead	0.52	Low
TCGA-D8-A1JN	620	Alive	0.52	Low
TCGA-D8-A1XV	461	Alive	0.52	Low
TCGA-EW-A1OV	789	Alive	0.53	Low
TCGA-E9-A54Y	725	Alive	0.59	Low
TCGA-C8-A1HO	375	Alive	0.62	Low
TCGA-AR-A0TY	1699	Dead	0.65	Low
TCGA-AO-A03R	2091	Alive	0.67	Low
TCGA-AR-A0TV	2288	Alive	0.7	Low
TCGA-C8-A12X	385	Alive	0.72	Low
TCGA-UU-A93S	116	Dead	0.72	Low
TCGA-GM-A2DM	3226	Alive	0.77	Low
TCGA-AC-A62Y	530	Alive	0.82	Low
TCGA-AR-A0TR	160	Dead	0.82	Low
TCGA-AN-A0AK	224	Alive	0.84	Low
TCGA-BH-A0W3	728	Alive	0.88	Low
TCGA-EW-A6SA	510	Alive	0.93	Low
TCGA-E9-A1R7	1467	Alive	1.06	Low
TCGA-BH-A1FL	1673	Dead	1.08	Low
TCGA-E2-A155	640	Alive	1.13	Low
TCGA-AR-A24Z	3001	Alive	1.14	Low
TCGA-E9-A1RE	1419	Alive	1.17	Low
TCGA-A7-A0DC	906	Alive	1.22	Low
TCGA-AO-A0JL	1683	Alive	1.22	Low
TCGA-A8-A09X	426	Dead	1.24	Low
TCGA-BH-A0BS	2612	Alive	1.29	Low
TCGA-A2-A0D4	767	Alive	1.33	Low
TCGA-A2-A0ET	1066	Alive	1.35	Low
TCGA-AQ-A54N	78	Alive	1.37	Low
TCGA-E2-A156	726	Alive	1.44	Low

TCGA-BH-A18L	811	Dead	1.45	Low
TCGA-AC-A7VB	250	Alive	1.46	Low
TCGA-AN-A0XL	163	Alive	1.5	Low
TCGA-A2-A0YF	1535	Alive	1.59	Low
TCGA-BH-A8FY	295	Dead	1.66	Low
TCGA-AR-A0U3	4080	Alive	1.71	Low
TCGA-C8-A12U	385	Alive	1.73	Low
TCGA-E2-A15J	1640	Alive	1.77	Low
TCGA-AN-A0FJ	242	Alive	1.8	Low
TCGA-BH-A0HL	72	Alive	1.8	Low
TCGA-A2-A0CU	158	Dead	1.91	Low
TCGA-D8-A1JI	577	Alive	1.93	Low
TCGA-S3-AA12	574	Alive	1.96	Low
TCGA-A7-A3IZ	322	Alive	2.03	Low
TCGA-A7-A3RF	408	Alive	2.04	Low
TCGA-D8-A1XF	463	Alive	2.1	Low
TCGA-EW-A1OX	911	Alive	2.13	Low
TCGA-A2-A4S3	666	Alive	2.15	Low
TCGA-A8-A07W	304	Alive	2.22	Low
TCGA-E2-A1IK	1800	Alive	2.22	Low
TCGA-PL-A8LX	5	Alive	2.23	Low
TCGA-B6-A0IB	3941	Dead	2.26	Low
TCGA-A2-A25D	552	Alive	2.28	Low
TCGA-A2-A0CW	3283	Alive	2.3	Low
TCGA-AR-A24U	3128	Alive	2.32	Low
TCGA-AC-A4ZE	890	Alive	2.35	Low
TCGA-LL-A6FP	677	Alive	2.35	Low
TCGA-A2-A3XU	912	Dead	2.38	Low
TCGA-A2-A25B	1291	Alive	2.41	Low
TCGA-D8-A1XW	1309	Alive	2.41	Low
TCGA-A8-A08I	365	Alive	2.43	Low
TCGA-A2-A1FX	1847	Alive	2.44	Low
TCGA-B6-A0RM	2373	Dead	2.44	Low
TCGA-C8-A26Y	394	Alive	2.45	Low
TCGA-AR-A1AR	524	Dead	2.47	Low
TCGA-BH-A1EN	2127	Dead	2.54	Low
TCGA-E2-A1LE	879	Dead	2.54	Low
TCGA-A2-A0SU	1662	Alive	2.58	Low
TCGA-A2-A3XV	996	Alive	2.58	Low
TCGA-AN-A0FF	172	Alive	2.58	Low

TCGA-AR-A2LH	616	Dead	2.63	Low
TCGA-BH-A209	3959	Dead	2.66	Low
TCGA-A8-A079	274	Alive	2.71	Low
TCGA-E2-A14T	2311	Alive	2.72	Low
TCGA-A8-A0A7	30	Alive	2.75	Low
TCGA-BH-A1F2	959	Dead	2.75	Low
TCGA-C8-A274	508	Alive	2.77	Low
TCGA-A7-A4SF	545	Alive	2.79	Low
TCGA-LL-A6FQ	80	Alive	2.83	Low
TCGA-BH-A42T	320	Dead	2.87	Low
TCGA-A8-A09Q	761	Alive	2.94	Low
TCGA-AQ-A04H	754	Alive	2.94	Low
TCGA-AR-A256	2854	Dead	2.96	Low
TCGA-A2-A0YT	723	Dead	2.97	Low
TCGA-BH-A18T	224	Dead	2.99	Low
TCGA-E2-A572	1208	Alive	3	Low
TCGA-A2-A1G4	595	Alive	3.01	Low
TCGA-AQ-A1H2	475	Alive	3.01	Low
TCGA-AR-A0TQ	2991	Alive	3.01	Low
TCGA-BH-A0BP	2296	Dead	3.01	Low
TCGA-E2-A109	1417	Alive	3.08	Low
TCGA-AC-A8OP	614	Alive	3.11	Low
TCGA-AN-A0AT	10	Alive	3.17	Low
TCGA-BH-A1EW	1694	Dead	3.24	Low
TCGA-BH-A0E6	293	Alive	3.27	Low
TCGA-BH-A18S	2009	Dead	3.27	Low
TCGA-A2-A0YG	666	Alive	3.28	Low
TCGA-A2-A0ER	2263	Alive	3.31	Low
TCGA-B6-A1KF	3088	Alive	3.31	Low
TCGA-AN-A0FT	214	Alive	3.32	Low
TCGA-A2-A0ES	2190	Alive	3.34	Low
TCGA-E9-A3HO	1158	Alive	3.36	Low
TCGA-AC-A2FG	1853	Alive	3.37	Low
TCGA-AR-A0U2	2551	Dead	3.41	Low
TCGA-A8-A091	1004	Alive	3.43	Low
TCGA-E2-A15T	1563	Alive	3.45	Low
TCGA-A8-A0A9	822	Alive	3.51	Low
TCGA-A2-A0EP	3603	Alive	3.65	Low
TCGA-AO-A03P	2911	Dead	3.67	Low
TCGA-E2-A1IE	2362	Alive	3.74	Low

TCGA-OL-A66H	812	Alive	3.75	Low
TCGA-AR-A0TZ	3262	Dead	3.83	Low
TCGA-C8-A1HN	394	Alive	3.96	Low
TCGA-A8-A0A1	365	Alive	4.02	Low
TCGA-BH-A0DO	1644	Alive	4.02	Low
TCGA-A1-A0SQ	554	Alive	4.03	Low
TCGA-AN-A0FW	11	Alive	4.05	Low
TCGA-D8-A1X9	727	Alive	4.05	Low
TCGA-C8-A26X	376	Alive	4.13	Low
TCGA-GM-A3XL	2108	Alive	4.15	Low
TCGA-A2-A0D3	1873	Alive	4.19	Low
TCGA-E2-A15D	526	Alive	4.2	Low
TCGA-EW-A1IZ	554	Alive	4.28	Low
TCGA-BH-A0B7	2559	Alive	4.29	Low
TCGA-AR-A24S	2976	Alive	4.4	Low
TCGA-D8-A27W	373	Alive	4.42	Low
TCGA-HN-A2NL	79	Alive	4.43	Low
TCGA-AR-A0TT	3316	Alive	4.49	Low
TCGA-E2-A1LB	2306	Alive	4.49	Low
TCGA-A7-A4SC	446	Alive	4.61	Low
TCGA-AR-A1AV	1864	Alive	4.63	Low
TCGA-E2-A107	1047	Alive	4.63	Low
TCGA-E9-A5UO	785	Alive	4.72	Low
TCGA-AN-A0XT	10	Alive	4.75	Low
TCGA-E9-A249	217	Alive	4.75	Low
TCGA-A8-A07O	304	Alive	4.78	Low
TCGA-EW-A1J1	575	Alive	4.81	Low
TCGA-C8-A12M	358	Alive	4.83	Low
TCGA-A2-A0T1	521	Alive	4.87	Low
TCGA-BH-A0BO	2197	Alive	4.87	Low
TCGA-A2-A0YJ	566	Alive	4.88	Low
TCGA-C8-A3M7	1034	Dead	4.92	Low
TCGA-E2-A15M	336	Dead	4.95	Low
TCGA-BH-A1EU	1286	Dead	4.96	Low
TCGA-E9-A2JT	288	Alive	4.96	Low
TCGA-AR-A2LE	5062	Alive	4.99	Low
TCGA-AR-A0TU	709	Alive	5.01	Low
TCGA-A2-A3KD	1206	Alive	5.04	Low
TCGA-AO-A12F	1842	Alive	5.1	Low
TCGA-PE-A5DC	1430	Dead	5.15	Low

TCGA-BH-A18H	652	Alive	5.18	Low
TCGA-A8-A06Q	31	Alive	5.24	Low
TCGA-A7-A0CJ	931	Alive	5.28	Low
TCGA-B6-A1KI	2236	Alive	5.28	Low
TCGA-AR-A1AX	2629	Alive	5.29	Low
TCGA-AO-A0JI	1528	Alive	5.3	Low
TCGA-A8-A085	1124	Alive	5.32	Low
TCGA-D8-A1XZ	466	Alive	5.33	Low
TCGA-BH-A0B0	2477	Alive	5.37	Low
TCGA-AC-A62X	417	Alive	5.41	Low
TCGA-A2-A0CO	3492	Dead	5.43	Low
TCGA-AR-A1AL	2971	Alive	5.43	Low
TCGA-D8-A27R	307	Alive	5.48	Low
TCGA-D8-A1JF	366	Alive	5.51	Low
TCGA-WT-AB41	1611	Alive	5.52	Low
TCGA-AC-A6NO	51	Alive	5.54	Low
TCGA-GM-A3NW	3361	Alive	5.54	Low
TCGA-PL-A8LZ	302	Alive	5.55	Low
TCGA-C8-A26V	616	Alive	5.57	Low
TCGA-BH-A0DX	2156	Alive	5.58	Low
TCGA-E2-A14P	1246	Alive	5.61	Low
TCGA-BH-A0DH	1156	Alive	5.65	Low
TCGA-BH-A0HO	76	Alive	5.66	Low
TCGA-AN-A046	10	Alive	5.68	Low
TCGA-A7-A4SB	418	Alive	5.74	Low
TCGA-AN-A04D	52	Alive	5.76	Low
TCGA-E2-A1IU	337	Alive	5.76	Low
TCGA-OL-A66P	428	Alive	5.76	Low
TCGA-A8-A09E	1492	Alive	5.81	Low
TCGA-AC-A2FO	2255	Alive	5.82	Low
TCGA-AR-A1AP	2856	Alive	5.85	Low
TCGA-B6-A0X4	860	Dead	5.9	Low
TCGA-A7-A13G	718	Alive	5.92	Low
TCGA-A8-A08F	1004	Alive	5.95	Low
TCGA-AC-A23H	174	Dead	5.95	Low
TCGA-A2-A4S1	820	Alive	5.96	Low
TCGA-D8-A1XR	482	Alive	6	Low
TCGA-E9-A22H	1232	Alive	6.05	Low
TCGA-A8-A09C	31	Alive	6.07	Low
TCGA-OL-A6VR	1220	Alive	6.08	Low

TCGA-EW-A1P1	1210	Alive	6.09	Low
TCGA-E2-A158	450	Alive	6.17	Low
TCGA-BH-A18N	1148	Dead	6.18	Low
TCGA-EW-A1P6	562	Alive	6.35	Low
TCGA-BH-A0H5	1620	Alive	6.4	Low
TCGA-E2-A15C	694	Alive	6.4	Low
TCGA-C8-A135	393	Alive	6.45	Low
TCGA-E9-A248	59	Alive	6.47	Low
TCGA-A8-A0A4	396	Alive	6.53	Low
TCGA-AR-A2LQ	1233	Alive	6.55	Low
TCGA-BH-A1FG	3736	Dead	6.55	Low
TCGA-E9-A1R6	339	Alive	6.57	Low
TCGA-C8-A1HM	375	Alive	6.63	Low
TCGA-C8-A3M8	394	Alive	6.67	Low
TCGA-E2-A14X	972	Alive	6.74	Low
TCGA-AC-A2FB	1234	Alive	6.81	Low
TCGA-E2-A14S	1009	Alive	6.83	Low
TCGA-A2-A3XT	2770	Alive	6.86	Low
TCGA-D8-A145	410	Alive	6.86	Low
TCGA-GM-A2DO	2596	Alive	6.89	Low
TCGA-A2-A04V	1920	Dead	6.93	Low
TCGA-S3-AA17	424	Alive	6.94	Low
TCGA-A2-A1FV	714	Alive	7	Low
TCGA-D8-A27G	409	Alive	7.12	Low
TCGA-A2-A259	1596	Alive	7.15	Low
TCGA-S3-AA0Z	629	Alive	7.19	Low
TCGA-AR-A2LL	2012	Alive	7.22	Low
TCGA-3C-AAAU	4047	Alive	7.24	Low
TCGA-EW-A1OY	908	Alive	7.24	Low
TCGA-BH-A28Q	1119	Alive	7.32	Low
TCGA-D8-A1X8	783	Alive	7.32	Low
TCGA-C8-A12W	385	Alive	7.34	Low
TCGA-BH-A0AY	777	Alive	7.39	Low
TCGA-A2-A0CL	3015	Alive	7.41	Low
TCGA-AO-A0J2	997	Alive	7.41	Low
TCGA-E2-A15O	1545	Alive	7.42	Low
TCGA-BH-A0H9	1247	Alive	7.43	Low
TCGA-B6-A0RO	4929	Alive	7.48	Low
TCGA-E2-A1L6	1648	Alive	7.48	Low
TCGA-AC-A2B8	677	Alive	7.56	Low

TCGA-B6-A0WZ	6292	Alive	7.6	Low
TCGA-PL-A8LY	8	Alive	7.66	Low
TCGA-A8-A07C	1034	Alive	7.71	Low
TCGA-A8-A08S	1004	Alive	7.74	Low
TCGA-A2-A0D2	1027	Alive	7.76	Low
TCGA-OL-A5RU	1219	Alive	7.78	Low
TCGA-A8-A08C	881	Alive	7.79	Low
TCGA-E2-A108	837	Alive	7.79	Low
TCGA-A2-A0YH	659	Alive	7.8	Low
TCGA-D8-A140	403	Alive	7.85	Low
TCGA-S3-A6ZH	641	Alive	7.87	Low
TCGA-AC-A62V	348	Dead	7.9	Low
TCGA-E2-A154	591	Alive	7.95	Low
TCGA-PE-A5DD	1953	Alive	7.95	Low
TCGA-A2-A0SY	1347	Alive	8.01	Low
TCGA-E9-A1NE	1088	Alive	8.01	Low
TCGA-A7-A13E	614	Dead	8.11	Low
TCGA-BH-A1FD	1009	Dead	8.12	Low
TCGA-A7-A425	447	Alive	8.25	Low
TCGA-AN-A0FL	231	Alive	8.29	Low
TCGA-E9-A1R4	186	Alive	8.35	Low
TCGA-A2-A3XY	1093	Dead	8.42	Low
TCGA-S3-AA11	421	Alive	8.44	Low
TCGA-BH-A1FJ	1927	Dead	8.45	Low
TCGA-E9-A245	26	Alive	8.47	Low
TCGA-D8-A1JB	1688	Alive	8.53	Low
TCGA-OL-A66L	1301	Alive	8.55	Low
TCGA-AN-A0FK	213	Alive	8.56	Low
TCGA-AC-A3TN	456	Alive	8.62	Low
TCGA-E2-A14W	974	Alive	8.62	Low
TCGA-A2-A0YI	1505	Alive	8.65	Low
TCGA-BH-A18P	921	Dead	8.79	Low
TCGA-E2-A15K	275	Alive	8.8	Low
TCGA-B6-A0IO	5042	Alive	8.88	Low
TCGA-AC-A2FK	2650	Alive	8.89	Low
TCGA-EW-A2FS	1604	Alive	8.9	Low
TCGA-BH-A0E7	1363	Alive	8.92	Low
TCGA-E2-A14N	1434	Alive	8.93	Low
TCGA-OL-A5D8	973	Alive	9.1	Low
TCGA-AC-A6IX	373	Alive	9.11	Low

TCGA-D8-A27K	1461	Alive	9.12	Low
TCGA-D8-A3Z5	1015	Alive	9.18	Low
TCGA-A8-A09M	1006	Alive	9.25	Low
TCGA-BH-A0HN	516	Alive	9.3	Low
TCGA-A8-A08J	1127	Dead	9.31	Low
TCGA-AR-A0TP	4275	Alive	9.41	Low
TCGA-E9-A1QZ	755	Alive	9.42	Low
TCGA-A1-A0SJ	416	Alive	9.51	Low
TCGA-A8-A06Y	791	Alive	9.52	Low
TCGA-A8-A0A6	640	Alive	9.58	Low
TCGA-B6-A0RQ	4267	Dead	9.6	Low
TCGA-EW-A1P8	239	Dead	9.68	Low
TCGA-AR-A2LK	1649	Dead	9.72	Low
TCGA-A8-A099	304	Alive	9.85	Low
TCGA-E2-A15I	1692	Alive	9.89	Low
TCGA-E9-A1RA	1369	Alive	9.89	Low
TCGA-A8-A06X	943	Dead	9.94	Low
TCGA-BH-A0B6	2483	Alive	9.94	Low
TCGA-BH-A6R8	293	Alive	10	Low
TCGA-GM-A2DK	2645	Alive	10.01	Low
TCGA-D8-A1Y0	472	Alive	10.06	Low
TCGA-LL-A441	996	Alive	10.08	Low
TCGA-EW-A1PE	320	Alive	10.17	Low
TCGA-C8-A26W	381	Alive	10.3	Low
TCGA-AN-A0FZ	10	Alive	10.32	Low
TCGA-A2-A25C	523	Alive	10.37	Low
TCGA-AR-A252	2838	Alive	10.37	Low
TCGA-AO-A12E	2142	Alive	10.38	Low
TCGA-D8-A1X5	565	Alive	10.47	Low
TCGA-C8-A8HR	408	Alive	10.48	Low
TCGA-LL-A8F5	596	Alive	10.49	Low
TCGA-E2-A106	2541	Alive	10.5	Low
TCGA-GM-A2DF	2155	Alive	10.54	Low
TCGA-AR-A2LN	1161	Alive	10.57	Low
TCGA-C8-A134	383	Alive	10.59	Low
TCGA-EW-A1PA	575	Alive	10.6	Low
TCGA-AO-A126	3307	Alive	10.66	Low
TCGA-A2-A04X	1686	Alive	10.81	Low
TCGA-A8-A07Z	1371	Alive	10.81	Low
TCGA-AN-A0AR	10	Alive	10.82	Low

TCGA-AN-A03X	10	Alive	10.84	Low
TCGA-BH-A1EX	1508	Dead	10.86	Low
TCGA-AO-A0JM	2184	Alive	10.89	Low
TCGA-EW-A1J6	875	Alive	10.9	Low
TCGA-LL-A5YL	519	Alive	10.91	Low
TCGA-B6-A0I8	749	Dead	10.95	Low
TCGA-A2-A3XX	1439	Dead	10.97	Low
TCGA-LL-A5YN	447	Alive	10.97	Low
TCGA-B6-A0IK	571	Dead	10.98	Low
TCGA-BH-A0RX	170	Alive	10.99	Low
TCGA-E2-A10A	1229	Alive	10.99	Low
TCGA-A8-A08L	304	Dead	11.1	Low
TCGA-AR-A0TS	2558	Alive	11.13	Low
TCGA-C8-A27A	747	Alive	11.2	Low
TCGA-LD-A7W5	216	Alive	11.22	Low
TCGA-C8-A1HE	375	Alive	11.25	Low
TCGA-E2-A56Z	252	Alive	11.27	Low
TCGA-A2-A25E	3204	Alive	11.32	Low
TCGA-AO-A03O	2483	Dead	11.35	Low
TCGA-A7-A26E	954	Alive	11.41	Low
TCGA-E2-A105	1308	Alive	11.54	Low
TCGA-A8-A06P	396	Alive	11.57	Low
TCGA-A8-A08R	30	Alive	11.63	Low
TCGA-OL-A5RV	1062	Alive	11.68	Low
TCGA-AR-A24N	3035	Alive	11.71	Low
TCGA-AR-A1AW	2632	Alive	11.73	Low
TCGA-AR-A24K	1548	Alive	11.76	Low
TCGA-A8-A06O	396	Alive	11.9	Low
TCGA-B6-A0IH	3418	Dead	11.92	Low
TCGA-AC-A23C	585	Alive	12.03	Low
TCGA-AR-A24R	3430	Alive	12.03	Low
TCGA-A2-A0CR	3283	Alive	12.04	Low
TCGA-GI-A2C8	225	Alive	12.05	Low
TCGA-A2-A0T4	624	Alive	12.2	Low
TCGA-D8-A1JC	480	Alive	12.23	Low
TCGA-E2-A2P6	1051	Alive	12.25	Low
TCGA-A2-A0EX	752	Alive	12.26	Low
TCGA-A2-A25F	322	Alive	12.36	Low
TCGA-E2-A14O	1359	Alive	12.42	Low
TCGA-BH-A1F8	763	Dead	12.44	Low

TCGA-AO-A0J6	1140	Alive	12.51	Low
TCGA-C8-A131	411	Alive	12.51	Low
TCGA-Z7-A8R5	3287	Alive	12.54	Low
TCGA-BH-A18F	1001	Alive	12.55	Low
TCGA-E9-A243	612	Alive	12.6	Low
TCGA-A2-A1G1	584	Alive	12.65	Low
TCGA-AO-A1KQ	1882	Alive	12.68	Low
TCGA-LL-A7T0	376	Alive	12.71	Low
TCGA-AR-A2LO	1198	Alive	12.84	Low
TCGA-AC-A8OS	70	Alive	13.17	Low
TCGA-A8-A07U	760	Alive	13.2	Low
TCGA-OL-A66N	792	Alive	13.2	Low
TCGA-E2-A1LI	3121	Alive	13.22	Low
TCGA-AO-A12A	3112	Alive	13.31	Low
TCGA-BH-A0B5	2136	Alive	13.34	Low
TCGA-B6-A0WS	2965	Dead	13.36	Low
TCGA-AN-A0XS	10	Alive	13.4	Low
TCGA-A8-A07P	334	Alive	13.48	Low
TCGA-OL-A66J	1996	Alive	13.52	Low
TCGA-AR-A1AY	1026	Alive	13.59	Low
TCGA-A8-A06T	1614	Alive	13.62	Low
TCGA-E9-A2JS	904	Dead	13.79	Low
TCGA-E9-A1R2	1063	Alive	13.8	Low
TCGA-EW-A3E8	1035	Alive	13.84	Low
TCGA-A7-A2KD	679	Alive	13.88	Low
TCGA-AO-A1KS	350	Alive	13.88	Low
TCGA-BH-A0H3	1928	Alive	13.88	Low
TCGA-AN-A0AM	5	Alive	13.95	Low
TCGA-B6-A0RN	8008	Alive	13.98	Low
TCGA-A8-A076	1642	Alive	14.05	Low
TCGA-E2-A15S	428	Alive	14.09	Low
TCGA-OL-A6VQ	600	Alive	14.14	Low
TCGA-E9-A22D	1248	Alive	14.18	Low
TCGA-BH-A1FH	1034	Dead	14.24	Low
TCGA-A7-A0CD	1165	Alive	14.25	Low
TCGA-E2-A14Q	1163	Alive	14.27	Low
TCGA-B6-A2IU	5176	Alive	14.38	Low
TCGA-AC-A2BK	2222	Alive	14.39	Low
TCGA-AC-A5EH	511	Alive	14.43	Low
TCGA-BH-A0BV	1519	Alive	14.58	Low

TCGA-3C-AALI	4005	Alive	14.68	Low
TCGA-B6-A0RL	2469	Dead	14.77	Low
TCGA-A8-A06U	883	Dead	14.78	Low
TCGA-B6-A0WV	2417	Dead	14.84	Low
TCGA-AC-A2FE	2636	Dead	14.85	Low
TCGA-AO-A03V	1351	Alive	14.9	Low
TCGA-D8-A1XA	839	Alive	15.01	Low
TCGA-A8-A09I	1371	Alive	15.02	Low
TCGA-GM-A2DI	2590	Alive	15.03	Low
TCGA-A8-A09R	273	Alive	15.26	Low
TCGA-OL-A5RX	878	Alive	15.32	Low
TCGA-E2-A15A	710	Alive	15.36	Low
TCGA-D8-A1JL	611	Alive	15.4	Low
TCGA-BH-A0DD	2486	Alive	15.41	Low
TCGA-AR-A1AK	3159	Alive	15.42	Low
TCGA-JL-A3YX	352	Alive	15.48	Low
TCGA-E9-A228	1285	Alive	15.56	Low
TCGA-BH-A18G	149	Alive	15.63	Low
TCGA-A8-A08G	607	Alive	15.67	Low
TCGA-A2-A0T6	575	Alive	15.72	Low
TCGA-C8-A12Z	382	Alive	15.73	Low
TCGA-AC-A2FF	2759	Alive	15.78	Low
TCGA-D8-A27F	488	Alive	15.97	Low
TCGA-D8-A141	626	Alive	16	Low
TCGA-AO-A0J8	680	Alive	16.03	Low
TCGA-AN-A0XV	162	Alive	16.04	Low
TCGA-C8-A12P	358	Alive	16.05	Low
TCGA-E9-A1R5	92	Alive	16.07	Low
TCGA-A1-A0SM	242	Alive	16.1	Low
TCGA-C8-A273	513	Alive	16.13	Low
TCGA-A8-A09N	31	Alive	16.15	Low
TCGA-GM-A2DH	2193	Alive	16.17	Low
TCGA-D8-A1JK	612	Alive	16.2	Low
TCGA-E9-A1RD	34	Alive	16.21	Low
TCGA-E2-A10B	1141	Alive	16.22	Low
TCGA-D8-A1JU	447	Alive	16.24	Low
TCGA-AQ-A1H3	989	Alive	16.27	Low
TCGA-AC-A3BB	987	Alive	16.29	Low
TCGA-D8-A1Y3	430	Alive	16.41	Low
TCGA-GM-A2DC	2535	Alive	16.41	Low

TCGA-C8-A12Q	385	Dead	16.42	Low
TCGA-BH-A1FU	1688	Dead	16.46	Low
TCGA-BH-A0EI	1926	Alive	16.61	Low
TCGA-GM-A3NY	1162	Alive	16.64	Low
TCGA-BH-A0DG	2041	Alive	16.68	Low
TCGA-LL-A50Y	762	Alive	16.73	Low
TCGA-BH-AB28	287	Alive	16.74	Low
TCGA-BH-A0EA	991	Dead	16.75	Low
TCGA-EW-A1OW	694	Alive	16.8	Low
TCGA-AO-A0JJ	1887	Alive	16.92	Low
TCGA-AN-A0XP	9	Alive	17.04	Low
TCGA-OK-A5Q2	64	Alive	17.12	Low
TCGA-AR-A24Q	3172	Alive	17.18	Low
TCGA-A7-A426	364	Alive	17.19	Low
TCGA-BH-A8FZ	574	Alive	17.22	Low
TCGA-A7-A3J0	313	Alive	17.3	Low
TCGA-D8-A1JG	1612	Alive	17.33	Low
TCGA-A7-A13H	899	Alive	17.35	Low
TCGA-GM-A3XG	1330	Alive	17.35	Low
TCGA-S3-A6ZF	572	Alive	17.41	Low
TCGA-A8-A09B	365	Alive	17.42	Low
TCGA-BH-A0E1	477	Alive	17.42	Low
TCGA-A8-A07L	975	Alive	17.48	Low
TCGA-E9-A1ND	1266	Alive	17.49	Low
TCGA-AC-A5XU	455	Alive	17.5	Low
TCGA-BH-A0DP	476	Alive	17.57	Low
TCGA-AR-A250	2707	Alive	17.66	Low
TCGA-E2-A153	707	Alive	17.8	Low
TCGA-C8-A1HF	332	Alive	17.82	Low
TCGA-BH-A18R	1142	Dead	17.83	Low
TCGA-D8-A1Y1	302	Dead	17.88	Low
TCGA-AC-A3EH	197	Dead	17.97	Low
TCGA-B6-A0WT	5739	Alive	18.02	Low
TCGA-AR-A1AI	3296	Alive	18.04	Low
TCGA-AR-A1AO	2618	Alive	18.07	Low
TCGA-XX-A899	467	Alive	18.11	Low
TCGA-E2-A15E	630	Alive	18.22	Low
TCGA-A8-A092	942	Alive	18.24	Low
TCGA-BH-A0HP	414	Alive	18.35	Low
TCGA-E9-A5FK	812	Alive	18.39	Low

TCGA-A2-A0YK	588	Alive	18.42	Low
TCGA-XX-A89A	488	Alive	18.42	High
TCGA-BH-A0DV	2064	Alive	18.45	High
TCGA-A2-A0EM	3094	Alive	18.47	High
TCGA-E9-A3X8	926	Alive	18.57	High
TCGA-C8-A137	379	Alive	18.59	High
TCGA-C8-A12L	363	Alive	18.6	High
TCGA-A8-A075	518	Alive	18.64	High
TCGA-C8-A12V	385	Alive	18.65	High
TCGA-E2-A1IH	1026	Alive	18.7	High
TCGA-A7-A0DA	1085	Alive	18.74	High
TCGA-A2-A0EW	1884	Dead	18.77	High
TCGA-AO-A0JC	1547	Alive	18.83	High
TCGA-D8-A1XY	503	Alive	18.84	High
TCGA-C8-A1HI	343	Alive	18.89	High
TCGA-AC-A6IV	568	Alive	18.96	High
TCGA-A2-A0CK	4159	Alive	18.99	High
TCGA-E2-A15F	658	Alive	19.01	High
TCGA-AN-A0XR	10	Alive	19.02	High
TCGA-GM-A5PV	412	Alive	19.02	High
TCGA-A2-A0T3	1516	Alive	19.06	High
TCGA-AQ-A7U7	584	Dead	19.13	High
TCGA-D8-A1Y2	433	Alive	19.19	High
TCGA-EW-A1J5	477	Alive	19.21	High
TCGA-A8-A0AB	518	Alive	19.33	High
TCGA-BH-A1EY	538	Dead	19.5	High
TCGA-E2-A3DX	1325	Alive	19.57	High
TCGA-A8-A082	549	Alive	19.6	High
TCGA-A8-A09D	1522	Alive	19.65	High
TCGA-EW-A1J3	504	Alive	19.73	High
TCGA-A2-A04Y	1099	Alive	19.74	High
TCGA-A2-A04T	2246	Alive	19.82	High
TCGA-A2-A0YC	990	Alive	19.93	High
TCGA-D8-A146	643	Alive	19.94	High
TCGA-AN-A0FS	210	Alive	20.01	High
TCGA-A2-A3XS	1032	Dead	20.03	High
TCGA-A7-A13F	765	Alive	20.08	High
TCGA-AR-A2LM	1935	Alive	20.09	High
TCGA-AC-A3OD	451	Alive	20.2	High
TCGA-BH-A0BZ	2255	Alive	20.23	High

TCGA-BH-A1F5	2712	Dead	20.27	High
TCGA-AR-A0TX	1972	Alive	20.3	High
TCGA-E9-A3QA	918	Alive	20.57	High
TCGA-AO-A03M	1866	Alive	20.58	High
TCGA-BH-A28O	1120	Alive	20.59	High
TCGA-C8-A8HP	396	Alive	20.66	High
TCGA-A8-A07J	365	Alive	20.7	High
TCGA-B6-A0I5	8556	Alive	20.72	High
TCGA-BH-A1F6	2965	Dead	20.74	High
TCGA-A2-A0EN	4088	Alive	20.81	High
TCGA-E9-A1RB	976	Dead	20.81	High
TCGA-AO-A03L	2442	Alive	20.84	High
TCGA-D8-A27N	519	Alive	20.86	High
TCGA-EW-A1PF	439	Alive	20.87	High
TCGA-A2-A0YD	769	Alive	20.94	High
TCGA-D8-A73U	492	Alive	21	High
TCGA-LL-A440	759	Alive	21	High
TCGA-A2-A1G6	501	Alive	21.01	High
TCGA-A7-A3IY	345	Alive	21.31	High
TCGA-A2-A25A	3276	Alive	21.51	High
TCGA-BH-A18Q	1692	Dead	21.6	High
TCGA-A8-A08T	3409	Dead	21.63	High
TCGA-D8-A27L	499	Alive	21.66	High
TCGA-B6-A0I9	362	Dead	21.67	High
TCGA-BH-A5J0	715	Alive	21.78	High
TCGA-E9-A1N6	678	Dead	21.85	High
TCGA-E9-A24A	747	Alive	21.9	High
TCGA-A2-A0EQ	2426	Alive	21.97	High
TCGA-D8-A1J9	532	Alive	21.98	High
TCGA-AR-A0TW	3009	Alive	22.01	High
TCGA-AR-A1AJ	3072	Alive	22.05	High
TCGA-D8-A1XG	448	Alive	22.05	High
TCGA-A2-A0D1	1051	Alive	22.13	High
TCGA-D8-A1JE	575	Alive	22.18	High
TCGA-B6-A409	573	Dead	22.26	High
TCGA-EW-A424	715	Alive	22.33	High
TCGA-OL-A66K	1275	Dead	22.38	High
TCGA-EW-A1P5	703	Alive	22.46	High
TCGA-BH-A0AU	1914	Alive	22.56	High
TCGA-E9-A1R0	860	Alive	22.58	High

TCGA-A7-A0DB	1007	Alive	22.61	High
TCGA-BH-A0AW	622	Alive	22.64	High
TCGA-E2-A15R	1732	Alive	22.64	High
TCGA-3C-AALJ	1474	Alive	22.67	High
TCGA-C8-A12O	385	Alive	22.75	High
TCGA-A8-A09T	579	Alive	22.8	High
TCGA-AC-A3HN	496	Alive	22.91	High
TCGA-AR-A1AS	1150	Alive	22.96	High
TCGA-BH-A8G0	662	Alive	23.02	High
TCGA-AO-A0JF	1980	Alive	23.06	High
TCGA-AR-A5QM	2231	Alive	23.15	High
TCGA-A8-A095	1277	Alive	23.3	High
TCGA-BH-A0BJ	660	Alive	23.31	High
TCGA-E9-A247	1186	Alive	23.31	High
TCGA-BH-A0BT	2365	Alive	23.39	High
TCGA-E9-A1N8	1039	Alive	23.49	High
TCGA-D8-A1JP	639	Alive	23.54	High
TCGA-PE-A5DE	2645	Alive	23.54	High
TCGA-AO-A129	3286	Alive	23.55	High
TCGA-EW-A1J2	403	Alive	23.6	High
TCGA-AC-A2BM	3022	Alive	23.81	High
TCGA-BH-A0BF	1324	Dead	23.89	High
TCGA-LD-A9QF	323	Alive	23.98	High
TCGA-BH-A0DS	78	Alive	24	High
TCGA-D8-A1XM	538	Alive	24	High
TCGA-BH-A0C1	1411	Dead	24.07	High
TCGA-D8-A1XU	395	Alive	24.08	High
TCGA-BH-A1ET	2520	Dead	24.11	High
TCGA-A2-A4S2	643	Alive	24.13	High
TCGA-D8-A142	425	Alive	24.17	High
TCGA-AR-A2LJ	2632	Alive	24.19	High
TCGA-E2-A1B5	984	Alive	24.33	High
TCGA-E2-A10E	865	Alive	24.43	High
TCGA-E2-A152	2128	Alive	24.54	High
TCGA-D8-A143	431	Alive	24.59	High
TCGA-A8-A08X	1308	Alive	24.62	High
TCGA-BH-A1FB	3669	Dead	24.66	High
TCGA-E2-A15P	595	Alive	24.91	High
TCGA-GM-A4E0	2191	Alive	24.97	High
TCGA-BH-A0W5	1288	Alive	24.99	High

TCGA-A1-A0SN	1196	Alive	25.02	High
TCGA-BH-A0C0	1270	Alive	25.13	High
TCGA-E2-A1IL	118	Alive	25.22	High
TCGA-LL-A9Q3	532	Alive	25.28	High
TCGA-A7-A3J1	343	Alive	25.42	High
TCGA-BH-A0DE	2372	Alive	25.55	High
TCGA-B6-A0RS	3063	Dead	25.57	High
TCGA-BH-A0B8	1569	Alive	25.71	High
TCGA-BH-A0BD	554	Alive	25.83	High
TCGA-A8-A084	458	Alive	25.91	High
TCGA-B6-A1KN	4233	Alive	25.94	High
TCGA-AO-A0JE	2335	Alive	25.96	High
TCGA-BH-A18M	2207	Dead	26.08	High
TCGA-E2-A1B1	2653	Alive	26.1	High
TCGA-BH-A203	1174	Dead	26.17	High
TCGA-A7-A5ZW	326	Alive	26.35	High
TCGA-AC-A3YI	707	Alive	26.36	High
TCGA-A8-A08A	30	Alive	26.41	High
TCGA-E2-A1L9	598	Alive	26.68	High
TCGA-AN-A03Y	10	Alive	26.8	High
TCGA-A2-A0CV	3011	Alive	26.93	High
TCGA-AC-A3QQ	734	Alive	26.93	High
TCGA-BH-A18U	1563	Dead	27.08	High
TCGA-AR-A24L	2866	Dead	27.16	High
TCGA-BH-A1FN	2192	Dead	27.23	High
TCGA-EW-A6SD	1010	Alive	27.23	High
TCGA-BH-A18K	2763	Dead	27.27	High
TCGA-BH-A0E2	435	Alive	27.47	High
TCGA-BH-A0GY	923	Alive	27.5	High
TCGA-AR-A24W	1550	Alive	27.54	High
TCGA-OL-A6VO	858	Alive	27.54	High
TCGA-BH-A0HU	392	Alive	27.56	High
TCGA-AR-A5QN	1013	Alive	27.57	High
TCGA-E2-A9RU	538	Alive	27.63	High
TCGA-AR-A1AN	2920	Alive	27.7	High
TCGA-V7-A7HQ	2033	Alive	27.71	High
TCGA-B6-A0IP	3926	Dead	27.73	High
TCGA-BH-A0HX	829	Alive	27.83	High
TCGA-LL-A5YP	450	Alive	28.03	High
TCGA-A2-A1FZ	683	Alive	28.13	High

TCGA-AR-A255	2161	Alive	28.24	High
TCGA-D8-A1JA	502	Alive	28.44	High
TCGA-EW-A1PC	187	Alive	28.46	High
TCGA-LL-A5YM	466	Alive	28.53	High
TCGA-A8-A07E	608	Alive	28.65	High
TCGA-BH-A0E9	2489	Alive	28.66	High
TCGA-C8-A26Z	470	Alive	28.75	High
TCGA-AC-A3W7	471	Alive	28.77	High
TCGA-E9-A227	975	Alive	28.86	High
TCGA-A8-A09V	457	Alive	28.87	High
TCGA-A8-A08Z	1217	Alive	29.05	High
TCGA-C8-A275	1	Alive	29.13	High
TCGA-LL-A7SZ	594	Alive	29.27	High
TCGA-BH-A42V	635	Alive	29.4	High
TCGA-A8-A07I	426	Alive	29.54	High
TCGA-A8-A07B	1308	Alive	29.59	High
TCGA-B6-A401	2596	Alive	29.76	High
TCGA-BH-A2L8	612	Alive	29.79	High
TCGA-LL-A740	441	Alive	29.87	High
TCGA-E2-A570	931	Alive	29.96	High
TCGA-A8-A08P	943	Alive	30.16	High
TCGA-D8-A4Z1	659	Alive	30.28	High
TCGA-EW-A1PG	1051	Alive	30.39	High
TCGA-AC-A3TM	762	Alive	30.42	High
TCGA-E2-A1BD	1133	Alive	30.45	High
TCGA-A7-A0D9	1139	Alive	30.47	High
TCGA-OL-A5D6	1104	Dead	30.75	High
TCGA-EW-A1PD	424	Alive	31.06	High
TCGA-GM-A2DN	3091	Alive	31.24	High
TCGA-AC-A3W5	504	Alive	31.26	High
TCGA-A7-A56D	448	Alive	31.38	High
TCGA-EW-A1OZ	1229	Alive	31.38	High
TCGA-A2-A0EV	968	Alive	31.58	High
TCGA-D8-A1XL	606	Alive	31.6	High
TCGA-E9-A22G	1239	Alive	31.72	High
TCGA-B6-A40C	2164	Alive	31.83	High
TCGA-A2-A04R	3709	Alive	31.88	High
TCGA-AC-A2QI	588	Alive	32.09	High
TCGA-E2-A1B6	867	Alive	32.13	High
TCGA-A8-A09A	304	Alive	32.17	High

TCGA-AQ-A04L	3957	Alive	32.25	High
TCGA-D8-A27I	439	Alive	32.35	High
TCGA-GM-A2D9	1812	Dead	32.54	High
TCGA-BH-A0C7	2767	Alive	32.56	High
TCGA-AN-A0FV	10	Alive	32.65	High
TCGA-A1-A0SI	635	Alive	32.67	High
TCGA-OL-A66O	528	Alive	32.67	High
TCGA-E2-A1IF	1138	Alive	32.7	High
TCGA-A2-A0CQ	2695	Alive	32.87	High
TCGA-A8-A097	365	Alive	32.87	High
TCGA-D8-A1J8	431	Alive	32.87	High
TCGA-EW-A1P3	1611	Alive	32.89	High
TCGA-AN-A049	19	Alive	32.92	High
TCGA-A2-A4RY	648	Alive	32.97	High
TCGA-E2-A576	1043	Alive	33	High
TCGA-AO-A03N	2031	Alive	33.05	High
TCGA-AO-A0JD	2190	Alive	33.11	High
TCGA-D8-A13Y	1728	Alive	33.22	High
TCGA-W8-A86G	347	Alive	33.22	High
TCGA-A1-A0SF	1463	Alive	33.42	High
TCGA-E2-A10F	878	Alive	33.42	High
TCGA-AR-A24P	84	Alive	33.56	High
TCGA-AR-A1AM	2991	Alive	33.58	High
TCGA-E9-A1RG	647	Alive	33.73	High
TCGA-AC-A2QH	1005	Alive	33.8	High
TCGA-D8-A27P	49	Alive	34.28	High
TCGA-AC-A23E	698	Alive	34.55	High
TCGA-B6-A0I1	2361	Dead	34.59	High
TCGA-BH-A202	795	Alive	34.69	High
TCGA-A7-A4SA	454	Alive	34.75	High
TCGA-AO-A1KR	2513	Alive	34.78	High
TCGA-AN-A0FY	10	Alive	34.83	High
TCGA-BH-A0HQ	1121	Alive	35.09	High
TCGA-LL-A5YO	440	Alive	35.25	High
TCGA-B6-A0RT	2721	Alive	35.29	High
TCGA-B6-A0IG	4456	Dead	35.34	High
TCGA-E9-A6HE	847	Alive	35.66	High
TCGA-E2-A1B4	1004	Dead	35.69	High
TCGA-GM-A2DB	2406	Alive	35.79	High
TCGA-D8-A1XD	522	Alive	35.86	High

TCGA-LD-A66U	646	Alive	35.96	High
TCGA-AC-A3W6	602	Alive	36	High
TCGA-EW-A6SC	952	Alive	36.1	High
TCGA-EW-A1IW	371	Alive	36.35	High
TCGA-BH-A0HI	620	Alive	36.57	High
TCGA-D8-A1JH	426	Alive	36.7	High
TCGA-A2-A04P	548	Dead	36.83	High
TCGA-B6-A0RI	7126	Alive	37.08	High
TCGA-BH-A18V	1556	Dead	37.12	High
TCGA-B6-A0WY	3461	Dead	37.45	High
TCGA-AO-A1KP	2953	Alive	37.47	High
TCGA-E2-A1AZ	2329	Alive	37.51	High
TCGA-D8-A1XT	506	Alive	37.57	High
TCGA-D8-A1XO	1682	Alive	37.64	High
TCGA-D8-A13Z	635	Alive	37.79	High
TCGA-A2-A3XZ	1532	Alive	37.9	High
TCGA-A2-A0T5	531	Alive	37.93	High
TCGA-A2-A3Y0	1546	Alive	38.09	High
TCGA-BH-A1FE	2273	Dead	38.25	High
TCGA-D8-A27T	398	Alive	38.47	High
TCGA-AO-A0JA	655	Alive	38.48	High
TCGA-BH-A1ES	3462	Dead	38.52	High
TCGA-AO-A03T	2124	Alive	38.57	High
TCGA-A8-A093	546	Alive	38.61	High
TCGA-BH-A201	856	Alive	38.97	High
TCGA-D8-A1JD	552	Alive	39.04	High
TCGA-C8-A278	297	Alive	39.21	High
TCGA-AR-A254	2605	Alive	39.24	High
TCGA-A8-A07F	577	Alive	39.48	High
TCGA-AO-A0JB	1542	Alive	39.67	High
TCGA-B6-A0WW	558	Dead	39.75	High
TCGA-BH-A0W7	1363	Alive	39.86	High
TCGA-A8-A086	396	Alive	40	High
TCGA-BH-A42U	3364	Alive	40	High
TCGA-AR-A2LR	1742	Alive	40.3	High
TCGA-C8-A12N	358	Alive	40.31	High
TCGA-D8-A1XQ	499	Alive	40.36	High
TCGA-E2-A14Z	563	Dead	40.36	High
TCGA-BH-A0H6	747	Alive	40.55	High
TCGA-A7-A0CH	1079	Alive	40.56	High

TCGA-C8-A130	370	Alive	40.61	High
TCGA-E2-A1IO	1855	Alive	40.79	High
TCGA-A8-A07R	273	Alive	41.42	High
TCGA-AN-A041	7	Alive	41.5	High
TCGA-BH-A0DQ	98	Alive	41.68	High
TCGA-E2-A1IJ	865	Alive	41.75	High
TCGA-A2-A3KC	1102	Alive	41.9	High
TCGA-E9-A1NH	576	Alive	42.49	High
TCGA-C8-A1HG	345	Alive	42.52	High
TCGA-B6-A40B	3152	Alive	42.55	High
TCGA-BH-A0DT	2403	Alive	42.57	High
TCGA-E9-A229	1148	Alive	42.61	High
TCGA-E2-A15H	393	Alive	42.66	High
TCGA-E2-A2P5	821	Dead	43.43	High
TCGA-A2-A0T0	533	Alive	43.58	High
TCGA-A2-A0CX	1728	Alive	43.59	High
TCGA-AQ-A0Y5	172	Dead	43.77	High
TCGA-E2-A14V	1042	Alive	43.84	High
TCGA-D8-A3Z6	563	Alive	43.91	High
TCGA-BH-A0DI	912	Alive	43.99	High
TCGA-A7-A26H	724	Alive	44.13	High
TCGA-A2-A0CT	2289	Alive	44.31	High
TCGA-AC-A3QP	675	Alive	44.33	High
TCGA-EW-A423	533	Alive	44.7	High
TCGA-BH-A18I	1093	Alive	44.88	High
TCGA-BH-A0AZ	1919	Alive	45.04	High
TCGA-A2-A4RW	222	Alive	45.4	High
TCGA-AN-A0FN	218	Alive	45.52	High
TCGA-AO-A1KO	622	Alive	46.17	High
TCGA-HN-A2OB	1900	Dead	46.31	High
TCGA-A2-A0EU	1043	Alive	46.49	High
TCGA-AC-A23G	2248	Alive	46.51	High
TCGA-A2-A0YE	554	Alive	46.58	High
TCGA-E9-A1NG	786	Dead	46.59	High
TCGA-A8-A08O	943	Alive	46.65	High
TCGA-S3-AA10	586	Alive	46.79	High
TCGA-AN-A0AS	10	Alive	46.86	High
TCGA-AN-A0FD	196	Alive	47.04	High
TCGA-EW-A2FR	1673	Alive	47.09	High
TCGA-BH-A0BC	974	Alive	47.1	High

TCGA-BH-A0B4	1191	Alive	47.41	High
TCGA-E2-A1L7	1836	Alive	47.56	High
TCGA-E9-A1RH	1417	Alive	47.58	High
TCGA-D8-A1JJ	611	Alive	47.65	High
TCGA-BH-A0HY	1545	Alive	48.16	High
TCGA-B6-A0RH	6456	Dead	48.49	High
TCGA-A1-A0SD	437	Alive	48.63	High
TCGA-E2-A1IG	2140	Alive	48.72	High
TCGA-A7-A26I	661	Alive	48.96	High
TCGA-AR-A24V	3203	Alive	49.03	High
TCGA-BH-A0DK	423	Alive	49.05	High
TCGA-AN-A0XO	375	Alive	49.18	High
TCGA-A8-A06R	547	Alive	49.52	High
TCGA-MS-A51U	681	Alive	49.56	High
TCGA-A2-A1FW	528	Alive	49.85	High
TCGA-A2-A04N	4354	Alive	49.92	High
TCGA-A7-A6VX	317	Alive	50.19	High
TCGA-BH-A0HK	178	Alive	50.58	High
TCGA-BH-A0BR	2330	Alive	50.64	High
TCGA-BH-A0B1	1148	Alive	51.04	High
TCGA-WT-AB44	883	Alive	51.31	High
TCGA-BH-A0H7	702	Alive	51.54	High
TCGA-AQ-A54O	1001	Alive	51.58	High
TCGA-3C-AALK	1448	Alive	51.72	High
TCGA-C8-A132	383	Alive	52.12	High
TCGA-A2-A0CZ	1616	Alive	52.38	High
TCGA-E2-A1BC	501	Alive	52.51	High
TCGA-E2-A1IN	675	Alive	52.86	High
TCGA-AR-A5QP	1185	Alive	52.93	High
TCGA-5L-AAT1	1471	Alive	52.97	High
TCGA-AQ-A04J	819	Alive	53	High
TCGA-BH-A0EB	745	Alive	53.01	High
TCGA-OL-A5S0	620	Alive	53.23	High
TCGA-B6-A0RG	2082	Alive	53.35	High
TCGA-E9-A226	1048	Dead	53.52	High
TCGA-A2-A0CM	754	Dead	53.54	High
TCGA-BH-A0GZ	328	Alive	53.68	High
TCGA-BH-A0BW	2371	Alive	53.8	High
TCGA-EW-A6S9	463	Alive	53.92	High
TCGA-AC-A2QJ	446	Dead	54.02	High

TCGA-A7-A26J	627	Alive	54.04	High
TCGA-A2-A0YM	965	Alive	54.48	High
TCGA-BH-A1FM	1388	Dead	55.1	High
TCGA-AN-A0XW	170	Alive	55.63	High
TCGA-BH-A0HA	1611	Alive	55.67	High
TCGA-E9-A1R3	78	Alive	56.36	High
TCGA-C8-A138	380	Alive	57.53	High
TCGA-E9-A22E	1269	Alive	57.66	High
TCGA-A7-A5ZX	336	Alive	58.11	High
TCGA-Z7-A8R6	3256	Alive	58.11	High
TCGA-C8-A1HJ	5	Alive	58.82	High
TCGA-AO-A12C	2372	Alive	59.1	High
TCGA-BH-A0BQ	2255	Alive	59.27	High
TCGA-GM-A2DD	2282	Alive	59.53	High
TCGA-GM-A2DA	6593	Dead	59.72	High
TCGA-BH-A0HB	806	Alive	59.78	High
TCGA-A2-A0YL	1474	Alive	60.22	High
TCGA-D8-A1XB	552	Alive	60.36	High
TCGA-LL-A73Z	227	Dead	60.61	High
TCGA-A2-A0CP	2813	Alive	60.99	High
TCGA-JL-A3YW	360	Alive	61.24	High
TCGA-A1-A0SH	1437	Alive	61.4	High
TCGA-GM-A5PX	551	Alive	61.74	High
TCGA-OL-A5RY	752	Alive	62.18	High
TCGA-AO-A12D	2515	Alive	62.48	High
TCGA-A8-A0A2	579	Alive	62.54	High
TCGA-BH-A1FC	3472	Dead	62.67	High
TCGA-B6-A402	2134	Alive	63.16	High
TCGA-A8-A07G	577	Alive	63.19	High
TCGA-A2-A0T7	631	Alive	63.55	High
TCGA-BH-A0BM	1876	Alive	64.33	High
TCGA-E9-A244	21	Alive	64.36	High
TCGA-AN-A0AJ	303	Alive	65.2	High
TCGA-AN-A0XN	10	Alive	65.26	High
TCGA-AN-A0FX	10	Alive	65.39	High
TCGA-B6-A0IJ	7106	Alive	66.15	High
TCGA-BH-A0W4	759	Alive	66.61	High
TCGA-BH-A0B9	1572	Alive	67.17	High
TCGA-GM-A3XN	2019	Alive	67.42	High
TCGA-OL-A5DA	1783	Alive	68.11	High

TCGA-B6-A0X1	7455	Dead	68.49	High
TCGA-EW-A1IY	258	Alive	68.85	High
TCGA-AR-A0U0	1988	Alive	69.67	High
TCGA-A2-A0SV	825	Dead	70.05	High
TCGA-D8-A1XK	441	Alive	70.87	High
TCGA-E9-A1RF	200	Alive	72.02	High
TCGA-E2-A1L8	2240	Alive	72.18	High
TCGA-A8-A08B	1156	Alive	72.44	High
TCGA-AR-A0U4	3261	Alive	72.48	High
TCGA-A2-A04U	2654	Alive	73.78	High
TCGA-E2-A15L	626	Alive	74.33	High
TCGA-OL-A5D7	1780	Alive	75.02	High
TCGA-BH-A0B3	1203	Alive	75.63	High
TCGA-E2-A150	1935	Alive	75.68	High
TCGA-BH-A18J	612	Dead	75.83	High
TCGA-C8-A8HQ	380	Alive	76.55	High
TCGA-A2-A0T2	255	Dead	76.68	High
TCGA-AR-A1AU	2868	Alive	79.05	High
TCGA-C8-A12Y	1476	Alive	79.26	High
TCGA-AN-A04A	90	Alive	79.83	High
TCGA-E9-A22A	1189	Alive	79.94	High
TCGA-BH-A0DZ	495	Alive	80.51	High
TCGA-4H-AAAK	348	Alive	80.85	High
TCGA-E2-A1LL	1309	Alive	81.19	High
TCGA-BH-A1EV	365	Dead	81.5	High
TCGA-GM-A2DL	3519	Alive	81.99	High
TCGA-5L-AAT0	1477	Alive	83.88	High
TCGA-AC-A6IW	413	Alive	85.67	High
TCGA-AR-A1AQ	3021	Alive	86.26	High
TCGA-A2-A0EO	2442	Alive	86.44	High
TCGA-AO-A1KT	541	Alive	86.89	High
TCGA-EW-A6SB	760	Alive	87.09	High
TCGA-E2-A159	762	Alive	89.29	High
TCGA-AN-A0XU	10	Alive	90.63	High
TCGA-A2-A0CS	2348	Dead	93.22	High
TCGA-S3-AA15	525	Alive	96.6	High
TCGA-A2-A0SX	1534	Alive	96.98	High
TCGA-BH-A208	1759	Dead	97.61	High
TCGA-E9-A295	375	Alive	98.03	High
TCGA-E2-A1LA	748	Alive	98.8	High

TCGA-AR-A24T	3202	Alive	98.88	High
TCGA-S3-AA14	529	Alive	99.74	High
TCGA-AR-A251	3030	Alive	100.39	High
TCGA-D8-A147	584	Alive	101.3	High
TCGA-UL-AAZ6	518	Alive	102.2	High
TCGA-EW-A1P7	915	Alive	102.24	High
TCGA-A2-A04Q	2385	Alive	104.13	High
TCGA-B6-A0RE	7777	Alive	104.56	High
TCGA-D8-A27V	381	Alive	105.7	High
TCGA-D8-A1JM	590	Alive	105.9	High
TCGA-C8-A27B	439	Alive	109.37	High
TCGA-E2-A1LH	3247	Alive	110.36	High
TCGA-GI-A2C9	3342	Alive	110.87	High
TCGA-AO-A0J9	1613	Alive	114.37	High
TCGA-BH-A0BL	2278	Alive	117.63	High
TCGA-OL-A66I	714	Alive	120.19	High
TCGA-A2-A0CY	1673	Alive	121.55	High
TCGA-A2-A0D0	2048	Alive	125.62	High
TCGA-BH-A5IZ	567	Alive	130.31	High
TCGA-BH-A0HF	727	Alive	134.63	High
TCGA-BH-A0BG	1871	Alive	138.59	High
TCGA-A2-A4RX	742	Alive	144.3	High
TCGA-A7-A6VY	266	Alive	150.47	High
TCGA-AO-A0J4	1587	Alive	161.37	High
TCGA-D8-A27H	397	Alive	162.29	High
TCGA-BH-A1F0	785	Dead	169.27	High
TCGA-B6-A0I6	991	Dead	172.05	High
TCGA-E2-A14Y	2109	Alive	180.52	High
TCGA-BH-A0E0	134	Alive	202.32	High
TCGA-BH-A0AV	1820	Alive	202.82	High
TCGA-AR-A1AH	3807	Alive	205.25	High
TCGA-A2-A0ST	3017	Alive	206.61	High
TCGA-LL-A6FR	489	Alive	211.74	High
TCGA-A7-A13D	965	Alive	215.7	High
TCGA-D8-A27M	410	Alive	217.36	High
TCGA-B6-A400	215	Alive	221.05	High
TCGA-AC-A8OQ	34	Alive	222.78	High
TCGA-E2-A1LK	266	Dead	228.31	High
TCGA-LL-A73Y	477	Alive	244.66	High
TCGA-EW-A1PB	608	Alive	254.63	High

TCGA-B6-A0IQ	4285	Alive	258.25	High
TCGA-A7-A6VV	313	Alive	269.63	High
TCGA-A1-A0SP	584	Alive	304.63	High
TCGA-E2-A14R	1174	Alive	308.15	High
TCGA-E2-A573	1062	Alive	331.16	High
TCGA-BH-A0EE	943	Alive	344.77	High
TCGA-A7-A0CE	1074	Alive	357.32	High
TCGA-BH-A6R9	160	Alive	370.11	High
TCGA-E2-A574	1179	Alive	381.59	High
TCGA-EW-A1PH	607	Alive	426.87	High
TCGA-E2-A1B0	1631	Alive	433.53	High
TCGA-EW-A3U0	532	Alive	434.5	High
TCGA-AO-A128	3248	Alive	435.82	High
TCGA-OL-A5RW	1106	Alive	473.13	High
TCGA-EW-A1P4	907	Alive	484.81	High
TCGA-B6-A0I2	4361	Alive	621.42	High
TCGA-E9-A5FL	24	Alive	653.75	High
TCGA-AN-A0AL	227	Alive	723.43	High
TCGA-A7-A4SD	441	Alive	727.86	High
TCGA-A7-A6VW	285	Alive	847.77	High
TCGA-A7-A4SE	644	Alive	878.68	High
TCGA-A2-A3XW	1712	Alive	1115.52	High
TCGA-E2-A1LG	1523	Alive	1373.16	High
TCGA-E2-A1II	1025	Alive	1734.1	High

Case Processing Summary		N	Percent
Cases available in analysis	Event[a]	70	13.90%
	Censored	398	79.30%
	Total	468	93.20%
Cases dropped	Cases with missing values	0	0.00%
	Cases with negative time	0	0.00%
	Censored cases before the earliest event in a stratum	34	6.80%
	Total	34	6.80%
Total		502	100.00%

Patient	Days	Status	Expression	Group
TCGA-AC-A7VC	1	Alive	0	Low
TCGA-AC-A8OR	40	Alive	0	Low
TCGA-BH-A0H0	461	Alive	0	Low
TCGA-D8-A1X6	541	Alive	0	Low
TCGA-AC-A5XS	588	Alive	0	Low
TCGA-A2-A4S0	706	Alive	0	Low
TCGA-E9-A54X	727	Alive	0	Low
TCGA-LQ-A4E4	849	Alive	0	Low
TCGA-A1-A0SO	852	Alive	0	Low
TCGA-A8-A09K	912	Alive	0	Low
TCGA-E9-A3Q9	1001	Alive	0	Low
TCGA-E2-A10C	1220	Alive	0	Low
TCGA-E2-A14U	1318	Alive	0	Low
TCGA-B6-A1KC	1326	Alive	0	Low
TCGA-BH-A0HW	1561	Alive	0	Low
TCGA-E2-A1LS	1604	Alive	0	Low
TCGA-D8-A1XC	377	Dead	0	Low
TCGA-A2-A0SW	1365	Dead	0	Low
TCGA-A2-A0EY	1925	Alive	0	Low
TCGA-B6-A0X5	2097	Dead	0	Low
TCGA-BH-A204	2534	Dead	0.23	Low
TCGA-A8-A06Z	31	Alive	0.25	Low
TCGA-LL-A442	889	Alive	0.26	Low
TCGA-AN-A0G0	16	Alive	0.29	Low
TCGA-AC-A2FM	792	Dead	0.33	Low
TCGA-AN-A04C	54	Alive	0.35	Low

TCGA-A8-A09W	30	Alive	0.42	Low
TCGA-D8-A73W	385	Dead	0.42	Low
TCGA-AO-A12B	2989	Alive	0.42	Low
TCGA-AR-A24H	4894	Alive	0.47	Low
TCGA-C8-A1HK	366	Alive	0.5	Low
TCGA-OL-A5RZ	679	Alive	0.51	Low
TCGA-D8-A1XV	461	Alive	0.52	Low
TCGA-D8-A1JN	620	Alive	0.52	Low
TCGA-AR-A1AT	1272	Dead	0.52	Low
TCGA-EW-A1OV	789	Alive	0.53	Low
TCGA-E9-A54Y	725	Alive	0.59	Low
TCGA-C8-A1HO	375	Alive	0.62	Low
TCGA-AR-A0TY	1699	Dead	0.65	Low
TCGA-AO-A03R	2091	Alive	0.67	Low
TCGA-AR-A0TV	2288	Alive	0.7	Low
TCGA-C8-A12X	385	Alive	0.72	Low
TCGA-UU-A93S	116	Dead	0.72	Low
TCGA-GM-A2DM	3226	Alive	0.77	Low
TCGA-AC-A62Y	530	Alive	0.82	Low
TCGA-AR-A0TR	160	Dead	0.82	Low
TCGA-AN-A0AK	224	Alive	0.84	Low
TCGA-BH-A0W3	728	Alive	0.88	Low
TCGA-EW-A6SA	510	Alive	0.93	Low
TCGA-E9-A1R7	1467	Alive	1.06	Low
TCGA-BH-A1FL	1673	Dead	1.08	Low
TCGA-E2-A155	640	Alive	1.13	Low
TCGA-AR-A24Z	3001	Alive	1.14	Low
TCGA-E9-A1RE	1419	Alive	1.17	Low
TCGA-A7-A0DC	906	Alive	1.22	Low
TCGA-AO-A0JL	1683	Alive	1.22	Low
TCGA-A8-A09X	426	Dead	1.24	Low
TCGA-BH-A0BS	2612	Alive	1.29	Low
TCGA-A2-A0D4	767	Alive	1.33	Low
TCGA-A2-A0ET	1066	Alive	1.35	Low
TCGA-AQ-A54N	78	Alive	1.37	Low
TCGA-E2-A156	726	Alive	1.44	Low
TCGA-BH-A18L	811	Dead	1.45	Low
TCGA-AC-A7VB	250	Alive	1.46	Low
TCGA-AN-A0XL	163	Alive	1.5	Low
TCGA-A2-A0YF	1535	Alive	1.59	Low

TCGA-BH-A8FY	295	Dead	1.66	Low
TCGA-AR-A0U3	4080	Alive	1.71	Low
TCGA-C8-A12U	385	Alive	1.73	Low
TCGA-E2-A15J	1640	Alive	1.77	Low
TCGA-BH-A0HL	72	Alive	1.8	Low
TCGA-AN-A0FJ	242	Alive	1.8	Low
TCGA-A2-A0CU	158	Dead	1.91	Low
TCGA-D8-A1JI	577	Alive	1.93	Low
TCGA-S3-AA12	574	Alive	1.96	Low
TCGA-A7-A3IZ	322	Alive	2.03	Low
TCGA-A7-A3RF	408	Alive	2.04	Low
TCGA-D8-A1XF	463	Alive	2.1	Low
TCGA-EW-A1OX	911	Alive	2.13	Low
TCGA-A2-A4S3	666	Alive	2.15	Low
TCGA-A8-A07W	304	Alive	2.22	Low
TCGA-E2-A1IK	1800	Alive	2.22	Low
TCGA-PL-A8LX	5	Alive	2.23	Low
TCGA-B6-A0IB	3941	Dead	2.26	Low
TCGA-A2-A25D	552	Alive	2.28	Low
TCGA-A2-A0CW	3283	Alive	2.3	Low
TCGA-AR-A24U	3128	Alive	2.32	Low
TCGA-LL-A6FP	677	Alive	2.35	Low
TCGA-AC-A4ZE	890	Alive	2.35	Low
TCGA-A2-A3XU	912	Dead	2.38	Low
TCGA-A2-A25B	1291	Alive	2.41	Low
TCGA-D8-A1XW	1309	Alive	2.41	Low
TCGA-A8-A08I	365	Alive	2.43	Low
TCGA-A2-A1FX	1847	Alive	2.44	Low
TCGA-B6-A0RM	2373	Dead	2.44	Low
TCGA-C8-A26Y	394	Alive	2.45	Low
TCGA-AR-A1AR	524	Dead	2.47	Low
TCGA-E2-A1LE	879	Dead	2.54	Low
TCGA-BH-A1EN	2127	Dead	2.54	Low
TCGA-AN-A0FF	172	Alive	2.58	Low
TCGA-A2-A3XV	996	Alive	2.58	Low
TCGA-A2-A0SU	1662	Alive	2.58	Low
TCGA-AR-A2LH	616	Dead	2.63	Low
TCGA-BH-A209	3959	Dead	2.66	Low
TCGA-A8-A079	274	Alive	2.71	Low
TCGA-E2-A14T	2311	Alive	2.72	Low

TCGA-A8-A0A7	30	Alive	2.75	Low
TCGA-BH-A1F2	959	Dead	2.75	Low
TCGA-C8-A274	508	Alive	2.77	Low
TCGA-A7-A4SF	545	Alive	2.79	Low
TCGA-LL-A6FQ	80	Alive	2.83	Low
TCGA-BH-A42T	320	Dead	2.87	Low
TCGA-AQ-A04H	754	Alive	2.94	Low
TCGA-A8-A09Q	761	Alive	2.94	Low
TCGA-AR-A256	2854	Dead	2.96	Low
TCGA-A2-A0YT	723	Dead	2.97	Low
TCGA-BH-A18T	224	Dead	2.99	Low
TCGA-E2-A572	1208	Alive	3	Low
TCGA-AQ-A1H2	475	Alive	3.01	Low
TCGA-A2-A1G4	595	Alive	3.01	Low
TCGA-AR-A0TQ	2991	Alive	3.01	Low
TCGA-BH-A0BP	2296	Dead	3.01	Low
TCGA-E2-A109	1417	Alive	3.08	Low
TCGA-AC-A8OP	614	Alive	3.11	Low
TCGA-AN-A0AT	10	Alive	3.17	Low
TCGA-BH-A1EW	1694	Dead	3.24	Low
TCGA-BH-A0E6	293	Alive	3.27	Low
TCGA-BH-A18S	2009	Dead	3.27	Low
TCGA-A2-A0YG	666	Alive	3.28	Low
TCGA-A2-A0ER	2263	Alive	3.31	Low
TCGA-B6-A1KF	3088	Alive	3.31	Low
TCGA-AN-A0FT	214	Alive	3.32	Low
TCGA-A2-A0ES	2190	Alive	3.34	Low
TCGA-E9-A3HO	1158	Alive	3.36	Low
TCGA-AC-A2FG	1853	Alive	3.37	Low
TCGA-AR-A0U2	2551	Dead	3.41	Low
TCGA-A8-A091	1004	Alive	3.43	Low
TCGA-E2-A15T	1563	Alive	3.45	Low
TCGA-A8-A0A9	822	Alive	3.51	Low
TCGA-A2-A0EP	3603	Alive	3.65	Low
TCGA-AO-A03P	2911	Dead	3.67	Low
TCGA-E2-A1IE	2362	Alive	3.74	Low
TCGA-OL-A66H	812	Alive	3.75	Low
TCGA-AR-A0TZ	3262	Dead	3.83	Low
TCGA-C8-A1HN	394	Alive	3.96	Low
TCGA-A8-A0A1	365	Alive	4.02	Low

TCGA-BH-A0DO	1644	Alive	4.02	Low
TCGA-A1-A0SQ	554	Alive	4.03	Low
TCGA-AN-A0FW	11	Alive	4.05	Low
TCGA-D8-A1X9	727	Alive	4.05	Low
TCGA-C8-A26X	376	Alive	4.13	Low
TCGA-GM-A3XL	2108	Alive	4.15	Low
TCGA-A2-A0D3	1873	Alive	4.19	Low
TCGA-E2-A15D	526	Alive	4.2	Low
TCGA-EW-A1IZ	554	Alive	4.28	Low
TCGA-BH-A0B7	2559	Alive	4.29	Low
TCGA-AR-A24S	2976	Alive	4.4	Low
TCGA-D8-A27W	373	Alive	4.42	Low
TCGA-HN-A2NL	79	Alive	4.43	Low
TCGA-E2-A1LB	2306	Alive	4.49	Low
TCGA-AR-A0TT	3316	Alive	4.49	Low
TCGA-A7-A4SC	446	Alive	4.61	Low
TCGA-E2-A107	1047	Alive	4.63	Low
TCGA-AR-A1AV	1864	Alive	4.63	Low
TCGA-E9-A5UO	785	Alive	4.72	Low
TCGA-AN-A0XT	10	Alive	4.75	Low
TCGA-E9-A249	217	Alive	4.75	Low
TCGA-A8-A07O	304	Alive	4.78	Low
TCGA-EW-A1J1	575	Alive	4.81	Low
TCGA-C8-A12M	358	Alive	4.83	Low
TCGA-A2-A0T1	521	Alive	4.87	Low
TCGA-BH-A0BO	2197	Alive	4.87	Low
TCGA-A2-A0YJ	566	Alive	4.88	Low
TCGA-C8-A3M7	1034	Dead	4.92	Low
TCGA-E2-A15M	336	Dead	4.95	Low
TCGA-E9-A2JT	288	Alive	4.96	Low
TCGA-BH-A1EU	1286	Dead	4.96	Low
TCGA-AR-A2LE	5062	Alive	4.99	Low
TCGA-AR-A0TU	709	Alive	5.01	Low
TCGA-A2-A3KD	1206	Alive	5.04	Low
TCGA-AO-A12F	1842	Alive	5.1	Low
TCGA-PE-A5DC	1430	Dead	5.15	Low
TCGA-BH-A18H	652	Alive	5.18	Low
TCGA-A8-A06Q	31	Alive	5.24	Low
TCGA-A7-A0CJ	931	Alive	5.28	Low
TCGA-B6-A1KI	2236	Alive	5.28	Low

TCGA-AR-A1AX	2629	Alive	5.29	Low
TCGA-AO-A0JI	1528	Alive	5.3	Low
TCGA-A8-A085	1124	Alive	5.32	Low
TCGA-D8-A1XZ	466	Alive	5.33	Low
TCGA-BH-A0B0	2477	Alive	5.37	Low
TCGA-AC-A62X	417	Alive	5.41	Low
TCGA-AR-A1AL	2971	Alive	5.43	Low
TCGA-A2-A0CO	3492	Dead	5.43	Low
TCGA-D8-A27R	307	Alive	5.48	Low
TCGA-D8-A1JF	366	Alive	5.51	Low
TCGA-WT-AB41	1611	Alive	5.52	Low
TCGA-AC-A6NO	51	Alive	5.54	Low
TCGA-GM-A3NW	3361	Alive	5.54	Low
TCGA-PL-A8LZ	302	Alive	5.55	Low
TCGA-C8-A26V	616	Alive	5.57	Low
TCGA-BH-A0DX	2156	Alive	5.58	Low
TCGA-E2-A14P	1246	Alive	5.61	Low
TCGA-BH-A0DH	1156	Alive	5.65	Low
TCGA-BH-A0HO	76	Alive	5.66	Low
TCGA-AN-A046	10	Alive	5.68	Low
TCGA-A7-A4SB	418	Alive	5.74	Low
TCGA-AN-A04D	52	Alive	5.76	Low
TCGA-E2-A1IU	337	Alive	5.76	Low
TCGA-OL-A66P	428	Alive	5.76	Low
TCGA-A8-A09E	1492	Alive	5.81	Low
TCGA-AC-A2FO	2255	Alive	5.82	Low
TCGA-AR-A1AP	2856	Alive	5.85	Low
TCGA-B6-A0X4	860	Dead	5.9	Low
TCGA-A7-A13G	718	Alive	5.92	Low
TCGA-A8-A08F	1004	Alive	5.95	Low
TCGA-AC-A23H	174	Dead	5.95	Low
TCGA-A2-A4S1	820	Alive	5.96	Low
TCGA-D8-A1XR	482	Alive	6	Low
TCGA-E9-A22H	1232	Alive	6.05	Low
TCGA-A8-A09C	31	Alive	6.07	Low
TCGA-OL-A6VR	1220	Alive	6.08	Low
TCGA-EW-A1P1	1210	Alive	6.09	Low
TCGA-E2-A158	450	Alive	6.17	Low
TCGA-BH-A18N	1148	Dead	6.18	Low
TCGA-EW-A1P6	562	Alive	6.35	Low

TCGA-E2-A15C	694	Alive	6.4	Low
TCGA-BH-A0H5	1620	Alive	6.4	Low
TCGA-C8-A135	393	Alive	6.45	Low
TCGA-E9-A248	59	Alive	6.47	Low
TCGA-A8-A0A4	396	Alive	6.53	Low
TCGA-AR-A2LQ	1233	Alive	6.55	Low
TCGA-BH-A1FG	3736	Dead	6.55	Low
TCGA-E9-A1R6	339	Alive	6.57	Low
TCGA-C8-A1HM	375	Alive	6.63	Low
TCGA-C8-A3M8	394	Alive	6.67	Low
TCGA-E2-A14X	972	Alive	6.74	Low
TCGA-AC-A2FB	1234	Alive	6.81	Low
TCGA-E2-A14S	1009	Alive	6.83	Low
TCGA-D8-A145	410	Alive	6.86	Low
TCGA-A2-A3XT	2770	Alive	6.86	Low
TCGA-GM-A2DO	2596	Alive	6.89	Low
TCGA-A2-A04V	1920	Dead	6.93	Low
TCGA-S3-AA17	424	Alive	6.94	Low
TCGA-A2-A1FV	714	Alive	7	Low
TCGA-D8-A27G	409	Alive	7.12	Low
TCGA-A2-A259	1596	Alive	7.15	Low
TCGA-S3-AA0Z	629	Alive	7.19	Low
TCGA-AR-A2LL	2012	Alive	7.22	Low
TCGA-EW-A1OY	908	Alive	7.24	Low
TCGA-3C-AAAU	4047	Alive	7.24	Low
TCGA-D8-A1XO	1682	Alive	37.64	High
TCGA-D8-A13Z	635	Alive	37.79	High
TCGA-A2-A3XZ	1532	Alive	37.9	High
TCGA-A2-A0T5	531	Alive	37.93	High
TCGA-A2-A3Y0	1546	Alive	38.09	High
TCGA-BH-A1FE	2273	Dead	38.25	High
TCGA-D8-A27T	398	Alive	38.47	High
TCGA-AO-A0JA	655	Alive	38.48	High
TCGA-BH-A1ES	3462	Dead	38.52	High
TCGA-AO-A03T	2124	Alive	38.57	High
TCGA-A8-A093	546	Alive	38.61	High
TCGA-BH-A201	856	Alive	38.97	High
TCGA-D8-A1JD	552	Alive	39.04	High
TCGA-C8-A278	297	Alive	39.21	High
TCGA-AR-A254	2605	Alive	39.24	High

TCGA-A8-A07F	577	Alive	39.48	High
TCGA-AO-A0JB	1542	Alive	39.67	High
TCGA-B6-A0WW	558	Dead	39.75	High
TCGA-BH-A0W7	1363	Alive	39.86	High
TCGA-A8-A086	396	Alive	40	High
TCGA-BH-A42U	3364	Alive	40	High
TCGA-AR-A2LR	1742	Alive	40.3	High
TCGA-C8-A12N	358	Alive	40.31	High
TCGA-D8-A1XQ	499	Alive	40.36	High
TCGA-E2-A14Z	563	Dead	40.36	High
TCGA-BH-A0H6	747	Alive	40.55	High
TCGA-A7-A0CH	1079	Alive	40.56	High
TCGA-C8-A130	370	Alive	40.61	High
TCGA-E2-A1IO	1855	Alive	40.79	High
TCGA-A8-A07R	273	Alive	41.42	High
TCGA-AN-A041	7	Alive	41.5	High
TCGA-BH-A0DQ	98	Alive	41.68	High
TCGA-E2-A1IJ	865	Alive	41.75	High
TCGA-A2-A3KC	1102	Alive	41.9	High
TCGA-E9-A1NH	576	Alive	42.49	High
TCGA-C8-A1HG	345	Alive	42.52	High
TCGA-B6-A40B	3152	Alive	42.55	High
TCGA-BH-A0DT	2403	Alive	42.57	High
TCGA-E9-A229	1148	Alive	42.61	High
TCGA-E2-A15H	393	Alive	42.66	High
TCGA-E2-A2P5	821	Dead	43.43	High
TCGA-A2-A0T0	533	Alive	43.58	High
TCGA-A2-A0CX	1728	Alive	43.59	High
TCGA-AQ-A0Y5	172	Dead	43.77	High
TCGA-E2-A14V	1042	Alive	43.84	High
TCGA-D8-A3Z6	563	Alive	43.91	High
TCGA-BH-A0DI	912	Alive	43.99	High
TCGA-A7-A26H	724	Alive	44.13	High
TCGA-A2-A0CT	2289	Alive	44.31	High
TCGA-AC-A3QP	675	Alive	44.33	High
TCGA-EW-A423	533	Alive	44.7	High
TCGA-BH-A18I	1093	Alive	44.88	High
TCGA-BH-A0AZ	1919	Alive	45.04	High
TCGA-A2-A4RW	222	Alive	45.4	High
TCGA-AN-A0FN	218	Alive	45.52	High

TCGA-AO-A1KO	622	Alive	46.17	High
TCGA-HN-A2OB	1900	Dead	46.31	High
TCGA-A2-A0EU	1043	Alive	46.49	High
TCGA-AC-A23G	2248	Alive	46.51	High
TCGA-A2-A0YE	554	Alive	46.58	High
TCGA-E9-A1NG	786	Dead	46.59	High
TCGA-A8-A08O	943	Alive	46.65	High
TCGA-S3-AA10	586	Alive	46.79	High
TCGA-AN-A0AS	10	Alive	46.86	High
TCGA-AN-A0FD	196	Alive	47.04	High
TCGA-EW-A2FR	1673	Alive	47.09	High
TCGA-BH-A0BC	974	Alive	47.1	High
TCGA-BH-A0B4	1191	Alive	47.41	High
TCGA-E2-A1L7	1836	Alive	47.56	High
TCGA-E9-A1RH	1417	Alive	47.58	High
TCGA-D8-A1JJ	611	Alive	47.65	High
TCGA-BH-A0HY	1545	Alive	48.16	High
TCGA-B6-A0RH	6456	Dead	48.49	High
TCGA-A1-A0SD	437	Alive	48.63	High
TCGA-E2-A1IG	2140	Alive	48.72	High
TCGA-A7-A26I	661	Alive	48.96	High
TCGA-AR-A24V	3203	Alive	49.03	High
TCGA-BH-A0DK	423	Alive	49.05	High
TCGA-AN-A0XO	375	Alive	49.18	High
TCGA-A8-A06R	547	Alive	49.52	High
TCGA-MS-A51U	681	Alive	49.56	High
TCGA-A2-A1FW	528	Alive	49.85	High
TCGA-A2-A04N	4354	Alive	49.92	High
TCGA-A7-A6VX	317	Alive	50.19	High
TCGA-BH-A0HK	178	Alive	50.58	High
TCGA-BH-A0BR	2330	Alive	50.64	High
TCGA-BH-A0B1	1148	Alive	51.04	High
TCGA-WT-AB44	883	Alive	51.31	High
TCGA-BH-A0H7	702	Alive	51.54	High
TCGA-AQ-A54O	1001	Alive	51.58	High
TCGA-3C-AALK	1448	Alive	51.72	High
TCGA-C8-A132	383	Alive	52.12	High
TCGA-A2-A0CZ	1616	Alive	52.38	High
TCGA-E2-A1BC	501	Alive	52.51	High
TCGA-E2-A1IN	675	Alive	52.86	High

TCGA-AR-A5QP	1185	Alive	52.93	High
TCGA-5L-AAT1	1471	Alive	52.97	High
TCGA-AQ-A04J	819	Alive	53	High
TCGA-BH-A0EB	745	Alive	53.01	High
TCGA-OL-A5S0	620	Alive	53.23	High
TCGA-B6-A0RG	2082	Alive	53.35	High
TCGA-E9-A226	1048	Dead	53.52	High
TCGA-A2-A0CM	754	Dead	53.54	High
TCGA-BH-A0GZ	328	Alive	53.68	High
TCGA-BH-A0BW	2371	Alive	53.8	High
TCGA-EW-A6S9	463	Alive	53.92	High
TCGA-AC-A2QJ	446	Dead	54.02	High
TCGA-A7-A26J	627	Alive	54.04	High
TCGA-A2-A0YM	965	Alive	54.48	High
TCGA-BH-A1FM	1388	Dead	55.1	High
TCGA-AN-A0XW	170	Alive	55.63	High
TCGA-BH-A0HA	1611	Alive	55.67	High
TCGA-E9-A1R3	78	Alive	56.36	High
TCGA-C8-A138	380	Alive	57.53	High
TCGA-E9-A22E	1269	Alive	57.66	High
TCGA-A7-A5ZX	336	Alive	58.11	High
TCGA-Z7-A8R6	3256	Alive	58.11	High
TCGA-C8-A1HJ	5	Alive	58.82	High
TCGA-AO-A12C	2372	Alive	59.1	High
TCGA-BH-A0BQ	2255	Alive	59.27	High
TCGA-GM-A2DD	2282	Alive	59.53	High
TCGA-GM-A2DA	6593	Dead	59.72	High
TCGA-BH-A0HB	806	Alive	59.78	High
TCGA-A2-A0YL	1474	Alive	60.22	High
TCGA-D8-A1XB	552	Alive	60.36	High
TCGA-LL-A73Z	227	Dead	60.61	High
TCGA-A2-A0CP	2813	Alive	60.99	High
TCGA-JL-A3YW	360	Alive	61.24	High
TCGA-A1-A0SH	1437	Alive	61.4	High
TCGA-GM-A5PX	551	Alive	61.74	High
TCGA-OL-A5RY	752	Alive	62.18	High
TCGA-AO-A12D	2515	Alive	62.48	High
TCGA-A8-A0A2	579	Alive	62.54	High
TCGA-BH-A1FC	3472	Dead	62.67	High
TCGA-B6-A402	2134	Alive	63.16	High

TCGA-A8-A07G	577	Alive	63.19	High
TCGA-A2-A0T7	631	Alive	63.55	High
TCGA-BH-A0BM	1876	Alive	64.33	High
TCGA-E9-A244	21	Alive	64.36	High
TCGA-AN-A0AJ	303	Alive	65.2	High
TCGA-AN-A0XN	10	Alive	65.26	High
TCGA-AN-A0FX	10	Alive	65.39	High
TCGA-B6-A0IJ	7106	Alive	66.15	High
TCGA-BH-A0W4	759	Alive	66.61	High
TCGA-BH-A0B9	1572	Alive	67.17	High
TCGA-GM-A3XN	2019	Alive	67.42	High
TCGA-OL-A5DA	1783	Alive	68.11	High
TCGA-B6-A0X1	7455	Dead	68.49	High
TCGA-EW-A1IY	258	Alive	68.85	High
TCGA-AR-A0U0	1988	Alive	69.67	High
TCGA-A2-A0SV	825	Dead	70.05	High
TCGA-D8-A1XK	441	Alive	70.87	High
TCGA-E9-A1RF	200	Alive	72.02	High
TCGA-E2-A1L8	2240	Alive	72.18	High
TCGA-A8-A08B	1156	Alive	72.44	High
TCGA-AR-A0U4	3261	Alive	72.48	High
TCGA-A2-A04U	2654	Alive	73.78	High
TCGA-E2-A15L	626	Alive	74.33	High
TCGA-OL-A5D7	1780	Alive	75.02	High
TCGA-BH-A0B3	1203	Alive	75.63	High
TCGA-E2-A150	1935	Alive	75.68	High
TCGA-BH-A18J	612	Dead	75.83	High
TCGA-C8-A8HQ	380	Alive	76.55	High
TCGA-A2-A0T2	255	Dead	76.68	High
TCGA-AR-A1AU	2868	Alive	79.05	High
TCGA-C8-A12Y	1476	Alive	79.26	High
TCGA-AN-A04A	90	Alive	79.83	High
TCGA-E9-A22A	1189	Alive	79.94	High
TCGA-BH-A0DZ	495	Alive	80.51	High
TCGA-4H-AAAK	348	Alive	80.85	High
TCGA-E2-A1LL	1309	Alive	81.19	High
TCGA-BH-A1EV	365	Dead	81.5	High
TCGA-GM-A2DL	3519	Alive	81.99	High
TCGA-5L-AAT0	1477	Alive	83.88	High
TCGA-AC-A6IW	413	Alive	85.67	High

TCGA-AR-A1AQ	3021	Alive	86.26	High
TCGA-A2-A0EO	2442	Alive	86.44	High
TCGA-AO-A1KT	541	Alive	86.89	High
TCGA-EW-A6SB	760	Alive	87.09	High
TCGA-E2-A159	762	Alive	89.29	High
TCGA-AN-A0XU	10	Alive	90.63	High
TCGA-A2-A0CS	2348	Dead	93.22	High
TCGA-S3-AA15	525	Alive	96.6	High
TCGA-A2-A0SX	1534	Alive	96.98	High
TCGA-BH-A208	1759	Dead	97.61	High
TCGA-E9-A295	375	Alive	98.03	High
TCGA-E2-A1LA	748	Alive	98.8	High
TCGA-AR-A24T	3202	Alive	98.88	High
TCGA-S3-AA14	529	Alive	99.74	High
TCGA-AR-A251	3030	Alive	100.39	High
TCGA-D8-A147	584	Alive	101.3	High
TCGA-UL-AAZ6	518	Alive	102.2	High
TCGA-EW-A1P7	915	Alive	102.24	High
TCGA-A2-A04Q	2385	Alive	104.13	High
TCGA-B6-A0RE	7777	Alive	104.56	High
TCGA-D8-A27V	381	Alive	105.7	High
TCGA-D8-A1JM	590	Alive	105.9	High
TCGA-C8-A27B	439	Alive	109.37	High
TCGA-E2-A1LH	3247	Alive	110.36	High
TCGA-GI-A2C9	3342	Alive	110.87	High
TCGA-AO-A0J9	1613	Alive	114.37	High
TCGA-BH-A0BL	2278	Alive	117.63	High
TCGA-OL-A66I	714	Alive	120.19	High
TCGA-A2-A0CY	1673	Alive	121.55	High
TCGA-A2-A0D0	2048	Alive	125.62	High
TCGA-BH-A5IZ	567	Alive	130.31	High
TCGA-BH-A0HF	727	Alive	134.63	High
TCGA-BH-A0BG	1871	Alive	138.59	High
TCGA-A2-A4RX	742	Alive	144.3	High
TCGA-A7-A6VY	266	Alive	150.47	High
TCGA-AO-A0J4	1587	Alive	161.37	High
TCGA-D8-A27H	397	Alive	162.29	High
TCGA-BH-A1F0	785	Dead	169.27	High
TCGA-B6-A0I6	991	Dead	172.05	High
TCGA-E2-A14Y	2109	Alive	180.52	High

TCGA-BH-A0E0	134	Alive	202.32	High
TCGA-BH-A0AV	1820	Alive	202.82	High
TCGA-AR-A1AH	3807	Alive	205.25	High
TCGA-A2-A0ST	3017	Alive	206.61	High
TCGA-LL-A6FR	489	Alive	211.74	High
TCGA-A7-A13D	965	Alive	215.7	High
TCGA-D8-A27M	410	Alive	217.36	High
TCGA-B6-A400	215	Alive	221.05	High
TCGA-AC-A8OQ	34	Alive	222.78	High
TCGA-E2-A1LK	266	Dead	228.31	High
TCGA-LL-A73Y	477	Alive	244.66	High
TCGA-EW-A1PB	608	Alive	254.63	High
TCGA-B6-A0IQ	4285	Alive	258.25	High
TCGA-A7-A6VV	313	Alive	269.63	High
TCGA-A1-A0SP	584	Alive	304.63	High
TCGA-E2-A14R	1174	Alive	308.15	High
TCGA-E2-A573	1062	Alive	331.16	High
TCGA-BH-A0EE	943	Alive	344.77	High
TCGA-A7-A0CE	1074	Alive	357.32	High
TCGA-BH-A6R9	160	Alive	370.11	High
TCGA-E2-A574	1179	Alive	381.59	High
TCGA-EW-A1PH	607	Alive	426.87	High
TCGA-E2-A1B0	1631	Alive	433.53	High
TCGA-EW-A3U0	532	Alive	434.5	High
TCGA-AO-A128	3248	Alive	435.82	High
TCGA-OL-A5RW	1106	Alive	473.13	High
TCGA-EW-A1P4	907	Alive	484.81	High
TCGA-B6-A0I2	4361	Alive	621.42	High
TCGA-E9-A5FL	24	Alive	653.75	High
TCGA-AN-A0AL	227	Alive	723.43	High
TCGA-A7-A4SD	441	Alive	727.86	High
TCGA-A7-A6VW	285	Alive	847.77	High
TCGA-A7-A4SE	644	Alive	878.68	High
TCGA-A2-A3XW	1712	Alive	1115.52	High
TCGA-E2-A1LG	1523	Alive	1373.16	High
TCGA-E2-A1II	1025	Alive	1734.1	High

Supplementary Table 2.2: The TCGA-BRCA patient data for *FOXQ1(for FOXQ1 refer to supplementary table 2.1), FOXF2, and FOXM1* expressions in each patient that were used for the multivariate Cox's regression.

Case Processing Summary

		N	Percent
Cases available in analysis	Event	135	13.40%
	Censored	813	80.80%
	Total	948	94.20%
Cases dropped	Cases with missing values	0	0.00%
	Cases with negative time	0	0.00%
	Censored cases before the earliest event in a stratum	58	5.80%
	Total	58	5.80%
Total		1006	100.00%

FOXQ1	0=Low	503	0
	1=High	503	1
FOXF2	0=Low	503	0
	1=High	503	1
FOXM1	0=Low	503	0
	1=High	503	1

Patient	Days	Status	FOXF2 Expression	Group
TCGA-AQ-A54N	78	Alive	0	Low
TCGA-E9-A54X	727	Alive	0.99	Low
TCGA-AR-A0TR	160	Dead	1.92	Low
TCGA-B6-A0RL	2469	Dead	2.15	Low
TCGA-B6-A0X1	7455	Dead	2.17	Low
TCGA-D8-A1XC	377	Dead	2.21	Low
TCGA-AN-A0FJ	242	Alive	3	Low
TCGA-AC-A8OR	40	Alive	3.46	Low
TCGA-AN-A0FL	231	Alive	3.68	Low
TCGA-OL-A6VR	1220	Alive	3.96	Low
TCGA-AC-A2BK	2222	Alive	4.16	Low
TCGA-E2-A156	726	Alive	4.31	Low
TCGA-AN-A04D	52	Alive	4.61	Low

TCGA-D8-A1JN	620	Alive	4.66	Low
TCGA-BH-A0HW	1561	Alive	4.75	Low
TCGA-A7-A3J0	313	Alive	5.16	Low
TCGA-EW-A1PB	608	Alive	5.16	Low
TCGA-BH-A0EE	943	Alive	5.36	Low
TCGA-A2-A0ET	1066	Alive	5.42	Low
TCGA-A2-A0CY	1673	Alive	6.14	Low
TCGA-GM-A2DM	3226	Alive	6.19	Low
TCGA-LL-A442	889	Alive	6.49	Low
TCGA-E9-A54Y	725	Alive	6.52	Low
TCGA-GM-A3XL	2108	Alive	6.58	Low
TCGA-AR-A1AI	3296	Alive	6.81	Low
TCGA-A8-A06Z	31	Alive	7.09	Low
TCGA-PL-A8LX	5	Alive	7.12	Low
TCGA-D8-A1XV	461	Alive	7.73	Low
TCGA-E9-A5UO	785	Alive	7.86	Low
TCGA-A7-A0DC	906	Alive	7.94	Low
TCGA-UU-A93S	116	Dead	7.96	Low
TCGA-E2-A14N	1434	Alive	8.04	Low
TCGA-A8-A06Q	31	Alive	8.27	Low
TCGA-AO-A1KR	2513	Alive	8.7	Low
TCGA-EW-A1OX	911	Alive	8.94	Low
TCGA-A1-A0SO	852	Alive	9.19	Low
TCGA-BH-A1FJ	1927	Dead	9.27	Low
TCGA-AR-A0U2	2551	Dead	9.3	Low
TCGA-A2-A0YJ	566	Alive	9.36	Low
TCGA-LL-A6FP	677	Alive	9.41	Low
TCGA-A8-A08I	365	Alive	9.49	Low
TCGA-BH-A0E0	134	Alive	9.75	Low
TCGA-S3-AA0Z	629	Alive	9.93	Low
TCGA-E2-A14U	1318	Alive	9.97	Low
TCGA-EW-A6SA	510	Alive	10.24	Low
TCGA-C8-A12U	385	Alive	10.38	Low
TCGA-A2-A4S0	706	Alive	10.43	Low
TCGA-BH-A0W3	728	Alive	10.54	Low
TCGA-AR-A0U0	1988	Alive	10.57	Low
TCGA-AN-A0AT	10	Alive	10.67	Low
TCGA-BH-A18L	811	Dead	10.98	Low
TCGA-BH-A18S	2009	Dead	11.1	Low
TCGA-A8-A07W	304	Alive	11.12	Low

TCGA-AR-A0TU	709	Alive	11.27	Low
TCGA-S3-AA12	574	Alive	11.27	Low
TCGA-E2-A15T	1563	Alive	11.29	Low
TCGA-E2-A14R	1174	Alive	11.46	Low
TCGA-D8-A1X6	541	Alive	11.48	Low
TCGA-A8-A09T	579	Alive	11.79	Low
TCGA-AR-A0TV	2288	Alive	11.9	Low
TCGA-BH-A209	3959	Dead	12.13	Low
TCGA-B6-A0I2	4361	Alive	12.18	Low
TCGA-C8-A12X	385	Alive	12.23	Low
TCGA-C8-A26Y	394	Alive	12.24	Low
TCGA-A8-A07O	304	Alive	12.26	Low
TCGA-HN-A2NL	79	Alive	12.26	Low
TCGA-OL-A5RZ	679	Alive	12.28	Low
TCGA-AR-A24H	4894	Alive	12.37	Low
TCGA-E9-A228	1285	Alive	12.39	Low
TCGA-AR-A256	2854	Dead	12.43	Low
TCGA-A2-A0YF	1535	Alive	12.49	Low
TCGA-A1-A0SQ	554	Alive	12.51	Low
TCGA-BH-A0B9	1572	Alive	12.54	Low
TCGA-A7-A3RF	408	Alive	12.59	Low
TCGA-B6-A0IB	3941	Dead	12.61	Low
TCGA-AO-A03O	2483	Dead	12.66	Low
TCGA-A2-A1G4	595	Alive	12.88	Low
TCGA-BH-A0HL	72	Alive	12.91	Low
TCGA-D8-A1JI	577	Alive	13.12	Low
TCGA-AO-A0JL	1683	Alive	13.45	Low
TCGA-BH-A0H0	461	Alive	13.46	Low
TCGA-C8-A1HM	375	Alive	13.73	Low
TCGA-OL-A6VO	858	Alive	13.77	Low
TCGA-AN-A04C	54	Alive	13.83	Low
TCGA-BH-A8FY	295	Dead	13.87	Low
TCGA-AN-A0G0	16	Alive	14.36	Low
TCGA-C8-A27B	439	Alive	14.36	Low
TCGA-AR-A1AH	3807	Alive	14.42	Low
TCGA-E2-A572	1208	Alive	14.49	Low
TCGA-A7-A4SF	545	Alive	14.5	Low
TCGA-E2-A1II	1025	Alive	14.6	Low
TCGA-AC-A7VB	250	Alive	14.63	Low
TCGA-A8-A09K	912	Alive	14.76	Low

TCGA-E2-A1IU	337	Alive	14.8	Low
TCGA-AR-A0TY	1699	Dead	14.83	Low
TCGA-E2-A15J	1640	Alive	14.84	Low
TCGA-A8-A06Y	791	Alive	14.91	Low
TCGA-C8-A1HK	366	Alive	15	Low
TCGA-E2-A1LS	1604	Alive	15.02	Low
TCGA-D8-A147	584	Alive	15.09	Low
TCGA-B6-A0RQ	4267	Dead	15.17	Low
TCGA-BH-A18T	224	Dead	15.26	Low
TCGA-GM-A3XG	1330	Alive	15.27	Low
TCGA-AQ-A1H2	475	Alive	15.3	Low
TCGA-LQ-A4E4	849	Alive	15.46	Low
TCGA-A2-A3XV	996	Alive	15.91	Low
TCGA-B6-A0X4	860	Dead	15.94	Low
TCGA-BH-A0HN	516	Alive	16.15	Low
TCGA-BH-A1EN	2127	Dead	16.19	Low
TCGA-E2-A107	1047	Alive	16.2	Low
TCGA-A7-A3IZ	322	Alive	16.24	Low
TCGA-GM-A5PV	412	Alive	16.25	Low
TCGA-D8-A143	431	Alive	16.27	Low
TCGA-BH-A0HO	76	Alive	16.4	Low
TCGA-A8-A099	304	Alive	16.5	Low
TCGA-BH-A0BS	2612	Alive	16.51	Low
TCGA-AR-A1AT	1272	Dead	16.59	Low
TCGA-A7-A0CJ	931	Alive	16.61	Low
TCGA-BH-A204	2534	Dead	16.8	Low
TCGA-C8-A274	508	Alive	16.87	Low
TCGA-C8-A26V	616	Alive	16.93	Low
TCGA-PL-A8LY	8	Alive	16.97	Low
TCGA-EW-A1OY	908	Alive	17.05	Low
TCGA-A8-A07Z	1371	Alive	17.2	Low
TCGA-AR-A0TZ	3262	Dead	17.23	Low
TCGA-B6-A0X5	2097	Dead	17.29	Low
TCGA-AO-A0JD	2190	Alive	17.31	Low
TCGA-AO-A12B	2989	Alive	17.34	Low
TCGA-3C-AAAU	4047	Alive	17.58	Low
TCGA-AO-A128	3248	Alive	17.64	Low
TCGA-BH-A18Q	1692	Dead	17.79	Low
TCGA-BH-A5IZ	567	Alive	17.9	Low
TCGA-AC-A5XS	588	Alive	18.12	Low

TCGA-A8-A09E	1492	Alive	18.21	Low
TCGA-AR-A0U3	4080	Alive	18.25	Low
TCGA-AR-A0U4	3261	Alive	18.55	Low
TCGA-AC-A62X	417	Alive	19.15	Low
TCGA-B6-A402	2134	Alive	19.15	Low
TCGA-E9-A1N8	1039	Alive	19.26	Low
TCGA-A2-A4S3	666	Alive	19.37	Low
TCGA-AR-A0TW	3009	Alive	19.38	Low
TCGA-A2-A0CW	3283	Alive	19.54	Low
TCGA-AR-A24Z	3001	Alive	19.69	Low
TCGA-A8-A08F	1004	Alive	19.98	Low
TCGA-E2-A10C	1220	Alive	19.98	Low
TCGA-B6-A0IO	5042	Alive	20.07	Low
TCGA-A8-A08B	1156	Alive	20.32	Low
TCGA-A2-A0ER	2263	Alive	20.49	Low
TCGA-E2-A1IK	1800	Alive	20.56	Low
TCGA-BH-A1F5	2712	Dead	20.63	Low
TCGA-D8-A1XK	441	Alive	20.91	Low
TCGA-A2-A0EY	1925	Alive	21.22	Low
TCGA-B6-A0RO	4929	Alive	21.23	Low
TCGA-AN-A0AR	10	Alive	21.28	Low
TCGA-B6-A1KC	1326	Alive	21.28	Low
TCGA-WT-AB41	1611	Alive	21.29	Low
TCGA-AN-A0FF	172	Alive	21.35	Low
TCGA-A2-A3XT	2770	Alive	21.47	Low
TCGA-A8-A092	942	Alive	21.48	Low
TCGA-E2-A14W	974	Alive	21.56	Low
TCGA-B6-A0IQ	4285	Alive	21.6	Low
TCGA-BH-A18N	1148	Dead	21.62	Low
TCGA-E9-A249	217	Alive	21.63	Low
TCGA-A8-A08A	30	Alive	21.71	Low
TCGA-A2-A0YT	723	Dead	21.85	Low
TCGA-A2-A0YG	666	Alive	21.99	Low
TCGA-AQ-A04H	754	Alive	22.04	Low
TCGA-D8-A1XW	1309	Alive	22.27	Low
TCGA-C8-A1HN	394	Alive	22.43	Low
TCGA-LL-A6FQ	80	Alive	22.61	Low
TCGA-AR-A1AW	2632	Alive	22.7	Low
TCGA-GM-A2DN	3091	Alive	22.75	Low
TCGA-UL-AAZ6	518	Alive	22.76	Low

TCGA-BH-A0BW	2371	Alive	22.84	Low
TCGA-B6-A0RM	2373	Dead	22.97	Low
TCGA-D8-A1Y3	430	Alive	23.04	Low
TCGA-BH-A6R8	293	Alive	23.11	Low
TCGA-C8-A12L	363	Alive	23.35	Low
TCGA-OL-A66H	812	Alive	23.35	Low
TCGA-E9-A3Q9	1001	Alive	23.45	Low
TCGA-C8-A12V	385	Alive	23.52	Low
TCGA-B6-A0IJ	7106	Alive	23.54	Low
TCGA-C8-A12M	358	Alive	23.6	Low
TCGA-AO-A03P	2911	Dead	23.71	Low
TCGA-AO-A12E	2142	Alive	23.77	Low
TCGA-E2-A15O	1545	Alive	23.9	Low
TCGA-BH-A1FD	1009	Dead	24.07	Low
TCGA-S3-AA11	421	Alive	24.43	Low
TCGA-AO-A0J2	997	Alive	24.5	Low
TCGA-A2-A04X	1686	Alive	24.51	Low
TCGA-E9-A22H	1232	Alive	24.71	Low
TCGA-A8-A09W	30	Alive	25.16	Low
TCGA-AN-A0AK	224	Alive	25.19	Low
TCGA-A2-A0CU	158	Dead	25.2	Low
TCGA-A8-A06X	943	Dead	25.34	Low
TCGA-AR-A2LE	5062	Alive	25.45	Low
TCGA-D8-A73W	385	Dead	25.5	Low
TCGA-AR-A251	3030	Alive	25.7	Low
TCGA-AR-A0TP	4275	Alive	25.71	Low
TCGA-AO-A03R	2091	Alive	26.04	Low
TCGA-E9-A3HO	1158	Alive	26.46	Low
TCGA-S3-AA17	424	Alive	26.46	Low
TCGA-AN-A046	10	Alive	26.51	Low
TCGA-A2-A0ST	3017	Alive	26.52	Low
TCGA-B6-A1KF	3088	Alive	26.52	Low
TCGA-GM-A2DO	2596	Alive	26.57	Low
TCGA-BH-A1FG	3736	Dead	26.58	Low
TCGA-E2-A14S	1009	Alive	26.71	Low
TCGA-E9-A1R7	1467	Alive	26.74	Low
TCGA-A2-A25B	1291	Alive	27.22	Low
TCGA-E2-A14O	1359	Alive	27.25	Low
TCGA-AO-A1KQ	1882	Alive	27.32	Low
TCGA-BH-A0C0	1270	Alive	27.41	Low

TCGA-BH-A0DH	1156	Alive	27.47	Low
TCGA-AN-A03Y	10	Alive	27.51	Low
TCGA-B6-A0WZ	6292	Alive	27.51	Low
TCGA-EW-A1J1	575	Alive	27.59	Low
TCGA-E9-A3QA	918	Alive	27.74	Low
TCGA-A8-A09Q	761	Alive	27.8	Low
TCGA-BH-A0DD	2486	Alive	28.01	Low
TCGA-B6-A2IU	5176	Alive	28.04	Low
TCGA-AO-A1KS	350	Alive	28.09	Low
TCGA-GM-A3NW	3361	Alive	28.09	Low
TCGA-A8-A0A1	365	Alive	28.11	Low
TCGA-A8-A079	274	Alive	28.12	Low
TCGA-A7-A0CE	1074	Alive	28.14	Low
TCGA-AR-A1AR	524	Dead	28.18	Low
TCGA-EW-A1PE	320	Alive	28.29	Low
TCGA-A7-A4SD	441	Alive	28.36	Low
TCGA-AC-A62Y	530	Alive	28.43	Low
TCGA-BH-A0E7	1363	Alive	28.49	Low
TCGA-E9-A1ND	1266	Alive	28.49	Low
TCGA-A7-A3IY	345	Alive	28.64	Low
TCGA-C8-A1HJ	5	Alive	28.71	Low
TCGA-BH-A18G	149	Alive	28.75	Low
TCGA-A7-A0CH	1079	Alive	28.78	Low
TCGA-E2-A1IE	2362	Alive	28.9	Low
TCGA-A8-A08G	607	Alive	29.02	Low
TCGA-A7-A13G	718	Alive	29.06	Low
TCGA-BH-A1EW	1694	Dead	29.12	Low
TCGA-EW-A1P5	703	Alive	29.31	Low
TCGA-A8-A06U	883	Dead	29.56	Low
TCGA-A8-A07B	1308	Alive	29.59	Low
TCGA-A8-A07P	334	Alive	29.72	Low
TCGA-EW-A1P8	239	Dead	29.75	Low
TCGA-PE-A5DD	1953	Alive	29.82	Low
TCGA-A2-A0D3	1873	Alive	29.99	Low
TCGA-BH-A0AW	622	Alive	29.99	Low
TCGA-D8-A1XQ	499	Alive	30.05	Low
TCGA-LL-A7T0	376	Alive	30.13	Low
TCGA-E2-A106	2541	Alive	30.42	Low
TCGA-A8-A08S	1004	Alive	30.65	Low
TCGA-E2-A15F	658	Alive	30.84	Low

TCGA-AN-A0AM	5	Alive	31.03	Low
TCGA-BH-A18H	652	Alive	31.06	Low
TCGA-E9-A248	59	Alive	31.08	Low
TCGA-E2-A109	1417	Alive	31.1	Low
TCGA-AR-A1AV	1864	Alive	31.23	Low
TCGA-A8-A091	1004	Alive	31.33	Low
TCGA-AN-A0XU	10	Alive	31.36	Low
TCGA-BH-A1FL	1673	Dead	31.42	Low
TCGA-AO-A0JI	1528	Alive	31.43	Low
TCGA-LL-A50Y	762	Alive	31.43	Low
TCGA-A2-A3Y0	1546	Alive	31.52	Low
TCGA-AR-A2LL	2012	Alive	31.77	Low
TCGA-EW-A1J6	875	Alive	31.8	Low
TCGA-A2-A0CM	754	Dead	31.84	Low
TCGA-AC-A23H	174	Dead	31.84	Low
TCGA-E2-A14T	2311	Alive	31.85	Low
TCGA-AR-A24K	1548	Alive	32.04	Low
TCGA-E9-A1RE	1419	Alive	32.09	Low
TCGA-C8-A8HP	396	Alive	32.2	Low
TCGA-AR-A1AJ	3072	Alive	32.49	Low
TCGA-A2-A1FX	1847	Alive	32.5	Low
TCGA-A8-A08C	881	Alive	32.51	Low
TCGA-BH-A0E9	2489	Alive	32.56	Low
TCGA-AO-A12F	1842	Alive	32.67	Low
TCGA-A8-A07U	760	Alive	32.79	Low
TCGA-AC-A62V	348	Dead	32.87	Low
TCGA-E2-A155	640	Alive	33.01	Low
TCGA-AR-A0TT	3316	Alive	33.03	Low
TCGA-A2-A1FW	528	Alive	33.23	Low
TCGA-E2-A14P	1246	Alive	33.24	Low
TCGA-BH-A18R	1142	Dead	33.28	Low
TCGA-BH-A1F8	763	Dead	33.28	Low
TCGA-E2-A10A	1229	Alive	33.62	Low
TCGA-EW-A1IZ	554	Alive	33.78	Low
TCGA-A2-A25D	552	Alive	33.89	Low
TCGA-E9-A1R6	339	Alive	33.93	Low
TCGA-AN-A0XP	9	Alive	34.08	Low
TCGA-AC-A3TN	456	Alive	34.12	Low
TCGA-C8-A1HO	375	Alive	34.24	Low
TCGA-BH-A0H9	1247	Alive	34.41	Low

TCGA-E2-A15K	275	Alive	34.45	Low
TCGA-A8-A0A6	640	Alive	34.58	Low
TCGA-AN-A0FW	11	Alive	34.62	Low
TCGA-LL-A5YM	466	Alive	34.65	Low
TCGA-AN-A0XR	10	Alive	34.73	Low
TCGA-D8-A1XZ	466	Alive	34.76	Low
TCGA-A8-A09X	426	Dead	34.77	Low
TCGA-A8-A0AB	518	Alive	34.8	Low
TCGA-AR-A24R	3430	Alive	34.99	Low
TCGA-BH-A1EX	1508	Dead	35.18	Low
TCGA-BH-A0BG	1871	Alive	35.2	Low
TCGA-A8-A08L	304	Dead	35.22	Low
TCGA-E9-A245	26	Alive	35.29	Low
TCGA-E2-A14X	972	Alive	35.45	Low
TCGA-LL-A8F5	596	Alive	35.68	Low
TCGA-GM-A2DH	2193	Alive	35.72	Low
TCGA-S3-AA10	586	Alive	35.73	Low
TCGA-AR-A24U	3128	Alive	35.75	Low
TCGA-BH-A0EA	991	Dead	35.89	Low
TCGA-A2-A0YM	965	Alive	35.93	Low
TCGA-B6-A0WV	2417	Dead	35.99	Low
TCGA-E2-A56Z	252	Alive	36.07	Low
TCGA-A7-A4SB	418	Alive	36.14	Low
TCGA-AR-A2LH	616	Dead	36.28	Low
TCGA-B6-A0I9	362	Dead	36.65	Low
TCGA-AO-A129	3286	Alive	36.68	Low
TCGA-A8-A082	549	Alive	36.8	Low
TCGA-E2-A150	1935	Alive	36.83	Low
TCGA-A2-A0YH	659	Alive	36.9	Low
TCGA-D8-A1XG	448	Alive	37.13	Low
TCGA-A2-A0CQ	2695	Alive	37.16	Low
TCGA-E9-A295	375	Alive	37.18	Low
TCGA-A2-A0T5	531	Alive	37.2	Low
TCGA-D8-A27F	488	Alive	37.36	Low
TCGA-D8-A1XF	463	Alive	37.39	Low
TCGA-OL-A5D8	973	Alive	37.63	Low
TCGA-D8-A1JF	366	Alive	37.68	Low
TCGA-D8-A1XA	839	Alive	37.73	Low
TCGA-D8-A27V	381	Alive	37.75	Low
TCGA-C8-A12Z	382	Alive	37.86	Low

TCGA-A8-A08J	1127	Dead	37.92	Low
TCGA-A8-A09I	1371	Alive	38.05	Low
TCGA-A8-A09M	1006	Alive	38.05	Low
TCGA-AR-A1AQ	3021	Alive	38.22	Low
TCGA-A2-A3XZ	1532	Alive	38.25	Low
TCGA-A2-A0SU	1662	Alive	38.31	Low
TCGA-A2-A0EQ	2426	Alive	38.55	Low
TCGA-AC-A2FB	1234	Alive	38.58	Low
TCGA-LL-A5YN	447	Alive	38.66	Low
TCGA-E2-A15E	630	Alive	38.97	Low
TCGA-A2-A0D4	767	Alive	39.14	Low
TCGA-AR-A1AP	2856	Alive	39.14	Low
TCGA-E2-A1LL	1309	Alive	39.15	Low
TCGA-AN-A0XT	10	Alive	39.26	Low
TCGA-AC-A7VC	1	Alive	39.34	Low
TCGA-AQ-A04J	819	Alive	39.35	Low
TCGA-AN-A0FK	213	Alive	39.45	Low
TCGA-A8-A076	1642	Alive	39.47	Low
TCGA-C8-A1HG	345	Alive	39.59	Low
TCGA-E2-A573	1062	Alive	39.7	Low
TCGA-E2-A9RU	538	Alive	39.76	Low
TCGA-C8-A1HE	375	Alive	39.92	Low
TCGA-E2-A1LB	2306	Alive	39.99	Low
TCGA-E9-A2JS	904	Dead	39.99	Low
TCGA-AC-A4ZE	890	Alive	40.02	Low
TCGA-AN-A0XL	163	Alive	40.05	Low
TCGA-A2-A0CT	2289	Alive	40.13	Low
TCGA-A8-A09N	31	Alive	40.58	Low
TCGA-D8-A1JL	611	Alive	40.58	Low
TCGA-EW-A1OV	789	Alive	40.61	Low
TCGA-BH-A42T	320	Dead	40.79	Low
TCGA-A2-A0SW	1365	Dead	40.8	Low
TCGA-BH-A0HX	829	Alive	40.8	Low
TCGA-E2-A1LG	1523	Alive	40.85	Low
TCGA-JL-A3YX	352	Alive	40.88	Low
TCGA-BH-A18P	921	Dead	41.01	Low
TCGA-PE-A5DC	1430	Dead	41.21	Low
TCGA-EW-A1P6	562	Alive	41.28	Low
TCGA-E2-A15D	526	Alive	41.33	Low
TCGA-A8-A07C	1034	Alive	41.49	Low

TCGA-BH-A18U	1563	Dead	41.51	Low
TCGA-D8-A3Z5	1015	Alive	41.81	Low
TCGA-A8-A09R	273	Alive	42.03	Low
TCGA-BH-A0RX	170	Alive	42.05	Low
TCGA-AC-A2BM	3022	Alive	42.09	Low
TCGA-B6-A0WT	5739	Alive	42.26	Low
TCGA-BH-A1EV	365	Dead	42.3	Low
TCGA-AN-A0FT	214	Alive	42.35	Low
TCGA-C8-A131	411	Alive	42.35	Low
TCGA-A8-A06T	1614	Alive	42.46	Low
TCGA-E2-A15R	1732	Alive	42.46	Low
TCGA-E2-A15M	336	Dead	42.49	Low
TCGA-D8-A1JA	502	Alive	42.52	Low
TCGA-AR-A1AY	1026	Alive	42.62	Low
TCGA-AO-A0J6	1140	Alive	42.64	Low
TCGA-GM-A2DC	2535	Alive	42.68	Low
TCGA-C8-A12P	358	Alive	42.8	Low
TCGA-A2-A0D1	1051	Alive	42.85	Low
TCGA-A2-A0D2	1027	Alive	42.88	Low
TCGA-A2-A3KD	1206	Alive	42.99	Low
TCGA-A8-A08P	943	Alive	43.02	Low
TCGA-S3-A6ZF	572	Alive	43.04	Low
TCGA-E9-A1RB	976	Dead	43.18	Low
TCGA-E9-A1RD	34	Alive	43.22	Low
TCGA-A2-A3XW	1712	Alive	43.23	Low
TCGA-D8-A1XL	606	Alive	43.37	Low
TCGA-A8-A075	518	Alive	43.38	Low
TCGA-E2-A15I	1692	Alive	43.45	Low
TCGA-A8-A06O	396	Alive	43.51	Low
TCGA-A1-A0SM	242	Alive	43.56	Low
TCGA-BH-A0H5	1620	Alive	43.65	Low
TCGA-AR-A1AS	1150	Alive	43.67	Low
TCGA-AR-A24S	2976	Alive	43.67	Low
TCGA-AO-A1KP	2953	Alive	43.77	Low
TCGA-C8-A275	1	Alive	43.84	Low
TCGA-BH-A0E1	477	Alive	43.95	Low
TCGA-D8-A1XR	482	Alive	44	Low
TCGA-D8-A27W	373	Alive	44.17	Low
TCGA-BH-A0HK	178	Alive	44.26	Low
TCGA-D8-A1X9	727	Alive	44.26	Low

TCGA-AC-A3EH	197	Dead	44.58	Low
TCGA-3C-AALI	4005	Alive	44.59	Low
TCGA-E2-A1L7	1836	Alive	44.64	Low
TCGA-D8-A1JG	1612	Alive	44.76	Low
TCGA-BH-A202	795	Alive	44.86	Low
TCGA-OL-A5D7	1780	Alive	44.92	Low
TCGA-D8-A1X5	565	Alive	44.94	Low
TCGA-S3-A6ZH	641	Alive	45.04	Low
TCGA-OL-A5RU	1219	Alive	45.36	Low
TCGA-E2-A14Q	1163	Alive	45.47	Low
TCGA-E9-A247	1186	Alive	45.47	Low
TCGA-OL-A5RV	1062	Alive	45.47	Low
TCGA-AR-A24N	3035	Alive	45.65	Low
TCGA-A2-A259	1596	Alive	45.72	Low
TCGA-GM-A2DK	2645	Alive	45.74	Low
TCGA-E2-A2P6	1051	Alive	45.86	Low
TCGA-E9-A22D	1248	Alive	45.89	Low
TCGA-BH-A0B8	1569	Alive	45.92	Low
TCGA-C8-A26X	376	Alive	45.93	Low
TCGA-A8-A0A9	822	Alive	45.99	Low
TCGA-B6-A0WW	558	Dead	46	Low
TCGA-D8-A13Y	1728	Alive	46	Low
TCGA-A7-A56D	448	Alive	46.06	Low
TCGA-A2-A04Y	1099	Alive	46.17	Low
TCGA-E2-A15C	694	Alive	46.4	Low
TCGA-E2-A105	1308	Alive	46.47	Low
TCGA-A8-A0A4	396	Alive	46.57	Low
TCGA-AC-A8OP	614	Alive	46.59	Low
TCGA-E2-A154	591	Alive	46.72	Low
TCGA-AO-A12A	3112	Alive	46.74	Low
TCGA-A2-A25C	523	Alive	46.76	Low
TCGA-E9-A1R4	186	Alive	46.89	Low
TCGA-GM-A2DB	2406	Alive	46.98	Low
TCGA-A2-A04Q	2385	Alive	47.05	Low
TCGA-A7-A0CD	1165	Alive	47.12	Low
TCGA-BH-A1F6	2965	Dead	47.15	Low
TCGA-BH-A0BT	2365	Alive	47.17	Low
TCGA-AQ-A0Y5	172	Dead	47.3	Low
TCGA-AR-A2LK	1649	Dead	47.36	Low
TCGA-D8-A1J8	431	Alive	47.38	Low

TCGA-B6-A0IK	571	Dead	47.4	Low
TCGA-A8-A09C	31	Alive	47.47	Low
TCGA-C8-A12W	385	Alive	47.48	Low
TCGA-OL-A66P	428	Alive	47.48	Low
TCGA-D8-A1JC	480	Alive	47.66	Low
TCGA-A7-A0D9	1139	Alive	47.76	Low
TCGA-AC-A2FM	792	Dead	47.78	Low
TCGA-BH-A0HB	806	Alive	47.82	Low
TCGA-A7-A13E	614	Dead	47.83	Low
TCGA-AO-A0JB	1542	Alive	47.88	Low
TCGA-AR-A0TQ	2991	Alive	47.89	Low
TCGA-V7-A7HQ	2033	Alive	48.04	Low
TCGA-BH-A1F2	959	Dead	48.3	Low
TCGA-AR-A1AX	2629	Alive	48.39	Low
TCGA-AC-A5EH	511	Alive	48.66	Low
TCGA-E2-A10B	1141	Alive	48.93	Low
TCGA-AR-A1AL	2971	Alive	49.16	Low
TCGA-D8-A1X8	783	Alive	49.34	Low
TCGA-BH-A0C1	1411	Dead	49.46	Low
TCGA-E9-A24A	747	Alive	49.49	Low
TCGA-BH-A0GY	923	Alive	49.59	Low
TCGA-A2-A04V	1920	Dead	49.7	Low
TCGA-LL-A441	996	Alive	49.75	Low
TCGA-AO-A03V	1351	Alive	49.8	Low
TCGA-E2-A1L6	1648	Alive	49.86	Low
TCGA-PL-A8LZ	302	Alive	49.96	Low
TCGA-A2-A0T3	1516	Alive	50	Low
TCGA-E9-A1QZ	755	Alive	50.13	Low
TCGA-LL-A7SZ	594	Alive	50.17	Low
TCGA-E2-A14Z	563	Dead	50.22	Low
TCGA-AC-A2FK	2650	Alive	50.24	Low
TCGA-BH-A0B6	2483	Alive	50.48	Low
TCGA-A2-A1FV	714	Alive	50.52	Low
TCGA-B6-A0RN	8008	Alive	50.58	Low
TCGA-AO-A0J8	680	Alive	50.6	Low
TCGA-B6-A0I8	749	Dead	50.67	Low
TCGA-AO-A126	3307	Alive	50.92	Low
TCGA-BH-A0EI	1926	Alive	50.98	Low
TCGA-A7-A13F	765	Alive	51	Low
TCGA-A7-A13H	899	Alive	51.01	Low

TCGA-EW-A1J5	477	Alive	51.05	Low
TCGA-A2-A0T2	255	Dead	51.27	Low
TCGA-D8-A1J9	532	Alive	51.28	Low
TCGA-BH-A0DO	1644	Alive	51.5	Low
TCGA-EW-A1J3	504	Alive	51.51	Low
TCGA-W8-A86G	347	Alive	51.73	Low
TCGA-A8-A07L	975	Alive	51.75	Low
TCGA-AR-A0TX	1972	Alive	51.78	Low
TCGA-AC-A23C	585	Alive	52.04	Low
TCGA-BH-A1EY	538	Dead	52.17	Low
TCGA-BH-A0E2	435	Alive	52.2	High
TCGA-E9-A2JT	288	Alive	52.41	High
TCGA-C8-A3M8	394	Alive	52.53	High
TCGA-A2-A0SY	1347	Alive	52.61	High
TCGA-A2-A0T4	624	Alive	52.71	High
TCGA-BH-A0H6	747	Alive	52.72	High
TCGA-E9-A244	21	Alive	52.92	High
TCGA-AO-A03T	2124	Alive	52.96	High
TCGA-GI-A2C9	3342	Alive	53.1	High
TCGA-A2-A0YC	990	Alive	53.53	High
TCGA-A2-A0T0	533	Alive	53.73	High
TCGA-AC-A6NO	51	Alive	53.78	High
TCGA-AO-A0JC	1547	Alive	53.85	High
TCGA-AR-A5QN	1013	Alive	53.92	High
TCGA-OK-A5Q2	64	Alive	54.01	High
TCGA-B6-A0IP	3926	Dead	54.06	High
TCGA-E2-A576	1043	Alive	54.08	High
TCGA-D8-A1Y1	302	Dead	54.18	High
TCGA-A2-A0SX	1534	Alive	54.27	High
TCGA-D8-A1JK	612	Alive	54.32	High
TCGA-Z7-A8R5	3287	Alive	54.36	High
TCGA-A2-A0EV	968	Alive	54.39	High
TCGA-E9-A1RH	1417	Alive	54.56	High
TCGA-E2-A159	762	Alive	54.65	High
TCGA-AC-A2FG	1853	Alive	54.68	High
TCGA-C8-A137	379	Alive	54.7	High
TCGA-E2-A10E	865	Alive	54.81	High
TCGA-AO-A1KO	622	Alive	54.87	High
TCGA-BH-A18F	1001	Alive	54.92	High
TCGA-A2-A0EM	3094	Alive	55.04	High

TCGA-A2-A4S2	643	Alive	55.15	High
TCGA-BH-A0DS	78	Alive	55.21	High
TCGA-A8-A085	1124	Alive	55.37	High
TCGA-AC-A3TM	762	Alive	55.39	High
TCGA-E2-A1B4	1004	Dead	55.52	High
TCGA-LL-A5YP	450	Alive	55.61	High
TCGA-E2-A153	707	Alive	55.62	High
TCGA-A2-A0EU	1043	Alive	55.63	High
TCGA-A7-A4SC	446	Alive	55.9	High
TCGA-BH-A1EU	1286	Dead	55.95	High
TCGA-AR-A252	2838	Alive	56	High
TCGA-A2-A0ES	2190	Alive	56.1	High
TCGA-C8-A278	297	Alive	56.15	High
TCGA-AC-A2B8	677	Alive	56.69	High
TCGA-AO-A12D	2515	Alive	56.71	High
TCGA-D8-A140	403	Alive	56.91	High
TCGA-C8-A3M7	1034	Dead	57.09	High
TCGA-BH-A0HU	392	Alive	57.13	High
TCGA-EW-A1PC	187	Alive	57.15	High
TCGA-B6-A0IG	4456	Dead	57.47	High
TCGA-E9-A1R2	1063	Alive	57.5	High
TCGA-B6-A0I5	8556	Alive	57.67	High
TCGA-A8-A09B	365	Alive	57.82	High
TCGA-BH-A0HI	620	Alive	58.02	High
TCGA-A2-A0T1	521	Alive	58.05	High
TCGA-BH-A0DX	2156	Alive	58.06	High
TCGA-A8-A09D	1522	Alive	58.14	High
TCGA-EW-A423	533	Alive	58.17	High
TCGA-AQ-A54O	1001	Alive	58.24	High
TCGA-AC-A3OD	451	Alive	58.41	High
TCGA-AO-A03M	1866	Alive	58.53	High
TCGA-BH-A18V	1556	Dead	58.66	High
TCGA-E2-A14V	1042	Alive	58.67	High
TCGA-BH-A0BP	2296	Dead	58.68	High
TCGA-D8-A27P	49	Alive	58.71	High
TCGA-D8-A1JB	1688	Alive	58.83	High
TCGA-A2-A0CX	1728	Alive	58.92	High
TCGA-A2-A0T6	575	Alive	58.95	High
TCGA-A7-A2KD	679	Alive	58.98	High
TCGA-AN-A049	19	Alive	59	High

TCGA-E9-A1R5	92	Alive	59.04	High
TCGA-A8-A095	1277	Alive	59.27	High
TCGA-AN-A03X	10	Alive	59.32	High
TCGA-LL-A5YL	519	Alive	59.37	High
TCGA-E2-A2P5	821	Dead	59.39	High
TCGA-A2-A0EX	752	Alive	59.54	High
TCGA-A8-A08T	3409	Dead	59.57	High
TCGA-AQ-A1H3	989	Alive	59.73	High
TCGA-D8-A4Z1	659	Alive	60.05	High
TCGA-E2-A1IL	118	Alive	60.07	High
TCGA-D8-A27G	409	Alive	60.54	High
TCGA-A2-A04P	548	Dead	60.68	High
TCGA-A2-A1G6	501	Alive	60.71	High
TCGA-A8-A084	458	Alive	60.72	High
TCGA-A2-A3XS	1032	Dead	61.06	High
TCGA-C8-A26Z	470	Alive	61.1	High
TCGA-PE-A5DE	2645	Alive	61.29	High
TCGA-B6-A40B	3152	Alive	61.43	High
TCGA-AN-A0AJ	303	Alive	61.61	High
TCGA-E9-A227	975	Alive	61.79	High
TCGA-AR-A0TS	2558	Alive	61.89	High
TCGA-EW-A6SD	1010	Alive	62.01	High
TCGA-A8-A06P	396	Alive	62.13	High
TCGA-A1-A0SJ	416	Alive	62.19	High
TCGA-BH-A1ET	2520	Dead	62.21	High
TCGA-GM-A4E0	2191	Alive	62.42	High
TCGA-B6-A409	573	Dead	62.64	High
TCGA-E2-A15P	595	Alive	62.68	High
TCGA-BH-A0HY	1545	Alive	62.87	High
TCGA-C8-A1HI	343	Alive	62.89	High
TCGA-C8-A1HF	332	Alive	62.96	High
TCGA-B6-A0RG	2082	Alive	63.01	High
TCGA-E2-A1AZ	2329	Alive	63.02	High
TCGA-E9-A1RA	1369	Alive	63.09	High
TCGA-B6-A0RS	3063	Dead	63.13	High
TCGA-AC-A2FE	2636	Dead	63.43	High
TCGA-OL-A66J	1996	Alive	63.54	High
TCGA-E9-A1N6	678	Dead	63.66	High
TCGA-BH-A203	1174	Dead	63.81	High
TCGA-BH-A8FZ	574	Alive	63.85	High

TCGA-E2-A1LE	879	Dead	63.94	High
TCGA-BH-A18J	612	Dead	63.95	High
TCGA-A7-A3J1	343	Alive	64.07	High
TCGA-BH-A0AU	1914	Alive	64.08	High
TCGA-BH-A0BV	1519	Alive	64.08	High
TCGA-A2-A0YI	1505	Alive	64.1	High
TCGA-E2-A10F	878	Alive	64.3	High
TCGA-A8-A07J	365	Alive	64.4	High
TCGA-D8-A27K	1461	Alive	64.8	High
TCGA-A2-A0EW	1884	Dead	64.82	High
TCGA-E2-A15A	710	Alive	64.94	High
TCGA-A8-A07E	608	Alive	65.04	High
TCGA-AR-A1AO	2618	Alive	65.05	High
TCGA-D8-A1XD	522	Alive	65.16	High
TCGA-LL-A9Q3	532	Alive	65.21	High
TCGA-BH-A0BO	2197	Alive	65.3	High
TCGA-BH-A0H3	1928	Alive	65.5	High
TCGA-OL-A66L	1301	Alive	65.53	High
TCGA-BH-A1ES	3462	Dead	65.57	High
TCGA-OL-A6VQ	600	Alive	65.66	High
TCGA-B6-A1KI	2236	Alive	65.73	High
TCGA-BH-AB28	287	Alive	65.76	High
TCGA-AN-A0XV	162	Alive	65.9	High
TCGA-E2-A1BD	1133	Alive	65.93	High
TCGA-A7-A425	447	Alive	66.02	High
TCGA-D8-A13Z	635	Alive	66.67	High
TCGA-AC-A8OS	70	Alive	66.73	High
TCGA-D8-A27R	307	Alive	67.09	High
TCGA-AR-A1AK	3159	Alive	67.22	High
TCGA-C8-A135	393	Alive	67.28	High
TCGA-B6-A1KN	4233	Alive	67.62	High
TCGA-OL-A5DA	1783	Alive	67.69	High
TCGA-A7-A0DB	1007	Alive	67.82	High
TCGA-GM-A2D9	1812	Dead	67.97	High
TCGA-OL-A66K	1275	Dead	67.97	High
TCGA-A2-A0CO	3492	Dead	68.09	High
TCGA-D8-A1JD	552	Alive	68.14	High
TCGA-GM-A2DL	3519	Alive	68.33	High
TCGA-E9-A1RG	647	Alive	68.39	High
TCGA-AN-A0FZ	10	Alive	68.44	High

TCGA-EW-A1P1	1210	Alive	68.46	High
TCGA-A7-A13D	965	Alive	68.65	High
TCGA-BH-A0W5	1288	Alive	68.73	High
TCGA-AR-A254	2605	Alive	68.88	High
TCGA-3C-AALJ	1474	Alive	68.9	High
TCGA-AR-A1AN	2920	Alive	68.91	High
TCGA-D8-A145	410	Alive	69.01	High
TCGA-BH-A0C7	2767	Alive	69.03	High
TCGA-A2-A1FZ	683	Alive	69.09	High
TCGA-E9-A1NE	1088	Alive	69.15	High
TCGA-D8-A1XY	503	Alive	69.4	High
TCGA-BH-A0DE	2372	Alive	69.47	High
TCGA-OL-A5RX	878	Alive	69.57	High
TCGA-EW-A1OZ	1229	Alive	69.66	High
TCGA-EW-A3E8	1035	Alive	69.78	High
TCGA-D8-A1XM	538	Alive	69.88	High
TCGA-BH-A0B7	2559	Alive	70.05	High
TCGA-BH-A0BD	554	Alive	70.31	High
TCGA-A2-A0YE	554	Alive	70.34	High
TCGA-A8-A093	546	Alive	70.35	High
TCGA-GM-A2DI	2590	Alive	70.41	High
TCGA-A2-A25E	3204	Alive	70.44	High
TCGA-A7-A26H	724	Alive	70.76	High
TCGA-BH-A0AY	777	Alive	70.84	High
TCGA-AN-A0XS	10	Alive	70.94	High
TCGA-AQ-A04L	3957	Alive	71.11	High
TCGA-A7-A6VX	317	Alive	71.21	High
TCGA-AC-A3QQ	734	Alive	71.32	High
TCGA-C8-A12Q	385	Dead	71.35	High
TCGA-E9-A226	1048	Dead	71.36	High
TCGA-EW-A1PA	575	Alive	71.4	High
TCGA-BH-A0HP	414	Alive	71.45	High
TCGA-B6-A401	2596	Alive	71.5	High
TCGA-B6-A0RH	6456	Dead	71.53	High
TCGA-E2-A1L8	2240	Alive	72.18	High
TCGA-E2-A570	931	Alive	72.23	High
TCGA-EW-A2FS	1604	Alive	72.3	High
TCGA-AR-A2LO	1198	Alive	72.42	High
TCGA-BH-A1FN	2192	Dead	72.45	High
TCGA-E9-A22G	1239	Alive	72.46	High

TCGA-E9-A243	612	Alive	72.81	High
TCGA-E9-A5FK	812	Alive	73.04	High
TCGA-D8-A1JM	590	Alive	73.06	High
TCGA-D8-A1JE	575	Alive	73.09	High
TCGA-EW-A1J2	403	Alive	73.32	High
TCGA-BH-A0B1	1148	Alive	73.4	High
TCGA-C8-A8HQ	380	Alive	73.79	High
TCGA-D8-A1XT	506	Alive	73.81	High
TCGA-B6-A0WS	2965	Dead	74	High
TCGA-AO-A0JM	2184	Alive	74.07	High
TCGA-BH-A0DP	476	Alive	74.15	High
TCGA-BH-A1FC	3472	Dead	74.73	High
TCGA-OL-A5D6	1104	Dead	74.83	High
TCGA-AN-A0FY	10	Alive	74.84	High
TCGA-AO-A0JF	1980	Alive	74.94	High
TCGA-A1-A0SF	1463	Alive	74.97	High
TCGA-A1-A0SN	1196	Alive	75.05	High
TCGA-AC-A8OQ	34	Alive	75.14	High
TCGA-D8-A73U	492	Alive	75.2	High
TCGA-C8-A26W	381	Alive	75.42	High
TCGA-E9-A1R3	78	Alive	75.9	High
TCGA-E2-A152	2128	Alive	75.99	High
TCGA-BH-A28Q	1119	Alive	76	High
TCGA-OL-A66N	792	Alive	76.22	High
TCGA-A2-A25F	322	Alive	76.49	High
TCGA-D8-A1XU	395	Alive	76.53	High
TCGA-A7-A26J	627	Alive	76.56	High
TCGA-EW-A1P4	907	Alive	76.69	High
TCGA-AC-A2FO	2255	Alive	76.8	High
TCGA-D8-A146	643	Alive	77.25	High
TCGA-A8-A09V	457	Alive	77.26	High
TCGA-EW-A1P7	915	Alive	77.4	High
TCGA-AN-A0XO	375	Alive	77.61	High
TCGA-GI-A2C8	225	Alive	77.64	High
TCGA-A2-A0EP	3603	Alive	77.74	High
TCGA-AR-A5QM	2231	Alive	78.35	High
TCGA-EW-A1IW	371	Alive	78.44	High
TCGA-EW-A1PF	439	Alive	78.45	High
TCGA-E2-A1B5	984	Alive	78.53	High
TCGA-D8-A1Y0	472	Alive	78.75	High

TCGA-A8-A0A2	579	Alive	78.76	High
TCGA-A7-A26E	954	Alive	79.37	High
TCGA-BH-A8G0	662	Alive	79.62	High
TCGA-OL-A66O	528	Alive	79.86	High
TCGA-BH-A0B5	2136	Alive	80.05	High
TCGA-AR-A24W	1550	Alive	80.06	High
TCGA-BH-A0H7	702	Alive	80.11	High
TCGA-E2-A108	837	Alive	80.45	High
TCGA-A8-A0A7	30	Alive	80.49	High
TCGA-WT-AB44	883	Alive	80.64	High
TCGA-E9-A1R0	860	Alive	80.95	High
TCGA-BH-A0GZ	328	Alive	81	High
TCGA-A2-A1G1	584	Alive	81.09	High
TCGA-AR-A2LN	1161	Alive	81.21	High
TCGA-E2-A1B6	867	Alive	81.21	High
TCGA-C8-A273	513	Alive	81.24	High
TCGA-AR-A2LQ	1233	Alive	81.44	High
TCGA-BH-A1FB	3669	Dead	81.6	High
TCGA-A7-A4SA	454	Alive	81.64	High
TCGA-AC-A6IX	373	Alive	82.4	High
TCGA-AC-A5XU	455	Alive	82.43	High
TCGA-XX-A899	467	Alive	82.68	High
TCGA-LD-A7W5	216	Alive	82.72	High
TCGA-A8-A086	396	Alive	82.82	High
TCGA-BH-A0DG	2041	Alive	82.96	High
TCGA-E9-A6HE	847	Alive	83.21	High
TCGA-A2-A0CS	2348	Dead	83.53	High
TCGA-E2-A14Y	2109	Alive	83.64	High
TCGA-B6-A0RT	2721	Alive	83.93	High
TCGA-5L-AAT1	1471	Alive	83.94	High
TCGA-E2-A1IG	2140	Alive	84.04	High
TCGA-E2-A15H	393	Alive	84.1	High
TCGA-A2-A04T	2246	Alive	84.15	High
TCGA-C8-A12N	358	Alive	84.25	High
TCGA-AC-A3BB	987	Alive	84.34	High
TCGA-A2-A0SV	825	Dead	84.39	High
TCGA-E2-A1B0	1631	Alive	84.66	High
TCGA-C8-A130	370	Alive	85.01	High
TCGA-A8-A07F	577	Alive	85.04	High
TCGA-A8-A097	365	Alive	85.04	High

TCGA-BH-A0BJ	660	Alive	85.36	High
TCGA-A2-A04R	3709	Alive	85.48	High
TCGA-C8-A8HR	408	Alive	85.56	High
TCGA-B6-A0I1	2361	Dead	86.32	High
TCGA-BH-A42V	635	Alive	86.45	High
TCGA-AC-A6IV	568	Alive	87.28	High
TCGA-A1-A0SP	584	Alive	87.56	High
TCGA-D8-A1XO	1682	Alive	87.82	High
TCGA-E2-A1IH	1026	Alive	87.93	High
TCGA-E9-A1NG	786	Dead	88	High
TCGA-BH-A0B0	2477	Alive	88.39	High
TCGA-BH-A5J0	715	Alive	88.51	High
TCGA-AO-A0JJ	1887	Alive	88.94	High
TCGA-LL-A5YO	440	Alive	89.77	High
TCGA-BH-A1FU	1688	Dead	90.52	High
TCGA-C8-A138	380	Alive	91.43	High
TCGA-A2-A4RY	648	Alive	91.54	High
TCGA-D8-A27L	499	Alive	92.07	High
TCGA-E9-A229	1148	Alive	92.08	High
TCGA-A7-A26I	661	Alive	92.39	High
TCGA-A2-A0YK	588	Alive	92.47	High
TCGA-A2-A0CK	4159	Alive	92.53	High
TCGA-XX-A89A	488	Alive	92.58	High
TCGA-AQ-A7U7	584	Dead	92.92	High
TCGA-E9-A1NH	576	Alive	93.02	High
TCGA-BH-A0HQ	1121	Alive	93.12	High
TCGA-AR-A250	2707	Alive	93.27	High
TCGA-4H-AAAK	348	Alive	93.62	High
TCGA-A8-A08X	1308	Alive	93.69	High
TCGA-AO-A0JE	2335	Alive	93.71	High
TCGA-D8-A1JH	426	Alive	93.8	High
TCGA-BH-A18K	2763	Dead	93.85	High
TCGA-E2-A1BC	501	Alive	93.87	High
TCGA-B6-A0IH	3418	Dead	93.9	High
TCGA-AR-A1AM	2991	Alive	94.01	High
TCGA-BH-A0DV	2064	Alive	94.04	High
TCGA-3C-AALK	1448	Alive	94.33	High
TCGA-E2-A1LA	748	Alive	94.35	High
TCGA-BH-A42U	3364	Alive	94.78	High
TCGA-Z7-A8R6	3256	Alive	95	High

TCGA-EW-A1PG	1051	Alive	95.03	High
TCGA-A2-A04U	2654	Alive	95.08	High
TCGA-A2-A0YD	769	Alive	95.34	High
TCGA-A8-A08O	943	Alive	95.39	High
TCGA-E2-A1B1	2653	Alive	95.55	High
TCGA-AR-A24P	84	Alive	96.05	High
TCGA-C8-A12O	385	Alive	96.35	High
TCGA-A2-A0CL	3015	Alive	96.37	High
TCGA-E2-A15S	428	Alive	97.2	High
TCGA-B6-A0RI	7126	Alive	97.71	High
TCGA-A1-A0SD	437	Alive	97.92	High
TCGA-D8-A141	626	Alive	98.37	High
TCGA-BH-A0BL	2278	Alive	98.48	High
TCGA-AO-A0JA	655	Alive	98.5	High
TCGA-A2-A0YL	1474	Alive	98.98	High
TCGA-E2-A3DX	1325	Alive	99.14	High
TCGA-A2-A4RW	222	Alive	99.27	High
TCGA-BH-A0DT	2403	Alive	99.45	High
TCGA-EW-A424	715	Alive	99.55	High
TCGA-A8-A08R	30	Alive	99.76	High
TCGA-AR-A24L	2866	Dead	99.77	High
TCGA-BH-A0DZ	495	Alive	100	High
TCGA-A8-A07I	426	Alive	100.1	High
TCGA-BH-A0HF	727	Alive	100.19	High
TCGA-A2-A04N	4354	Alive	100.63	High
TCGA-E2-A1L9	598	Alive	100.78	High
TCGA-A7-A426	364	Alive	101.22	High
TCGA-C8-A132	383	Alive	101.54	High
TCGA-AN-A0FS	210	Alive	101.55	High
TCGA-BH-A0E6	293	Alive	101.87	High
TCGA-BH-A0DK	423	Alive	102.16	High
TCGA-AR-A5QP	1185	Alive	102.25	High
TCGA-LL-A740	441	Alive	102.54	High
TCGA-A2-A0CR	3283	Alive	103.44	High
TCGA-EW-A6S9	463	Alive	103.63	High
TCGA-A2-A0CZ	1616	Alive	103.81	High
TCGA-BH-A0BZ	2255	Alive	103.86	High
TCGA-A2-A0T7	631	Alive	103.99	High
TCGA-AC-A23E	698	Alive	104.25	High
TCGA-GM-A5PX	551	Alive	104.34	High

TCGA-A2-A0CV	3011	Alive	104.58	High
TCGA-EW-A6SB	760	Alive	104.64	High
TCGA-BH-A0BF	1324	Dead	104.79	High
TCGA-BH-A0B4	1191	Alive	105.07	High
TCGA-BH-A0HA	1611	Alive	105.3	High
TCGA-AR-A255	2161	Alive	105.52	High
TCGA-E2-A1IJ	865	Alive	105.97	High
TCGA-A2-A3XY	1093	Dead	106.1	High
TCGA-C8-A27A	747	Alive	106.64	High
TCGA-AR-A2LM	1935	Alive	106.82	High
TCGA-EW-A1P3	1611	Alive	107.02	High
TCGA-GM-A3XN	2019	Alive	107.17	High
TCGA-D8-A142	425	Alive	107.3	High
TCGA-EW-A1IY	258	Alive	107.51	High
TCGA-BH-A18M	2207	Dead	107.62	High
TCGA-A2-A0EN	4088	Alive	107.66	High
TCGA-BH-A0W4	759	Alive	108.56	High
TCGA-D8-A27T	398	Alive	108.78	High
TCGA-D8-A1Y2	433	Alive	108.83	High
TCGA-AN-A0AS	10	Alive	109.03	High
TCGA-AN-A0XW	170	Alive	109.32	High
TCGA-E9-A1RF	200	Alive	109.56	High
TCGA-BH-A0B3	1203	Alive	109.8	High
TCGA-AO-A0J9	1613	Alive	110.3	High
TCGA-BH-A0EB	745	Alive	110.31	High
TCGA-B6-A0RE	7777	Alive	110.35	High
TCGA-BH-A18I	1093	Alive	111.39	High
TCGA-E2-A1IN	675	Alive	111.44	High
TCGA-GM-A3NY	1162	Alive	111.61	High
TCGA-AO-A03L	2442	Alive	112.77	High
TCGA-LL-A440	759	Alive	113.01	High
TCGA-AR-A2LJ	2632	Alive	113.72	High
TCGA-LL-A6FR	489	Alive	113.97	High
TCGA-AC-A3HN	496	Alive	114.29	High
TCGA-B6-A40C	2164	Alive	114.42	High
TCGA-BH-A1FM	1388	Dead	114.54	High
TCGA-A8-A09A	304	Alive	114.64	High
TCGA-BH-A0BR	2330	Alive	115.02	High
TCGA-AC-A3YI	707	Alive	115.38	High
TCGA-AC-A2FF	2759	Alive	115.62	High

TCGA-A8-A08Z	1217	Alive	115.86	High
TCGA-E2-A1IF	1138	Alive	115.94	High
TCGA-BH-A0DI	912	Alive	116.6	High
TCGA-EW-A6SC	952	Alive	116.71	High
TCGA-A8-A07R	273	Alive	116.75	High
TCGA-AN-A0FV	10	Alive	116.75	High
TCGA-D8-A1XB	552	Alive	117.06	High
TCGA-C8-A12Y	1476	Alive	117.37	High
TCGA-C8-A134	383	Alive	117.75	High
TCGA-BH-A0BM	1876	Alive	118.47	High
TCGA-D8-A27M	410	Alive	118.84	High
TCGA-MS-A51U	681	Alive	119.46	High
TCGA-A7-A0DA	1085	Alive	119.48	High
TCGA-AC-A3W7	471	Alive	119.57	High
TCGA-BH-A0W7	1363	Alive	119.57	High
TCGA-BH-A1FE	2273	Dead	119.59	High
TCGA-A2-A3XX	1439	Dead	119.61	High
TCGA-D8-A1JJ	611	Alive	120.01	High
TCGA-BH-A201	856	Alive	120.29	High
TCGA-OL-A5RY	752	Alive	120.29	High
TCGA-JL-A3YW	360	Alive	120.68	High
TCGA-AR-A1AU	2868	Alive	120.83	High
TCGA-A8-A07G	577	Alive	121.22	High
TCGA-LD-A66U	646	Alive	121.35	High
TCGA-D8-A3Z6	563	Alive	121.89	High
TCGA-A2-A0CP	2813	Alive	122.65	High
TCGA-BH-A0BC	974	Alive	122.89	High
TCGA-D8-A1JU	447	Alive	123.09	High
TCGA-D8-A27N	519	Alive	123.15	High
TCGA-B6-A0WY	3461	Dead	123.88	High
TCGA-AO-A03N	2031	Alive	124.19	High
TCGA-GM-A2DA	6593	Dead	124.86	High
TCGA-AC-A3W5	504	Alive	125.05	High
TCGA-BH-A28O	1120	Alive	125.4	High
TCGA-A2-A4S1	820	Alive	125.93	High
TCGA-A1-A0SI	635	Alive	127.13	High
TCGA-A2-A25A	3276	Alive	127.49	High
TCGA-BH-A2L8	612	Alive	127.78	High
TCGA-AN-A0XN	10	Alive	129.02	High
TCGA-S3-AA14	529	Alive	129.61	High

TCGA-BH-A1FH	1034	Dead	131.59	High
TCGA-BH-A0BQ	2255	Alive	135.8	High
TCGA-GM-A2DD	2282	Alive	137.74	High
TCGA-LL-A73Z	227	Dead	137.74	High
TCGA-A7-A6VW	285	Alive	138.52	High
TCGA-AO-A0J4	1587	Alive	138.68	High
TCGA-EW-A1PD	424	Alive	138.75	High
TCGA-AN-A0FD	196	Alive	139.23	High
TCGA-AO-A1KT	541	Alive	140.71	High
TCGA-AO-A12C	2372	Alive	141	High
TCGA-E2-A1IO	1855	Alive	142.01	High
TCGA-AC-A3QP	675	Alive	142.53	High
TCGA-A1-A0SH	1437	Alive	142.66	High
TCGA-E2-A1LI	3121	Alive	142.73	High
TCGA-AN-A0AL	227	Alive	142.91	High
TCGA-AC-A2QI	588	Alive	143.61	High
TCGA-AN-A041	7	Alive	144.09	High
TCGA-AC-A3W6	602	Alive	144.41	High
TCGA-AR-A24V	3203	Alive	144.97	High
TCGA-D8-A1JP	639	Alive	145.53	High
TCGA-A2-A0EO	2442	Alive	145.98	High
TCGA-A7-A5ZX	336	Alive	146.09	High
TCGA-LD-A9QF	323	Alive	147.82	High
TCGA-A7-A6VV	313	Alive	151.62	High
TCGA-AC-A23G	2248	Alive	151.89	High
TCGA-E9-A22A	1189	Alive	155.46	High
TCGA-S3-AA15	525	Alive	155.53	High
TCGA-D8-A27I	439	Alive	156.51	High
TCGA-E9-A3X8	926	Alive	157.38	High
TCGA-BH-A0DQ	98	Alive	160.6	High
TCGA-OL-A5S0	620	Alive	162.72	High
TCGA-A7-A5ZW	326	Alive	164.38	High
TCGA-A2-A3KC	1102	Alive	164.39	High
TCGA-LL-A73Y	477	Alive	165.41	High
TCGA-E2-A15L	626	Alive	166.84	High
TCGA-5L-AAT0	1477	Alive	167.77	High
TCGA-HN-A2OB	1900	Dead	168.17	High
TCGA-GM-A2DF	2155	Alive	170.18	High
TCGA-E9-A22E	1269	Alive	171.1	High
TCGA-A7-A4SE	644	Alive	171.28	High

TCGA-EW-A2FR	1673	Alive	174.57	High
TCGA-A2-A3XU	912	Dead	181.72	High
TCGA-OL-A5RW	1106	Alive	183.32	High
TCGA-E9-A5FL	24	Alive	183.46	High
TCGA-B6-A0I6	991	Dead	184.01	High
TCGA-EW-A1OW	694	Alive	185.24	High
TCGA-BH-A0AZ	1919	Alive	186.39	High
TCGA-AN-A04A	90	Alive	186.97	High
TCGA-D8-A27H	397	Alive	187.97	High
TCGA-A8-A06R	547	Alive	188.31	High
TCGA-E2-A158	450	Alive	190.22	High
TCGA-AR-A24T	3202	Alive	192.61	High
TCGA-AN-A0FN	218	Alive	214.77	High
TCGA-EW-A1PH	607	Alive	216.86	High
TCGA-A2-A0D0	2048	Alive	221.99	High
TCGA-E2-A1LH	3247	Alive	222.27	High
TCGA-A7-A6VY	266	Alive	234.52	High
TCGA-AC-A2QJ	446	Dead	236.64	High
TCGA-A2-A4RX	742	Alive	252.68	High
TCGA-AR-A24Q	3172	Alive	279.48	High
TCGA-AR-A2LR	1742	Alive	280.14	High
TCGA-AN-A0FX	10	Alive	289	High
TCGA-AC-A2QH	1005	Alive	319.87	High
TCGA-B6-A400	215	Alive	322.94	High
TCGA-EW-A3U0	532	Alive	342.43	High
TCGA-BH-A208	1759	Dead	344.26	High
TCGA-BH-A0AV	1820	Alive	348.56	High
TCGA-E2-A574	1179	Alive	370.93	High
TCGA-E2-A1LK	266	Dead	380.32	High
TCGA-OL-A66I	714	Alive	471.15	High
TCGA-BH-A6R9	160	Alive	567.18	High
TCGA-BH-A1F0	785	Dead	673.19	High
TCGA-AC-A6IW	413	Alive	1947.86	High

Patient	Days	Status	FOXM1 Expression	Group
TCGA-E9-A1R3	78	Alive	10.61	Low
TCGA-A2-A1G6	501	Alive	47.79	Low
TCGA-A2-A0CV	3011	Alive	48.44	Low
TCGA-D8-A1JU	447	Alive	51.31	Low
TCGA-E2-A1BC	501	Alive	53.08	Low
TCGA-BH-A0BM	1876	Alive	61.36	Low
TCGA-GM-A5PX	551	Alive	64.7	Low
TCGA-D8-A1XY	503	Alive	65.81	Low
TCGA-GM-A2DC	2535	Alive	66.75	Low
TCGA-WT-AB44	883	Alive	67.17	Low
TCGA-B6-A0RQ	4267	Dead	67.87	Low
TCGA-AC-A2FK	2650	Alive	67.9	Low
TCGA-GI-A2C8	225	Alive	73.8	Low
TCGA-AR-A2LN	1161	Alive	74.57	Low
TCGA-B6-A0IH	3418	Dead	76.78	Low
TCGA-E2-A14U	1318	Alive	79.51	Low
TCGA-AC-A2QI	588	Alive	83.98	Low
TCGA-EW-A1PG	1051	Alive	86.09	Low
TCGA-E9-A3Q9	1001	Alive	88.34	Low
TCGA-A7-A5ZX	336	Alive	89.42	Low
TCGA-AO-A1KO	622	Alive	92.31	Low
TCGA-AR-A2LM	1935	Alive	93.21	Low
TCGA-GM-A3XG	1330	Alive	95.92	Low
TCGA-A2-A0D3	1873	Alive	103.52	Low
TCGA-HN-A2OB	1900	Dead	103.75	Low
TCGA-W8-A86G	347	Alive	106.1	Low
TCGA-BH-A0EA	991	Dead	108.31	Low
TCGA-E2-A15I	1692	Alive	109.67	Low
TCGA-A2-A0T6	575	Alive	112.91	Low
TCGA-E2-A1B4	1004	Dead	116.59	Low
TCGA-BH-A28O	1120	Alive	118.05	Low
TCGA-EW-A1J2	403	Alive	120.79	Low
TCGA-B6-A0RN	8008	Alive	123.15	Low
TCGA-GM-A5PV	412	Alive	127.17	Low
TCGA-BH-A0BO	2197	Alive	128.46	Low
TCGA-5L-AAT0	1477	Alive	129.16	Low
TCGA-AR-A0TR	160	Dead	129.66	Low
TCGA-A7-A5ZW	326	Alive	130.03	Low

TCGA-BH-A8G0	662	Alive	132.42	Low
TCGA-BH-A0DO	1644	Alive	132.71	Low
TCGA-A2-A0CP	2813	Alive	134.18	Low
TCGA-Z7-A8R5	3287	Alive	136.02	Low
TCGA-5L-AAT1	1471	Alive	137.95	Low
TCGA-BH-A28Q	1119	Alive	142.71	Low
TCGA-A2-A0EX	752	Alive	143.3	Low
TCGA-E9-A3X8	926	Alive	143.4	Low
TCGA-BH-A0BP	2296	Dead	145.75	Low
TCGA-A2-A259	1596	Alive	148.1	Low
TCGA-BH-A18S	2009	Dead	149.73	Low
TCGA-A2-A0CO	3492	Dead	152.63	Low
TCGA-OL-A5RX	878	Alive	153.54	Low
TCGA-BH-A1FH	1034	Dead	157.03	Low
TCGA-BH-A1ET	2520	Dead	158.61	Low
TCGA-OL-A66N	792	Alive	159.93	Low
TCGA-A2-A0YI	1505	Alive	160.63	Low
TCGA-AR-A1AM	2991	Alive	161.39	Low
TCGA-LL-A6FP	677	Alive	165.02	Low
TCGA-BH-A0DV	2064	Alive	166.93	Low
TCGA-A8-A07J	365	Alive	167.43	Low
TCGA-BH-A42U	3364	Alive	167.89	Low
TCGA-AC-A3YI	707	Alive	169.38	Low
TCGA-GM-A4E0	2191	Alive	169.46	Low
TCGA-AC-A3QP	675	Alive	171.13	Low
TCGA-E2-A15D	526	Alive	172.7	Low
TCGA-A2-A0ES	2190	Alive	176.7	Low
TCGA-A2-A0CZ	1616	Alive	178.7	Low
TCGA-E9-A1NH	576	Alive	180.28	Low
TCGA-E2-A15P	595	Alive	180.46	Low
TCGA-BH-A0H6	747	Alive	180.95	Low
TCGA-D8-A4Z1	659	Alive	183.52	Low
TCGA-E2-A3DX	1325	Alive	188.18	Low
TCGA-GM-A2DM	3226	Alive	192.16	Low
TCGA-GM-A2DI	2590	Alive	193.02	Low
TCGA-AC-A2FO	2255	Alive	193.49	Low
TCGA-BH-A0H3	1928	Alive	193.5	Low
TCGA-AR-A24W	1550	Alive	193.79	Low
TCGA-D8-A3Z5	1015	Alive	194.74	Low
TCGA-BH-A0DS	78	Alive	195.34	Low

TCGA-OL-A66L	1301	Alive	196.18	Low
TCGA-AC-A5XS	588	Alive	196.77	Low
TCGA-A7-A0D9	1139	Alive	202.57	Low
TCGA-AC-A2FG	1853	Alive	203	Low
TCGA-BH-A1FB	3669	Dead	203.2	Low
TCGA-D8-A73U	492	Alive	203.97	Low
TCGA-AR-A24V	3203	Alive	205.57	Low
TCGA-BH-A42V	635	Alive	207.7	Low
TCGA-D8-A1JB	1688	Alive	208.56	Low
TCGA-AC-A3W7	471	Alive	209.21	Low
TCGA-E2-A572	1208	Alive	210.06	Low
TCGA-D8-A1JH	426	Alive	210.7	Low
TCGA-BH-A0AZ	1919	Alive	211.69	Low
TCGA-GM-A2DK	2645	Alive	213.13	Low
TCGA-E2-A153	707	Alive	216.66	Low
TCGA-A8-A0A6	640	Alive	216.91	Low
TCGA-D8-A27L	499	Alive	217.62	Low
TCGA-AC-A3TN	456	Alive	219.23	Low
TCGA-D8-A1JN	620	Alive	220.3	Low
TCGA-V7-A7HQ	2033	Alive	222.69	Low
TCGA-E2-A15C	694	Alive	223.42	Low
TCGA-A7-A0DC	906	Alive	224.3	Low
TCGA-A2-A4S0	706	Alive	224.44	Low
TCGA-BH-A1EU	1286	Dead	226.7	Low
TCGA-A2-A4RY	648	Alive	226.92	Low
TCGA-E9-A5FK	812	Alive	227.35	Low
TCGA-AC-A3BB	987	Alive	229.49	Low
TCGA-OL-A5RU	1219	Alive	232.41	Low
TCGA-B6-A1KI	2236	Alive	232.95	Low
TCGA-B6-A0RO	4929	Alive	233.07	Low
TCGA-BH-A0W5	1288	Alive	234.06	Low
TCGA-D8-A1X5	565	Alive	234.55	Low
TCGA-OL-A6VR	1220	Alive	236.24	Low
TCGA-A8-A06P	396	Alive	236.5	Low
TCGA-C8-A12N	358	Alive	237.44	Low
TCGA-B6-A0X4	860	Dead	238.28	Low
TCGA-AQ-A0Y5	172	Dead	239.76	Low
TCGA-GM-A3NY	1162	Alive	240.13	Low
TCGA-GM-A2D9	1812	Dead	241.74	Low
TCGA-A7-A13G	718	Alive	242.34	Low

TCGA-AR-A24T	3202	Alive	243.51	Low
TCGA-A7-A13H	899	Alive	245.03	Low
TCGA-BH-A0B6	2483	Alive	245.74	Low
TCGA-AQ-A1H2	475	Alive	247.4	Low
TCGA-E2-A1B5	984	Alive	248.16	Low
TCGA-AO-A0JF	1980	Alive	248.25	Low
TCGA-D8-A27V	381	Alive	249.03	Low
TCGA-A8-A06R	547	Alive	249.72	Low
TCGA-OL-A6VQ	600	Alive	249.74	Low
TCGA-A2-A0EW	1884	Dead	256.02	Low
TCGA-BH-A1EY	538	Dead	257.67	Low
TCGA-OL-A66K	1275	Dead	260.18	Low
TCGA-E2-A1IJ	865	Alive	260.64	Low
TCGA-BH-A1F5	2712	Dead	262.54	Low
TCGA-D8-A146	643	Alive	263.13	Low
TCGA-BH-A8FZ	574	Alive	263.37	Low
TCGA-E2-A106	2541	Alive	264.69	Low
TCGA-OL-A66J	1996	Alive	270.28	Low
TCGA-AC-A62Y	530	Alive	272.15	Low
TCGA-AQ-A54O	1001	Alive	272.38	Low
TCGA-MS-A51U	681	Alive	274.47	Low
TCGA-EW-A3E8	1035	Alive	275.14	Low
TCGA-BH-A0DQ	98	Alive	281.57	Low
TCGA-A8-A08Z	1217	Alive	282.37	Low
TCGA-BH-A0HN	516	Alive	282.85	Low
TCGA-LL-A440	759	Alive	283.51	Low
TCGA-D8-A27K	1461	Alive	283.66	Low
TCGA-AR-A2LE	5062	Alive	286.83	Low
TCGA-A2-A0EN	4088	Alive	286.9	Low
TCGA-E2-A1IL	118	Alive	287.3	Low
TCGA-A7-A0CH	1079	Alive	288.57	Low
TCGA-A8-A08C	881	Alive	288.86	Low
TCGA-A2-A0EM	3094	Alive	290.63	Low
TCGA-D8-A1XO	1682	Alive	291.79	Low
TCGA-A2-A4S1	820	Alive	296.08	Low
TCGA-A2-A04N	4354	Alive	297.14	Low
TCGA-A8-A07G	577	Alive	297.25	Low
TCGA-A2-A0YD	769	Alive	298.3	Low
TCGA-C8-A1HI	343	Alive	298.92	Low
TCGA-D8-A145	410	Alive	300.11	Low

TCGA-AC-A2B8	677	Alive	301.47	Low
TCGA-D8-A1XU	395	Alive	302.05	Low
TCGA-A2-A4S2	643	Alive	304.79	Low
TCGA-BH-A1FG	3736	Dead	307.04	Low
TCGA-AN-A0XS	10	Alive	308.52	Low
TCGA-A2-A0YK	588	Alive	311.37	Low
TCGA-AN-A0FS	210	Alive	312.44	Low
TCGA-E9-A1R4	186	Alive	312.84	Low
TCGA-BH-A0HQ	1121	Alive	313.19	Low
TCGA-A2-A0EO	2442	Alive	313.43	Low
TCGA-E9-A1R5	92	Alive	313.51	Low
TCGA-BH-A0DT	2403	Alive	315.5	Low
TCGA-E2-A156	726	Alive	318.68	Low
TCGA-BH-A6R8	293	Alive	319.59	Low
TCGA-BH-A0BQ	2255	Alive	319.62	Low
TCGA-BH-A1EV	365	Dead	320.97	Low
TCGA-BH-A0E9	2489	Alive	321.33	Low
TCGA-AN-A0FT	214	Alive	323	Low
TCGA-AC-A8OS	70	Alive	323.71	Low
TCGA-BH-A0DH	1156	Alive	324.79	Low
TCGA-LL-A50Y	762	Alive	325.55	Low
TCGA-AR-A2LQ	1233	Alive	327.53	Low
TCGA-A7-A0DB	1007	Alive	328.01	Low
TCGA-EW-A1P1	1210	Alive	330.03	Low
TCGA-AC-A23E	698	Alive	334.15	Low
TCGA-AC-A8OR	40	Alive	334.29	Low
TCGA-PL-A8LX	5	Alive	334.43	Low
TCGA-D8-A27P	49	Alive	336.04	Low
TCGA-BH-A0DP	476	Alive	337.07	Low
TCGA-BH-A0BJ	660	Alive	337.26	Low
TCGA-OL-A5RV	1062	Alive	337.99	Low
TCGA-AN-A0XP	9	Alive	339.95	Low
TCGA-B6-A401	2596	Alive	340.65	Low
TCGA-AC-A2FB	1234	Alive	342.71	Low
TCGA-B6-A0I5	8556	Alive	344.47	Low
TCGA-E9-A24A	747	Alive	344.52	Low
TCGA-D8-A1XM	538	Alive	344.58	Low
TCGA-AN-A0XT	10	Alive	346.31	Low
TCGA-A8-A08T	3409	Dead	346.99	Low
TCGA-BH-A0HI	620	Alive	347.1	Low

TCGA-BH-A6R9	160	Alive	347.69	Low
TCGA-AO-A12C	2372	Alive	352.54	Low
TCGA-D8-A1JI	577	Alive	352.9	Low
TCGA-BH-A0EB	745	Alive	353.18	Low
TCGA-A1-A0SH	1437	Alive	353.32	Low
TCGA-LL-A9Q3	532	Alive	353.4	Low
TCGA-A8-A06Y	791	Alive	353.92	Low
TCGA-A2-A0CR	3283	Alive	354.52	Low
TCGA-BH-A0DE	2372	Alive	355.56	Low
TCGA-AN-A03X	10	Alive	355.61	Low
TCGA-BH-A18H	652	Alive	357.47	Low
TCGA-OL-A5DA	1783	Alive	357.71	Low
TCGA-AO-A03V	1351	Alive	358.24	Low
TCGA-AC-A6IV	568	Alive	359.36	Low
TCGA-BH-A0B0	2477	Alive	359.56	Low
TCGA-A2-A0EV	968	Alive	359.79	Low
TCGA-E9-A229	1148	Alive	360.01	Low
TCGA-E2-A1IU	337	Alive	361.42	Low
TCGA-A7-A26H	724	Alive	365.02	Low
TCGA-AO-A0J8	680	Alive	365.23	Low
TCGA-D8-A27I	439	Alive	365.46	Low
TCGA-D8-A1XC	377	Dead	365.63	Low
TCGA-LD-A66U	646	Alive	365.63	Low
TCGA-AC-A23G	2248	Alive	366.18	Low
TCGA-A7-A3J1	343	Alive	367.19	Low
TCGA-D8-A3Z6	563	Alive	367.33	Low
TCGA-E9-A1NG	786	Dead	370.26	Low
TCGA-D8-A141	626	Alive	370.68	Low
TCGA-AO-A12A	3112	Alive	373.95	Low
TCGA-A7-A426	364	Alive	375.62	Low
TCGA-A2-A0EP	3603	Alive	376.73	Low
TCGA-AC-A2FE	2636	Dead	378.22	Low
TCGA-WT-AB41	1611	Alive	378.75	Low
TCGA-A2-A1FZ	683	Alive	380.11	Low
TCGA-E9-A1RA	1369	Alive	380.26	Low
TCGA-BH-A1EX	1508	Dead	382	Low
TCGA-E2-A1IO	1855	Alive	384.03	Low
TCGA-LL-A5YM	466	Alive	385.23	Low
TCGA-A2-A4RW	222	Alive	385.3	Low
TCGA-E2-A1IN	675	Alive	386.69	Low

TCGA-A8-A09B	365	Alive	386.85	Low
TCGA-GM-A3NW	3361	Alive	387.35	Low
TCGA-BH-A0H5	1620	Alive	389.56	Low
TCGA-AO-A0JC	1547	Alive	389.58	Low
TCGA-BH-A0E7	1363	Alive	391.93	Low
TCGA-A2-A0CS	2348	Dead	393.46	Low
TCGA-AR-A1AL	2971	Alive	393.47	Low
TCGA-BH-A2L8	612	Alive	397.14	Low
TCGA-A2-A0T2	255	Dead	397.46	Low
TCGA-A2-A1FV	714	Alive	397.87	Low
TCGA-A8-A099	304	Alive	399.73	Low
TCGA-E2-A108	837	Alive	401.18	Low
TCGA-A8-A06T	1614	Alive	402.56	Low
TCGA-E2-A14Q	1163	Alive	404.24	Low
TCGA-BH-A0DI	912	Alive	404.96	Low
TCGA-E2-A1LB	2306	Alive	409.4	Low
TCGA-LL-A6FQ	80	Alive	412.91	Low
TCGA-A8-A091	1004	Alive	414.09	Low
TCGA-E2-A1B1	2653	Alive	414.1	Low
TCGA-A7-A26E	954	Alive	414.58	Low
TCGA-4H-AAAK	348	Alive	414.81	Low
TCGA-A7-A3IY	345	Alive	414.97	Low
TCGA-AR-A252	2838	Alive	415.27	Low
TCGA-A8-A0A2	579	Alive	415.59	Low
TCGA-AR-A5QP	1185	Alive	419.03	Low
TCGA-BH-A18N	1148	Dead	423.59	Low
TCGA-A8-A09T	579	Alive	425.5	Low
TCGA-E2-A1L8	2240	Alive	426.04	Low
TCGA-A2-A0SY	1347	Alive	426.55	Low
TCGA-E2-A1L9	598	Alive	429.43	Low
TCGA-BH-A8FY	295	Dead	430.05	Low
TCGA-LL-A740	441	Alive	430.57	Low
TCGA-BH-A0BT	2365	Alive	431.35	Low
TCGA-EW-A1J1	575	Alive	434.74	Low
TCGA-AN-A0FN	218	Alive	439.19	Low
TCGA-C8-A274	508	Alive	439.21	Low
TCGA-A8-A093	546	Alive	439.6	Low
TCGA-GM-A3XN	2019	Alive	444.09	Low
TCGA-AR-A2LJ	2632	Alive	444.97	Low
TCGA-BH-A0HO	76	Alive	446.15	Low

TCGA-AR-A1AV	1864	Alive	447.28	Low
TCGA-B6-A0RH	6456	Dead	450.09	Low
TCGA-AN-A0FD	196	Alive	451.6	Low
TCGA-S3-AA14	529	Alive	451.62	Low
TCGA-A8-A0A1	365	Alive	452.57	Low
TCGA-E2-A1LS	1604	Alive	455.91	Low
TCGA-EW-A423	533	Alive	456.6	Low
TCGA-AC-A2FF	2759	Alive	458.31	Low
TCGA-E2-A1L6	1648	Alive	459.79	Low
TCGA-BH-A0EI	1926	Alive	460.8	Low
TCGA-A8-A08A	30	Alive	464.43	Low
TCGA-E2-A570	931	Alive	465.18	Low
TCGA-A2-A25A	3276	Alive	465.86	Low
TCGA-D8-A1XG	448	Alive	466.18	Low
TCGA-E9-A227	975	Alive	466.86	Low
TCGA-E9-A2JT	288	Alive	467.13	Low
TCGA-OL-A5D6	1104	Dead	468.36	Low
TCGA-C8-A3M7	1034	Dead	469.9	Low
TCGA-E2-A1BD	1133	Alive	470.72	Low
TCGA-LL-A73Z	227	Dead	471	Low
TCGA-E9-A1RD	34	Alive	471.9	Low
TCGA-E9-A1RF	200	Alive	474.6	Low
TCGA-BH-A201	856	Alive	478.91	Low
TCGA-A8-A09V	457	Alive	484.45	Low
TCGA-PL-A8LY	8	Alive	484.58	Low
TCGA-AO-A12B	2989	Alive	485.51	Low
TCGA-A2-A0EU	1043	Alive	485.82	Low
TCGA-E2-A15J	1640	Alive	490.25	Low
TCGA-A1-A0SD	437	Alive	490.84	Low
TCGA-EW-A1P5	703	Alive	490.85	Low
TCGA-GM-A2DA	6593	Dead	492.2	Low
TCGA-BH-A208	1759	Dead	496.98	Low
TCGA-D8-A1XB	552	Alive	497.54	Low
TCGA-B6-A0WY	3461	Dead	498.7	Low
TCGA-B6-A0I8	749	Dead	499.75	Low
TCGA-BH-A18M	2207	Dead	500.06	Low
TCGA-LL-A442	889	Alive	500.78	Low
TCGA-AC-A3EH	197	Dead	503.06	Low
TCGA-A7-A56D	448	Alive	504.36	Low
TCGA-AN-A0XO	375	Alive	504.45	Low

TCGA-AR-A0TW	3009	Alive	509.51	Low
TCGA-E2-A14Z	563	Dead	509.75	Low
TCGA-BH-A0W4	759	Alive	510.25	Low
TCGA-A2-A0T7	631	Alive	515.06	Low
TCGA-BH-A5J0	715	Alive	515.45	Low
TCGA-AO-A126	3307	Alive	515.62	Low
TCGA-LL-A5YN	447	Alive	519.72	Low
TCGA-D8-A1JE	575	Alive	520.34	Low
TCGA-3C-AALK	1448	Alive	521.01	Low
TCGA-EW-A1P6	562	Alive	522.04	Low
TCGA-A7-A4SC	446	Alive	522.25	Low
TCGA-E2-A1IG	2140	Alive	524.38	Low
TCGA-BH-A0DX	2156	Alive	524.95	Low
TCGA-A8-A07P	334	Alive	525.32	Low
TCGA-AQ-A7U7	584	Dead	526.32	Low
TCGA-EW-A1PE	320	Alive	526.43	Low
TCGA-LD-A7W5	216	Alive	527.11	Low
TCGA-BH-A0HA	1611	Alive	527.13	Low
TCGA-XX-A899	467	Alive	530.5	Low
TCGA-A2-A3XV	996	Alive	531.34	Low
TCGA-AN-A0XN	10	Alive	531.87	Low
TCGA-AC-A3HN	496	Alive	531.92	Low
TCGA-A7-A0CD	1165	Alive	535.63	Low
TCGA-E2-A15E	630	Alive	537.52	Low
TCGA-D8-A1X6	541	Alive	538.41	Low
TCGA-AN-A0FV	10	Alive	538.97	Low
TCGA-E9-A54X	727	Alive	539.67	Low
TCGA-A2-A3XW	1712	Alive	542.81	Low
TCGA-B6-A2IU	5176	Alive	544.4	Low
TCGA-D8-A73W	385	Dead	545.2	Low
TCGA-A2-A0ET	1066	Alive	546.71	Low
TCGA-LD-A9QF	323	Alive	547.4	Low
TCGA-B6-A0RM	2373	Dead	547.56	Low
TCGA-A1-A0SF	1463	Alive	549.23	Low
TCGA-AC-A5EH	511	Alive	550.21	Low
TCGA-BH-AB28	287	Alive	551.5	Low
TCGA-AR-A2LL	2012	Alive	552.96	Low
TCGA-EW-A6SC	952	Alive	553.39	Low
TCGA-A8-A085	1124	Alive	553.72	Low
TCGA-AR-A2LH	616	Dead	554.13	Low

TCGA-AC-A3QQ	734	Alive	556.9	Low
TCGA-A2-A4RX	742	Alive	557.15	Low
TCGA-EW-A2FR	1673	Alive	558.09	Low
TCGA-AO-A0JB	1542	Alive	560	Low
TCGA-BH-A0DG	2041	Alive	563.42	Low
TCGA-A2-A0T5	531	Alive	563.61	Low
TCGA-C8-A138	380	Alive	565.04	Low
TCGA-AC-A3OD	451	Alive	566.23	Low
TCGA-C8-A12M	358	Alive	566.85	Low
TCGA-A8-A086	396	Alive	567.2	Low
TCGA-AR-A1AN	2920	Alive	567.22	Low
TCGA-E9-A22E	1269	Alive	568.01	Low
TCGA-D8-A1X8	783	Alive	568.56	Low
TCGA-BH-A0HK	178	Alive	569.64	Low
TCGA-AR-A5QN	1013	Alive	569.89	Low
TCGA-BH-A0HP	414	Alive	571.96	Low
TCGA-AN-A04A	90	Alive	573.61	Low
TCGA-AC-A2QJ	446	Dead	577.39	Low
TCGA-BH-A0BS	2612	Alive	578.24	Low
TCGA-A2-A25C	523	Alive	580.1	Low
TCGA-E2-A10F	878	Alive	581.85	Low
TCGA-AC-A3W6	602	Alive	582.32	Low
TCGA-A8-A0A7	30	Alive	583.34	Low
TCGA-EW-A1PF	439	Alive	585.18	Low
TCGA-EW-A1P7	915	Alive	589.81	Low
TCGA-OL-A66P	428	Alive	590.11	Low
TCGA-D8-A27N	519	Alive	591.31	Low
TCGA-XX-A89A	488	Alive	591.88	Low
TCGA-A2-A0YL	1474	Alive	592.15	Low
TCGA-D8-A1X9	727	Alive	592.94	Low
TCGA-B6-A0WT	5739	Alive	593	Low
TCGA-AO-A0JJ	1887	Alive	593.15	Low
TCGA-A2-A0YC	990	Alive	594.24	Low
TCGA-E2-A1IK	1800	Alive	596.25	Low
TCGA-D8-A1XV	461	Alive	597.45	Low
TCGA-BH-A0W7	1363	Alive	597.87	Low
TCGA-AC-A8OP	614	Alive	600.31	Low
TCGA-A7-A3RF	408	Alive	601.87	Low
TCGA-LL-A5YL	519	Alive	602.47	Low
TCGA-E9-A295	375	Alive	603.21	Low

TCGA-EW-A2FS	1604	Alive	604.05	Low
TCGA-AR-A5QM	2231	Alive	604.33	Low
TCGA-E9-A249	217	Alive	609.03	Low
TCGA-AQ-A1H3	989	Alive	609.15	Low
TCGA-EW-A6SD	1010	Alive	610	Low
TCGA-AN-A0AS	10	Alive	610.35	Low
TCGA-E9-A1R0	860	Alive	610.45	Low
TCGA-D8-A1JA	502	Alive	610.88	Low
TCGA-AN-A0FZ	10	Alive	613.73	Low
TCGA-A8-A09A	304	Alive	614.93	Low
TCGA-AN-A0XL	163	Alive	617.72	Low
TCGA-BH-A0GZ	328	Alive	621.06	Low
TCGA-E9-A5UO	785	Alive	623.76	Low
TCGA-EW-A1OX	911	Alive	625.65	Low
TCGA-AN-A041	7	Alive	626.93	Low
TCGA-C8-A1HE	375	Alive	627.13	Low
TCGA-BH-A18G	149	Alive	627.43	Low
TCGA-D8-A27T	398	Alive	630.26	Low
TCGA-E2-A1IF	1138	Alive	632.97	Low
TCGA-OL-A5D8	973	Alive	633.07	Low
TCGA-A8-A09Q	761	Alive	633.21	Low
TCGA-BH-A0B7	2559	Alive	634.31	Low
TCGA-A8-A09D	1522	Alive	634.88	Low
TCGA-BH-A0H7	702	Alive	636.49	Low
TCGA-BH-A0AY	777	Alive	636.89	Low
TCGA-AO-A12D	2515	Alive	641.28	Low
TCGA-S3-AA11	421	Alive	641.33	Low
TCGA-E9-A1R2	1063	Alive	645	Low
TCGA-A2-A0CT	2289	Alive	647.68	Low
TCGA-EW-A1J6	875	Alive	648.98	Low
TCGA-AC-A6NO	51	Alive	649.19	Low
TCGA-AC-A23C	585	Alive	649.79	Low
TCGA-AQ-A04L	3957	Alive	653.49	Low
TCGA-AN-A0XV	162	Alive	653.77	Low
TCGA-A8-A08O	943	Alive	658.12	Low
TCGA-AN-A0FL	231	Alive	662.27	Low
TCGA-D8-A1XW	1309	Alive	664.77	Low
TCGA-EW-A1PD	424	Alive	664.86	Low
TCGA-D8-A1Y2	433	Alive	666.1	Low
TCGA-BH-A0H9	1247	Alive	669.15	Low

TCGA-GM-A2DN	3091	Alive	670.13	Low
TCGA-AR-A1AS	1150	Alive	670.19	Low
TCGA-D8-A1XQ	499	Alive	670.7	Low
TCGA-A1-A0SQ	554	Alive	670.72	Low
TCGA-E9-A1RE	1419	Alive	670.77	Low
TCGA-PE-A5DE	2645	Alive	672.1	Low
TCGA-LL-A6FR	489	Alive	673.02	Low
TCGA-A2-A0YF	1535	Alive	673.49	Low
TCGA-S3-AA12	574	Alive	673.52	Low
TCGA-D8-A140	403	Alive	676.65	Low
TCGA-A8-A097	365	Alive	679.38	Low
TCGA-D8-A1XA	839	Alive	679.48	Low
TCGA-E2-A1IH	1026	Alive	680.89	Low
TCGA-D8-A1XD	522	Alive	682.29	Low
TCGA-BH-A0GY	923	Alive	684.4	Low
TCGA-A7-A4SA	454	Alive	684.54	Low
TCGA-A2-A0SU	1662	Alive	684.59	Low
TCGA-OL-A66H	812	Alive	687.8	Low
TCGA-A8-A09K	912	Alive	689.27	Low
TCGA-A2-A0CK	4159	Alive	691.62	Low
TCGA-E2-A10B	1141	Alive	695.82	Low
TCGA-BH-A18I	1093	Alive	697.16	Low
TCGA-B6-A0WS	2965	Dead	699.65	Low
TCGA-AO-A0JE	2335	Alive	699.66	Low
TCGA-A8-A07F	577	Alive	706.16	Low
TCGA-EW-A1IZ	554	Alive	706.71	Low
TCGA-BH-A0HB	806	Alive	706.8	Low
TCGA-EW-A1J3	504	Alive	708.11	Low
TCGA-B6-A0IP	3926	Dead	708.56	Low
TCGA-EW-A424	715	Alive	711.46	Low
TCGA-AR-A1AW	2632	Alive	711.95	Low
TCGA-BH-A1FL	1673	Dead	714.88	Low
TCGA-AR-A255	2161	Alive	716.79	Low
TCGA-B6-A0RI	7126	Alive	717.14	Low
TCGA-C8-A132	383	Alive	718.07	Low
TCGA-A2-A0CQ	2695	Alive	719.79	Low
TCGA-AR-A254	2605	Alive	720.57	Low
TCGA-C8-A12Y	1476	Alive	724.4	Low
TCGA-E2-A154	591	Alive	727.55	Low
TCGA-A2-A3KC	1102	Alive	729.84	Low

TCGA-JL-A3YW	360	Alive	731.15	Low
TCGA-E9-A5FL	24	Alive	732.36	Low
TCGA-E2-A56Z	252	Alive	735.84	Low
TCGA-EW-A1IY	258	Alive	736.28	Low
TCGA-BH-A1FU	1688	Dead	736.29	Low
TCGA-E9-A245	26	Alive	738.24	Low
TCGA-A8-A0A4	396	Alive	744.17	Low
TCGA-AR-A1AX	2629	Alive	746.88	Low
TCGA-A1-A0SM	242	Alive	751.48	Low
TCGA-D8-A27G	409	Alive	755.17	Low
TCGA-BH-A0HF	727	Alive	756.72	Low
TCGA-AR-A0TZ	3262	Dead	759.02	Low
TCGA-A8-A09R	273	Alive	761.22	Low
TCGA-AQ-A54N	78	Alive	761.41	Low
TCGA-A2-A3KD	1206	Alive	762.33	Low
TCGA-D8-A1JF	366	Alive	762.75	Low
TCGA-E2-A14T	2311	Alive	763.42	Low
TCGA-BH-A0AW	622	Alive	763.58	Low
TCGA-AR-A24U	3128	Alive	764.69	Low
TCGA-AC-A2BM	3022	Alive	765.8	Low
TCGA-A1-A0SI	635	Alive	768.96	Low
TCGA-AR-A1AO	2618	Alive	770.29	Low
TCGA-E2-A10A	1229	Alive	770.86	Low
TCGA-B6-A0WZ	6292	Alive	771.09	Low
TCGA-C8-A12Q	385	Dead	772.38	Low
TCGA-D8-A1XR	482	Alive	773.29	High
TCGA-AR-A1AP	2856	Alive	774.95	High
TCGA-AC-A3TM	762	Alive	777.08	High
TCGA-AN-A046	10	Alive	779	High
TCGA-AC-A2FM	792	Dead	779.03	High
TCGA-E9-A6HE	847	Alive	782.86	High
TCGA-AR-A0TT	3316	Alive	783.61	High
TCGA-AN-A0FK	213	Alive	787.1	High
TCGA-AR-A24P	84	Alive	789.16	High
TCGA-BH-A0DK	423	Alive	790.14	High
TCGA-A8-A06U	883	Dead	791.71	High
TCGA-A8-A0AB	518	Alive	793.81	High
TCGA-E2-A10E	865	Alive	798.12	High
TCGA-OL-A5RY	752	Alive	799.27	High
TCGA-EW-A6SA	510	Alive	805.31	High

TCGA-BH-A0BV	1519	Alive	811.63	High
TCGA-BH-A0B4	1191	Alive	818.61	High
TCGA-PE-A5DD	1953	Alive	820.37	High
TCGA-A8-A0A9	822	Alive	820.93	High
TCGA-AC-A6IX	373	Alive	822.47	High
TCGA-BH-A1F2	959	Dead	826.51	High
TCGA-A8-A09M	1006	Alive	828.35	High
TCGA-BH-A0BF	1324	Dead	831.55	High
TCGA-AO-A0J9	1613	Alive	831.64	High
TCGA-A2-A0CU	158	Dead	831.7	High
TCGA-E2-A576	1043	Alive	833.6	High
TCGA-BH-A0HW	1561	Alive	833.87	High
TCGA-E9-A54Y	725	Alive	836.03	High
TCGA-E9-A1R6	339	Alive	838.51	High
TCGA-D8-A1J9	532	Alive	838.71	High
TCGA-GM-A2DO	2596	Alive	839.65	High
TCGA-EW-A1J5	477	Alive	839.82	High
TCGA-AR-A24K	1548	Alive	840.55	High
TCGA-E2-A1LK	266	Dead	840.72	High
TCGA-BH-A0C1	1411	Dead	843.47	High
TCGA-AC-A23H	174	Dead	843.52	High
TCGA-AC-A4ZE	890	Alive	844.83	High
TCGA-E9-A226	1048	Dead	844.97	High
TCGA-B6-A40B	3152	Alive	845.89	High
TCGA-EW-A1P3	1611	Alive	850.76	High
TCGA-BH-A1ES	3462	Dead	858.43	High
TCGA-AR-A2LO	1198	Alive	860.3	High
TCGA-BH-A1EN	2127	Dead	866.04	High
TCGA-BH-A18J	612	Dead	868.53	High
TCGA-A2-A0EY	1925	Alive	869.26	High
TCGA-AR-A0TX	1972	Alive	871.59	High
TCGA-B6-A409	573	Dead	876.1	High
TCGA-A2-A04P	548	Dead	878.66	High
TCGA-C8-A3M8	394	Alive	883.31	High
TCGA-C8-A278	297	Alive	883.39	High
TCGA-BH-A0HX	829	Alive	884.49	High
TCGA-A7-A2KD	679	Alive	884.71	High
TCGA-E2-A152	2128	Alive	886.93	High
TCGA-BH-A0B8	1569	Alive	890.5	High
TCGA-E2-A155	640	Alive	894.61	High

TCGA-B6-A0IG	4456	Dead	896.41	High
TCGA-AR-A24L	2866	Dead	897.85	High
TCGA-AR-A1AU	2868	Alive	901.45	High
TCGA-BH-A0BR	2330	Alive	901.58	High
TCGA-E9-A1R7	1467	Alive	902.68	High
TCGA-D8-A142	425	Alive	905.24	High
TCGA-AC-A3W5	504	Alive	906.71	High
TCGA-B6-A0I1	2361	Dead	912.99	High
TCGA-A2-A0T1	521	Alive	913.44	High
TCGA-AN-A049	19	Alive	914.19	High
TCGA-AO-A1KP	2953	Alive	916.61	High
TCGA-C8-A12X	385	Alive	916.79	High
TCGA-BH-A0HL	72	Alive	918.49	High
TCGA-E9-A1QZ	755	Alive	921.59	High
TCGA-E2-A2P6	1051	Alive	926.42	High
TCGA-A2-A04Y	1099	Alive	926.98	High
TCGA-E2-A105	1308	Alive	928.2	High
TCGA-LL-A73Y	477	Alive	930.33	High
TCGA-E2-A15M	336	Dead	933.45	High
TCGA-A2-A04V	1920	Dead	934.1	High
TCGA-B6-A0IO	5042	Alive	934.17	High
TCGA-AR-A1AT	1272	Dead	935.88	High
TCGA-A2-A0CY	1673	Alive	940.73	High
TCGA-C8-A26V	616	Alive	941.34	High
TCGA-AO-A03L	2442	Alive	942.08	High
TCGA-OK-A5Q2	64	Alive	942.32	High
TCGA-AR-A24N	3035	Alive	942.92	High
TCGA-A8-A095	1277	Alive	944.66	High
TCGA-BH-A18K	2763	Dead	946.89	High
TCGA-E2-A14X	972	Alive	948.23	High
TCGA-E2-A15F	658	Alive	951	High
TCGA-A8-A06Z	31	Alive	952.38	High
TCGA-AO-A03T	2124	Alive	961.04	High
TCGA-JL-A3YX	352	Alive	961.2	High
TCGA-LL-A5YO	440	Alive	961.91	High
TCGA-C8-A26Z	470	Alive	965.13	High
TCGA-EW-A1OZ	1229	Alive	965.88	High
TCGA-UL-AAZ6	518	Alive	972.32	High
TCGA-A7-A425	447	Alive	972.94	High
TCGA-AO-A0JI	1528	Alive	980.45	High

TCGA-D8-A1JP	639	Alive	981.56	High
TCGA-E2-A158	450	Alive	989.52	High
TCGA-GM-A2DD	2282	Alive	991.55	High
TCGA-A8-A09E	1492	Alive	993.3	High
TCGA-A7-A3J0	313	Alive	995.7	High
TCGA-E9-A1RH	1417	Alive	997.61	High
TCGA-BH-A0B1	1148	Alive	999.6	High
TCGA-A8-A08B	1156	Alive	1003.66	High
TCGA-E2-A15T	1563	Alive	1008.35	High
TCGA-AR-A250	2707	Alive	1011.1	High
TCGA-A8-A07B	1308	Alive	1019.67	High
TCGA-D8-A1JJ	611	Alive	1020.2	High
TCGA-C8-A8HR	408	Alive	1023.27	High
TCGA-E2-A10C	1220	Alive	1025.69	High
TCGA-AC-A5XU	455	Alive	1026.8	High
TCGA-AR-A1AK	3159	Alive	1029.22	High
TCGA-BH-A0E6	293	Alive	1036.85	High
TCGA-A8-A06Q	31	Alive	1038.15	High
TCGA-BH-A1F0	785	Dead	1038.56	High
TCGA-D8-A1XT	506	Alive	1047.66	High
TCGA-E9-A1NE	1088	Alive	1049.04	High
TCGA-E2-A15L	626	Alive	1060.33	High
TCGA-BH-A18U	1563	Dead	1063.57	High
TCGA-A8-A09C	31	Alive	1065.06	High
TCGA-E2-A14S	1009	Alive	1068.06	High
TCGA-BH-A1FE	2273	Dead	1071.5	High
TCGA-A2-A0T0	533	Alive	1073.31	High
TCGA-BH-A0BC	974	Alive	1075.21	High
TCGA-A8-A08X	1308	Alive	1081.36	High
TCGA-GM-A2DL	3519	Alive	1082.37	High
TCGA-A8-A08L	304	Dead	1088.49	High
TCGA-AR-A24S	2976	Alive	1088.68	High
TCGA-EW-A1IW	371	Alive	1091.04	High
TCGA-AO-A128	3248	Alive	1091.07	High
TCGA-C8-A12V	385	Alive	1098.67	High
TCGA-B6-A1KC	1326	Alive	1104.48	High
TCGA-D8-A1JG	1612	Alive	1108.47	High
TCGA-B6-A40C	2164	Alive	1115.36	High
TCGA-BH-A1EW	1694	Dead	1115.51	High
TCGA-A2-A0D4	767	Alive	1118.21	High

TCGA-C8-A273	513	Alive	1118.58	High
TCGA-A7-A3IZ	322	Alive	1123.13	High
TCGA-A2-A0CL	3015	Alive	1127.23	High
TCGA-A7-A4SB	418	Alive	1127.86	High
TCGA-C8-A8HP	396	Alive	1133.63	High
TCGA-S3-A6ZH	641	Alive	1135.28	High
TCGA-E2-A15R	1732	Alive	1136.97	High
TCGA-E9-A22H	1232	Alive	1138.22	High
TCGA-BH-A0C0	1270	Alive	1141.98	High
TCGA-EW-A6S9	463	Alive	1143.27	High
TCGA-AO-A03N	2031	Alive	1149.06	High
TCGA-A2-A25D	552	Alive	1149.72	High
TCGA-B6-A1KN	4233	Alive	1151.4	High
TCGA-C8-A135	393	Alive	1151.58	High
TCGA-A8-A076	1642	Alive	1153.95	High
TCGA-BH-A0W3	728	Alive	1154.09	High
TCGA-AC-A8OQ	34	Alive	1154.39	High
TCGA-EW-A1OV	789	Alive	1155.86	High
TCGA-A8-A06O	396	Alive	1159.48	High
TCGA-A1-A0SJ	416	Alive	1164.78	High
TCGA-AN-A0FF	172	Alive	1167.26	High
TCGA-BH-A0H0	461	Alive	1174.3	High
TCGA-A2-A1FX	1847	Alive	1175.38	High
TCGA-E2-A574	1179	Alive	1183.18	High
TCGA-B6-A0WW	558	Dead	1183.95	High
TCGA-A2-A3XZ	1532	Alive	1198.05	High
TCGA-A8-A07E	608	Alive	1207.83	High
TCGA-E2-A159	762	Alive	1208.58	High
TCGA-E2-A1LE	879	Dead	1214.8	High
TCGA-A7-A0DA	1085	Alive	1214.92	High
TCGA-BH-A1F8	763	Dead	1215.18	High
TCGA-C8-A26X	376	Alive	1215.88	High
TCGA-BH-A0HY	1545	Alive	1217.74	High
TCGA-AO-A12E	2142	Alive	1219.17	High
TCGA-AO-A0JA	655	Alive	1219.75	High
TCGA-B6-A0RG	2082	Alive	1222.94	High
TCGA-BH-A1FM	1388	Dead	1223.92	High
TCGA-BH-A0DZ	495	Alive	1224.51	High
TCGA-BH-A0RX	170	Alive	1226.13	High
TCGA-S3-AA17	424	Alive	1227.73	High

TCGA-BH-A0EE	943	Alive	1230.25	High
TCGA-A8-A084	458	Alive	1232.8	High
TCGA-AQ-A04H	754	Alive	1234.65	High
TCGA-D8-A1Y1	302	Dead	1235.02	High
TCGA-BH-A0BZ	2255	Alive	1243.19	High
TCGA-BH-A18F	1001	Alive	1243.25	High
TCGA-OL-A66O	528	Alive	1243.94	High
TCGA-EW-A1OY	908	Alive	1244.14	High
TCGA-AN-A0FW	11	Alive	1245.95	High
TCGA-BH-A18P	921	Dead	1247.35	High
TCGA-A2-A25B	1291	Alive	1248.77	High
TCGA-A2-A0CX	1728	Alive	1252.02	High
TCGA-BH-A0BW	2371	Alive	1255.5	High
TCGA-3C-AALJ	1474	Alive	1256.03	High
TCGA-D8-A1XL	606	Alive	1261.71	High
TCGA-C8-A26Y	394	Alive	1265.58	High
TCGA-A7-A26J	627	Alive	1266.99	High
TCGA-E2-A14W	974	Alive	1268.3	High
TCGA-A2-A1G4	595	Alive	1270.93	High
TCGA-B6-A0IK	571	Dead	1273.72	High
TCGA-A8-A08J	1127	Dead	1278.32	High
TCGA-C8-A131	411	Alive	1290.79	High
TCGA-A2-A3XU	912	Dead	1297.67	High
TCGA-A8-A06X	943	Dead	1302.8	High
TCGA-D8-A1XZ	466	Alive	1306.29	High
TCGA-EW-A1PH	607	Alive	1312.87	High
TCGA-3C-AAAU	4047	Alive	1313.95	High
TCGA-A8-A07Z	1371	Alive	1316.52	High
TCGA-A2-A04R	3709	Alive	1317.54	High
TCGA-GM-A2DB	2406	Alive	1319.63	High
TCGA-A8-A082	549	Alive	1322.79	High
TCGA-C8-A1HO	375	Alive	1323.03	High
TCGA-E9-A22D	1248	Alive	1323.28	High
TCGA-LL-A7T0	376	Alive	1325.4	High
TCGA-E2-A1LA	748	Alive	1330.57	High
TCGA-A8-A07I	426	Alive	1336.69	High
TCGA-A2-A0ER	2263	Alive	1342.9	High
TCGA-OL-A5S0	620	Alive	1343.88	High
TCGA-E2-A1IE	2362	Alive	1356.66	High
TCGA-BH-A202	795	Alive	1359.67	High

TCGA-BH-A204	2534	Dead	1361.88	High
TCGA-A8-A08I	365	Alive	1365.1	High
TCGA-A2-A0T4	624	Alive	1372.94	High
TCGA-A7-A0CJ	931	Alive	1381.99	High
TCGA-AR-A251	3030	Alive	1384.5	High
TCGA-AN-A0XR	10	Alive	1386.73	High
TCGA-A7-A6VX	317	Alive	1388.45	High
TCGA-E9-A248	59	Alive	1391.09	High
TCGA-LQ-A4E4	849	Alive	1393.62	High
TCGA-AR-A0U0	1988	Alive	1393.85	High
TCGA-B6-A0RS	3063	Dead	1421.36	High
TCGA-A8-A09W	30	Alive	1428.69	High
TCGA-E2-A15H	393	Alive	1428.69	High
TCGA-AR-A1AR	524	Dead	1433.06	High
TCGA-AC-A62V	348	Dead	1435.61	High
TCGA-C8-A12O	385	Alive	1455.4	High
TCGA-A2-A0SX	1534	Alive	1455.64	High
TCGA-E2-A14O	1359	Alive	1456.75	High
TCGA-A8-A08G	607	Alive	1458.55	High
TCGA-B6-A0WV	2417	Dead	1462.15	High
TCGA-LL-A7SZ	594	Alive	1462.24	High
TCGA-C8-A12Z	382	Alive	1465	High
TCGA-A2-A1FW	528	Alive	1475.34	High
TCGA-E2-A15K	275	Alive	1479.54	High
TCGA-S3-A6ZF	572	Alive	1485.34	High
TCGA-A8-A08P	943	Alive	1488.14	High
TCGA-AR-A2LK	1649	Dead	1491.73	High
TCGA-AN-A03Y	10	Alive	1494.07	High
TCGA-A2-A0SW	1365	Dead	1494.42	High
TCGA-E2-A1B0	1631	Alive	1495.05	High
TCGA-AO-A0JL	1683	Alive	1495.09	High
TCGA-D8-A1JC	480	Alive	1495.37	High
TCGA-AN-A0XW	170	Alive	1498.86	High
TCGA-C8-A137	379	Alive	1501.24	High
TCGA-E9-A1RG	647	Alive	1502.12	High
TCGA-AR-A24R	3430	Alive	1502.48	High
TCGA-BH-A1FJ	1927	Dead	1506.5	High
TCGA-E9-A1N6	678	Dead	1507.2	High
TCGA-AO-A03M	1866	Alive	1507.37	High
TCGA-E9-A228	1285	Alive	1515.96	High

TCGA-E2-A15O	1545	Alive	1519.65	High
TCGA-A8-A08S	1004	Alive	1522.47	High
TCGA-D8-A1JD	552	Alive	1525.47	High
TCGA-B6-A0I9	362	Dead	1525.54	High
TCGA-BH-A1FD	1009	Dead	1530.68	High
TCGA-A2-A3XS	1032	Dead	1537.21	High
TCGA-BH-A1FN	2192	Dead	1543.16	High
TCGA-B6-A0IB	3941	Dead	1546.69	High
TCGA-A2-A04X	1686	Alive	1548.05	High
TCGA-A2-A0YT	723	Dead	1562.04	High
TCGA-A2-A0SV	825	Dead	1564.89	High
TCGA-E2-A1LH	3247	Alive	1565.62	High
TCGA-E9-A22A	1189	Alive	1566.13	High
TCGA-A8-A07W	304	Alive	1567.27	High
TCGA-BH-A0AU	1914	Alive	1569.83	High
TCGA-PL-A8LZ	302	Alive	1572.31	High
TCGA-D8-A27H	397	Alive	1574.16	High
TCGA-C8-A1HG	345	Alive	1579.26	High
TCGA-A8-A08F	1004	Alive	1580.21	High
TCGA-BH-A0C7	2767	Alive	1584.55	High
TCGA-C8-A26W	381	Alive	1585.31	High
TCGA-D8-A1Y0	472	Alive	1596.54	High
TCGA-A8-A075	518	Alive	1598.33	High
TCGA-AC-A7VC	1	Alive	1605.82	High
TCGA-BH-A0E2	435	Alive	1606.62	High
TCGA-3C-AALI	4005	Alive	1608.33	High
TCGA-A2-A0YG	666	Alive	1633.09	High
TCGA-A7-A26I	661	Alive	1639.07	High
TCGA-C8-A1HK	366	Alive	1640.09	High
TCGA-BH-A0BG	1871	Alive	1640.45	High
TCGA-AO-A0JM	2184	Alive	1643.43	High
TCGA-AR-A1AJ	3072	Alive	1650.68	High
TCGA-AO-A1KT	541	Alive	1651.36	High
TCGA-AN-A04C	54	Alive	1652.2	High
TCGA-PE-A5DC	1430	Dead	1653.09	High
TCGA-A2-A0YH	659	Alive	1656.35	High
TCGA-E2-A9RU	538	Alive	1662.28	High
TCGA-A2-A25E	3204	Alive	1665.05	High
TCGA-A2-A3XX	1439	Dead	1666.02	High
TCGA-E9-A3HO	1158	Alive	1668.64	High

TCGA-BH-A0B5	2136	Alive	1673.76	High
TCGA-GM-A2DF	2155	Alive	1677.47	High
TCGA-E2-A109	1417	Alive	1683.01	High
TCGA-BH-A1F6	2965	Dead	1687.32	High
TCGA-B6-A0RL	2469	Dead	1691.56	High
TCGA-A2-A04U	2654	Alive	1693.96	High
TCGA-D8-A1JK	612	Alive	1700.4	High
TCGA-AO-A03P	2911	Dead	1702.07	High
TCGA-UU-A93S	116	Dead	1710.3	High
TCGA-A8-A09I	1371	Alive	1710.72	High
TCGA-B6-A0RT	2721	Alive	1725.11	High
TCGA-D8-A1J8	431	Alive	1735.25	High
TCGA-AN-A0FY	10	Alive	1747.89	High
TCGA-AO-A1KS	350	Alive	1748.33	High
TCGA-A2-A25F	322	Alive	1753.41	High
TCGA-BH-A0E1	477	Alive	1754.26	High
TCGA-AC-A62X	417	Alive	1767.22	High
TCGA-BH-A0BD	554	Alive	1770.88	High
TCGA-A8-A09N	31	Alive	1784.28	High
TCGA-A7-A6VV	313	Alive	1797.01	High
TCGA-A7-A4SF	545	Alive	1799.07	High
TCGA-AR-A0TY	1699	Dead	1799.61	High
TCGA-A2-A3XY	1093	Dead	1803.41	High
TCGA-D8-A27W	373	Alive	1808.99	High
TCGA-AN-A0FX	10	Alive	1809.25	High
TCGA-C8-A1HN	394	Alive	1821.25	High
TCGA-BH-A0HU	392	Alive	1832.75	High
TCGA-E9-A247	1186	Alive	1839.55	High
TCGA-AO-A03O	2483	Dead	1848.94	High
TCGA-C8-A8HQ	380	Alive	1850.43	High
TCGA-C8-A275	1	Alive	1851.29	High
TCGA-A1-A0SN	1196	Alive	1856.43	High
TCGA-A2-A0EQ	2426	Alive	1857.48	High
TCGA-LL-A441	996	Alive	1857.95	High
TCGA-EW-A1PA	575	Alive	1859.61	High
TCGA-C8-A1HF	332	Alive	1867.98	High
TCGA-E2-A15A	710	Alive	1868.5	High
TCGA-E2-A1LL	1309	Alive	1874.86	High
TCGA-E9-A243	612	Alive	1876.27	High
TCGA-AO-A03R	2091	Alive	1880.1	High

TCGA-E9-A2JS	904	Dead	1884.24	High
TCGA-A7-A13D	965	Alive	1887.96	High
TCGA-BH-A42T	320	Dead	1893.47	High
TCGA-AC-A2BK	2222	Alive	1905.14	High
TCGA-E2-A1LG	1523	Alive	1916.95	High
TCGA-E9-A1ND	1266	Alive	1929.88	High
TCGA-D8-A27R	307	Alive	1937.28	High
TCGA-B6-A402	2134	Alive	1941.02	High
TCGA-AR-A24Z	3001	Alive	1941.92	High
TCGA-OL-A5RW	1106	Alive	1988.12	High
TCGA-C8-A12P	358	Alive	2000.78	High
TCGA-AR-A0TV	2288	Alive	2012.89	High
TCGA-AN-A0AJ	303	Alive	2028.61	High
TCGA-A2-A0T3	1516	Alive	2033.01	High
TCGA-A8-A092	942	Alive	2062.28	High
TCGA-S3-AA15	525	Alive	2068.94	High
TCGA-BH-A0E0	134	Alive	2084.87	High
TCGA-EW-A3U0	532	Alive	2088.63	High
TCGA-D8-A1Y3	430	Alive	2100.22	High
TCGA-BH-A18L	811	Dead	2102.45	High
TCGA-D8-A1XF	463	Alive	2114.1	High
TCGA-Z7-A8R6	3256	Alive	2121.88	High
TCGA-AC-A7VB	250	Alive	2133.54	High
TCGA-A2-A0D1	1051	Alive	2203.93	High
TCGA-E2-A150	1935	Alive	2223.4	High
TCGA-E2-A2P5	821	Dead	2231.56	High
TCGA-AO-A0J6	1140	Alive	2231.87	High
TCGA-C8-A27B	439	Alive	2257.24	High
TCGA-A2-A0ST	3017	Alive	2259.4	High
TCGA-A2-A04Q	2385	Alive	2282.97	High
TCGA-AR-A0TP	4275	Alive	2316.37	High
TCGA-OL-A5RZ	679	Alive	2343.52	High
TCGA-LL-A5YP	450	Alive	2347.67	High
TCGA-AR-A1AH	3807	Alive	2357.36	High
TCGA-A2-A4S3	666	Alive	2358.27	High
TCGA-C8-A27A	747	Alive	2360.37	High
TCGA-E9-A1N8	1039	Alive	2363.88	High
TCGA-BH-A203	1174	Dead	2368.03	High
TCGA-A7-A13E	614	Dead	2391.15	High
TCGA-AR-A0U3	4080	Alive	2429.02	High

TCGA-OL-A66I	714	Alive	2432.89	High
TCGA-AO-A0J4	1587	Alive	2433.79	High
TCGA-GI-A2C9	3342	Alive	2435.29	High
TCGA-E2-A1B6	867	Alive	2437.44	High
TCGA-A2-A0CW	3283	Alive	2439	High
TCGA-AR-A24H	4894	Alive	2444.68	High
TCGA-AR-A0TQ	2991	Alive	2453.38	High
TCGA-AN-A0G0	16	Alive	2524.53	High
TCGA-E9-A1RB	976	Dead	2542.18	High
TCGA-AR-A1AI	3296	Alive	2554.11	High
TCGA-AO-A1KQ	1882	Alive	2568.48	High
TCGA-EW-A1OW	694	Alive	2575.45	High
TCGA-A2-A0CM	754	Dead	2585.73	High
TCGA-D8-A147	584	Alive	2591.6	High
TCGA-A8-A09X	426	Dead	2601.24	High
TCGA-D8-A13Z	635	Alive	2610.96	High
TCGA-E2-A107	1047	Alive	2634.93	High
TCGA-E2-A14P	1246	Alive	2649.34	High
TCGA-E2-A573	1062	Alive	2651.82	High
TCGA-BH-A0DD	2486	Alive	2661.85	High
TCGA-A7-A4SE	644	Alive	2673.99	High
TCGA-C8-A134	383	Alive	2705.89	High
TCGA-E2-A14Y	2109	Alive	2714.31	High
TCGA-B6-A0X5	2097	Dead	2719.59	High
TCGA-AN-A0AM	5	Alive	2742.57	High
TCGA-GM-A2DH	2193	Alive	2777.04	High
TCGA-AN-A0FJ	242	Alive	2793.76	High
TCGA-C8-A1HM	375	Alive	2801.96	High
TCGA-E2-A14V	1042	Alive	2804.53	High
TCGA-AO-A0JD	2190	Alive	2810.66	High
TCGA-BH-A209	3959	Dead	2821.96	High
TCGA-AR-A2LR	1742	Alive	2829.58	High
TCGA-OL-A6VO	858	Alive	2864.53	High
TCGA-E2-A1LI	3121	Alive	2896.81	High
TCGA-A7-A13F	765	Alive	2924.96	High
TCGA-E2-A1L7	1836	Alive	2939.32	High
TCGA-D8-A27M	410	Alive	2940.87	High
TCGA-BH-A18Q	1692	Dead	2950.18	High
TCGA-C8-A12U	385	Alive	2963.65	High
TCGA-A7-A6VY	266	Alive	2976.62	High

TCGA-EW-A1PB	608	Alive	3004.29	High
TCGA-B6-A1KF	3088	Alive	3016.8	High
TCGA-BH-A0BL	2278	Alive	3025.12	High
TCGA-AN-A0AT	10	Alive	3049	High
TCGA-AC-A6IW	413	Alive	3049.48	High
TCGA-BH-A0B3	1203	Alive	3092.41	High
TCGA-AN-A04D	52	Alive	3100.51	High
TCGA-AR-A0U2	2551	Dead	3149.74	High
TCGA-C8-A12W	385	Alive	3181.82	High
TCGA-AN-A0AK	224	Alive	3183.46	High
TCGA-AO-A12F	1842	Alive	3195.33	High
TCGA-EW-A1PC	187	Alive	3201.07	High
TCGA-A8-A07R	273	Alive	3211.38	High
TCGA-LL-A8F5	596	Alive	3238.94	High
TCGA-B6-A400	215	Alive	3269.79	High
TCGA-A7-A4SD	441	Alive	3272.6	High
TCGA-A8-A079	274	Alive	3283.57	High
TCGA-A8-A07O	304	Alive	3321.94	High
TCGA-E9-A244	21	Alive	3329.66	High
TCGA-E2-A14R	1174	Alive	3331.8	High
TCGA-C8-A12L	363	Alive	3336.96	High
TCGA-AR-A0TS	2558	Alive	3372.54	High
TCGA-AC-A2QH	1005	Alive	3510	High
TCGA-B6-A0RE	7777	Alive	3554.42	High
TCGA-AN-A0XU	10	Alive	3567.06	High
TCGA-AR-A256	2854	Dead	3596.06	High
TCGA-BH-A18R	1142	Dead	3627.42	High
TCGA-AR-A0U4	3261	Alive	3646.11	High
TCGA-A2-A0YJ	566	Alive	3648.67	High
TCGA-E2-A15S	428	Alive	3658.14	High
TCGA-AR-A1AQ	3021	Alive	3676.68	High
TCGA-B6-A0IQ	4285	Alive	3686.78	High
TCGA-A8-A08R	30	Alive	3769.69	High
TCGA-AQ-A04J	819	Alive	3792.26	High
TCGA-D8-A13Y	1728	Alive	3801.3	High
TCGA-AR-A24Q	3172	Alive	3864.72	High
TCGA-AR-A1AY	1026	Alive	3884.64	High
TCGA-AO-A1KR	2513	Alive	3952.33	High
TCGA-E9-A3QA	918	Alive	3963.92	High
TCGA-A7-A0CE	1074	Alive	4005.5	High

TCGA-S3-AA0Z	629	Alive	4024.41	High
TCGA-C8-A130	370	Alive	4027.71	High
TCGA-A8-A07C	1034	Alive	4036.77	High
TCGA-A8-A07U	760	Alive	4086.93	High
TCGA-BH-A0AV	1820	Alive	4105.32	High
TCGA-AO-A0J2	997	Alive	4142.09	High
TCGA-D8-A27F	488	Alive	4249.11	High
TCGA-B6-A0I2	4361	Alive	4283.96	High
TCGA-A2-A0D0	2048	Alive	4335.99	High
TCGA-EW-A1P4	907	Alive	4399.72	High
TCGA-AN-A0AL	227	Alive	4434.48	High
TCGA-A2-A1G1	584	Alive	4439.59	High
TCGA-A7-A6VW	285	Alive	4499.48	High
TCGA-A2-A0YE	554	Alive	4569.37	High
TCGA-A2-A3XT	2770	Alive	4596.62	High
TCGA-D8-A1JL	611	Alive	4608.75	High
TCGA-A1-A0SO	852	Alive	4650.27	High
TCGA-A2-A3Y0	1546	Alive	4744.21	High
TCGA-GM-A3XL	2108	Alive	4764.61	High
TCGA-E2-A14N	1434	Alive	4798.93	High
TCGA-EW-A6SB	760	Alive	4808.99	High
TCGA-BH-A0B9	1572	Alive	4950.32	High
TCGA-A8-A07L	975	Alive	5023.77	High
TCGA-D8-A143	431	Alive	5242.56	High
TCGA-B6-A0I6	991	Dead	5537.95	High
TCGA-AO-A129	3286	Alive	5576.61	High
TCGA-BH-A1FC	3472	Dead	5581.71	High
TCGA-C8-A1HJ	5	Alive	5636.76	High
TCGA-S3-AA10	586	Alive	5757.73	High
TCGA-D8-A1XK	441	Alive	6005.73	High
TCGA-A2-A0YM	965	Alive	6036.05	High
TCGA-BH-A18T	224	Dead	6261.51	High
TCGA-E2-A1II	1025	Alive	6337.97	High
TCGA-B6-A0IJ	7106	Alive	6345.69	High
TCGA-AR-A0TU	709	Alive	6782.6	High
TCGA-OL-A5D7	1780	Alive	6815.01	High
TCGA-A2-A0D2	1027	Alive	6954.29	High
TCGA-BH-A5IZ	567	Alive	7024.43	High
TCGA-BH-A18V	1556	Dead	7356.47	High
TCGA-E9-A22G	1239	Alive	7624.48	High

TCGA-HN-A2NL	79	Alive	7683.88	High
TCGA-A2-A04T	2246	Alive	7889.5	High
TCGA-AN-A0AR	10	Alive	8071.34	High
TCGA-EW-A1P8	239	Dead	8366.4	High
TCGA-B6-A0X1	7455	Dead	9101.6	High
TCGA-E2-A1AZ	2329	Alive	9446.08	High
TCGA-A1-A0SP	584	Alive	10027.18	High
TCGA-D8-A1JM	590	Alive	10098.32	High

Supplementary Table 2.3: The TCGA-BRCA patient data for *FOXQ1*expression in BC subtypes that were used for the adjusted Cox's regression

FOXQ1	Low	503	
	High	503	

BC_subtype_cat = HER2

Case Processing Summary

		N	Percent
Cases available in analysis	Event	17	22.10%
	Censored	55	71.40%
	Total	72	93.50%
Cases dropped	Cases with missing values	0	0.00%
	Cases with negative time	0	0.00%
	Censored cases before the earliest event in a stratum	5	6.50%
	Total	5	6.50%
Total		77	100.00%

BC_subtype_cat = Luminal

Case Processing Summary

		N	Percent
Cases available in analysis	Event	88	12.40%
	Censored	580	82.00%
	Total	668	94.50%
Cases dropped	Cases with missing values	0	0.00%
	Cases with negative time	0	0.00%
	Censored cases before the earliest event in a stratum	39	5.50%
	Total	39	5.50%
Total		707	100.00%

BC_subtype_cat = TNBC

Case Processing Summary

		N	Percent
Cases available in analysis	Event	23	13.10%
	Censored	134	76.60%
	Total	157	89.70%
Cases dropped	Cases with missing values	0	0.00%
	Cases with negative time	0	0.00%
	Censored cases before the earliest event in a stratum	18	10.30%
	Total	18	10.30%
Total		175	100.00%

Patient	BC Subtype	Days	Status	FOXQ1 Expression	Group
TCGA-A1-A0SO	TNBC	852	Alive	0	Low
TCGA-AC-A7VC	TNBC	1	Alive	0	Low
TCGA-E2-A1LS	TNBC	1604	Alive	0	Low
TCGA-AN-A0G0	TNBC	16	Alive	0.29	Low
TCGA-AO-A0JL	TNBC	1683	Alive	1.22	Low
TCGA-AQ-A54N	TNBC	78	Alive	1.37	Low
TCGA-AN-A0FJ	TNBC	242	Alive	1.8	Low
TCGA-AN-A0AT	TNBC	10	Alive	3.17	Low
TCGA-BH-A0E6	TNBC	293	Alive	3.27	Low
TCGA-B6-A1KF	TNBC	3088	Alive	3.31	Low
TCGA-GM-A3XL	TNBC	2108	Alive	4.15	Low
TCGA-HN-A2NL	TNBC	79	Alive	4.43	Low
TCGA-A8-A07O	TNBC	304	Alive	4.78	Low
TCGA-A2-A0YJ	TNBC	566	Alive	4.88	Low
TCGA-AR-A0TU	TNBC	709	Alive	5.01	Low
TCGA-AO-A12F	TNBC	1842	Alive	5.1	Low
TCGA-AC-A62X	TNBC	417	Alive	5.41	Low
TCGA-PL-A8LZ	TNBC	302	Alive	5.55	Low
TCGA-AN-A04D	TNBC	52	Alive	5.76	Low
TCGA-A2-A4S1	TNBC	820	Alive	5.96	Low
TCGA-E2-A158	TNBC	450	Alive	6.17	Low
TCGA-E2-A14X	TNBC	972	Alive	6.74	Low
TCGA-A2-A3XT	TNBC	2770	Alive	6.86	Low
TCGA-S3-AA0Z	TNBC	629	Alive	7.19	Low
TCGA-A8-A07C	TNBC	1034	Alive	7.71	Low
TCGA-A2-A0D2	TNBC	1027	Alive	7.76	Low
TCGA-AN-A0FL	TNBC	231	Alive	8.29	Low

TCGA-E2-A14N	TNBC	1434	Alive	8.93	Low
TCGA-AR-A0TP	TNBC	4275	Alive	9.41	Low
TCGA-LL-A8F5	TNBC	596	Alive	10.49	Low
TCGA-GM-A2DF	TNBC	2155	Alive	10.54	Low
TCGA-C8-A134	TNBC	383	Alive	10.59	Low
TCGA-AN-A0AR	TNBC	10	Alive	10.82	Low
TCGA-BH-A0RX	TNBC	170	Alive	10.99	Low
TCGA-AR-A0TS	TNBC	2558	Alive	11.13	Low
TCGA-A8-A08R	TNBC	30	Alive	11.63	Low
TCGA-A2-A25F	TNBC	322	Alive	12.36	Low
TCGA-AO-A0J6	TNBC	1140	Alive	12.51	Low
TCGA-C8-A131	TNBC	411	Alive	12.51	Low
TCGA-E9-A243	TNBC	612	Alive	12.6	Low
TCGA-A2-A1G1	TNBC	584	Alive	12.65	Low
TCGA-A8-A07U	TNBC	760	Alive	13.2	Low
TCGA-E2-A1LI	TNBC	3121	Alive	13.22	Low
TCGA-AR-A1AY	TNBC	1026	Alive	13.59	Low
TCGA-AC-A2BK	TNBC	2222	Alive	14.39	Low
TCGA-D8-A1JL	TNBC	611	Alive	15.4	Low
TCGA-BH-A18G	TNBC	149	Alive	15.63	Low
TCGA-D8-A27F	TNBC	488	Alive	15.97	Low
TCGA-D8-A1JK	TNBC	612	Alive	16.2	Low
TCGA-EW-A1OW	TNBC	694	Alive	16.8	Low
TCGA-AR-A24Q	TNBC	3172	Alive	17.18	Low
TCGA-E9-A1ND	TNBC	1266	Alive	17.49	Low
TCGA-AR-A1AI	TNBC	3296	Alive	18.04	Low
TCGA-AN-A04C	Her2	54	Alive	0.35	Low
TCGA-C8-A1HK	Her2	366	Alive	0.5	Low
TCGA-OL-A5RZ	Her2	679	Alive	0.51	Low

TCGA-EW-A1OV	Her2	789	Alive	0.53	Low
TCGA-AR-A24U	Her2	3128	Alive	2.32	Low
TCGA-C8-A26Y	Her2	394	Alive	2.45	Low
TCGA-A2-A3XV	Her2	996	Alive	2.58	Low
TCGA-A8-A0A7	Her2	30	Alive	2.75	Low
TCGA-A7-A4SF	Her2	545	Alive	2.79	Low
TCGA-C8-A26X	Her2	376	Alive	4.13	Low
TCGA-BH-A0B7	Her2	2559	Alive	4.29	Low
TCGA-E2-A1LB	Her2	2306	Alive	4.49	Low
TCGA-A2-A0T1	Her2	521	Alive	4.87	Low
TCGA-D8-A1JF	Her2	366	Alive	5.51	Low
TCGA-E2-A14P	Her2	1246	Alive	5.61	Low
TCGA-OL-A66P	Her2	428	Alive	5.76	Low
TCGA-C8-A135	Her2	393	Alive	6.45	Low
TCGA-E9-A248	Her2	59	Alive	6.47	Low
TCGA-AO-A0J2	Her2	997	Alive	7.41	Low
TCGA-A2-A04X	Her2	1686	Alive	10.81	Low
TCGA-AC-A5EH	Her2	511	Alive	14.43	Low
TCGA-3C-AALI	Her2	4005	Alive	14.68	Low
TCGA-C8-A12Z	Her2	382	Alive	15.73	Low
TCGA-C8-A12P	Her2	358	Alive	16.05	Low
TCGA-GM-A2DH	Her2	2193	Alive	16.17	Low
TCGA-D8-A1JG	Her2	1612	Alive	17.33	Low
TCGA-C8-A1HF	Her2	332	Alive	17.82	Low
TCGA-A2-A4S0	Luminal	706	Alive	0	Low
TCGA-A8-A09K	Luminal	912	Alive	0	Low
TCGA-AC-A5XS	Luminal	588	Alive	0	Low
TCGA-AC-A8OR	Luminal	40	Alive	0	Low
TCGA-E2-A14U	Luminal	1318	Alive	0	Low
TCGA-E9-A3Q9	Luminal	1001	Alive	0	Low
TCGA-LQ-A4E4	Luminal	849	Alive	0	Low
TCGA-LL-A442	Luminal	889	Alive	0.26	Low
TCGA-AO-A12B	Luminal	2989	Alive	0.42	Low
TCGA-D8-A1JN	Luminal	620	Alive	0.52	Low
TCGA-D8-A1XV	Luminal	461	Alive	0.52	Low
TCGA-C8-A1HO	Luminal	375	Alive	0.62	Low
TCGA-C8-A12X	Luminal	385	Alive	0.72	Low
TCGA-GM-A2DM	Luminal	3226	Alive	0.77	Low
TCGA-AC-A62Y	Luminal	530	Alive	0.82	Low
TCGA-A7-A0DC	Luminal	906	Alive	1.22	Low

TCGA-BH-A0BS	Luminal	2612	Alive	1.29	Low
TCGA-A2-A0ET	Luminal	1066	Alive	1.35	Low
TCGA-E2-A156	Luminal	726	Alive	1.44	Low
TCGA-AN-A0XL	Luminal	163	Alive	1.5	Low
TCGA-A2-A0YF	Luminal	1535	Alive	1.59	Low
TCGA-AR-A0U3	Luminal	4080	Alive	1.71	Low
TCGA-E2-A15J	Luminal	1640	Alive	1.77	Low
TCGA-BH-A0HL	Luminal	72	Alive	1.8	Low
TCGA-S3-AA12	Luminal	574	Alive	1.96	Low
TCGA-A7-A3IZ	Luminal	322	Alive	2.03	Low
TCGA-A7-A3RF	Luminal	408	Alive	2.04	Low
TCGA-E2-A1IK	Luminal	1800	Alive	2.22	Low
TCGA-PL-A8LX	Luminal	5	Alive	2.23	Low
TCGA-A2-A25D	Luminal	552	Alive	2.28	Low
TCGA-AC-A4ZE	Luminal	890	Alive	2.35	Low
TCGA-LL-A6FP	Luminal	677	Alive	2.35	Low
TCGA-A2-A0SU	Luminal	1662	Alive	2.58	Low
TCGA-E2-A14T	Luminal	2311	Alive	2.72	Low
TCGA-LL-A6FQ	Luminal	80	Alive	2.83	Low
TCGA-E2-A572	Luminal	1208	Alive	3	Low
TCGA-AQ-A1H2	Luminal	475	Alive	3.01	Low
TCGA-AC-A8OP	Luminal	614	Alive	3.11	Low
TCGA-A2-A0ER	Luminal	2263	Alive	3.31	Low
TCGA-AN-A0FT	Luminal	214	Alive	3.32	Low
TCGA-A2-A0ES	Luminal	2190	Alive	3.34	Low
TCGA-AC-A2FG	Luminal	1853	Alive	3.37	Low
TCGA-A8-A091	Luminal	1004	Alive	3.43	Low
TCGA-A8-A0A9	Luminal	822	Alive	3.51	Low
TCGA-A2-A0EP	Luminal	3603	Alive	3.65	Low
TCGA-E2-A1IE	Luminal	2362	Alive	3.74	Low
TCGA-OL-A66H	Luminal	812	Alive	3.75	Low
TCGA-A8-A0A1	Luminal	365	Alive	4.02	Low
TCGA-BH-A0DO	Luminal	1644	Alive	4.02	Low
TCGA-A1-A0SQ	Luminal	554	Alive	4.03	Low
TCGA-AN-A0FW	Luminal	11	Alive	4.05	Low
TCGA-D8-A1X9	Luminal	727	Alive	4.05	Low
TCGA-A2-A0D3	Luminal	1873	Alive	4.19	Low
TCGA-E2-A15D	Luminal	526	Alive	4.2	Low
TCGA-EW-A1IZ	Luminal	554	Alive	4.28	Low
TCGA-A7-A4SC	Luminal	446	Alive	4.61	Low

TCGA-E2-A107	Luminal	1047	Alive	4.63	Low
TCGA-AN-A0XT	Luminal	10	Alive	4.75	Low
TCGA-EW-A1J1	Luminal	575	Alive	4.81	Low
TCGA-BH-A0BO	Luminal	2197	Alive	4.87	Low
TCGA-E9-A2JT	Luminal	288	Alive	4.96	Low
TCGA-AR-A2LE	Luminal	5062	Alive	4.99	Low
TCGA-A2-A3KD	Luminal	1206	Alive	5.04	Low
TCGA-BH-A18H	Luminal	652	Alive	5.18	Low
TCGA-B6-A1KI	Luminal	2236	Alive	5.28	Low
TCGA-AR-A1AX	Luminal	2629	Alive	5.29	Low
TCGA-AO-A0JI	Luminal	1528	Alive	5.3	Low
TCGA-BH-A0B0	Luminal	2477	Alive	5.37	Low
TCGA-AR-A1AL	Luminal	2971	Alive	5.43	Low
TCGA-WT-AB41	Luminal	1611	Alive	5.52	Low
TCGA-AC-A6NO	Luminal	51	Alive	5.54	Low
TCGA-GM-A3NW	Luminal	3361	Alive	5.54	Low
TCGA-BH-A0DX	Luminal	2156	Alive	5.58	Low
TCGA-BH-A0DH	Luminal	1156	Alive	5.65	Low
TCGA-BH-A0HO	Luminal	76	Alive	5.66	Low
TCGA-AN-A046	Luminal	10	Alive	5.68	Low
TCGA-A7-A4SB	Luminal	418	Alive	5.74	Low
TCGA-E2-A1IU	Luminal	337	Alive	5.76	Low
TCGA-AC-A2FO	Luminal	2255	Alive	5.82	Low
TCGA-AR-A1AP	Luminal	2856	Alive	5.85	Low
TCGA-A7-A13G	Luminal	718	Alive	5.92	Low
TCGA-OL-A6VR	Luminal	1220	Alive	6.08	Low
TCGA-EW-A1P6	Luminal	562	Alive	6.35	Low
TCGA-BH-A0H5	Luminal	1620	Alive	6.4	Low
TCGA-E2-A15C	Luminal	694	Alive	6.4	Low
TCGA-A8-A0A4	Luminal	396	Alive	6.53	Low
TCGA-E9-A1R6	Luminal	339	Alive	6.57	Low
TCGA-AC-A2FB	Luminal	1234	Alive	6.81	Low
TCGA-D8-A145	Luminal	410	Alive	6.86	Low
TCGA-A2-A1FV	Luminal	714	Alive	7	Low
TCGA-D8-A27G	Luminal	409	Alive	7.12	Low
TCGA-A2-A259	Luminal	1596	Alive	7.15	Low
TCGA-3C-AAAU	Luminal	4047	Alive	7.24	Low
TCGA-BH-A28Q	Luminal	1119	Alive	7.32	Low
TCGA-D8-A1X8	Luminal	783	Alive	7.32	Low
TCGA-BH-A0AY	Luminal	777	Alive	7.39	Low

TCGA-E2-A15O	Luminal	1545	Alive	7.42	Low
TCGA-BH-A0H9	Luminal	1247	Alive	7.43	Low
TCGA-B6-A0RO	Luminal	4929	Alive	7.48	Low
TCGA-E2-A1L6	Luminal	1648	Alive	7.48	Low
TCGA-AC-A2B8	Luminal	677	Alive	7.56	Low
TCGA-B6-A0WZ	Luminal	6292	Alive	7.6	Low
TCGA-OL-A5RU	Luminal	1219	Alive	7.78	Low
TCGA-A8-A08C	Luminal	881	Alive	7.79	Low
TCGA-D8-A140	Luminal	403	Alive	7.85	Low
TCGA-S3-A6ZH	Luminal	641	Alive	7.87	Low
TCGA-E2-A154	Luminal	591	Alive	7.95	Low
TCGA-PE-A5DD	Luminal	1953	Alive	7.95	Low
TCGA-A2-A0SY	Luminal	1347	Alive	8.01	Low
TCGA-E9-A1NE	Luminal	1088	Alive	8.01	Low
TCGA-A7-A425	Luminal	447	Alive	8.25	Low
TCGA-S3-AA11	Luminal	421	Alive	8.44	Low
TCGA-E9-A245	Luminal	26	Alive	8.47	Low
TCGA-D8-A1JB	Luminal	1688	Alive	8.53	Low
TCGA-OL-A66L	Luminal	1301	Alive	8.55	Low
TCGA-AN-A0FK	Luminal	213	Alive	8.56	Low
TCGA-AC-A3TN	Luminal	456	Alive	8.62	Low
TCGA-A2-A0YI	Luminal	1505	Alive	8.65	Low
TCGA-B6-A0IO	Luminal	5042	Alive	8.88	Low
TCGA-EW-A2FS	Luminal	1604	Alive	8.9	Low
TCGA-BH-A0E7	Luminal	1363	Alive	8.92	Low
TCGA-OL-A5D8	Luminal	973	Alive	9.1	Low
TCGA-AC-A6IX	Luminal	373	Alive	9.11	Low
TCGA-D8-A27K	Luminal	1461	Alive	9.12	Low
TCGA-D8-A3Z5	Luminal	1015	Alive	9.18	Low
TCGA-BH-A0HN	Luminal	516	Alive	9.3	Low
TCGA-E9-A1QZ	Luminal	755	Alive	9.42	Low
TCGA-A1-A0SJ	Luminal	416	Alive	9.51	Low
TCGA-A8-A06Y	Luminal	791	Alive	9.52	Low
TCGA-A8-A0A6	Luminal	640	Alive	9.58	Low
TCGA-A8-A099	Luminal	304	Alive	9.85	Low
TCGA-E2-A15I	Luminal	1692	Alive	9.89	Low
TCGA-E9-A1RA	Luminal	1369	Alive	9.89	Low
TCGA-BH-A0B6	Luminal	2483	Alive	9.94	Low
TCGA-BH-A6R8	Luminal	293	Alive	10	Low
TCGA-GM-A2DK	Luminal	2645	Alive	10.01	Low

TCGA-D8-A1Y0	Luminal	472	Alive	10.06	Low
TCGA-EW-A1PE	Luminal	320	Alive	10.17	Low
TCGA-AN-A0FZ	Luminal	10	Alive	10.32	Low
TCGA-AR-A252	Luminal	2838	Alive	10.37	Low
TCGA-AO-A12E	Luminal	2142	Alive	10.38	Low
TCGA-E2-A106	Luminal	2541	Alive	10.5	Low
TCGA-AR-A2LN	Luminal	1161	Alive	10.57	Low
TCGA-EW-A1PA	Luminal	575	Alive	10.6	Low
TCGA-AO-A126	Luminal	3307	Alive	10.66	Low
TCGA-A8-A07Z	Luminal	1371	Alive	10.81	Low
TCGA-AN-A03X	Luminal	10	Alive	10.84	Low
TCGA-LL-A5YL	Luminal	519	Alive	10.91	Low
TCGA-LL-A5YN	Luminal	447	Alive	10.97	Low
TCGA-E2-A10A	Luminal	1229	Alive	10.99	Low
TCGA-LD-A7W5	Luminal	216	Alive	11.22	Low
TCGA-C8-A1HE	Luminal	375	Alive	11.25	Low
TCGA-A7-A26E	Luminal	954	Alive	11.41	Low
TCGA-E2-A105	Luminal	1308	Alive	11.54	Low
TCGA-A8-A06P	Luminal	396	Alive	11.57	Low
TCGA-OL-A5RV	Luminal	1062	Alive	11.68	Low
TCGA-AC-A23C	Luminal	585	Alive	12.03	Low
TCGA-A2-A0CR	Luminal	3283	Alive	12.04	Low
TCGA-GI-A2C8	Luminal	225	Alive	12.05	Low
TCGA-A2-A0T4	Luminal	624	Alive	12.2	Low
TCGA-E2-A2P6	Luminal	1051	Alive	12.25	Low
TCGA-A2-A0EX	Luminal	752	Alive	12.26	Low
TCGA-Z7-A8R5	Luminal	3287	Alive	12.54	Low
TCGA-BH-A18F	Luminal	1001	Alive	12.55	Low
TCGA-AR-A2LO	Luminal	1198	Alive	12.84	Low
TCGA-AC-A8OS	Luminal	70	Alive	13.17	Low
TCGA-OL-A66N	Luminal	792	Alive	13.2	Low
TCGA-AO-A12A	Luminal	3112	Alive	13.31	Low
TCGA-BH-A0B5	Luminal	2136	Alive	13.34	Low
TCGA-AN-A0XS	Luminal	10	Alive	13.4	Low
TCGA-A8-A07P	Luminal	334	Alive	13.48	Low
TCGA-OL-A66J	Luminal	1996	Alive	13.52	Low
TCGA-A8-A06T	Luminal	1614	Alive	13.62	Low
TCGA-E9-A1R2	Luminal	1063	Alive	13.8	Low
TCGA-EW-A3E8	Luminal	1035	Alive	13.84	Low
TCGA-BH-A0H3	Luminal	1928	Alive	13.88	Low

TCGA-B6-A0RN	Luminal	8008	Alive	13.98	Low
TCGA-OL-A6VQ	Luminal	600	Alive	14.14	Low
TCGA-A7-A0CD	Luminal	1165	Alive	14.25	Low
TCGA-E2-A14Q	Luminal	1163	Alive	14.27	Low
TCGA-B6-A2IU	Luminal	5176	Alive	14.38	Low
TCGA-BH-A0BV	Luminal	1519	Alive	14.58	Low
TCGA-AO-A03V	Luminal	1351	Alive	14.9	Low
TCGA-D8-A1XA	Luminal	839	Alive	15.01	Low
TCGA-GM-A2DI	Luminal	2590	Alive	15.03	Low
TCGA-OL-A5RX	Luminal	878	Alive	15.32	Low
TCGA-AR-A1AK	Luminal	3159	Alive	15.42	Low
TCGA-JL-A3YX	Luminal	352	Alive	15.48	Low
TCGA-A2-A0T6	Luminal	575	Alive	15.72	Low
TCGA-AC-A2FF	Luminal	2759	Alive	15.78	Low
TCGA-D8-A141	Luminal	626	Alive	16	Low
TCGA-AO-A0J8	Luminal	680	Alive	16.03	Low
TCGA-AN-A0XV	Luminal	162	Alive	16.04	Low
TCGA-E9-A1R5	Luminal	92	Alive	16.07	Low
TCGA-C8-A273	Luminal	513	Alive	16.13	Low
TCGA-E9-A1RD	Luminal	34	Alive	16.21	Low
TCGA-E2-A10B	Luminal	1141	Alive	16.22	Low
TCGA-D8-A1JU	Luminal	447	Alive	16.24	Low
TCGA-AQ-A1H3	Luminal	989	Alive	16.27	Low
TCGA-AC-A3BB	Luminal	987	Alive	16.29	Low
TCGA-GM-A2DC	Luminal	2535	Alive	16.41	Low
TCGA-BH-A0EI	Luminal	1926	Alive	16.61	Low
TCGA-GM-A3NY	Luminal	1162	Alive	16.64	Low
TCGA-BH-A0DG	Luminal	2041	Alive	16.68	Low
TCGA-LL-A50Y	Luminal	762	Alive	16.73	Low
TCGA-BH-AB28	Luminal	287	Alive	16.74	Low
TCGA-AO-A0JJ	Luminal	1887	Alive	16.92	Low
TCGA-AN-A0XP	Luminal	9	Alive	17.04	Low
TCGA-OK-A5Q2	Luminal	64	Alive	17.12	Low
TCGA-A7-A426	Luminal	364	Alive	17.19	Low
TCGA-A7-A3J0	Luminal	313	Alive	17.3	Low
TCGA-A7-A13H	Luminal	899	Alive	17.35	Low
TCGA-GM-A3XG	Luminal	1330	Alive	17.35	Low
TCGA-A8-A09B	Luminal	365	Alive	17.42	Low
TCGA-BH-A0E1	Luminal	477	Alive	17.42	Low
TCGA-AC-A5XU	Luminal	455	Alive	17.5	Low

TCGA-BH-A0DP	Luminal	476	Alive	17.57	Low
TCGA-E2-A153	Luminal	707	Alive	17.8	Low
TCGA-B6-A0WT	Luminal	5739	Alive	18.02	Low
TCGA-XX-A899	Luminal	467	Alive	18.11	Low
TCGA-E2-A15E	Luminal	630	Alive	18.22	Low
TCGA-BH-A0HP	Luminal	414	Alive	18.35	Low
TCGA-E9-A5FK	Luminal	812	Alive	18.39	Low
TCGA-A2-A0EY	Luminal	1925	Alive	0	Low
TCGA-B6-A1KC	Luminal	1326	Alive	0	Low
TCGA-BH-A0H0	Luminal	461	Alive	0	Low
TCGA-BH-A0HW	Luminal	1561	Alive	0	Low
TCGA-D8-A1X6	Luminal	541	Alive	0	Low
TCGA-E2-A10C	Luminal	1220	Alive	0	Low
TCGA-E9-A54X	Luminal	727	Alive	0	Low
TCGA-A8-A06Z	Luminal	31	Alive	0.25	Low
TCGA-A8-A09W	Luminal	30	Alive	0.42	Low
TCGA-AR-A24H	Luminal	4894	Alive	0.47	Low
TCGA-E9-A54Y	Luminal	725	Alive	0.59	Low
TCGA-AR-A0TV	Luminal	2288	Alive	0.7	Low
TCGA-AN-A0AK	Luminal	224	Alive	0.84	Low
TCGA-BH-A0W3	Luminal	728	Alive	0.88	Low
TCGA-E9-A1R7	Luminal	1467	Alive	1.06	Low
TCGA-E2-A155	Luminal	640	Alive	1.13	Low
TCGA-AR-A24Z	Luminal	3001	Alive	1.14	Low
TCGA-E9-A1RE	Luminal	1419	Alive	1.17	Low
TCGA-A2-A0D4	Luminal	767	Alive	1.33	Low
TCGA-AC-A7VB	Luminal	250	Alive	1.46	Low
TCGA-C8-A12U	Luminal	385	Alive	1.73	Low
TCGA-D8-A1JI	Luminal	577	Alive	1.93	Low
TCGA-D8-A1XF	Luminal	463	Alive	2.1	Low
TCGA-EW-A1OX	Luminal	911	Alive	2.13	Low
TCGA-A2-A4S3	Luminal	666	Alive	2.15	Low
TCGA-A8-A07W	Luminal	304	Alive	2.22	Low
TCGA-A2-A0CW	Luminal	3283	Alive	2.3	Low
TCGA-A2-A25B	Luminal	1291	Alive	2.41	Low
TCGA-A8-A08I	Luminal	365	Alive	2.43	Low
TCGA-A2-A1FX	Luminal	1847	Alive	2.44	Low
TCGA-AN-A0FF	Luminal	172	Alive	2.58	Low
TCGA-A8-A079	Luminal	274	Alive	2.71	Low
TCGA-C8-A274	Luminal	508	Alive	2.77	Low

TCGA-A8-A09Q	Luminal	761	Alive	2.94	Low
TCGA-AQ-A04H	Luminal	754	Alive	2.94	Low
TCGA-A2-A1G4	Luminal	595	Alive	3.01	Low
TCGA-AR-A0TQ	Luminal	2991	Alive	3.01	Low
TCGA-E2-A109	Luminal	1417	Alive	3.08	Low
TCGA-A2-A0YG	Luminal	666	Alive	3.28	Low
TCGA-E9-A3HO	Luminal	1158	Alive	3.36	Low
TCGA-E2-A15T	Luminal	1563	Alive	3.45	Low
TCGA-C8-A1HN	Luminal	394	Alive	3.96	Low
TCGA-AR-A24S	Luminal	2976	Alive	4.4	Low
TCGA-D8-A27W	Luminal	373	Alive	4.42	Low
TCGA-AR-A0TT	Luminal	3316	Alive	4.49	Low
TCGA-E9-A5UO	Luminal	785	Alive	4.72	Low
TCGA-E9-A249	Luminal	217	Alive	4.75	Low
TCGA-C8-A12M	Luminal	358	Alive	4.83	Low
TCGA-A8-A06Q	Luminal	31	Alive	5.24	Low
TCGA-A7-A0CJ	Luminal	931	Alive	5.28	Low
TCGA-D8-A1XZ	Luminal	466	Alive	5.33	Low
TCGA-D8-A27R	Luminal	307	Alive	5.48	Low
TCGA-C8-A26V	Luminal	616	Alive	5.57	Low
TCGA-A8-A09E	Luminal	1492	Alive	5.81	Low
TCGA-A8-A08F	Luminal	1004	Alive	5.95	Low
TCGA-D8-A1XR	Luminal	482	Alive	6	Low
TCGA-E9-A22H	Luminal	1232	Alive	6.05	Low
TCGA-A8-A09C	Luminal	31	Alive	6.07	Low
TCGA-C8-A1HM	Luminal	375	Alive	6.63	Low
TCGA-C8-A3M8	Luminal	394	Alive	6.67	Low
TCGA-E2-A14S	Luminal	1009	Alive	6.83	Low
TCGA-GM-A2DO	Luminal	2596	Alive	6.89	Low
TCGA-S3-AA17	Luminal	424	Alive	6.94	Low
TCGA-AR-A2LL	Luminal	2012	Alive	7.22	Low
TCGA-EW-A1OY	Luminal	908	Alive	7.24	Low
TCGA-C8-A12W	Luminal	385	Alive	7.34	Low
TCGA-A8-A08S	Luminal	1004	Alive	7.74	Low
TCGA-A2-A0YH	Luminal	659	Alive	7.8	Low
TCGA-E9-A1R4	Luminal	186	Alive	8.35	Low
TCGA-E2-A15K	Luminal	275	Alive	8.8	Low
TCGA-A8-A09M	Luminal	1006	Alive	9.25	Low
TCGA-C8-A26W	Luminal	381	Alive	10.3	Low
TCGA-A2-A25C	Luminal	523	Alive	10.37	Low

TCGA-D8-A1X5	Luminal	565	Alive	10.47	Low
TCGA-AO-A0JM	Luminal	2184	Alive	10.89	Low
TCGA-EW-A1J6	Luminal	875	Alive	10.9	Low
TCGA-C8-A27A	Luminal	747	Alive	11.2	Low
TCGA-E2-A56Z	Luminal	252	Alive	11.27	Low
TCGA-A2-A25E	Luminal	3204	Alive	11.32	Low
TCGA-AR-A24N	Luminal	3035	Alive	11.71	Low
TCGA-AR-A1AW	Luminal	2632	Alive	11.73	Low
TCGA-AR-A24K	Luminal	1548	Alive	11.76	Low
TCGA-A8-A06O	Luminal	396	Alive	11.9	Low
TCGA-AR-A24R	Luminal	3430	Alive	12.03	Low
TCGA-D8-A1JC	Luminal	480	Alive	12.23	Low
TCGA-E2-A14O	Luminal	1359	Alive	12.42	Low
TCGA-LL-A7T0	Luminal	376	Alive	12.71	Low
TCGA-A7-A2KD	Luminal	679	Alive	13.88	Low
TCGA-AO-A1KS	Luminal	350	Alive	13.88	Low
TCGA-AN-A0AM	Luminal	5	Alive	13.95	Low
TCGA-A8-A076	Luminal	1642	Alive	14.05	Low
TCGA-E2-A15S	Luminal	428	Alive	14.09	Low
TCGA-E9-A22D	Luminal	1248	Alive	14.18	Low
TCGA-A8-A09I	Luminal	1371	Alive	15.02	Low
TCGA-A8-A09R	Luminal	273	Alive	15.26	Low
TCGA-E2-A15A	Luminal	710	Alive	15.36	Low
TCGA-E9-A228	Luminal	1285	Alive	15.56	Low
TCGA-A8-A08G	Luminal	607	Alive	15.67	Low
TCGA-A8-A09N	Luminal	31	Alive	16.15	Low
TCGA-D8-A1Y3	Luminal	430	Alive	16.41	Low
TCGA-S3-A6ZF	Luminal	572	Alive	17.41	Low
TCGA-A8-A07L	Luminal	975	Alive	17.48	Low
TCGA-AR-A250	Luminal	2707	Alive	17.66	Low
TCGA-A8-A092	Luminal	942	Alive	18.24	Low
TCGA-AO-A03R	Normal	2091	Alive	0.67	Low
TCGA-D8-A1XW	Normal	1309	Alive	2.41	Low
TCGA-EW-A1P1	Normal	1210	Alive	6.09	Low
TCGA-AR-A2LQ	Normal	1233	Alive	6.55	Low
TCGA-A2-A0CL	Normal	3015	Alive	7.41	Low
TCGA-PL-A8LY	Normal	8	Alive	7.66	Low
TCGA-E2-A108	Normal	837	Alive	7.79	Low
TCGA-AC-A2FK	Normal	2650	Alive	8.89	Low
TCGA-LL-A441	Normal	996	Alive	10.08	Low

TCGA-C8-A8HR	Normal	408	Alive	10.48	Low
TCGA-BH-A8FZ	Normal	574	Alive	17.22	Low
TCGA-AR-A1AO	Normal	2618	Alive	18.07	Low
TCGA-A2-A0YK	Normal	588	Alive	18.42	Low
TCGA-A2-A3XU	TNBC	912	Dead	2.38	Low
TCGA-AR-A1AR	TNBC	524	Dead	2.47	Low
TCGA-AR-A256	TNBC	2854	Dead	2.96	Low
TCGA-BH-A18T	TNBC	224	Dead	2.99	Low
TCGA-A7-A13E	TNBC	614	Dead	8.11	Low
TCGA-A2-A3XY	TNBC	1093	Dead	8.42	Low
TCGA-EW-A1P8	TNBC	239	Dead	9.68	Low
TCGA-A2-A3XX	TNBC	1439	Dead	10.97	Low
TCGA-AR-A1AT	Her2	1272	Dead	0.52	Low
TCGA-UU-A93S	Her2	116	Dead	0.72	Low
TCGA-A8-A09X	Her2	426	Dead	1.24	Low
TCGA-BH-A1EN	Her2	2127	Dead	2.54	Low
TCGA-E2-A1LE	Her2	879	Dead	2.54	Low
TCGA-AC-A23H	Her2	174	Dead	5.95	Low
TCGA-BH-A18P	Her2	921	Dead	8.79	Low
TCGA-A8-A08J	Her2	1127	Dead	9.31	Low
TCGA-B6-A0IK	Her2	571	Dead	10.98	Low
TCGA-A8-A08L	Her2	304	Dead	11.1	Low
TCGA-C8-A12Q	Her2	385	Dead	16.42	Low
TCGA-BH-A18R	Her2	1142	Dead	17.83	Low
TCGA-D8-A1XC	Luminal	377	Dead	0	Low
TCGA-AC-A2FM	Luminal	792	Dead	0.33	Low
TCGA-D8-A73W	Luminal	385	Dead	0.42	Low
TCGA-AR-A0TR	Luminal	160	Dead	0.82	Low
TCGA-BH-A1FL	Luminal	1673	Dead	1.08	Low
TCGA-BH-A8FY	Luminal	295	Dead	1.66	Low
TCGA-A2-A0CU	Luminal	158	Dead	1.91	Low
TCGA-B6-A0RM	Luminal	2373	Dead	2.44	Low
TCGA-BH-A0BP	Luminal	2296	Dead	3.01	Low
TCGA-BH-A1EW	Luminal	1694	Dead	3.24	Low
TCGA-BH-A18S	Luminal	2009	Dead	3.27	Low
TCGA-AR-A0TZ	Luminal	3262	Dead	3.83	Low
TCGA-C8-A3M7	Luminal	1034	Dead	4.92	Low
TCGA-E2-A15M	Luminal	336	Dead	4.95	Low
TCGA-BH-A1EU	Luminal	1286	Dead	4.96	Low
TCGA-PE-A5DC	Luminal	1430	Dead	5.15	Low

TCGA-A2-A0CO	Luminal	3492	Dead	5.43	Low
TCGA-B6-A0X4	Luminal	860	Dead	5.9	Low
TCGA-BH-A18N	Luminal	1148	Dead	6.18	Low
TCGA-BH-A1FG	Luminal	3736	Dead	6.55	Low
TCGA-A2-A04V	Luminal	1920	Dead	6.93	Low
TCGA-BH-A1EX	Luminal	1508	Dead	10.86	Low
TCGA-B6-A0I8	Luminal	749	Dead	10.95	Low
TCGA-B6-A0IH	Luminal	3418	Dead	11.92	Low
TCGA-B6-A0WS	Luminal	2965	Dead	13.36	Low
TCGA-BH-A1FH	Luminal	1034	Dead	14.24	Low
TCGA-A8-A06U	Luminal	883	Dead	14.78	Low
TCGA-AC-A2FE	Luminal	2636	Dead	14.85	Low
TCGA-BH-A0EA	Luminal	991	Dead	16.75	Low
TCGA-AC-A3EH	Luminal	197	Dead	17.97	Low
TCGA-B6-A0X5	Luminal	2097	Dead	0	Low
TCGA-A2-A0SW	Luminal	1365	Dead	0	Low
TCGA-BH-A204	Luminal	2534	Dead	0.23	Low
TCGA-AR-A0TY	Luminal	1699	Dead	0.65	Low
TCGA-BH-A18L	Luminal	811	Dead	1.45	Low
TCGA-B6-A0IB	Luminal	3941	Dead	2.26	Low
TCGA-BH-A209	Luminal	3959	Dead	2.66	Low
TCGA-BH-A1F2	Luminal	959	Dead	2.75	Low
TCGA-BH-A42T	Luminal	320	Dead	2.87	Low
TCGA-A2-A0YT	Luminal	723	Dead	2.97	Low
TCGA-AR-A0U2	Luminal	2551	Dead	3.41	Low
TCGA-AO-A03P	Luminal	2911	Dead	3.67	Low
TCGA-BH-A1FD	Luminal	1009	Dead	8.12	Low
TCGA-BH-A1FJ	Luminal	1927	Dead	8.45	Low
TCGA-AR-A2LK	Luminal	1649	Dead	9.72	Low
TCGA-A8-A06X	Luminal	943	Dead	9.94	Low
TCGA-AO-A03O	Luminal	2483	Dead	11.35	Low
TCGA-BH-A1F8	Luminal	763	Dead	12.44	Low
TCGA-E9-A2JS	Luminal	904	Dead	13.79	Low
TCGA-B6-A0RL	Luminal	2469	Dead	14.77	Low
TCGA-B6-A0WV	Luminal	2417	Dead	14.84	Low
TCGA-D8-A1Y1	Luminal	302	Dead	17.88	Low
TCGA-AR-A2LH	Normal	616	Dead	2.63	Low
TCGA-B6-A0RQ	Normal	4267	Dead	9.6	Low
TCGA-BH-A1FU	Normal	1688	Dead	16.46	Low

TCGA-C8-A12V	TNBC	385	Alive	18.65	High
TCGA-A7-A0DA	TNBC	1085	Alive	18.74	High
TCGA-A2-A04T	TNBC	2246	Alive	19.82	High
TCGA-E9-A3QA	TNBC	918	Alive	20.57	High
TCGA-AR-A1AJ	TNBC	3072	Alive	22.05	High
TCGA-E9-A1N8	TNBC	1039	Alive	23.49	High
TCGA-AO-A129	TNBC	3286	Alive	23.55	High
TCGA-D8-A142	TNBC	425	Alive	24.17	High
TCGA-D8-A143	TNBC	431	Alive	24.59	High
TCGA-OL-A6VO	TNBC	858	Alive	27.54	High
TCGA-LL-A5YP	TNBC	450	Alive	28.03	High
TCGA-E9-A22G	TNBC	1239	Alive	31.72	High
TCGA-E2-A1B6	TNBC	867	Alive	32.13	High
TCGA-AC-A2QH	TNBC	1005	Alive	33.8	High
TCGA-AO-A1KR	TNBC	2513	Alive	34.78	High
TCGA-B6-A0RT	TNBC	2721	Alive	35.29	High
TCGA-E2-A1AZ	TNBC	2329	Alive	37.51	High
TCGA-A2-A3Y0	TNBC	1546	Alive	38.09	High
TCGA-AR-A2LR	TNBC	1742	Alive	40.3	High
TCGA-D8-A1XQ	TNBC	499	Alive	40.36	High
TCGA-A8-A07R	TNBC	273	Alive	41.42	High
TCGA-A2-A0T0	TNBC	533	Alive	43.58	High
TCGA-A2-A0YE	TNBC	554	Alive	46.58	High
TCGA-S3-AA10	TNBC	586	Alive	46.79	High
TCGA-A7-A26I	TNBC	661	Alive	48.96	High
TCGA-AQ-A04J	TNBC	819	Alive	53	High
TCGA-OL-A5S0	TNBC	620	Alive	53.23	High
TCGA-BH-A0BW	TNBC	2371	Alive	53.8	High
TCGA-A2-A0YM	TNBC	965	Alive	54.48	High
TCGA-C8-A1HJ	TNBC	5	Alive	58.82	High
TCGA-B6-A402	TNBC	2134	Alive	63.16	High
TCGA-E9-A244	TNBC	21	Alive	64.36	High
TCGA-AN-A0FX	TNBC	10	Alive	65.39	High
TCGA-B6-A0IJ	TNBC	7106	Alive	66.15	High
TCGA-BH-A0B9	TNBC	1572	Alive	67.17	High
TCGA-AR-A0U0	TNBC	1988	Alive	69.67	High
TCGA-D8-A1XK	TNBC	441	Alive	70.87	High
TCGA-AR-A0U4	TNBC	3261	Alive	72.48	High
TCGA-A2-A04U	TNBC	2654	Alive	73.78	High

TCGA-OL-A5D7	TNBC	1780	Alive	75.02	High
TCGA-BH-A0B3	TNBC	1203	Alive	75.63	High
TCGA-E2-A150	TNBC	1935	Alive	75.68	High
TCGA-E2-A1LL	TNBC	1309	Alive	81.19	High
TCGA-AC-A6IW	TNBC	413	Alive	85.67	High
TCGA-AR-A1AQ	TNBC	3021	Alive	86.26	High
TCGA-EW-A6SB	TNBC	760	Alive	87.09	High
TCGA-E2-A159	TNBC	762	Alive	89.29	High
TCGA-AN-A0XU	TNBC	10	Alive	90.63	High
TCGA-S3-AA15	TNBC	525	Alive	96.6	High
TCGA-A2-A0SX	TNBC	1534	Alive	96.98	High
TCGA-AR-A251	TNBC	3030	Alive	100.39	High
TCGA-D8-A147	TNBC	584	Alive	101.3	High
TCGA-A2-A04Q	TNBC	2385	Alive	104.13	High
TCGA-B6-A0RE	TNBC	7777	Alive	104.56	High
TCGA-D8-A1JM	TNBC	590	Alive	105.9	High
TCGA-C8-A27B	TNBC	439	Alive	109.37	High
TCGA-E2-A1LH	TNBC	3247	Alive	110.36	High
TCGA-GI-A2C9	TNBC	3342	Alive	110.87	High
TCGA-BH-A0BL	TNBC	2278	Alive	117.63	High
TCGA-OL-A66I	TNBC	714	Alive	120.19	High
TCGA-A2-A0D0	TNBC	2048	Alive	125.62	High
TCGA-BH-A5IZ	TNBC	567	Alive	130.31	High
TCGA-BH-A0BG	TNBC	1871	Alive	138.59	High
TCGA-A2-A4RX	TNBC	742	Alive	144.3	High
TCGA-A7-A6VY	TNBC	266	Alive	150.47	High
TCGA-AO-A0J4	TNBC	1587	Alive	161.37	High
TCGA-D8-A27H	TNBC	397	Alive	162.29	High
TCGA-E2-A14Y	TNBC	2109	Alive	180.52	High
TCGA-BH-A0E0	TNBC	134	Alive	202.32	High
TCGA-BH-A0AV	TNBC	1820	Alive	202.82	High
TCGA-AR-A1AH	TNBC	3807	Alive	205.25	High
TCGA-A2-A0ST	TNBC	3017	Alive	206.61	High
TCGA-LL-A6FR	TNBC	489	Alive	211.74	High
TCGA-A7-A13D	TNBC	965	Alive	215.7	High
TCGA-D8-A27M	TNBC	410	Alive	217.36	High
TCGA-B6-A400	TNBC	215	Alive	221.05	High
TCGA-AC-A8OQ	TNBC	34	Alive	222.78	High
TCGA-LL-A73Y	TNBC	477	Alive	244.66	High
TCGA-EW-A1PB	TNBC	608	Alive	254.63	High

TCGA-B6-A0IQ	TNBC	4285	Alive	258.25	High
TCGA-A7-A6VV	TNBC	313	Alive	269.63	High
TCGA-A1-A0SP	TNBC	584	Alive	304.63	High
TCGA-E2-A14R	TNBC	1174	Alive	308.15	High
TCGA-E2-A573	TNBC	1062	Alive	331.16	High
TCGA-A7-A0CE	TNBC	1074	Alive	357.32	High
TCGA-E2-A574	TNBC	1179	Alive	381.59	High
TCGA-EW-A1PH	TNBC	607	Alive	426.87	High
TCGA-EW-A3U0	TNBC	532	Alive	434.5	High
TCGA-AO-A128	TNBC	3248	Alive	435.82	High
TCGA-OL-A5RW	TNBC	1106	Alive	473.13	High
TCGA-EW-A1P4	TNBC	907	Alive	484.81	High
TCGA-B6-A0I2	TNBC	4361	Alive	621.42	High
TCGA-E9-A5FL	TNBC	24	Alive	653.75	High
TCGA-AN-A0AL	TNBC	227	Alive	723.43	High
TCGA-A7-A4SD	TNBC	441	Alive	727.86	High
TCGA-A7-A6VW	TNBC	285	Alive	847.77	High
TCGA-A7-A4SE	TNBC	644	Alive	878.68	High
TCGA-E2-A1LG	TNBC	1523	Alive	1373.16	High
TCGA-E2-A1II	TNBC	1025	Alive	1734.1	High
TCGA-C8-A137	Her2	379	Alive	18.59	High
TCGA-C8-A12L	Her2	363	Alive	18.6	High
TCGA-AR-A0TX	Her2	1972	Alive	20.3	High
TCGA-C8-A8HP	Her2	396	Alive	20.66	High
TCGA-A2-A0EQ	Her2	2426	Alive	21.97	High
TCGA-A2-A0D1	Her2	1051	Alive	22.13	High
TCGA-BH-A0AW	Her2	622	Alive	22.64	High
TCGA-E2-A152	Her2	2128	Alive	24.54	High
TCGA-A8-A08X	Her2	1308	Alive	24.62	High
TCGA-AO-A0JE	Her2	2335	Alive	25.96	High
TCGA-EW-A6SD	Her2	1010	Alive	27.23	High
TCGA-D8-A1JA	Her2	502	Alive	28.44	High
TCGA-C8-A275	Her2	1	Alive	29.13	High
TCGA-A8-A07I	Her2	426	Alive	29.54	High
TCGA-AC-A3W5	Her2	504	Alive	31.26	High
TCGA-AN-A0FV	Her2	10	Alive	32.65	High
TCGA-LL-A5YO	Her2	440	Alive	35.25	High
TCGA-GM-A2DB	Her2	2406	Alive	35.79	High
TCGA-D8-A1XT	Her2	506	Alive	37.57	High
TCGA-D8-A13Z	Her2	635	Alive	37.79	High

TCGA-A2-A3XZ	Her2	1532	Alive	37.9	High
TCGA-C8-A278	Her2	297	Alive	39.21	High
TCGA-AR-A254	Her2	2605	Alive	39.24	High
TCGA-A2-A0CX	Her2	1728	Alive	43.59	High
TCGA-E2-A14V	Her2	1042	Alive	43.84	High
TCGA-EW-A2FR	Her2	1673	Alive	47.09	High
TCGA-E9-A1RH	Her2	1417	Alive	47.58	High
TCGA-C8-A138	Her2	380	Alive	57.53	High
TCGA-JL-A3YW	Her2	360	Alive	61.24	High
TCGA-AO-A12D	Her2	2515	Alive	62.48	High
TCGA-A8-A08B	Her2	1156	Alive	72.44	High
TCGA-BH-A0EE	Her2	943	Alive	344.77	High
TCGA-E2-A1B0	Her2	1631	Alive	433.53	High
TCGA-BH-A0DV	Luminal	2064	Alive	18.45	High
TCGA-XX-A89A	Luminal	488	Alive	18.42	High
TCGA-A2-A0EM	Luminal	3094	Alive	18.47	High
TCGA-E9-A3X8	Luminal	926	Alive	18.57	High
TCGA-E2-A1IH	Luminal	1026	Alive	18.7	High
TCGA-AO-A0JC	Luminal	1547	Alive	18.83	High
TCGA-D8-A1XY	Luminal	503	Alive	18.84	High
TCGA-C8-A1HI	Luminal	343	Alive	18.89	High
TCGA-AC-A6IV	Luminal	568	Alive	18.96	High
TCGA-A2-A0CK	Luminal	4159	Alive	18.99	High
TCGA-E2-A15F	Luminal	658	Alive	19.01	High
TCGA-GM-A5PV	Luminal	412	Alive	19.02	High
TCGA-EW-A1J5	Luminal	477	Alive	19.21	High
TCGA-A8-A0AB	Luminal	518	Alive	19.33	High
TCGA-E2-A3DX	Luminal	1325	Alive	19.57	High
TCGA-A8-A09D	Luminal	1522	Alive	19.65	High
TCGA-EW-A1J3	Luminal	504	Alive	19.73	High
TCGA-A2-A0YC	Luminal	990	Alive	19.93	High
TCGA-D8-A146	Luminal	643	Alive	19.94	High
TCGA-AN-A0FS	Luminal	210	Alive	20.01	High
TCGA-AR-A2LM	Luminal	1935	Alive	20.09	High
TCGA-AC-A3OD	Luminal	451	Alive	20.2	High
TCGA-AO-A03M	Luminal	1866	Alive	20.58	High
TCGA-A8-A07J	Luminal	365	Alive	20.7	High
TCGA-B6-A0I5	Luminal	8556	Alive	20.72	High
TCGA-A2-A0EN	Luminal	4088	Alive	20.81	High
TCGA-AO-A03L	Luminal	2442	Alive	20.84	High

TCGA-EW-A1PF	Luminal	439	Alive	20.87	High
TCGA-A2-A0YD	Luminal	769	Alive	20.94	High
TCGA-D8-A73U	Luminal	492	Alive	21	High
TCGA-LL-A440	Luminal	759	Alive	21	High
TCGA-A7-A3IY	Luminal	345	Alive	21.31	High
TCGA-D8-A27L	Luminal	499	Alive	21.66	High
TCGA-BH-A5J0	Luminal	715	Alive	21.78	High
TCGA-E9-A24A	Luminal	747	Alive	21.9	High
TCGA-AR-A0TW	Luminal	3009	Alive	22.01	High
TCGA-D8-A1XG	Luminal	448	Alive	22.05	High
TCGA-EW-A424	Luminal	715	Alive	22.33	High
TCGA-EW-A1P5	Luminal	703	Alive	22.46	High
TCGA-E9-A1R0	Luminal	860	Alive	22.58	High
TCGA-A7-A0DB	Luminal	1007	Alive	22.61	High
TCGA-E2-A15R	Luminal	1732	Alive	22.64	High
TCGA-C8-A12O	Luminal	385	Alive	22.75	High
TCGA-A8-A09T	Luminal	579	Alive	22.8	High
TCGA-AC-A3HN	Luminal	496	Alive	22.91	High
TCGA-AR-A1AS	Luminal	1150	Alive	22.96	High
TCGA-BH-A8G0	Luminal	662	Alive	23.02	High
TCGA-AO-A0JF	Luminal	1980	Alive	23.06	High
TCGA-AR-A5QM	Luminal	2231	Alive	23.15	High
TCGA-BH-A0BJ	Luminal	660	Alive	23.31	High
TCGA-E9-A247	Luminal	1186	Alive	23.31	High
TCGA-BH-A0BT	Luminal	2365	Alive	23.39	High
TCGA-D8-A1JP	Luminal	639	Alive	23.54	High
TCGA-PE-A5DE	Luminal	2645	Alive	23.54	High
TCGA-EW-A1J2	Luminal	403	Alive	23.6	High
TCGA-BH-A0DS	Luminal	78	Alive	24	High
TCGA-D8-A1XM	Luminal	538	Alive	24	High
TCGA-D8-A1XU	Luminal	395	Alive	24.08	High
TCGA-A2-A4S2	Luminal	643	Alive	24.13	High
TCGA-AR-A2LJ	Luminal	2632	Alive	24.19	High
TCGA-E2-A1B5	Luminal	984	Alive	24.33	High
TCGA-E2-A10E	Luminal	865	Alive	24.43	High
TCGA-E2-A15P	Luminal	595	Alive	24.91	High
TCGA-GM-A4E0	Luminal	2191	Alive	24.97	High
TCGA-BH-A0W5	Luminal	1288	Alive	24.99	High
TCGA-E2-A1IL	Luminal	118	Alive	25.22	High
TCGA-LL-A9Q3	Luminal	532	Alive	25.28	High

TCGA-A7-A3J1	Luminal	343	Alive	25.42	High
TCGA-BH-A0DE	Luminal	2372	Alive	25.55	High
TCGA-BH-A0B8	Luminal	1569	Alive	25.71	High
TCGA-E2-A1B1	Luminal	2653	Alive	26.1	High
TCGA-A7-A5ZW	Luminal	326	Alive	26.35	High
TCGA-A8-A08A	Luminal	30	Alive	26.41	High
TCGA-E2-A1L9	Luminal	598	Alive	26.68	High
TCGA-A2-A0CV	Luminal	3011	Alive	26.93	High
TCGA-AC-A3QQ	Luminal	734	Alive	26.93	High
TCGA-BH-A0E2	Luminal	435	Alive	27.47	High
TCGA-BH-A0GY	Luminal	923	Alive	27.5	High
TCGA-AR-A24W	Luminal	1550	Alive	27.54	High
TCGA-AR-A5QN	Luminal	1013	Alive	27.57	High
TCGA-AR-A1AN	Luminal	2920	Alive	27.7	High
TCGA-V7-A7HQ	Luminal	2033	Alive	27.71	High
TCGA-BH-A0HX	Luminal	829	Alive	27.83	High
TCGA-A2-A1FZ	Luminal	683	Alive	28.13	High
TCGA-AR-A255	Luminal	2161	Alive	28.24	High
TCGA-A8-A07E	Luminal	608	Alive	28.65	High
TCGA-BH-A0E9	Luminal	2489	Alive	28.66	High
TCGA-C8-A26Z	Luminal	470	Alive	28.75	High
TCGA-AC-A3W7	Luminal	471	Alive	28.77	High
TCGA-E9-A227	Luminal	975	Alive	28.86	High
TCGA-A8-A09V	Luminal	457	Alive	28.87	High
TCGA-A8-A08Z	Luminal	1217	Alive	29.05	High
TCGA-LL-A7SZ	Luminal	594	Alive	29.27	High
TCGA-BH-A42V	Luminal	635	Alive	29.4	High
TCGA-A8-A07B	Luminal	1308	Alive	29.59	High
TCGA-B6-A401	Luminal	2596	Alive	29.76	High
TCGA-BH-A2L8	Luminal	612	Alive	29.79	High
TCGA-LL-A740	Luminal	441	Alive	29.87	High
TCGA-E2-A570	Luminal	931	Alive	29.96	High
TCGA-D8-A4Z1	Luminal	659	Alive	30.28	High
TCGA-AC-A3TM	Luminal	762	Alive	30.42	High
TCGA-E2-A1BD	Luminal	1133	Alive	30.45	High
TCGA-A7-A0D9	Luminal	1139	Alive	30.47	High
TCGA-GM-A2DN	Luminal	3091	Alive	31.24	High
TCGA-A7-A56D	Luminal	448	Alive	31.38	High
TCGA-A2-A0EV	Luminal	968	Alive	31.58	High
TCGA-B6-A40C	Luminal	2164	Alive	31.83	High

TCGA-AC-A2QI	Luminal	588	Alive	32.09	High
TCGA-A8-A09A	Luminal	304	Alive	32.17	High
TCGA-AQ-A04L	Luminal	3957	Alive	32.25	High
TCGA-D8-A27I	Luminal	439	Alive	32.35	High
TCGA-OL-A66O	Luminal	528	Alive	32.67	High
TCGA-E2-A1IF	Luminal	1138	Alive	32.7	High
TCGA-A2-A0CQ	Luminal	2695	Alive	32.87	High
TCGA-A8-A097	Luminal	365	Alive	32.87	High
TCGA-EW-A1P3	Luminal	1611	Alive	32.89	High
TCGA-AN-A049	Luminal	19	Alive	32.92	High
TCGA-E2-A576	Luminal	1043	Alive	33	High
TCGA-W8-A86G	Luminal	347	Alive	33.22	High
TCGA-A1-A0SF	Luminal	1463	Alive	33.42	High
TCGA-E2-A10F	Luminal	878	Alive	33.42	High
TCGA-AR-A24P	Luminal	84	Alive	33.56	High
TCGA-AR-A1AM	Luminal	2991	Alive	33.58	High
TCGA-D8-A27P	Luminal	49	Alive	34.28	High
TCGA-AC-A23E	Luminal	698	Alive	34.55	High
TCGA-A7-A4SA	Luminal	454	Alive	34.75	High
TCGA-BH-A0HQ	Luminal	1121	Alive	35.09	High
TCGA-E9-A6HE	Luminal	847	Alive	35.66	High
TCGA-D8-A1XD	Luminal	522	Alive	35.86	High
TCGA-LD-A66U	Luminal	646	Alive	35.96	High
TCGA-AC-A3W6	Luminal	602	Alive	36	High
TCGA-EW-A6SC	Luminal	952	Alive	36.1	High
TCGA-EW-A1IW	Luminal	371	Alive	36.35	High
TCGA-BH-A0HI	Luminal	620	Alive	36.57	High
TCGA-D8-A1JH	Luminal	426	Alive	36.7	High
TCGA-B6-A0RI	Luminal	7126	Alive	37.08	High
TCGA-D8-A1XO	Luminal	1682	Alive	37.64	High
TCGA-A2-A0T5	Luminal	531	Alive	37.93	High
TCGA-D8-A27T	Luminal	398	Alive	38.47	High
TCGA-AO-A0JA	Luminal	655	Alive	38.48	High
TCGA-A8-A093	Luminal	546	Alive	38.61	High
TCGA-BH-A201	Luminal	856	Alive	38.97	High
TCGA-A8-A07F	Luminal	577	Alive	39.48	High
TCGA-BH-A0W7	Luminal	1363	Alive	39.86	High
TCGA-A8-A086	Luminal	396	Alive	40	High
TCGA-C8-A12N	Luminal	358	Alive	40.31	High
TCGA-BH-A0H6	Luminal	747	Alive	40.55	High

TCGA-A7-A0CH	Luminal	1079	Alive	40.56	High
TCGA-E2-A1IO	Luminal	1855	Alive	40.79	High
TCGA-AN-A041	Luminal	7	Alive	41.5	High
TCGA-BH-A0DQ	Luminal	98	Alive	41.68	High
TCGA-E2-A1IJ	Luminal	865	Alive	41.75	High
TCGA-A2-A3KC	Luminal	1102	Alive	41.9	High
TCGA-E9-A1NH	Luminal	576	Alive	42.49	High
TCGA-B6-A40B	Luminal	3152	Alive	42.55	High
TCGA-BH-A0DT	Luminal	2403	Alive	42.57	High
TCGA-E9-A229	Luminal	1148	Alive	42.61	High
TCGA-E2-A15H	Luminal	393	Alive	42.66	High
TCGA-D8-A3Z6	Luminal	563	Alive	43.91	High
TCGA-BH-A0DI	Luminal	912	Alive	43.99	High
TCGA-A7-A26H	Luminal	724	Alive	44.13	High
TCGA-A2-A0CT	Luminal	2289	Alive	44.31	High
TCGA-AC-A3QP	Luminal	675	Alive	44.33	High
TCGA-EW-A423	Luminal	533	Alive	44.7	High
TCGA-BH-A18I	Luminal	1093	Alive	44.88	High
TCGA-BH-A0AZ	Luminal	1919	Alive	45.04	High
TCGA-A2-A4RW	Luminal	222	Alive	45.4	High
TCGA-AN-A0FN	Luminal	218	Alive	45.52	High
TCGA-A2-A0EU	Luminal	1043	Alive	46.49	High
TCGA-AC-A23G	Luminal	2248	Alive	46.51	High
TCGA-A8-A08O	Luminal	943	Alive	46.65	High
TCGA-AN-A0AS	Luminal	10	Alive	46.86	High
TCGA-AN-A0FD	Luminal	196	Alive	47.04	High
TCGA-BH-A0BC	Luminal	974	Alive	47.1	High
TCGA-A1-A0SD	Luminal	437	Alive	48.63	High
TCGA-E2-A1IG	Luminal	2140	Alive	48.72	High
TCGA-AR-A24V	Luminal	3203	Alive	49.03	High
TCGA-BH-A0DK	Luminal	423	Alive	49.05	High
TCGA-AN-A0XO	Luminal	375	Alive	49.18	High
TCGA-MS-A51U	Luminal	681	Alive	49.56	High
TCGA-A2-A04N	Luminal	4354	Alive	49.92	High
TCGA-BH-A0HK	Luminal	178	Alive	50.58	High
TCGA-BH-A0BR	Luminal	2330	Alive	50.64	High
TCGA-BH-A0B1	Luminal	1148	Alive	51.04	High
TCGA-WT-AB44	Luminal	883	Alive	51.31	High
TCGA-BH-A0H7	Luminal	702	Alive	51.54	High
TCGA-3C-AALK	Luminal	1448	Alive	51.72	High

TCGA-C8-A132	Luminal	383	Alive	52.12	High
TCGA-E2-A1BC	Luminal	501	Alive	52.51	High
TCGA-E2-A1IN	Luminal	675	Alive	52.86	High
TCGA-AR-A5QP	Luminal	1185	Alive	52.93	High
TCGA-5L-AAT1	Luminal	1471	Alive	52.97	High
TCGA-BH-A0EB	Luminal	745	Alive	53.01	High
TCGA-B6-A0RG	Luminal	2082	Alive	53.35	High
TCGA-BH-A0GZ	Luminal	328	Alive	53.68	High
TCGA-EW-A6S9	Luminal	463	Alive	53.92	High
TCGA-A7-A26J	Luminal	627	Alive	54.04	High
TCGA-AN-A0XW	Luminal	170	Alive	55.63	High
TCGA-BH-A0HA	Luminal	1611	Alive	55.67	High
TCGA-E9-A1R3	Luminal	78	Alive	56.36	High
TCGA-A7-A5ZX	Luminal	336	Alive	58.11	High
TCGA-AO-A12C	Luminal	2372	Alive	59.1	High
TCGA-BH-A0BQ	Luminal	2255	Alive	59.27	High
TCGA-BH-A0HB	Luminal	806	Alive	59.78	High
TCGA-A2-A0YL	Luminal	1474	Alive	60.22	High
TCGA-D8-A1XB	Luminal	552	Alive	60.36	High
TCGA-A2-A0CP	Luminal	2813	Alive	60.99	High
TCGA-A1-A0SH	Luminal	1437	Alive	61.4	High
TCGA-GM-A5PX	Luminal	551	Alive	61.74	High
TCGA-A8-A0A2	Luminal	579	Alive	62.54	High
TCGA-A8-A07G	Luminal	577	Alive	63.19	High
TCGA-A2-A0T7	Luminal	631	Alive	63.55	High
TCGA-BH-A0BM	Luminal	1876	Alive	64.33	High
TCGA-AN-A0XN	Luminal	10	Alive	65.26	High
TCGA-BH-A0W4	Luminal	759	Alive	66.61	High
TCGA-GM-A3XN	Luminal	2019	Alive	67.42	High
TCGA-OL-A5DA	Luminal	1783	Alive	68.11	High
TCGA-E9-A1RF	Luminal	200	Alive	72.02	High
TCGA-E2-A1L8	Luminal	2240	Alive	72.18	High
TCGA-E2-A15L	Luminal	626	Alive	74.33	High
TCGA-AR-A1AU	Luminal	2868	Alive	79.05	High
TCGA-C8-A12Y	Luminal	1476	Alive	79.26	High
TCGA-AN-A04A	Luminal	90	Alive	79.83	High
TCGA-BH-A0DZ	Luminal	495	Alive	80.51	High
TCGA-4H-AAAK	Luminal	348	Alive	80.85	High
TCGA-GM-A2DL	Luminal	3519	Alive	81.99	High
TCGA-5L-AAT0	Luminal	1477	Alive	83.88	High

TCGA-A2-A0EO	Luminal	2442	Alive	86.44	High
TCGA-E9-A295	Luminal	375	Alive	98.03	High
TCGA-E2-A1LA	Luminal	748	Alive	98.8	High
TCGA-AR-A24T	Luminal	3202	Alive	98.88	High
TCGA-S3-AA14	Luminal	529	Alive	99.74	High
TCGA-UL-AAZ6	Luminal	518	Alive	102.2	High
TCGA-D8-A27V	Luminal	381	Alive	105.7	High
TCGA-AO-A0J9	Luminal	1613	Alive	114.37	High
TCGA-BH-A0HF	Luminal	727	Alive	134.63	High
TCGA-A8-A075	Luminal	518	Alive	18.64	High
TCGA-AN-A0XR	Luminal	10	Alive	19.02	High
TCGA-A2-A0T3	Luminal	1516	Alive	19.06	High
TCGA-D8-A1Y2	Luminal	433	Alive	19.19	High
TCGA-A8-A082	Luminal	549	Alive	19.6	High
TCGA-A2-A04Y	Luminal	1099	Alive	19.74	High
TCGA-A7-A13F	Luminal	765	Alive	20.08	High
TCGA-BH-A0BZ	Luminal	2255	Alive	20.23	High
TCGA-D8-A27N	Luminal	519	Alive	20.86	High
TCGA-D8-A1J9	Luminal	532	Alive	21.98	High
TCGA-D8-A1JE	Luminal	575	Alive	22.18	High
TCGA-BH-A0AU	Luminal	1914	Alive	22.56	High
TCGA-3C-AALJ	Luminal	1474	Alive	22.67	High
TCGA-A8-A095	Luminal	1277	Alive	23.3	High
TCGA-AC-A2BM	Luminal	3022	Alive	23.81	High
TCGA-A1-A0SN	Luminal	1196	Alive	25.02	High
TCGA-BH-A0C0	Luminal	1270	Alive	25.13	High
TCGA-BH-A0BD	Luminal	554	Alive	25.83	High
TCGA-A8-A084	Luminal	458	Alive	25.91	High
TCGA-B6-A1KN	Luminal	4233	Alive	25.94	High
TCGA-AN-A03Y	Luminal	10	Alive	26.8	High
TCGA-BH-A0HU	Luminal	392	Alive	27.56	High
TCGA-E2-A9RU	Luminal	538	Alive	27.63	High
TCGA-EW-A1PC	Luminal	187	Alive	28.46	High
TCGA-LL-A5YM	Luminal	466	Alive	28.53	High
TCGA-A8-A08P	Luminal	943	Alive	30.16	High
TCGA-EW-A1OZ	Luminal	1229	Alive	31.38	High
TCGA-D8-A1XL	Luminal	606	Alive	31.6	High
TCGA-A2-A04R	Luminal	3709	Alive	31.88	High
TCGA-BH-A0C7	Luminal	2767	Alive	32.56	High
TCGA-A1-A0SI	Luminal	635	Alive	32.67	High

TCGA-D8-A1J8	Luminal	431	Alive	32.87	High
TCGA-AO-A03N	Luminal	2031	Alive	33.05	High
TCGA-AO-A0JD	Luminal	2190	Alive	33.11	High
TCGA-D8-A13Y	Luminal	1728	Alive	33.22	High
TCGA-E9-A1RG	Luminal	647	Alive	33.73	High
TCGA-BH-A202	Luminal	795	Alive	34.69	High
TCGA-AN-A0FY	Luminal	10	Alive	34.83	High
TCGA-AO-A1KP	Luminal	2953	Alive	37.47	High
TCGA-D8-A1JD	Luminal	552	Alive	39.04	High
TCGA-C8-A130	Luminal	370	Alive	40.61	High
TCGA-C8-A1HG	Luminal	345	Alive	42.52	High
TCGA-E2-A1L7	Luminal	1836	Alive	47.56	High
TCGA-D8-A1JJ	Luminal	611	Alive	47.65	High
TCGA-BH-A0HY	Luminal	1545	Alive	48.16	High
TCGA-A8-A06R	Luminal	547	Alive	49.52	High
TCGA-A2-A1FW	Luminal	528	Alive	49.85	High
TCGA-A7-A6VX	Luminal	317	Alive	50.19	High
TCGA-E9-A22E	Luminal	1269	Alive	57.66	High
TCGA-Z7-A8R6	Luminal	3256	Alive	58.11	High
TCGA-AN-A0AJ	Luminal	303	Alive	65.2	High
TCGA-EW-A1IY	Luminal	258	Alive	68.85	High
TCGA-C8-A8HQ	Luminal	380	Alive	76.55	High
TCGA-E9-A22A	Luminal	1189	Alive	79.94	High
TCGA-AO-A1KT	Luminal	541	Alive	86.89	High
TCGA-A2-A0CY	Luminal	1673	Alive	121.55	High
TCGA-BH-A28O	Normal	1120	Alive	20.59	High
TCGA-A2-A1G6	Normal	501	Alive	21.01	High
TCGA-A2-A25A	Normal	3276	Alive	21.51	High
TCGA-LD-A9QF	Normal	323	Alive	23.98	High
TCGA-AC-A3YI	Normal	707	Alive	26.36	High
TCGA-EW-A1PG	Normal	1051	Alive	30.39	High
TCGA-A2-A4RY	Normal	648	Alive	32.97	High
TCGA-AO-A03T	Normal	2124	Alive	38.57	High
TCGA-AO-A0JB	Normal	1542	Alive	39.67	High
TCGA-BH-A42U	Normal	3364	Alive	40	High
TCGA-AO-A1KO	Normal	622	Alive	46.17	High
TCGA-A2-A0CZ	Normal	1616	Alive	52.38	High
TCGA-GM-A2DD	Normal	2282	Alive	59.53	High
TCGA-OL-A5RY	Normal	752	Alive	62.18	High
TCGA-EW-A1P7	Normal	915	Alive	102.24	High

TCGA-BH-A6R9	Normal	160	Alive	370.11	High
TCGA-A2-A3XW	Normal	1712	Alive	1115.52	High
TCGA-A2-A3XS	TNBC	1032	Dead	20.03	High
TCGA-BH-A1F6	TNBC	2965	Dead	20.74	High
TCGA-BH-A18Q	TNBC	1692	Dead	21.6	High
TCGA-B6-A409	TNBC	573	Dead	22.26	High
TCGA-B6-A0I1	TNBC	2361	Dead	34.59	High
TCGA-A2-A04P	TNBC	548	Dead	36.83	High
TCGA-BH-A18V	TNBC	1556	Dead	37.12	High
TCGA-A2-A0CM	TNBC	754	Dead	53.54	High
TCGA-AC-A2QJ	TNBC	446	Dead	54.02	High
TCGA-BH-A1FC	TNBC	3472	Dead	62.67	High
TCGA-B6-A0X1	TNBC	7455	Dead	68.49	High
TCGA-A2-A0T2	TNBC	255	Dead	76.68	High
TCGA-BH-A1F0	TNBC	785	Dead	169.27	High
TCGA-B6-A0I6	TNBC	991	Dead	172.05	High
TCGA-E2-A1LK	TNBC	266	Dead	228.31	High
TCGA-B6-A0I9	Her2	362	Dead	21.67	High
TCGA-B6-A0RS	Her2	3063	Dead	25.57	High
TCGA-BH-A203	Her2	1174	Dead	26.17	High
TCGA-B6-A0RH	Her2	6456	Dead	48.49	High
TCGA-BH-A1EV	Her2	365	Dead	81.5	High
TCGA-A2-A0EW	Luminal	1884	Dead	18.77	High
TCGA-AQ-A7U7	Luminal	584	Dead	19.13	High
TCGA-BH-A1EY	Luminal	538	Dead	19.5	High
TCGA-BH-A1F5	Luminal	2712	Dead	20.27	High
TCGA-A8-A08T	Luminal	3409	Dead	21.63	High
TCGA-OL-A66K	Luminal	1275	Dead	22.38	High
TCGA-BH-A0C1	Luminal	1411	Dead	24.07	High
TCGA-BH-A1ET	Luminal	2520	Dead	24.11	High
TCGA-BH-A1FB	Luminal	3669	Dead	24.66	High
TCGA-BH-A18M	Luminal	2207	Dead	26.08	High
TCGA-AR-A24L	Luminal	2866	Dead	27.16	High
TCGA-BH-A18K	Luminal	2763	Dead	27.27	High
TCGA-B6-A0IP	Luminal	3926	Dead	27.73	High
TCGA-GM-A2D9	Luminal	1812	Dead	32.54	High
TCGA-B6-A0IG	Luminal	4456	Dead	35.34	High
TCGA-E2-A1B4	Luminal	1004	Dead	35.69	High
TCGA-B6-A0WY	Luminal	3461	Dead	37.45	High
TCGA-BH-A1FE	Luminal	2273	Dead	38.25	High

TCGA-BH-A1ES	Luminal	3462	Dead	38.52	High
TCGA-E2-A14Z	Luminal	563	Dead	40.36	High
TCGA-E2-A2P5	Luminal	821	Dead	43.43	High
TCGA-AQ-A0Y5	Luminal	172	Dead	43.77	High
TCGA-HN-A2OB	Luminal	1900	Dead	46.31	High
TCGA-E9-A1NG	Luminal	786	Dead	46.59	High
TCGA-GM-A2DA	Luminal	6593	Dead	59.72	High
TCGA-BH-A18J	Luminal	612	Dead	75.83	High
TCGA-A2-A0CS	Luminal	2348	Dead	93.22	High
TCGA-E9-A1RB	Luminal	976	Dead	20.81	High
TCGA-E9-A1N6	Luminal	678	Dead	21.85	High
TCGA-BH-A0BF	Luminal	1324	Dead	23.89	High
TCGA-BH-A18U	Luminal	1563	Dead	27.08	High
TCGA-BH-A1FN	Luminal	2192	Dead	27.23	High
TCGA-B6-A0WW	Luminal	558	Dead	39.75	High
TCGA-E9-A226	Luminal	1048	Dead	53.52	High
TCGA-BH-A1FM	Luminal	1388	Dead	55.1	High
TCGA-A2-A0SV	Luminal	825	Dead	70.05	High
TCGA-OL-A5D6	Normal	1104	Dead	30.75	High
TCGA-LL-A73Z	Normal	227	Dead	60.61	High
TCGA-BH-A208	Normal	1759	Dead	97.61	High